Large Artery Stiffness: Genes and Pathways

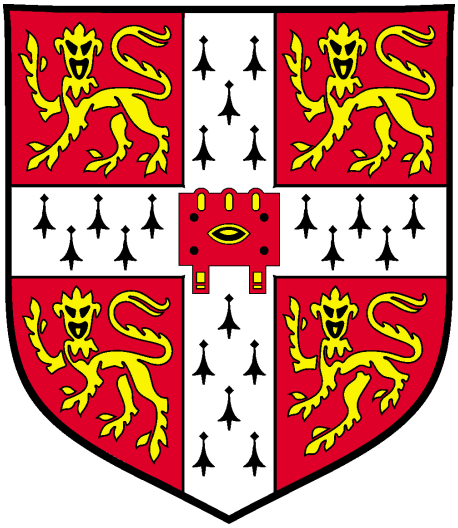

Raya AL MASKARI

Gonville & Caius College

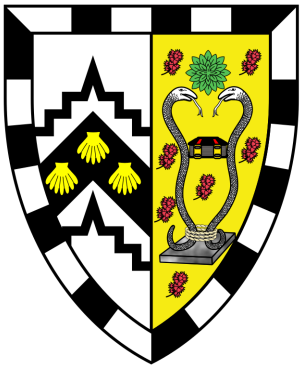

This dissertation is submitted for the Degree of Doctor of Philosophy

University of Cambridge

June 20, 2018

To Mohammed & Noor

DECLARATION

This thesis is the result of my own work and includes nothing which is the outcome of work done in collaboration except where specifically indicated in the text. It has not been submitted, nor is it in the process of being submitted, for any other qualification at the University of Cambridge or any other university.

In accordance with the Degree Committee for the Faculty of Medicine, this dissertation does not exceed 60,000 words.

Raya Al Maskari

June 20, 2018

"As you start to walk on the way, the way appears..."

Rumi

ACKNOWLEDGEMENTS

I wish to extend my gratitude to the many people without whom the completion of this thesis would not have been possible.

My supervisors Kevin O' Shaughnessy and Yasmin for their support during my time in the lab, Sarah Cleary for her technical help and encouragement throughout and Keith Siew whose passion for science I found contagious. I especially mention Iris Hardege, whose pragmatism and incredible repertoire of techniques have greatly shaped the outcome of this work. I am grateful for our friendship that has extended beyond the lab, and have no doubt it is one that will stand the test of time over the years to come.

My graduate tutor Ruth Scurr and Gonville & Caius College Master Sir Alan Fersht for their moral support at the most critical times, and my fellow Caians for the most enriching discussions that have stimulated my intellectual growth.

My parents whose unconditional love, unwavering support and boundless prayers have been the beacon of light guiding me through life. My brothers and sisters who have flown into Cambridge on many occasions to provide a helping hand and have supported me in ways I can never pay back. The love of my life, Ahmed, who sacrificed being away from myself and the kids so I can fulfill my ambitions, and has been my rock over the 9 years we've been together. My pride and joy, Mohammed and Noor, who are an infinite source of happiness, and of course the many people who were of tremendous help with the babysitting.

My thesis writing partner, Zein Azhari, who has kept me motivated and made the journey of thesis writing a thoroughly enjoyable one; I couldn't have wished for a better way to end my PhD. The many friends who became my home away from home and kept me grounded during the toughest times: Zahra Abbas, Maria Qigua, Roland Papp, Gerry Mako, Ada Teo, Joel Chappell, Jilles Fermont, Mohammed Abdalaal, Kristin Webster and Ellen.

Finally, I am very grateful to Cambridge Overseas Trust for their Honorary scholarship and HM The Sultan of Oman for the Merit Scholarship Programme that funded my PhD.

ABSTRACT

Aortic stiffness underlies systolic hypertension, promotes heart failure and is associated with increased cardiovascular morbidity and mortality. It is regarded as a primary driver of left ventricular hypertrophy and aortic aneurysms and is linked to the pathogenesis of cognitive impairment, stroke and renal failure. Like most cardiovascular traits, aortic stiffness is a complex trait and is moderately heritable, yet the precise molecular mechanisms that underpin the stiffening process remain poorly defined. This study aimed to employ multiple approaches to further identify the genetic basis of aortic stiffness in a large repository of human donor aortas that had undergone *ex vivo* pulse wave velocity (PWV) phenotyping.

The first part of this work sought to investigate the molecular basis of Loeys-Dietz type 4 syndrome in a pedigree with multiple cases of aortic aneurysms and dissections. A missense variant p.(Arg320Cys) was identified in a highly evolutionary conserved region of *TGFB2*. There was striking upregulation of TGFB1, TGFB2 and pSMAD2/3 on imunocytochemical straining and western blotting of the aortic tissue from the index case confirming the functional importance of the variant. This case highlighted the striking paradox of predicted loss-of-function mutations in *TGFB2* causing enhanced TGFβ signalling in this emerging familial aortopathy and underscored the significance of TGFβ signalling in aortic extracellular matrix biology.

The second part of this work attempted to characterise the biological basis for the susceptibility locus identified in the most recent genome wide analysis of carotid-femoral PWV. While the locus lies within the 14q32.2 gene desert, it contains regulatory elements, with the transcriptional regulator B-cell CLL/lymphoma 11B (*BCL11B*) and non-coding RNA DB129663 representing potential targets for these enhancers. The association of five lead SNPs from the genome-wide association studies (GWAS) meta-analysis was examined for *ex vivo* aortic stiffness and *BCL11B* and DB129663 aortic mRNA expression. Three of the five SNPs associated significantly with PWV and showed allele-specific differences in *BCL11B* mRNA. The risk alleles associated with lower *BCL11B* suggesting a protective role for *BCL11B*. Despite the strong association, BCL11B protein was not detected in the human aorta; however, qPCR for CD markers showed that *BCL11B* transcript correlated strongly

with markers for activated lymphocytes. In contrast, DB129663 transcripts were detected in 55% of the samples, and of the five SNPs only one showed allele-specific differences in aortic DB129663 transcripts. No significant differences were observed in PWV between samples expressing or lacking DB129663, and therefore the implication of this lncRNA in aortic stiffness remains elusive. The *BCL11B* transcript detected in the human aorta may reflect lymphocyte infiltration, suggesting that immune mechanisms contribute to the observed association with PWV.

For the final part of this work genetic associations with aortic stiffness were explored in a candidate gene-based study utilising tagging SNPs to effectively capture the genetic information from linkage disequilibrium blocks. Association analyses were performed in young, healthy ENIGMA study participants selected for high and low PWV values then validated in the remaining ENIGMA cohorts. The association of four lead SNPs was then examined for *ex vivo* aortic stiffness in human donor aortas. The tissue expression of these SNPs and their encoded proteins was also explored. Neither the aggrecan nor the fibulin-1 SNPs showed significant associations with *ex vivo* PWV in the donor aortas. The exonic aggrecan tagSNP rs2882676 displayed differential transcript abundance between homozygous allele carriers but this did not translate at the protein level. Both aggrecan and fibulin-1 were found in the aortic wall, but with marked differences in the distribution and glycosylation of aggrecan, reflecting loss of chondroitin-sulphate binding domains. These differences were age-dependent but the striking finding was the acceleration of this process in stiff versus elastic young aortas. These findings suggest that aggrecan and fibulin-1 have critical roles in determining the biomechanics of the aorta and their modification with age could underpin age-related aortic stiffening.

PUBLICATIONS

This thesis is based on the following publications and manuscript, which will be referred to in the text by their Arabic numerals:

1. **Raya Al Maskari**, Yasmin, S Cleary, Nikki Figg, Sarju Mehta, Doris Rassl, Ian Wilkinson and Kevin M O'Shaughnessy. A missense TGFB2 variant p.(Arg320Cys) causes a paradoxical and striking increase in aortic TGFB1/2 expression. *European Journal of Human Genetics* **25**, 157-160 (2017)

2. **Raya Al Maskari**, Iris Hardege, Sarah Cleary, Nicki Figg, Ye Li, Keith Siew, Ashraf Khir, Yong Yu, Pentao Liu, Ian Wilkinson, Kevin O'Shaughnessy and Yasmin. Functional characterisation of common BCL11B gene desert variants suggests an inflammation-mediated association of BCL11B with aortic stiffness. (Manuscript in review)

3. Yasmin, **Raya Al Maskari**, Carmel M McEniery, Sarah E Cleary, Keith Siew, Ye Li, Ashraf W Khir, John R Cockcroft, Ian B Wilkinson and Kevin M O'Shaughnessy. The matrix proteins aggrecan and fibulin-1 play a key role in determining aortic stiffness. *Scientific Reports* **8**, 8550 (2018)

Contents

List of Figures

List of Tables

List of Acronyms

ACAN	Aggrecan
ADAMTS	A disintegrin and metalloproteinase with thrombospondin motifs
AGE	Advanced glycation end-products
aPWV	Aortic pulse wave velocity
BCL11B	B cell-lymphoma/11B
cfPWV	Carotid-femoral pulse wave velocity
CLD	C-type lectin domain
CNS	Central nervous system
COUP-TF	Chicken ovalbumin upstream promoter transcription factor
CRP	Complement regulatory protein
CS	Chondroitin sulphate
CTGF	Connective tissue growth factor
CTIP2	COUP-TF interacting protein 2
CVD	Cardiovascular diseases
ECM	Extracellular matrix
EGF	Epidermal growth factor
EM	Elastic modulus
eQTL	Expression quantitative trait locus
FBLN1	Fibulin-1

GAG Glycosaminoglycan

GAPDH Glyceraldehyde 3-phosphate dehydrogenase

GWAS Genome wide association study

IFN γ Interferon γ

IGD Inter-globular domain

KS Keratan sulphate

LD Linkage disequilibrium

LDS Loeys-Dietz syndrome

lncRNA long-noncoding RNA

MMP Matrix metalloproteinases

NO Nitric oxide

NuRD Nucleosome remodelling and histone deacetylation complex

PBMC Peripheral blood mononuclear cells

PWV Pulse wave velocity

qPCR Quantitative polymerase chain reaction

RAAS Renin-angiotensin aldosterone system

SMC Smooth muscle cells

SNP Single nucleotide polymorphism

TCR T cell receptor

TGF β Transforming growth factor β

TNF α Tumour necrosis factor α

TSA Tyramide signal amplification

VNTR Variable number of tandem repeats

VSMC Vascular smooth muscle cells

1

Introduction

1.1 Background

Despite a decline in age-specific death rates in recent years, cardiovascular diseases (CVD) remain the largest single contributor to global morbidity and mortality, with 422 million prevalent cases and 18 million deaths predicted to have occurred globally in the year 2015 alone [1,2]. Following current trends, the number of CVD related deaths is projected to reach 25 million by 2030; this is largely driven by population growth and ageing populations [3]. In recognition of the rising global burden of CVD, the World Health Organisation set a target aimed at reducing 25% of premature deaths from CVD and other noncommunicable diseases by 2025 [2]. It is estimated that at least 5.7 million deaths can be prevented if the suggested interventional strategies aimed at targeting modifiable CVD risk factors, as well as secondary prevention of CVD are effectively implemented [4].

Mounting evidence has shown stiffening of the large arteries to be an important determinant of cardiovascular risk and therefore a potential target open for therapeutic intervention [5, 6]. Aortic stiffness underlies systolic hypertension, promotes heart failure, and is associated with increased cardiovascular morbidity and mortality [5, 7]. It is regarded as a primary driver of left ventricular hypertrophy and aortic aneurysms and is linked to the pathogenesis of cognitive impairment, stroke, cerebral microbleeds and renal failure [8–13]. Carotid-femoral pulse wave velocity (cfPWV), the current gold-standard measure of aortic stiffness, is a strong and independent predictor of cardiovascular events and all-cause mortality in both healthy individuals and high risk groups, including those with end-stage kidney disease, hypertension and diabetes [14–16].

Like most cardiovascular traits, aortic stiffness has a multifactorial aetiology and its cellular and molecular landscapes are complex. Evidence from family studies show aortic stiffness to be moderately heritable with 38-40% of cfPWV explained by variation in genetic factors [17, 18]. Genetic

studies of a host of monogenic aortopathies have informed our understanding of essential mechanisms that regulate aortic wall function. A combination of genome-wide studies, transcriptomic profiling and hypothesis-driven candidate gene studies have further provided a number of key insights into its molecular drivers, highlighting pathways related to extracellular matrix (ECM) structure and homeostasis, inflammation, calcification and blood pressure regulation [19]. Despite these advances, progress has been hampered by poor reproducibility of genetic associations and difficulties in assigning definitive causal pathways to susceptibility loci. Dissecting the complex genetic architecture of this trait will help identify the biological pathways that underpin the stiffening process and, eventually, novel drug targets and effective de-stiffening strategies. The present chapter aims to provide an overview of aortic function and the current understanding of genes and pathways that associate with aortic stiffness as well as summarise the evidence from the literature that supports the potential for therapeutic intervention.

1.2 The Aortic Wall

1.2.1 Histology

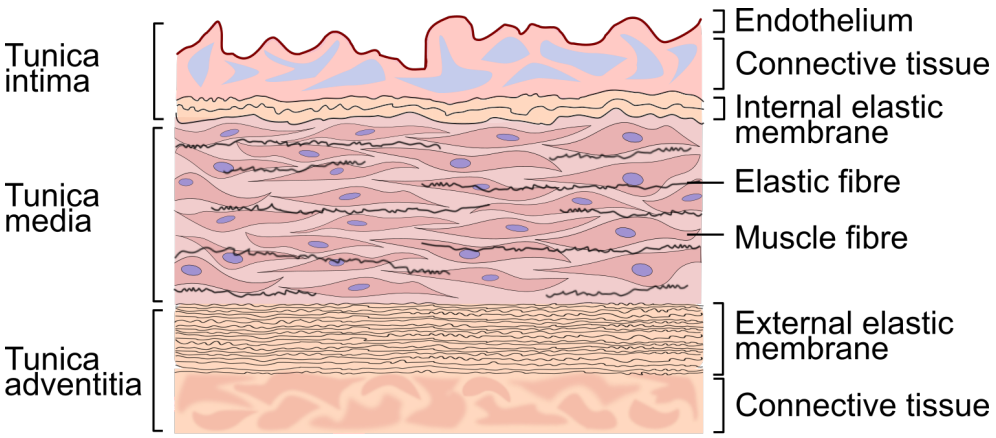

Figure 1.1: Schematic overview of the aortic wall layers

The arterial wall is made of three histologically distinct layers; the intima, media and adventitia (Figure 1.1), each comprising a unique assembly of cells and matrix. The intimal layer is composed of a single layer of endothelial cells, connective tissue and an internal elastic lamina; the media is made of vascular smooth muscle cells (VSMC) embedded in concentric layers of elastic fibres forming lamellar units, collagen and proteoglycans. The adventitial layer is mostly connective tissue containing nerve fibres and vasa vasorum [20]. The ECM provides mechanical structure and a framework supporting the various components of the aortic wall and also relays the signals required

for VSMC development, proliferation and adhesion, and regulates the bioavailability of various signalling molecules and growth factors [21].

1.2.2 Regional Heterogeneity

Properties of the aorta above and below the diaphragm differ in their embryonic origin, structural and mechanical properties, protease profiles and in their susceptibility to aortic pathologies. Embryologically, the thoracic region is derived from the neural crest while the abdominal aortic region from the mesoderm, as a result demonstrating distinct and diverse responses to local cytokines and growth factors [22]. Structurally, the abdominal aorta contains half the number of lamellar units contained in the thoracic aorta, is completely devoid of a vasa vasorum network and contains lower elastin and collagen content; the thoracic aorta therefore has greater distensibility and elasticity [22,23]. The disparate proportion in elastin and collagen content contributes to a heterogeneity of PWV along the arterial tree, with the thoracic portion being more elastic and distensible than the distal segments [22,24]. The two aortic segments are also suggested to display marginal discrepancies in the cellular sources and ratios of matrixmetalloproteinase (MMP)/ tissue inhibitor of metalloproteinase (TIMP) content [22]. Finally, thoracic and abdominal aortas vary in their predisposition to lipid accumulation and plaque progression as well as in the pathophysiological mechanisms that underly aneurysmal formation [22]. It stands to reason that molecular drivers of aortic stiffness may also display regional differences and must therefore be considered in the pursuit of its molecular basis.

1.2.3 Function

The aorta serves an important function as a conduit circulating blood to the peripheral organs from the left ventricle. A less recognised but equally fundamental function of the aorta is to act as a "cushioning" chamber for the heart, dampening the high-energy pulsations generated by the heart beats and supporting the perfusion of organs. These functions have been traditionally exemplified by the *Windkessel* model, which was developed by the quantitative physiologist Otto Frank in 1899 [25]. The origin of the term comes from the German word for 'air-chamber'. This was a water reservoir half-filled with air positioned behind the pumps of old fire hoses, which transformed the pulsing water output into a continuous stream. In a similar way, the *Windkessel* model of the arterial system allows for an unremitting blood flow to the periphery by storing 50% of the stroke volume during the systolic phase of the heart beat and propelling it to the peripheral circulation during diastole, thus ensuring sustained perfusion of organs throughout the cardiac cycle (Figure 1.5) [25].

The function of the aorta can further be illustrated by the aortic pressure waveform model. When the heart contracts, the pulse of blood ejected is accompanied by a pressure wave that originates from the ventricle walls. This pressure is transmitted in the forward direction, travelling away from the heart in waves at a speed known as the pulse wave velocity (PWV). The journey that the forward wave takes through the circulation is far from a straightforward one, as the propagating wave confronts many points of "mismatch" along its path [26]. The bifurcations and taperings of the circulatory system result in wave reflections that travel in an opposing direction to that of the forward wave, in other words, towards the heart and against the direction of blood flow [26]. In a healthy, compliant system where both cardiac and vascular events are meticulously synchronised, the reflected wave returns to the central aorta during late systole and early diastole giving rise to a secondary augmentation pressure at the aortic root. The precise timing of the return of the reflected wave with respect to the cardiac cycle is critical for the efficiency of the cardiovascular system. It allows for the augmentation of diastolic blood pressure, thereby enhancing coronary blood flow whilst ensuring that no additional pressure is produced during systole [26].

1.2.4 Load-Bearing Elements

The capacity of the artery to contract and expand to accommodate the cardiac cycle pressure oscillations is central to its function. The aortic wall is indeed viscoelastic in nature. This characteristic is the product of an intricate interplay of two structural proteins of the extracellular matrix that are inherently different, elastin and collagen. Elastin is 70-100% extensible, whilst collagen is only 2-4%; the latter is 1000 times stiffer than the former when both are stretched [27]. The distinct contribution of these proteins to the mechanical behaviour of the aortic wall was initially demonstrated in the mid 1900s by Roach and Burton who subjected human arterial samples to varying levels of pressure [28]. In their seminal work, they found that elastin fibres are load-bearing at low pressures, while collagen fibres are predominantly load-bearing at high pressures. Thus, elastin is responsible for the compliance and structural integrity of arteries at low physiological pressures, whereas collagen imparts the tensile strength to arteries at higher physiological pressures. As such, any change in the collagen to elastin ratio could detrimentally compromise the aorta's ability to accommodate changes in pressure. Indeed, this by-and-large, is the hallmark of arterial ageing.

1.2.5 Age-Related Changes

The arterial changes observed in ageing could be compared to a rubber band that has been stretched continuously for many years. Conceptually similar to the "wear and tear" of rubber due to repetitive

cycles of stretch and recoil, the cyclic stress and strain of arterial elastin leads to its "fracture and fatigue". This results in the fundamental degenerative process seen in arterial ageing: thinning, fraying and fragmentation of elastin fibres. The fracturing of rubber is estimated to occur after 1 x 10^9 oscillations, in cardiac time this is equivalent to 60-70 beats per minute over the course of 25-30 years in humans [29]. Theoretically, this is the age when aortic elastin fibres begin to fragment. It is for this reason that the process of arterial degeneration has been said to commence in childhood and to be "well developed" by early adulthood [30]. This stark difference in elastin fibre composition is clearly seen in Figure1.2.

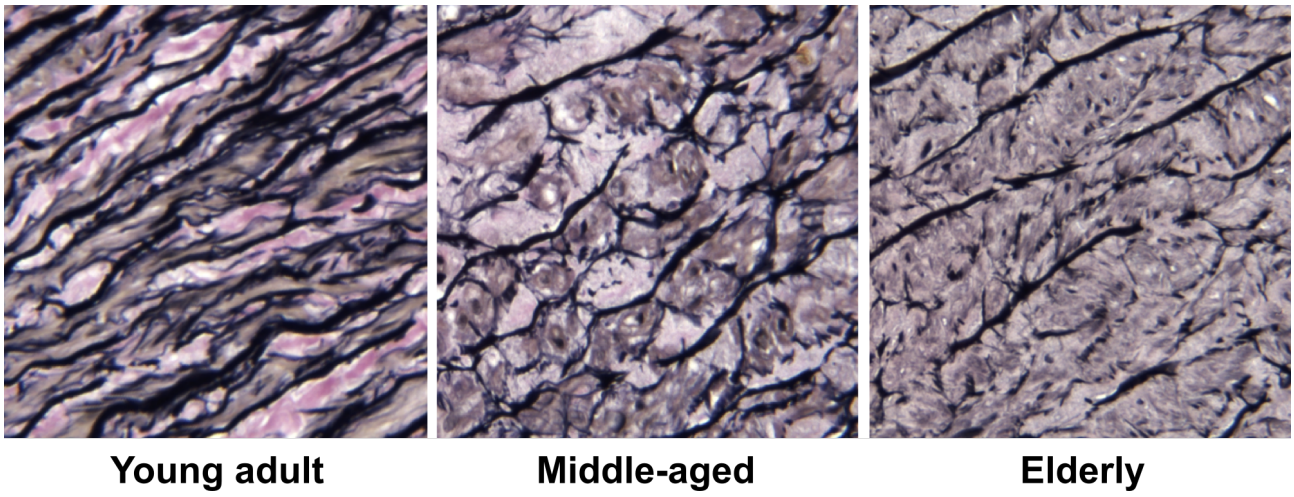

Figure 1.2: Verhoeff Van Gieson staining of human aortic sections showing the progressive fraying and fragmentation of elastin with age. The young adult represents a 28 year old subject, the middle-aged a 50 year old subject and the elderly an 81 year old subject.

In addition to the mechanical fatigue of elastin, several other factors accelerate its degradation. A pre-requisite for the proper mechanical functioning of elastin is a specific level of covalent cross-linkage of elastic fibres by lysyl oxidase. With age, this optimal degree of cross-linking is impacted by nitration and formation of advanced glycation end products (AGEs) [31,32]. Furthermore, inflammatory processes, oxidative stress, elevated cholesterol levels and metabolic dysfunction together enhance the precipitation of calcium apatite onto elastic fibres, giving rise to medial elastic fibre calcification (*elastocalcinosis*), which disrupts the elastic fibre network even further [33].

Arterial ageing is further accelerated by a host of other structural and cellular modifications to the aortic wall. These include an increase in the content and cross-linking of collagen, ECM accumulation, increased VSCM proliferation, migration, senescence and ossification, enhanced activity of proteolytic enzymes, reduced endothelial function and intima-medial layer thickening [34, 35]. Together, these lead to the dilatation, stiffening and thickening of the aortic walls which compromise its cushioning function and predispose aortic walls to a number of adverse effects and end-organ injury

(Figure 1.3). The aforementioned degenerative changes are more prominent in the proximal large central arteries (i.e., aorta and its major branches) which have a higher elastin content and receive most of the impact of repeated cyclic strain and stress compared to the peripheral muscular arteries (i.e., radial).

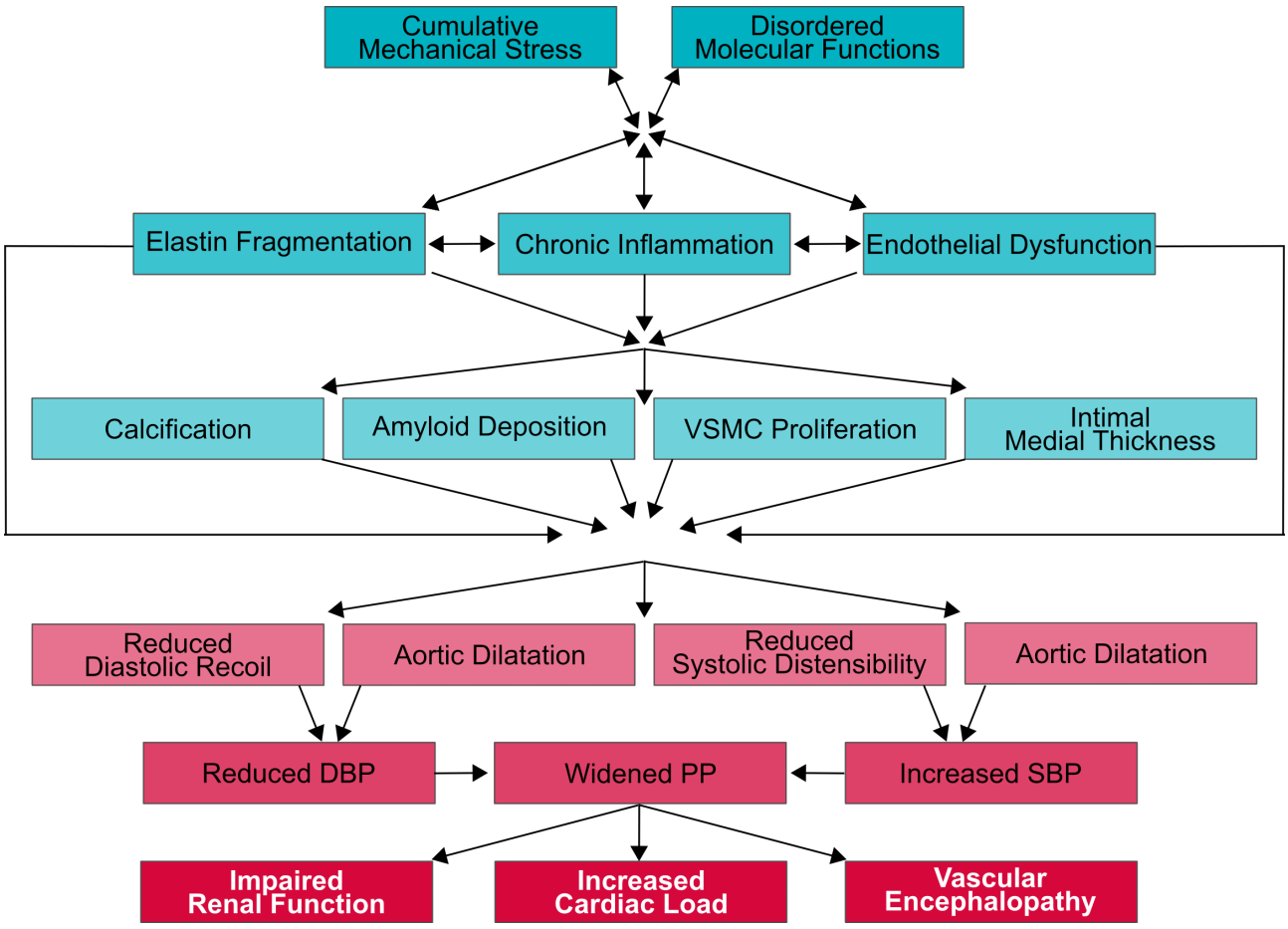

Figure 1.3: Theoretical model of arterial ageing. Age-associated mechanical stress predisposes to elastin fragmentation, endothelial damage and a state of chronic inflammation within the aortic wall. These factors synergistically promote further structural and cellular alterations to the aortic wall and compromise its cushioning efficiency. Image modified from Al Ghatrif and Lakatta [35].

1.3 Aortic Stiffness

1.3.1 Biological versus Pathological Stiffness

Arteries stiffen with age; however, it is not clear why arterial ageing and its associated complications manifest in some individuals more than others. There is no straightforward answer to this question, as the mechanisms underlying age-related arterial stiffness are complex. Records of aortic PWV in rural versus more urbanised communities in China and Cameroon have indicated that the physiological ageing of arteries can be aggravated by environmental, dietary and lifestyle factors

associated with modern societies [36,37] (Figure 1.4). For example, conditions such as diabetes, obesity, hypertension, high cholesterol, impaired glycaemic control, renal dysfunction and inflammation accelerate the progression of arterial ageing, thus accounting for some of the variability [38–43]. The pathogenesis and progression of aortic stiffness is further governed by a complex network of cellular, biochemical, enzymatic and genetic pathways which alter the capacity of the aorta to adapt and repair in the face of the ageing process.

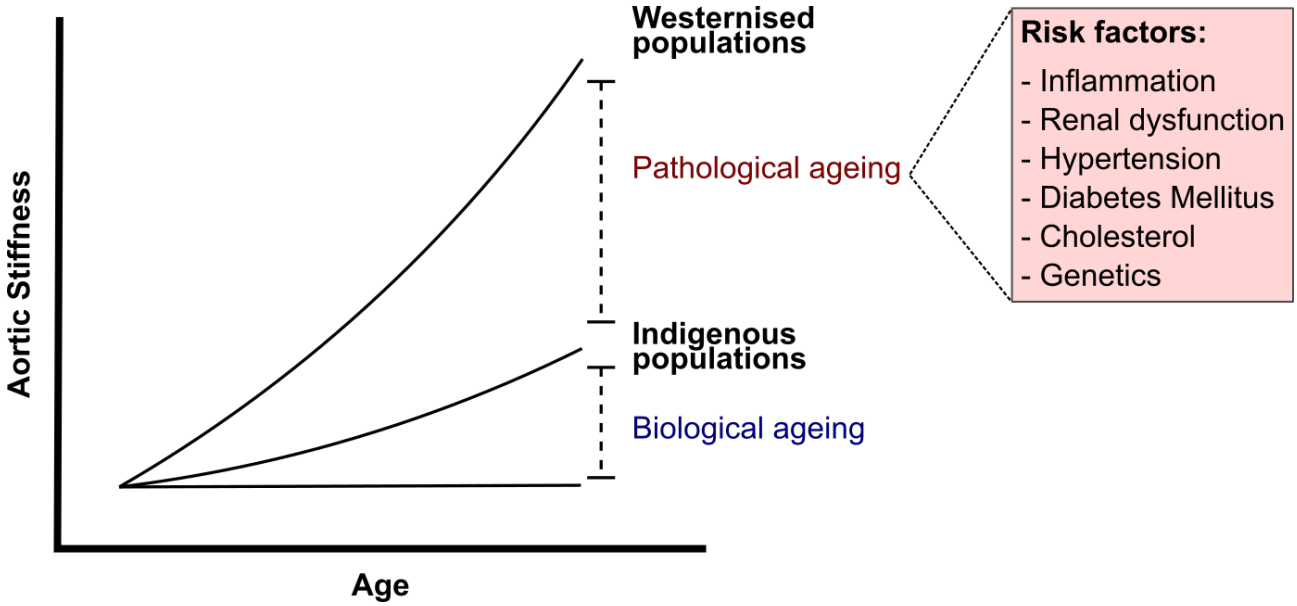

Figure 1.4: Graphic representation of biological versus pathological ageing. Image modified from Wilkinson and McEniery [44].

1.3.2 Haemodynamic and Clinical Consequences

Aortic stiffness is detrimental in several ways. The fraying of elastin fibres means that the mechanical load is now shifted to the more rigid collagen component of the aorta, compromising the cushioning function of the aorta and causing major changes to the aortic pressure waveform [26]. When the central arteries lose cushioning efficiency, the pressure pulsations travel further down the arterial tree into the vessels of the microcirculation which trigger microbleeds and microinfarcts, and increase the risk of stroke, cognitive impairment and renal failure. A rigid aorta is also inefficient at storing the stroke volume during systole; the entire stroke volume is thus propelled to the periphery during this phase, which disrupts the continuous perfusion of the peripheral system and reduces transit time with the capillaries (Figure 1.5). With respect to the changes in the aortic pressure waveform, a stiffened artery causes an early return of the reflected wave such that it falls within the systolic phase instead of the diastolic phase. The early return of reflected wave, coupled with a stiffened aorta, leads to a rise in systolic pressure and fall in diastolic pressure, giving rise to isolated systolic

hypertension. The raised systolic pressure also causes an increase in left ventricular load driving left ventricular hypertrophy and increased cardiac oxygen demand. Conversely, the reduced diastolic blood pressure makes the heart incapable of meeting this demand due to the compromised coronary perfusion, predisposing the heart to ischaemia and, ultimately to myocardial infarction or heart disease [26].

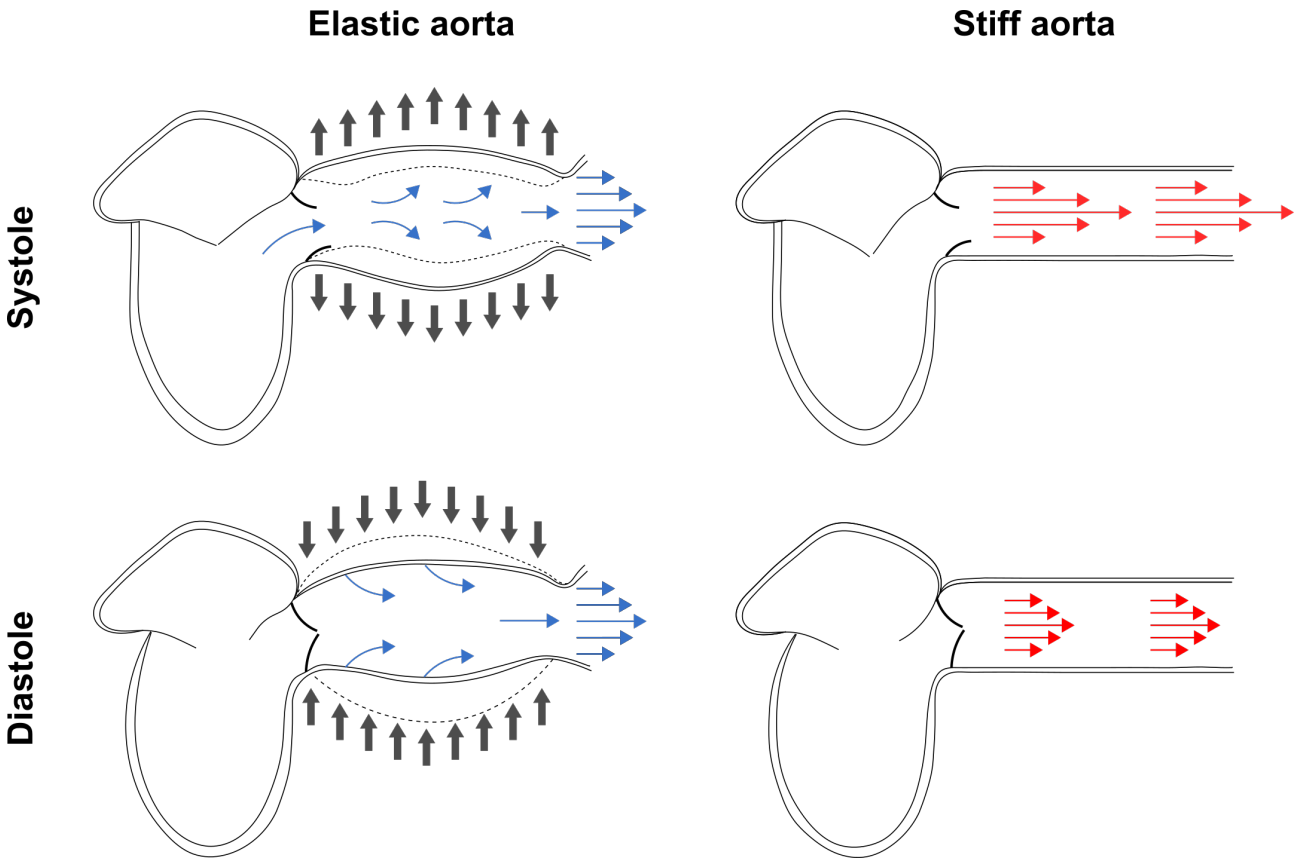

Figure 1.5: Impact of aortic stiffness on blood flow through the peripheral circulation. Image modified from Briet et al. [45].

1.3.3 Pulse Wave Velocity: An Index of Aortic Stiffness

PWV was recognised in 1922 as a marker of arterial elasticity and a fundamental index of "circulatory efficiency" by Bramwell and Hill [46] but the notion of arterial wave analysis and the assessment of arterial pulse has been known since the late Han dynasty when one of the first books 'the Pulse Classic', was written in 220 AD [47]. Moreover, the concept of forward pulse wave transmission was identified by Erasistratos as early as 280 BC, and he found that the pulse appeared earlier in arteries proximal to the heart than in those distal to the heart [48]. The field has since evolved into a quantitative discipline, particularly highlighting the haemodynamic and mechanical behaviour of the circulation. Aortic PWV is the current gold standard measure of arterial stiffness, measured

non-invasively between any two arterial sites (i.e. carotid and femoral arteries or carotid and radial arteries). It increases with age: typically 5m/s in a 20 year old adult vs. 12m/s in an 80 year old.

Aortic PWV is an independent and strong predictor of cardiovascular (CV) risk and all causes of mortality in a variety of patient groups and unselected subjects. A meta-analysis conducted by Vlachopoulos et al. encompassing 15,500 subjects indicated that a 1m/s increase in aPWV was associated with a 14% increase in the risk of CV events, 15% increase in CV mortality and 15% increase in all-cause mortality, even after accounting for classical risk factors [16]. The predictive risk of aortic stiffness in this meta-analysis was greater in high-risk groups, such as chronic kidney patients, diabetics, and hypertensives, than in low-risk groups. A more recent meta-analysis by Ben-Shlomo et al. [49] reported similar findings confirming the role of aPWV as a strong predictor of future CV events even after adjusting for the traditional CV risk factors. The authors demonstrated that incorporating PWV into the conventional CV risk prediction model improved the 10-year classification by 13% and, unlike the findings of Vlachopoulos et al., the predictive value of aPWV appeared stronger in the younger population while still predictive in the elderly.

In addition to PWV, other indexes of arterial distensibility include augmentation index (AIx), central aortic pressure, pulse pressure and aortic pressure augmentation which are, in strict terms, indexes of pressure waveform [50]. Pulse pressure is an important predictor of coronary heart disease and, although an indirect measurement of stiffness, an increase in pulse pressure is widely recognised as a surrogate marker for central artery stiffness and has been shown to be more strongly correlated with aPWV than other BP parameters [51,52]. This was first recognised by Bramwell and Hills who noted that "... other things being equal, [pulse pressure] will vary directly as the rigidity of the arterial walls" [46]. It is now well recognised that the steep rise in pulse pressure observed after the age 50-60 years is mainly attributed to large artery stiffness [52].

1.4 Dissecting the Genetic Components of Aortic Stiffness

1.4.1 Lessons from Monogenic Aortopathies

Some of our current understanding of the pathophysiology of arterial stiffness and its genetic contribution has stemmed from rare monogenic disorders that manifest abnormalities related to the arterial wall. The identification of genes underlying these syndromic aortopathies have also led to the identification of genetic predispositions to aortic stiffness in the general population.

1.4.1.1 Marfan Syndrome

Marfan syndrome is an autosomal dominant disorder of connective tissue estimated to affect about 1 in 5,000 people worldwide [53]. The disorder is caused by mutations in the *FBN1* gene, which encodes the microfibrillar component of the ECM, fibrillin-1 [54]. Aortic root dilatation and accompanying aortic regurgitation, dissection, and rupture are the main clinical manifestations and drivers of premature death in mutant carriers. Current evidence strongly supports excess TGFβ signalling, resulting from improper matrix sequestration and trafficking of TGFβ cytokine due to fibrillin-1 deficiency, in the disease pathogenesis of Marfan subjects [54]. TGFβ up-regulation is in fact a common final process in a number of syndromic and non-syndromic large vessel diseases, including Loeys-Dietz syndrome (LDS) and thoracic aortic aneurysm and dissection (TAAD) [55]. Associations of *FBN1* common variants with arterial stiffness in the general population have not been consistent; significant associations are reported in middle-aged men [56] and in patients with coronary artery disease [57] but not in apparently healthy subjects from a wide age range [58]. Similarly, functional *TGFB1* variants failed to show any significant or consistent associations with PWV nor with other stiffness indexes [59].

1.4.1.2 William's Syndrome

William's syndrome affects about 1 in 7500 people and is caused by a microdeletion within chromosome 7 (7q11.23) harbouring the elastin gene (*ELN*) [60]. Subjects typically display cardiovascular anomalies, including elastin arteriopathy, arterial wall hypertrophy, aortic stenosis and hypertension, as well as a host of other cognitive, endocrine and growth abnormalities [61]. Deletion of the *ELN* gene results in an atypical assembly of elastic fibres within the media, and despite having a thicker intima-medial layer; cases generally exhibit abnormally low stiffness measures, which is assumed to be driven by the dedifferentiation of VSMCs [62]. Despite the central role of elastin in supporting the visco-elastic properties of the arterial wall, only a handful of studies have reported associations of *ELN* gene polymorphisms with arterial stiffness [63–65].

1.4.1.3 Ehlers Danlos Syndrome

Vascular Ehler Danlos syndrome (vEDS) is a rare autosomal dominant disorder caused by missense or exon-skipping mutations in the pro α1 (III) chain of collagen type III (*COL3A1*) with an overall incidence of approximately 1 in 5000 births [66]. The mutations result in a range of symptoms, including arterial rupture and aneurysms, gastrointestinal and pulmonary complications, stroke and sudden death [66]. Mutations in *COL3A1* disrupt the triple helical structure and assembly of the α1

chains, interrupting the synthesis and secretion of collagen fibres, therefore weakening the integrity of connective tissues [67]. Collagen makes up between 20-50% of the dry weight of the aorta and, in addition to imparting structural rigidity to the aortic wall, it is also involved in the anchorage of VSMC and in promoting their contractile phenotype [27]. At least 13 of the 28 known members of the collagen superfamily have been described in human blood vessels, with types I and III being the isoforms most prominently found in arteries [68]. The accumulation of collagen is a hallmark of the degenerative process of aortic stiffness, yet there has been little evidence for a substantial association of collagen I or III SNPs with stiffness indexes [56, 69, 70]. A single SNP within *COL4A1*, encoding the basal membrane constituent collagen type V, was identified by GWAS in the Sardinia founder population but failed to replicate in the most recent GWAS meta-analysis of cfPWV [71, 72].

1.4.2 Linkage Studies

Linkage studies into cfPWV identified several susceptibility loci across multiple chromosomal regions, with β-adducin, neurokinin-1 receptor, α-2B adrenergic receptor, interleukin-6 (*IL-6*), insulin-like growth factor-1 receptor, myocyte-specific enhancer factor 2A, chondroitin synthase and proprotein convertases as candidate genes underlying the linkage peaks [17, 70]. However, there have been limited reproducibility between populations; with the exception of *IL-6* [73], none of the putative candidate genes were independently confirmed beyond the initial reports; possibly reflecting the highly polygenic nature of aortic stiffness and highlighting the challenges in attempting to construe biological context from suggestive loci.

1.4.3 SNP Associations and Transcriptomic Profiling

1.4.3.1 Extracellular Matrix Integrity and Homeostasis

The structural changes involved in arterial stiffness (Figure 1.6) are largely driven by cellular and noncellular factors that dysregulate the structural organisation and homeostasis of the ECM. A moderate number of SNPs and transcripts pertaining to these factors have been identified and can be categorised into genes that encode structural components of the ECM and alter their degradation (mainly MMPs), genes of the inflammatory pathway, and genes that promote aortic medial calcification.

1.4.3.1.1 Structural Elements

Microarray-based gene expression profiling of human aorta by Durier and colleagues [75] identified a wide range of genes that were differentially expressed between stiff and distensible aortas.

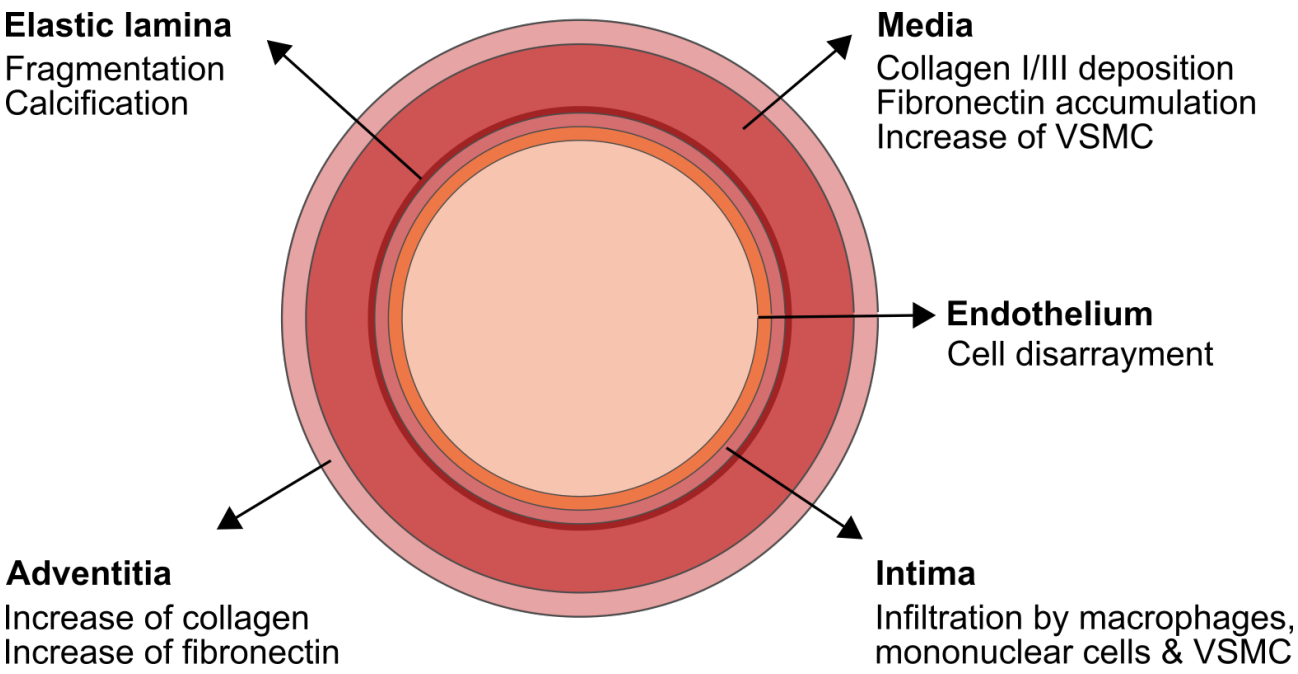

Figure 1.6: Morphological alterations in a stiffened artery. Image modified from Diez [74].

A significant proportion of the differentially expressed transcripts belonged to genes that regulate signalling, communication and transcription, as well as genes that mechanically regulate vascular function. Amongst the latter class were transcripts from the proteoglycan family (decorin, osteomodulin, aggrecan-1 and chondroitin sulphate proteoglycan-5) that impart structural organisation to the ECM and also regulate cellular migration and proliferation. A recent quantitative proteomic investigation in mammary arteries from nonatherosclerotic subjects corroborated these findings by demonstrating a significant down-regulation in the protein levels of proteoglycans in subjects with stiff arteries [76].

1.4.3.1.2 Matrix Metalloproteinases

MMPs are a group of proteolytic enzymes that have the capacity to catalyse the normal turnover of the ECM and also degrade its structural components [34]. The balance between matrix protein synthesis and degradation is tightly controlled by their endogenous inhibitors; as arteries age or undergo pathological changes, this balance is lost and MMP enzyme activity increases. MMP activity may also be augmented by other factors that are perturbed in a stiffened artery, including pro-inflammatory cytokines, endothelial dysfunction and enhanced renin-angiotensin aldosterone system (RAAS) activity [34]. Increased serum concentrations of MMP2 and MMP9 hence correlate strongly with arterial stiffness in healthy individuals and in isolated systolic hypertensives [77]. Several *MMP3* and *MMP9* functional polymorphisms have been found to associate with PWV in

healthy individuals, and in subjects with hypertension, isolated systolic hypertension and coronary artery disease [78–81].

1.4.3.1.3 The Inflammatory Pathway

Mechanical fatiguing of the aorta is suggested to promote a state of chronic, low profile inflammation that is characterised by a global profile of up-regulated inflammatory molecules, most notably TNF-α, TGF-β1, NFκB and monocyte chemoattractant protein (MCP-1) [82]. This pro-inflammatory state is initiated by a complex network of signalling cascades which is primarily driven by RAAS as illustrated in Figure 1.7.

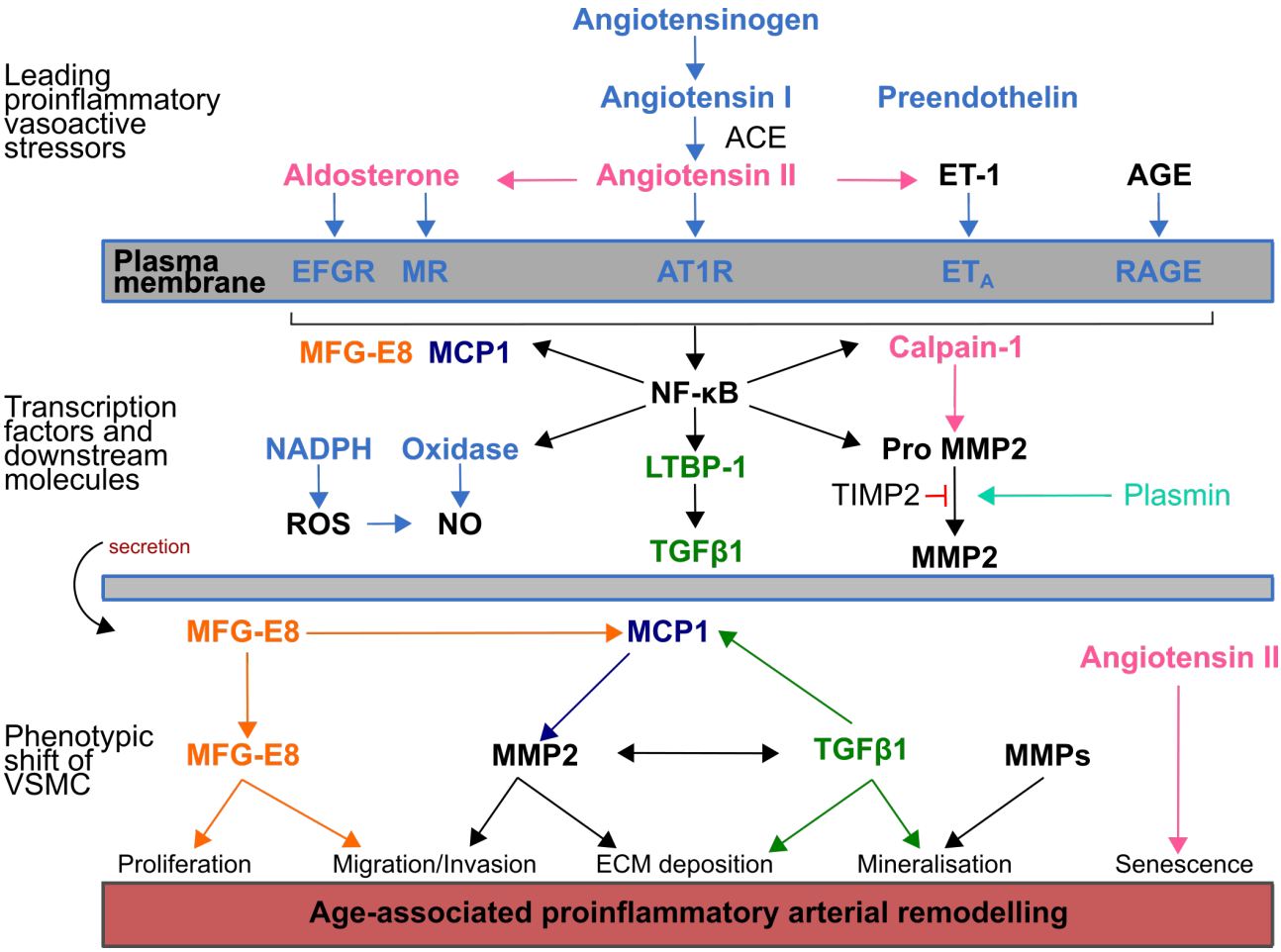

Figure 1.7: Cross-talk of signalling pathways involved in promoting proinflammatory arterial remodelling. ACE; angiotensin converting enzyme, AT1R; angiotensin II type 1 receptor, AGE; advanced glycation end products, ET-1; endothelin-1, ET$_A$; endothelin-1 receptor A, LTBP-1; latent-TGFβ-binding protein-1, MCP-1; monocyte chemoattractant protein-1, MFG-E8; milk fat globule epidermal growth factor-8, MR; aldosterone/mineralocorticoid receptor, RAGE; receptor for AGE, ROS; reactive oxygen species. Image modified from Wang et al. [83].

C-reactive protein (CRP) is an independent and important predictor of PWV and remains a strong predictor of current PWV over a 20 year follow up, highlighting the important role of low grade

inflammation in the pathogenesis and progression aortic stiffness [84]. Polymorphisms within *CRP* itself have not been found to associate with aortic PWV [85]. However, significant associations with PWV have been documented within several other inflammatory molecules and biomarkers, including the vascular and intercellular adhesion molecules (*VCAM1* and *ICAM1*, respectively), P-selectin and TNF receptor superfamily member 6 (*FAS*) [86,87]. Finally, the most recent GWAS meta-analysis in the *AortaGen Consortium* identified several genetic variants on chromosome 14 that strongly associated with cfPWV [72]. The locus lies in a gene desert that contains no annotated genes but is known to harbour gene regulatory elements and is flanked at its telomeric end by *BCL11B*, the most plausible candidate in the region [72, 88]. This is a transcription factor that regulates important aspects of the development and function of T lymphocytes and other immune cells, suggesting the association maybe driven by inflammatory mechanisms [89]. However, the biological significance of the GWAS signal remains unexplored.

1.4.3.1.4 Calcification

Aortic medial calcification is a hallmark of age-related ECM remodelling, and correlates strongly with PWV in the general population, in patients with end-stage renal dysfunction and independently of markers of atherosclerosis [18, 90, 91]. Several factors are believed to promote medial elastocalcinosis, amongst those is the transdifferentiation of VSMC into a mineralising form (*chondro-ossification*) and the induction of signalling pathways that accelerate calcium accumulation and down-regulate calcification inhibitors (e.g. osteopontin and osteonectin) [35]. Polymorphisms within several genes involved in calcium regulation have shown significant associations with PWV; these include *ATP2B1* (which encodes the calcium transporting ATPase 1), fetuin-A (an inhibitor of calcium-phosphate precipitation) and *ENPP1* (which encodes ectonucleotide pyrophosphatase / phosphodiesterase -1, a regulator of pyrophosphate and an inhibitor of calcification) [92–94]. Transcript abundance of *NPP1* in lymphoblastoid cell lines of subjects from the Twins UK Cohort was recently shown to correlate strongly with PWV and its progression over a 4 year follow-up period [95]. The same study identified *CTNNB1* as a common transcriptional regulator of *COL4A1* and *ENPP1* by network analysis, and osteopontin as a downstream effector of *ENPP1*. Taken together, the authors suggest COL4A1 to act in concert with ENPP1 in promoting arterial stiffness and, in addition to its role in calcification, propose ENPP1 to act via osteopontin in promoting further ECM remodelling by activating MMP2 and MMP9. This is supported by earlier observations of a strong correlation between enhanced transcription and enzymatic activity of MMP2 and MMP9 and elastin calcification [96]. Finally, a SNP in the calcium and integrin-binding protein-2 (*CIB2*), a regulator of intracellular calcium

levels, was identified also in the Twins UK Cohort [97]. The study utilised an integrated multi-'omics' approach, incorporating genomic, methylomic and transcriptomic profiling thus allowing for a biological interpretation of the data. The SNP from this study correlated with PWV and with increased transcription but reduced methylation of *CIBT* and was therefore suggested to alter the extent of vascular calcification amongst carriers of the minor allele.

1.4.3.2 Blood Pressure Regulation

Blood pressure is widely recognised as a key contributor of PWV and arterial wall remodelling; conversely, arterial distensibility is an early predictor of hypertension development in the general population, and is increasingly acknowledged as a potential therapeutic target for hypertension [5, 39, 98–100]. The bidirectional relationship between arterial stiffness and blood pressure has thus posed an ongoing debate in attempting to ascertain which of the two factors precedes the other [101]. It is therefore not surprising that genetic variants within systems that regulate blood pressure have been found to associate with aortic stiffness.

1.4.3.2.1 The Renin-Angiotensin Aldosterone System

The RAAS is largely known for its regulation of blood pressure and electrolyte homeostasis. Mounting evidence also supports its role in the functional and structural changes associated with arterial stiffness [102]. Inappropriate activation of RAAS leads to changes in NADPH oxidase activity, nitric oxide (NO) bioavailability and levels of reactive oxygen (ROS) species, and also activates a range of cytokines including TNF-α and interleukins 1, 6 and 17 (Figure 1.7) [34]. Moreover, angiotensin II is associated with increased MMP2/9 activity, it induces TGFβ signalling, enhances collagen accumulation and promotes VSMC proliferation and differentiation [103]. The stimulation of ROS by angiotensin II, together with the initiation of an inflammatory cascade, promotes endothelial dysfunction and atherosclerosis, therefore contributing to the progression of arterial remodelling and stiffness [104]. Aldosterone is similarly suggested to regulate the structure and function of the arterial wall by altering endothelial function, VSMC proliferation and collagen turnover [105]. A moderate number of functional polymorphisms within various components of the RAAS have shown significant associations with arterial stiffness across a range of populations in both healthy and hypertensive subjects. These include variants within angiotensinogen (*AGT*), angiotensin-converting enzyme (*ACE*), angiotensin II type 1 receptor (AT_1R) and aldosterone synthase (*CYP11B2*) [106–113]. Notwithstanding, RAAS polymorphisms associated only weakly with arterial stiffness in the Framingham Heart Study 100K Project, and none appeared in the top hits of the GWAS by Tarasov et al.

or in the GWAS meta-analysis, nor did components of the RAAS pathway appear within linkage peaks (with the exception of *CYP11B*) [70–72].

1.4.3.2.2 The Endothelium

The role of the endothelium in arterial wall mechanics is demonstrated by the observation of decreased index following endothelial removal [114]. Stiffening of the large artery is thus partly modulated by endothelium-derived vasoactive mediators such as NO and endothelin (ET-1) [115]. Endothelial NO is potent vasodilator and regulator of vascular function, and is involved in regulating VSMC proliferation, platelet stimulation and leukocyte adhesion [116]. Arterial stiffness indexes have been shown to decrease with local intra-arterial adiministration of NO-inducing drugs (glyceryl nitrite) and increase with NO-inhibiting drugs (L-NMMA), lending evidence to a role for this pathway in arterial stiffness mechanisms [117]. Variants within the NO synthase gene (*NOS3*) have been associated with arterial stiffness measures in the general population, in hypertensives and in diabetics [116, 118–122].

Endothelin is a potent vasoconstrictor which, together with its two VSMC receptors ETAR and ETBR, is involved in modulating vascular tone and vascular wall remodelling [123]. Experimental evidence supports an interaction between elements of the RAAS and ET-1 pathways [124]. In addition to their blood pressure lowering effects, ETAR antagonists have been shown to lower PWV in animals and in patients with chronic kidney disease presenting a potential therapeutic target for arterial stiffness [125]. Several studies have also supported an associations of genetic variants within the ET-1 system with arterial stiffness [123, 126].

1.4.3.2.3 The Sympathetic Nervous System

Arterial wall properties are thought to be affected by the level of sympathetic nervous activity [127]. This is supported by observations of increased radial and femoral artery distensibility following the depletion of adrenergic tone, decreased compliance of the radial artery following short-term sympathetic activation and also by evidence that tachycardia, a well-recognised sign of increased sympathetic activity, is a determinant of PWV [127]. Possible mechanisms suggested to underlie these observations include a direct effect on vasomotor tone, enhanced endothelial dysfunction, structural changes to the arterial wall and RAAS related mechanisms [127]. Genetic variants within three beta adrenergic receptors (*ADRB1*, *ADRB2*, *ADRB3*) associate with arterial stiffness independently of BP effects [128].

1.4.4 Potential For Therapeutic Intervention

Favourable interventional effects on arterial stiffness and wave reflection are supported by a growing body of evidence. Pharmacological treatments that have been reported to reduce stiffness include antihypertensive drugs (diuretics, beta blockers, ACE inhibitors, AT1 inhibitors and calcium channel blockers), nitrates, statins, antidiabetic agents, advanced-glycation end products (AGE) breakers and anti-inflammatory drugs [129]. While O'Rourke et al. argue that the direct pharmacological treatment of arterial stiffness to restore its elasticity is "impossible" [50,130], AGE breakers- which act by targeting AGE cross linked elastin and collagen and represent a class of drugs with direct actions on the arterial wall- have been shown to improve vascular compliance and reduce pulse pressure [131]. Moreover, aortic remodelling in mice models of Marfan syndrome was shown to be preventable by the blockade of NFκB; thus Boutouyrie et al. reason that direct de-stiffening of the arterial wall can be achieved with the identification of druggable targets and pathways [100].

Many studies have reported the effects of antihypertensive treatments on arterial stiffness, with drugs targeting the RAAS appearing to be more effective at reducing stiffness than other classes [132]. The reduction in arterial stiffness observed with antihypertensive treatments could, in part, be explained by the fact that PWV and other measurements of stiffness are dependent on BP levels; hence a decrease in BP, in theory, will associate with a decrease in PWV [133]. Assessment of arterial stiffness with BP lowering drugs in the longer run can reveal whether the improved outcome is solely due to changes occurring with decreased BP such as improved endothelial function and reduced distension pressure, or that these drugs confer additional mechanisms involving geometric and structural changes to the arterial wall [133]. Data from a 5.3 year follow up of antihypertensive treatment showed that PWV reduction continued beyond the initial phase of BP control even with the limited BP reduction, indicating that this might indeed be the case [134]; similar conclusions have been drawn from a meta-analysis involving short and long term treatments with antihypertensive drugs [135]. Moreover, the de-stiffening potency is not similar across antihypertensive drugs, further suggesting that the effect of these in reducing stiffness is beyond mere control of BP [135,136]. Drugs targeting the RAAS in particular appear to improve arterial compliance independent of BP lowering effects, presumably by modulating arterial wall collagen content, reversing SMC hypertrophy and reducing wall thickness [137]. This is supported by observations from animal studies of SHR rats receiving either ACE inhibitor or AT1 receptor blocker in combination with a normal sodium diet, where a reduction in BP was accompanied by a decrease in aortic collagen content and an improved arterial distensibility [133].

Therapeutic interventions targeting wave reflection by nitrates, angiotensin receptor blockers, calcium channel blockers and ACE inhibitors have also been proposed and are considered to be superior to BP reducing strategies [130]. The principle behind this approach is that dilation of muscular arteries, which make up the bulk of the arterial tree, by these agents "traps" the reflected wave in small peripheral arteries, preventing it from returning to the heart ultimately leading to a marked reduction in the scale of the reflected wave [130]. The long-term benefits of using nitrates for arterial stiffness are unknown and possibly limited given the problem of nitrate tachyphylaxis [130].

In view of the role of inflammation in remodelling of the aorta, anti-inflammatory drugs have also been suggested to improve arterial stiffness. Antibodies against TNF-α have shown improvements in stiffness in patients with inflammatory conditions [138]. In the same context, statins have been shown to improve stiffness measures in rheumatoid arthritis patients and prevent inflammation induced aortic stiffness [132]. It is recognised that statins protective effects on the CV system is not only accounted for by its lipid lowering effect but also by their "pleiotropic effects," including anti-inflammation, anti-oxidative stress and enhancement of endothelial function [139] which could account for their favourable effects on the aortic wall. For example, the administration of low dose atorvastatin appears to protect against arterial stiffness in diabetes-induced rats independently of its lipid-lowering effects [139], and improve stiffness measures in hypertensive and hyperlipidemic patients [140]. The exact mechanisms by which statins might confer protective effects on the arterial wall are not fully understood but data from animal studies indicate that atorvastatin prevents a number of angiotensin-II dependent modifications to the structure and function of the arterial wall. These include the reversal of angiotensin-II induced stiffness and oxidative stress, inhibition of angiotensin-II induced collagen accumulation and inhibition of intracellular signalling pathways that promote vascular fibrosis [141]. The stiffness reducing effect of statins remain inconclusive, with conflicting data suggesting increased PWV with their use and others reporting no significant changes [140].

In summary, it is evident that arterial stiffness can be modulated pharmacologically. Better elucidation of the mechanisms that drive the stiffening process will help to generate therapeutic targets that reverse or slow the impact of ageing on aortic function.

1.5 Aim and Objectives

Background: Aortic stiffness is an important predictor of cardiovascular endpoints. Like many cardiovascular traits, it has a multi-factorial aetiology and is moderately heritable and genetically complex. Despite over a decade of investigations, progress has been challenged by the lack of reproducibility and complexities of translating genetic markers and susceptibility loci into meaningful biological pathways. The precise genetic mechanisms that regulate the process of aortic stiffening therefore remain largely unknown.

Aim: Expand on the existing knowledge of the genetic landscape that governs the complex trait of large artery stiffening.

Objectives:

1. Examine the molecular basis of the hereditary large vessel disease, Loeys-Dietz type 4, in a pedigree with multiple cases of aortic aneurysms and dissections and ascertain its downstream effect on aortic TGFβ signalling.

2. Investigate the biological context of the GWAS signal identified in the *AortaGen Consortium* by characterising the impact of the lead SNPs on the putative targets (*BCL11B* and DB129663) and on *ex vivo* PWV in a repository of human donor aortas.

3. Validate significant SNP associations that had been previously identified in the ENIGMA cohort using a candidate gene approach [Publication 3] and investigate the expression patterns of the genes containing these SNPs (*ACAN* and *FBLN1*) and their encoded proteins in human donor aortas.

2

General Experimental Methodology

2.1 Study Samples

Aortic tissue samples (n=226) were harvested from organ donors via transplant coordinators at Addenbrooke's Hospital, Cambridge, UK. Fresh thoracic, abdominal and iliac arteries were collected and preserved in tissue medium at the time of organ donation. Tissues were cleared of blood vessels, adipose tissues and other residues, and then stored at -80°C. If sufficient tissue had been collected, 2 cm rings were excised for biophysical measurements and small sections were preserved in RNA*later*® stabilisation solution in preparation for RNA extraction. For a subset of the samples collected, patches of the tissues were fixed in 4% paraformaldehyde for immunochemical analyses. Section embedding and cutting was performed by Nickolas Figg (University of Cambridge, UK).

Demographic data, anthropometric information, biochemical and haemodynamic measurements, medical and drug history (past and at the time of death), cause of death, and other details that may have affected aortic stiffness were recorded. All samples and donor data were handled in accordance with the policies and procedures of the Human Tissue Act (UK), and the study was approved by both the local and regional ethics committees. Samples were collected by Yasmin (University of Cambridge, UK) and Sarah Cleary (University of Cambridge, UK).

2.2 Biomechanical Measurements

The aortic ring diameter and wall thickness were measured using digital callipers and the mean reading from three different locations was recorded. Young's modulus (EM) was derived from stress-strain data measured using an Instron 5542 tensile test machine (Instron Corp., USA) controlled by Bluehill (version 2) software. Each ring was cycled five times in the range of 0-180 mmHg at a constant rate of 10 mm/min. The EM at a load of 100 mmHg, which represents physiological

pressure conditions, was used to calculate the pulse wave velocity (PWV^{MK}) for each aorta using the Moens-Kortweg (MK) equation:

$$PWV^{\mathrm{MK}} = \sqrt{\times EM\frac{h}{2r\rho}} \tag{2.1}$$

where h is the wall thickness, r the arterial radius and ρ is blood density, which was taken to be 1.05 g/cm^3. The MK equation assumes an infinitely long and straight tube with homogenous elasticity and geometry [142]. Given the inhomogeneous nature of the arterial wall, identifying an h measure that best represents the portion of the arterial wall which contributes most to its stiffness is an obvious challenge. Nonetheless, the qualitative relationship between PWV derived using the MK equation and stiffness has been shown to be valid and is widely adopted in a variety of settings for arterial stiffness estimation [143]. Measurements were carried out by Ashraf Khir (Brunel University, Uxbridge, UK) and Ye Li (Brunel University, Uxbridge, UK).

2.3 DNA Extraction, Quantification and Quality Control

Genomic DNA was isolated from 25 mg of thawed aortic tissue, which was mechanically disrupted in lysis buffer using a TissueLyser LT (QIAGEN, Germany) and 30 oscillations for 2 min intervals to avoid overheating the sample. Complete tissue lysis was achieved following overnight incubation in proteinase K at 56°C. DNA was extracted using a QIAamp DNA Mini Kit (QIAGEN, Germany) and DNA quantity and purity was determined using a NanoDrop spectrophotometer (ND1000, USA). A 260/280 nm absorbance ratio of 1.7-1.9 was deemed suitable for downstream applications.

2.4 Single Nucleotide Polymorphism Genotyping

SNPs were genotyped using TaqMan® SNP genotyping assays (ThermoFisher Scientific, USA). A total of 20 ng DNA was amplified in a final reaction volume of 20 µl per well containing 7.5µl TaqMan® Genotyping Master Mix (ThermoFisher Scientific, USA), 1 µl SNP assay and 3.5 µl sterile, double filtered water. The polymerase chain reaction (PCR) thermal cycling conditions involved an initial denaturation step at 95°C for 10 min, followed by 40 cycles of 92°C for 15 s followed by 60°C for 1 min. Allelic discrimination was carried out using an ABI 7500 Detection System (ThermoFisher Scientific, USA).

2.5 Gene Expression Workflow

2.5.1 Reverse Transcription

Three reverse-transcription systems were compared: avian myeloblastosis virus (AMV) reverse transcriptase (Promega, USA), moloney murine leukaemia virus (MMLV) reverse transcriptase GoScript™ (Promega, USA), and genetically enhanced-MMLV reverse transcriptase SuperScript®IV (ThermoFisher Scientific, USA) as detailed below. Following cDNA synthesis, complementary RNA was removed by incubating the samples with 2 U/µl of E. coli RNase H (ThermoFisher Scientific, USA) at 37°C for 20 min. Samples were then stored at -20°C until further analysis.

2.5.1.1 AMV Reverse Transcription

Reverse transcription reactions were performed using 1 µg of total RNA primed with 0.5 µg hexamer oligonucleotides and hybridised at 70°C for 5 min followed by immediately chilling on ice for a further 5 min. The reverse transcription reaction comprised of 5 mM $MgCl_2$, 0.5 mM dNTP mix, 1× reverse transcription buffer, 20 U recombinant RNasin® ribonuclease inhibitor, and 15 U avian myeloblastosis virus (AMV) reverse transcriptase in a final volume of 20 µl. The PCR thermal conditions consisted of an initial annealing step at 22°C for 15 min, followed by extension at 42°C for 1 h, then AMV transcriptase inactivation at 95°C for 5 min, followed by 4°C for 5 min.

2.5.1.2 GoScript™ Reverse Transcription

Reverse transcription reactions were performed using 1 µg of total RNA primed with 0.5 µg hexamer oligonucleotides and hybridised at 70°C for 5 min following by immediately chilling on ice for a further 5 min. The reverse transcription reaction comprised of 5 mM of $MgCl_2$, 0.5 mM dNTP mix, 1× GoScript™ reaction buffer, 20 U recombinant RNasin® ribonuclease inhibitor, and 160 U GoScript™ reverse transcriptase in a final volume of 20 µl. The PCR thermal conditions consisted of an initial annealing step at 25°C for 5 min, followed by extension at 42°C for 1 h, then reverse transcriptase inactivation at 70°C for 5 min.

2.5.1.3 SuperScript®IV Reverse Transcription

Reverse transcription reactions were performed using 1 µg of total RNA primed with 0.5 µg hexamer oligonucleotides and denatured at 65°C for 5 min with 0.5 mM dNTP mix followed by immediately chilling on ice for 1 min. The cDNA synthesis mix comprised of 5 mM $MgCl_2$, 5 mM DTT, 1× SuperScript®IV buffer, 40 U RNaseOUT™ and 200 U of SuperScript®IV reverse transcriptase in a

final volume of 20 µl. The PCR thermal conditions consisted of an initial annealing step at 23°C for 10 min, followed by extension at 50°C for 10 min, then reverse transcriptase inactivation at 80°C for 10 min.

2.5.2 Assessment of Reverse Transcription Linearity

The efficiency of the reverse transcription step, which is significantly dependent on the choice of reverse transcriptase and RNA concentration, is an essential prerequisite for valid and reproducible quantitative PCR (qPCR) results [144]. In order to compare the linear range of the three reverse transcription systems, cDNA was prepared using each of the transcriptases for serially diluted RNA ranging from 1 µg to 10 ng, which was then used as the template in real-time PCR reactions using TaqMan® gene expression assays and Master Mix (ThermoFisher Scientific, USA). All reactions were performed in duplicate, and for each transcriptase the mean Ct values were plotted against the logarithm of the RNA mass and the correlation coefficient (R^2) of the curve was used as a measure of the linearity of the qPCR reaction.

The AMV enzyme system was found to be the least successful of the three methods assessed, demonstrating poor linearity of the standard curve (R^2= 0.30) compared to R^2= 0.98 for GoScript and R^2= 0.97 for Superscript IV (Figure 2.1). As a correlation coefficient of ≥0.98 is recommended for reliable gene expression quantification [145], the GoScript reverse transcription system was selected for reverse transcription of aortic RNA.

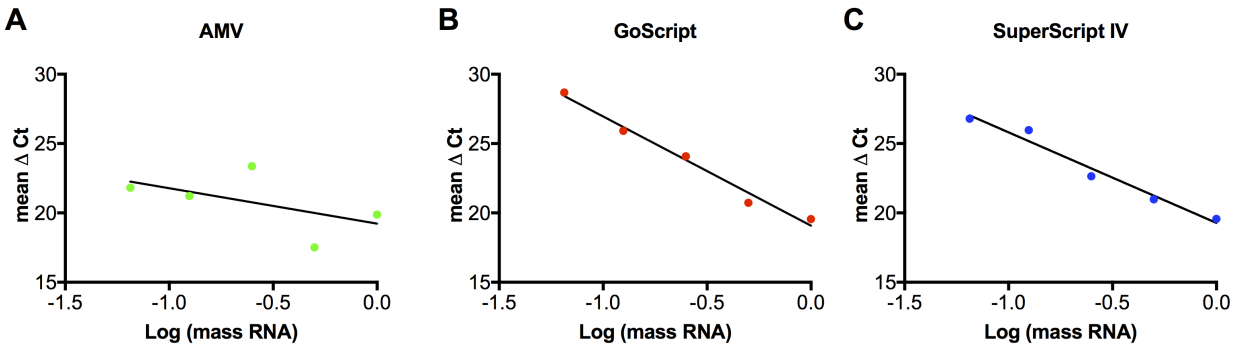

Figure 2.1: Comparison of the linearity of three reverse transcription systems. (A) AMV transcriptase displayed inferior linearity (R^2= 0.30) compared to the two MMLV transcriptases (B) and (C) which displayed linearity values of 0.98 and 0.97, respectively.

2.5.3 Real-Time Quantitative Polymerase Chain Reaction

RT-qPCR reactions were performed using TaqMan® chemistry, and each qPCR reaction comprised of 1.5 µl stock cDNA, 1 × TaqMan® gene expression assay (ThermoFisher Scientific, USA), 1× TaqMan®

Fast Advanced master mix (ThermoFisher Scientific, USA) and nuclease-free water (Promega, USA) to make a total volume of 15 µl. The thermal cycling conditions consisted of an initial 2 min incubation step at 50°C, followed by polymerase activation at 95°C for 20 s then 40 cycles of denaturation for 3 s at 95°C and annealing/extension for 30 s at 60°C. All samples were run in duplicate with a negative control included for each assay. Fluorescent signals were detected using an ABI 7500 Real Time PCR System (ThermoFisher Scientific, USA). Fold-differences in gene expression were calculated using the $2^{-\Delta Ct}$ method [146], where:

$$\Delta Ct = target\ gene\ Ct - reference\ gene\ Ct \tag{2.2}$$

and Ct is the threshold cycle generated by the ABI system.

2.5.4 Selection of a Reference Housekeeping Gene

The expression stability of six housekeeping genes (Table 2.1) was assessed using a geNorm kit (Primer Design, UK). Genes were selected from a panel of twelve commonly used reference genes from various functional groups. Twelve aortic tissue samples were selected for this validation process; six from each end of the PWV spectrum. The software qBase+ was used to rank the reference genes for stability of expression across the samples. This software assigns a stability value (M) for each reference gene by calculating the average pairwise variation of each gene and all other reference genes included in the test run. The software also determines the optimal number of reference genes required for accurate normalisation based on pairwise variation (V), starting with the most stably expressed reference gene and sequentially adding genes until a cut off geNorm V value of <0.15 is reached [147].

Table 2.1: Selection of reference genes included in the geNorm pilot study

Gene	Symbol
18S Ribosomal RNA	*18S*
ATP Synthase, H+ Transporting, Mitochondrial F1 Complex, Beta Polypeptide	*ATP5B*
Beta-Actin	*ACTB*
B-2-Microglobulin	*B2M*
Glyceraldehyde 3-Phosphate Dehydrogenase	*GAPDH*
Phospholipase A2	*YWHAZ*

As expected, transcript levels of the six reference genes varied, and the geNorm analysis identified that *GAPDH*, *ATP5B* and *ACTB* were the most stable reference genes for the twelve aortic samples,

while *18S* and *B2M* were the least stable (Figure 2.2A). The optimal number of reference genes determined by the geNorm algorithm was two, with the recommended combination being *GAPDH* and *ATP5B* (Figure 2.2B). The successive inclusion of additional genes was not found to confer any additional value for accurate normalisation (Figure 2.2B).

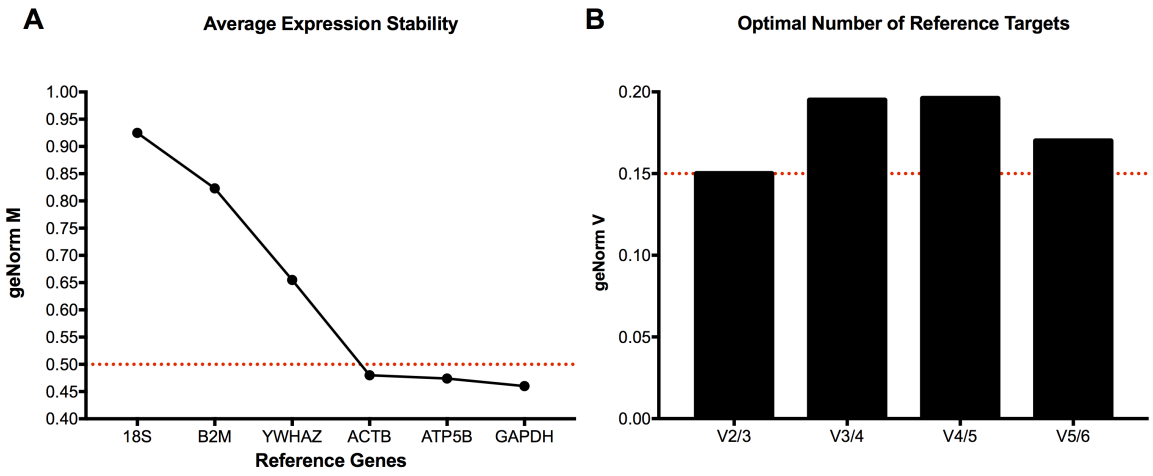

Figure 2.2: geNorm expression stability plots of six housekeeping genes. (A) Average expression stability of six candidate reference control genes in donor aortic samples (n=12). Genes with the lowest M values have the most stable expression. (B) Optimal number of reference genes. A V value with the recommended cut-off of 0.15 can be attained using two reference genes.

The findings from the geNorm analysis were then validated using a larger cohort of randomly selected aortic samples (n=20). The results of this validation experiment showed stable coefficient of variation (CV) and M values for *GAPDH* (mean CV=0.25, mean M=0.48), whereas there were large variations across the samples for *ATP5B* and *ACTB* (mean CV=0.76, mean M=3.2 and mean CV=0.98, mean M=3.95, respectively). As these values were above the acceptable stability values for heterogeneous samples (CV<0.5 and M<1), *ATP5B* and *ACTB* were excluded from the choice of valid reference genes. *GAPDH* was subsequently selected as the primary housekeeping gene suitable for qPCR normalisation for the aortic tissue samples.

2.5.5 Assessment of qPCR Amplification Efficiency

As the amplification efficiencies of the target and reference genes need to be comparable for valid quantitation using the $2^{-\Delta Ct}$ method [146], the efficiency of the gene expression assays was estimated using a 6-log dilution range of cDNA from three randomly selected aortic samples. Mean Ct values were plotted against the logarithm of the cDNA dilution factor and the assay efficiency was

determined using the equation:

$$E = [10^{1/-slope} - 1] \times 100 \tag{2.3}$$

All the assays tested exhibited comparable efficiencies (Table 2.2) and showed efficiencies within the acceptable range of 90-110%; therefore they were deemed suitable for quantitative gene expression analyses.

Table 2.2: Efficiency values of gene expression assays

Gene	Symbol	Assay ID	Efficiency (%)
B-Cell Lymphoma/11B	*BCL11B*	Hs01102259_m1	105.6
Protein Tyrosine Phosphatase, Receptor Type C	*CD45*	Hs04189704_m1	103.1
Interferon Stimulated Exonuclease Gene 20	*CD25*	Hs00907778_m1	104.7
CD8a Molecule	*CD8A*	Hs00233520_m1	102.5
Glycophorin A	*CD235A*	Hs01068072_m1	106.6
Aggrecan	*ACAN*	Hs00153936_m1	106.3
Fibulin 1	*FBLN1*	Hs00972609_m1	103.4
Glyceraldehyde 3-Phosphate Dehydrogenase	*GAPDH*	4326317E	101.2

2.6 Protein Extraction and Quantification

Cytoplasmic and nuclear protein fractions were extracted from 10 mg thawed aortic tissue using NE-PER™ nuclear and cytoplasmic extraction reagents (ThermoFisher Scientific, USA). Tissues were first rinsed in cold phosphate buffered saline (PBS) then pulverised on a pre-chilled petri dish. Samples were re-suspended in 100 µl cytoplasmic extraction reagent I (CERI) containing protease and phosphatase inhibitor cocktails (Calchem), before homogenisation using a TissueLyser LT (QIAGEN, Germany) at 30 oscillations for 2 min intervals until complete disintegration. The homogenate was incubated on ice for 10 min before adding 5.5 µl ice-cold cytoplasmic extraction reagent II (CERII) and incubating on ice for a further 1 min. The homogenate was subjected to centrifugation at 16,000 $\times$ g for 10 min and the supernatant, which contained the cytoplasmic fraction, was then stored at -80°C for later use. The pellet, containing the nuclei, was suspended in 50 µl ice-cold nuclear extraction reagent (NER) and vortexed every 10 min for a total of 40 min whilst being kept on ice throughout. The lysate was then subjected to centrifugation at 16,000 $\times$ g for 15 min and the supernatant containing the nuclear extract was stored at -80°C for later use. All protein extraction steps were carried out at 4°C. Protein was quantified using a bicinchoninic acid (BCA) assay (ThermoFisher Scientific, USA) and absorbance at 562 nm was measured using a Titertek Multiskan® Plus MKII plate reader.

2.7 Western Blotting

Protein lysates were incubated at 70°C for 10 min in lodium dodecyl sulphate (LDS) sample loading buffer (ThermoFisher Scientific, USA) and Bolt® sample reducing agent (ThermoFisher Scientific, USA). All Western blots were performed under reducing conditions unless otherwise stated. Proteins were separated by SDS-gel electrophoresis using 4-12% gradient Bis-Tris Plus Bolt® gels (ThermoFisher Scientific, USA) at 200 V for 30 min and then transferred to a 0.22 µM nitrocellulose membrane (ThermoFisher Scientific, USA) using an iBlot2 dry blotting system (ThermoFisher Scientific, USA) at 20 V for 7 min. Prior to transfer gels were equilibrated for 5 min in NuPage® transfer buffer (ThermoFisher Scientific, USA) containing 10% methanol. Membranes were blocked with 5% milk in tris-buffered saline (TBS) for 1 h at room temperature then incubated with primary antibodies in TBS-Tween (0.1% Tween 20) containing 5% milk for 16 h at 4°C. Membranes were washed in 3×TBS-Tween for 15 min before being incubated with secondary antibodies in TBS-Tween for 1 h at room temperature in the dark. The wash step was then repeated before visualisation of the protein bands which were detected using a LI-COR Odessey system and quantified using ImageStudioLite software.

2.8 Immunohistochemical Staining

Immunohistochemical (IHC) staining was performed on formalin-fixed, paraffin-embedded samples (FFPE). Sections (4 µm) were deparaffinised in Histo-Clear (National Diagnostics, USA) then dehydrated via submersion in graduated alcohols. Antigen retrieval was performed in either pH6 citrate buffer (Vector Laboratories, UK) or R-Universal epitope recovery buffer (Aptum Biologics Ltd, UK) using a 2100 Retriever pressure steamer (Aptum Biologics Ltd, UK). Tissue endogenous peroxidase activity was quenched by incubating the samples in 0.3% hydrogen peroxide (Sigma-Aldrich, USA) in 100% methanol for 15 min. A titration experiment was initially conducted to determine the optimal antibody concentration, and wherever possible a positive control tissue known to express the protein of interest was used during the optimisation step. All incubation steps were carried out in humidified chambers, and immunostaining experiments included a negative (no primary antibody) control. Three methods of target antigen amplification were used in this study; peroxidase anti peroxidase (PAP), horseradish peroxidase (HRP) labelled polymer, and avidin-biotin complex (ABC) methods (Sections 2.8.1-2.8.3).

Following chromogenic detection, sections were counterstained with Mayers haematoxylin (Sigma-

Aldrich, USA), rehydrated via submersion in graduated alcohols, cleared in Histo-Clear (National Diagnostics, USA) and then mounted using Histomount (National Diagnostics, USA). Fiji analysis software was used to adjust the image brightness and contrast for enhanced visibility, and images presented within each figure panel were processed in parallel.

2.8.1 Peroxidase Anti-Peroxidase Method

The PAP method (Figure 2.3A) utilises horseradish peroxidase and an immunological sandwich amplification to produce a signal. The PAP immune complex, composed of three peroxidase enzyme molecules and two anti-peroxidase IgG molecules, binds to the secondary antibody, thus linking it to the primary antibody which recognises the antigen of interest [148]. After quenching endogenous peroxidase activity, sections were blocked with 5% goat serum in PBS for 2 h at room temperature before being probed with the primary antibody for 16 h at $4°C$ in 3% goat serum in 0.1% Tween-20–PBS. This was followed by three 5 min washes in 0.1% Tween-20–PBS, before incubating the sections in the appropriate secondary antibody (goat anti-rabbit or goat anti-mouse) at a 1:100 dilution in 3% goat serum in 0.1% Tween-20–PBS for 1 h at room temperature, again followed by three 5 min washes in 0.1% Tween-20–PBS. The sections were then incubated in rabbit or mouse PAP complex at a 1:200 dilution in 3% goat serum in 0.1% Tween-20–PBS for 1 h at room temperature, followed by three 5 min washes in 0.1% Tween-20–PBS. For chromogenic detection, sections were incubated in 0.6 mg/mL of 3,3'-diaminobenzidine tetra-hydrochloride (DAB) in 0.05 M Tris-HCl buffer (pH 7.6) containing 0.03% hydrogen peroxide for 5-10 min. The reaction was quenched by immersion in deionised water. Sections were counterstained with haematoxylin, rehydrated, cleared and mounted as described earlier.

2.8.2 HRP Labelled Polymer Method

The HRP labelled polymer method utilises an enzyme-conjugated polymer backbone that carries multiple secondary antibody and HRP sites (Figure 2.3B), thus allowing for enhanced signal amplification which is particularly advantageous for antigens with low tissue expression. Following antigen retrieval, sections were blocked in Dual Enzyme Blocker solution (Dako, UK) for 30 min followed by three 5 min washes in 0.1% Tween-20–TBS and then probed with the primary antibody diluted in antibody diluent solution (Dako, UK) for 30 min at room temperature. This was followed by three 15 min washes in 0.1% Tween-20–TBS then incubation in the labelled secondary polymer (Dako, UK) for 30 min at room temperature. The washing step was repeated before the sections were incubated in DAB diluted in substrate buffer (pH 7.5) containing hydrogen peroxide until the

desired staining was achieved. The reaction was quenched in deionised water and sections were counterstained with haematoxylin, rehydrated, cleared and mounted as described earlier.

2.8.3 Avidin-Biotin Complex Method

The ABC method (Figure 2.3C) exploits the high affinity properties of avidin and biotin to enhance the resolution and sensitivity of chromogenic detection [149]. Using this method, biotinylated HRP irreversibly complexes with avidin in solution to form the ABC complex, which is then introduced to a biotinylated secondary antibody. Peroxidase activity was quenched as previously described and the sections blocked in 5% goat serum in PBS for 30 min at room temperature before probing with the primary antibody for 30 min at room temperature in 2.5% goat serum in 0.1% Tween-20–PBS. This was followed by a 5 min wash in 0.1% Tween-20–PBS before sections were incubated in the biotinylated secondary antibody (Vectastain Elite ABC Kit, Vector Laboratories, USA) diluted in PBS containing 1.5% goat serum. Meanwhile, the ABC complex was prepared by mixing equal volumes of avidin and biotinylated HRP solution (Vector Laboratories, USA), which was allowed to stand for 30 min. Sections were washed for 5 min in 0.1% Tween-20–PBS then incubated in the ABC complex solution for 30 min, followed by a further 5 min wash in buffer. This was followed by chromogenic detection with DAB and then haematoxylin counterstaining, rehydration, clearing in Histoclear and mounting as described earlier.

2.9 Immunofluorescence Staining

2.9.1 Standard Immunofluorescence

FFPE sections were deparaffinised and antigen retrieval was performed before permeabilising the sections with 0.05% Triton™ X-100–PBS for 5 min and blocking for 2 h at room temperature with 5% goat or donkey serum in 0.05% Triton™ X-100–PBS. Sections were probed with the primary antibody for 16 h at 4°C in 2% goat or donkey serum in 0.05% Triton™ X-100–PBS. Sections were rinsed in 0.05% Triton™ X-100–PBS for 5 min with agitation and then incubated in fluorochrome-conjugated secondary antibody in 2% goat or donkey serum in 0.05% Triton™ X-100–PBS for 1 h at room temperature in the dark. Sections were counterstained with Sytox® Orange (ThermoFisher Scientific, USA) at a 1:10,000 dilution in deionised water for 20 min at room temperature before mounting with ProLong® Gold Antifade Mountant (ThermoFisher Scientific, USA). Mountant was cured overnight before visualisation.

2.9.2 Immunofluorescence with Tyramide Signal Amplification

Standard immunofluorescence can be improved by incorporating a tyramide signal amplification (TSA) step (Figure 2.3D), which is estimated to enhance fluorophore detection by 100-fold, therefore providing a powerful strategy for detecting low abundant targets. This method involves using an HRP-conjugated secondary antibody and fluorochrome-labelled tyramide. The catalytic activity of HRP generates tyramide radicals, which bind covalently to tyrosine residues *in situ*, and the fluorophore is thus deposited in the vicinity of the site of synthesis allowing for fluorescent signal detection [150]. FFPE sections were deparaffinised and antigen retrieval performed as described earlier. As TSA is catalysed by peroxidase, endogenous peroxidase activity was quenched to prevent high background noise. This was performed using 3% hydrogen peroxide in methanol for 30 min. Next, sections were blocked in TNB buffer (0.1 M Tris-HCl (pH 7.5), 0.15 M NaCl and 0.5% blocking reagent (FP1012, PerkinElmer, USA) for 1 h at room temperature followed by primary antibody incubation in TNB buffer for 1 h at room temperature. Sections were washed in TNT wash buffer (0.1 M Tris-HCl, 0.15 M NaCl and 0.05% Tween-20), and then incubated in HRP-conjugated secondary antibody (Sigma-Aldrich, USA) diluted 1:1000 in TNB buffer for 1 h at room temperature before washing in TNT buffer. Sections were incubated in 200 µl TSA Plus Fluorescein working solution (PerkinElmer, USA) for 5 min and then washed in TNT buffer. Sections were counterstained with Sytox® Orange, mounted with ProLong® Gold and cured overnight before visualisation.

2.10 Confocal Microscopy

Confocal laser scanning microscopy (CLSM) images were acquired using a Leica SP8 (Leica Microsystems Heidelberg GmbH, Germany) inverted laser scanning confocal microscope using a 20 $\times$ 1.4 N.A. objective. Acquisition parameters were as follows: 12-bit, 1024 $\times$ 1024 pixels, 1.25 $\times$ and 3 $\times$ digital zooms, 8000 Hz scan speed, 16-line Kalman filtering and 2 frame accumulation. Fiji analysis software was used to adjust the image brightness and contrast for enhanced visibility. Images within each figure were processed in parallel, and all confocal images within figure panels were obtained using identical scan settings.

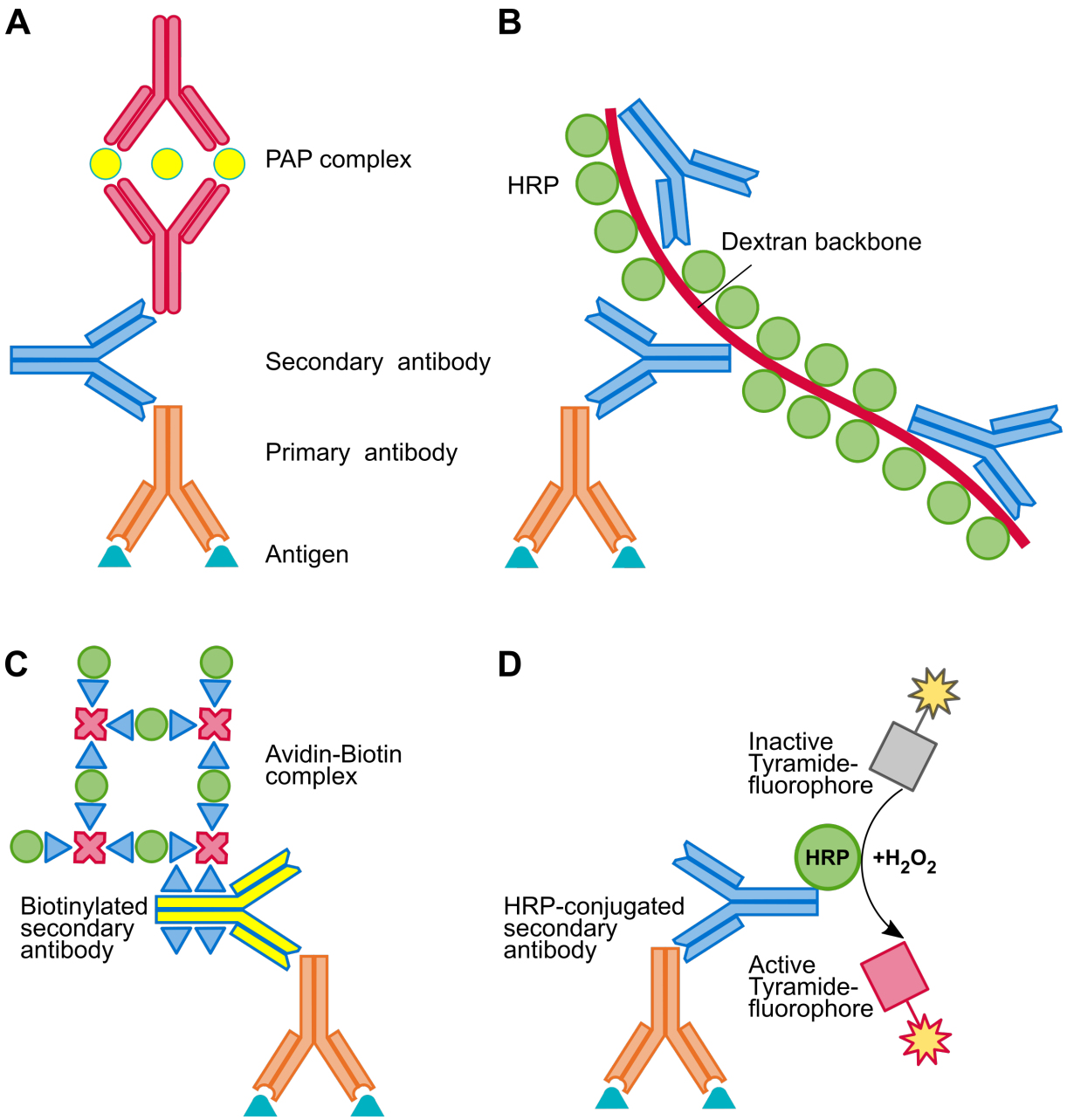

Figure 2.3: Schematic diagrams illustrating the principle behind different immunostaining methods. (A) Peroxidase anti-peroxidase method (B) HRP labelled polymer method (C) Avidin-biotin method, and (D) Tyramide signal amplification.

2.11 Statistical Analysis

Statistical analyses were conducted using SPSS version 23 and GraphPad Prism 7 software. Normally distributed data are presented as mean ± standard deviation (SD), while skewed data are presented as median and inter-quartile range (IQR). Non-normally distributed variables were log-transformed for statistical analyses. For each of the SNPs investigated, deviations from the Hardy-Weinberg equilibrium were tested using the χ^2 test. Allelic variation in gene expression was compared using the Student's t-tests with Welch's corrections. Associations between SNPs and PWV

were tested assuming an additive inheritance pattern in multiple linear regression models, and adjusting for confounders such as age, age^2, gender, height and weight, which are known to influence aortic PWV. For Western blot quantification statistical significance between groups was determined using the non-parametric Mann Whitney U test. In all tests, a p-value of <0.05 was considered to be statistically significant.

3

Lessons from a Monogenic Aneurysm Disorder: A Loeys-Dietz Type 4 Case Study

3.1 Abstract

Loeys-Dietz syndrome (LDS) is an autosomal dominant connective tissue disorder with a range of cardiovascular, skeletal, craniofacial and cutaneous manifestations. LDS type 4 is caused by mutations in TGF beta ligand 2 (*TGFB2*), and based on family pedigrees described to date, appears to have a milder clinical phenotype, often presenting with isolated aortic disease. Its molecular basis was investigated in a new pedigree and a missense variant p.(Arg320Cys) (NM_003238.3) was identified within a highly evolutionary conserved region of *TGFB2*, representing a new LDS type 4 pedigree with multiple cases of aortic aneurysms and dissections. There was striking up-regulation of TGFB1, TGFB2 and the canonical signal transducer pSMAD2/3 on immunostaining and Western blotting of aortic tissue from the subject, confirming the functional importance of this variant. This case highlights the striking paradox of predicted loss-of-function mutations in *TGFB2* causing enhanced TGFβ signalling in this emerging familial aortopathy.

3.2 Introduction

3.2.1 Background

The identification of molecular mechanisms operating in rare Mendelian and monogenic traits has been pivotal in discovering novel pathways contributing to complex traits and polygenic diseases with milder phenotypes. A classic example is the insight gained from the discovery of genes responsible for monogenic forms of hypertension in recognising the primacy of kidneys and adrenal glands in blood pressure regulation [151]. Likewise, mutations identified in rare monogenic aortopathies,

such as fibrillin-1 in Marfan syndrome [152], type III procollagen in vascular Ehlers-Danlos syndrome [153], and transforming growth factor β (TGFβ) signalling in LDS [154], have highlighted how the dynamic interplay of signalling molecules, extracellular matrix (ECM) composition, and vascular smooth muscle cell (VSMC) function is crucial to maintaining aortic wall function and integrity. LDS is an inherited autosomal dominant systemic disorder with a broad phenotypic spectrum of cardiovascular, skeletal, craniofacial, and cutaneous manifestations (OMIM 609192). Classic features of LDS include widespread arterial tortuosity, a bicuspid aortic valve, bifid uvula/cleft palate and hypertelorism [155]. Early and progressive aortic root dilatation is a distinct hallmark of LDS, predisposing to premature death from dissection and rupture of the aorta [155] (Figure 3.1). The specific molecular mechanisms which trigger aortic dissection are not known but is likely to be primed by the degeneration of the medial layer due to the cumulative effect of smooth muscle cell (SMC) apoptosis, elastic fibre fragmentation, impaired aortic remodelling, proteoglycan and glycosaminoglycan accumulation, enhanced inflammation, the up-regulation of matrix metalloproteinases (MMP), and precarious angiotensin II and TGFβ signalling [156].

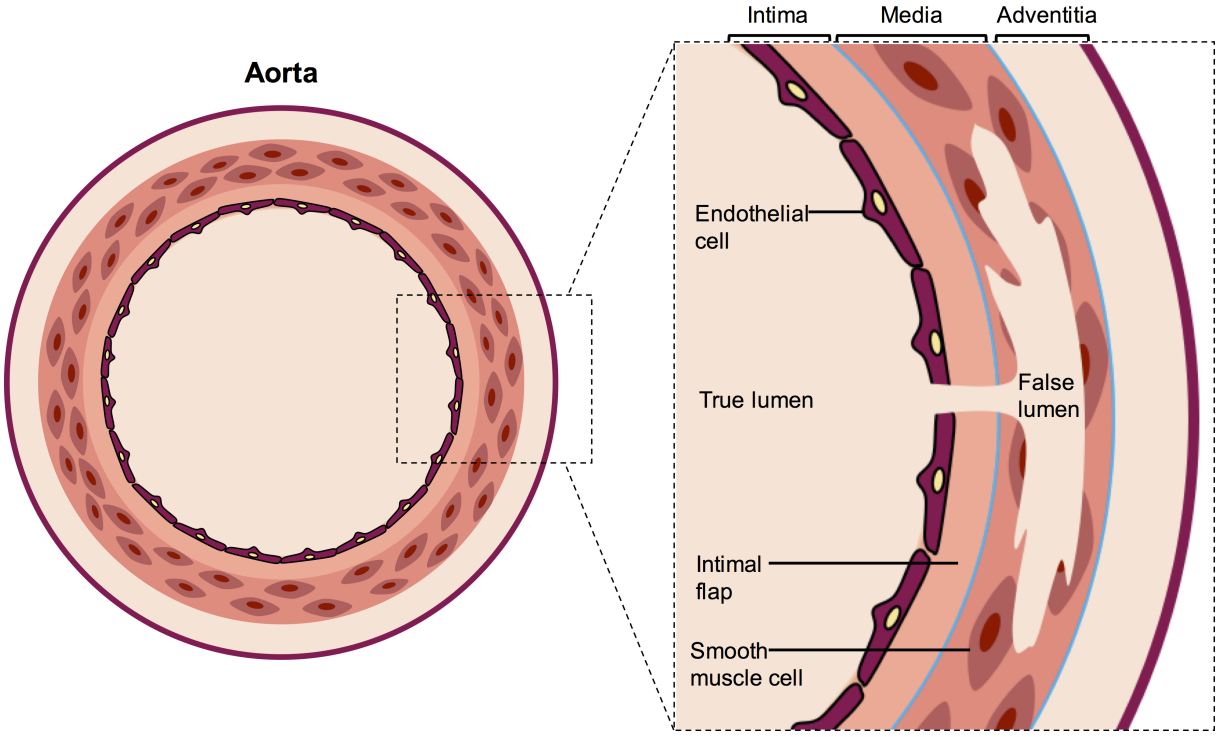

Figure 3.1: Aortic dissection. An intimal flap is formed when bleeding within the media drives the intima and adventitial layers apart. Image modified from Nienaber et al. [157].

TGFB1-3 are multipotent cytokines that regulate key processes, including cell proliferation, differentiation, apoptosis, angiogenesis and immune suppression, through signalling via serine/threonine kinase receptors (TGFBRI/II) and the downstream effectors known as SMAD proteins, as well as additional pathways collectively known as the SMAD-independent or non-canonical signalling path-

way (Figure 3.2) [158]. These signalling cascades modulate several genes involved in ECM synthesis and homeostasis, including fibronectin, fibrillar collagens, elastin, MMPs, proteinase inhibitors and proteoglycans, as well as TGFβ itself, thus generating a positive feedback loop [159–165].

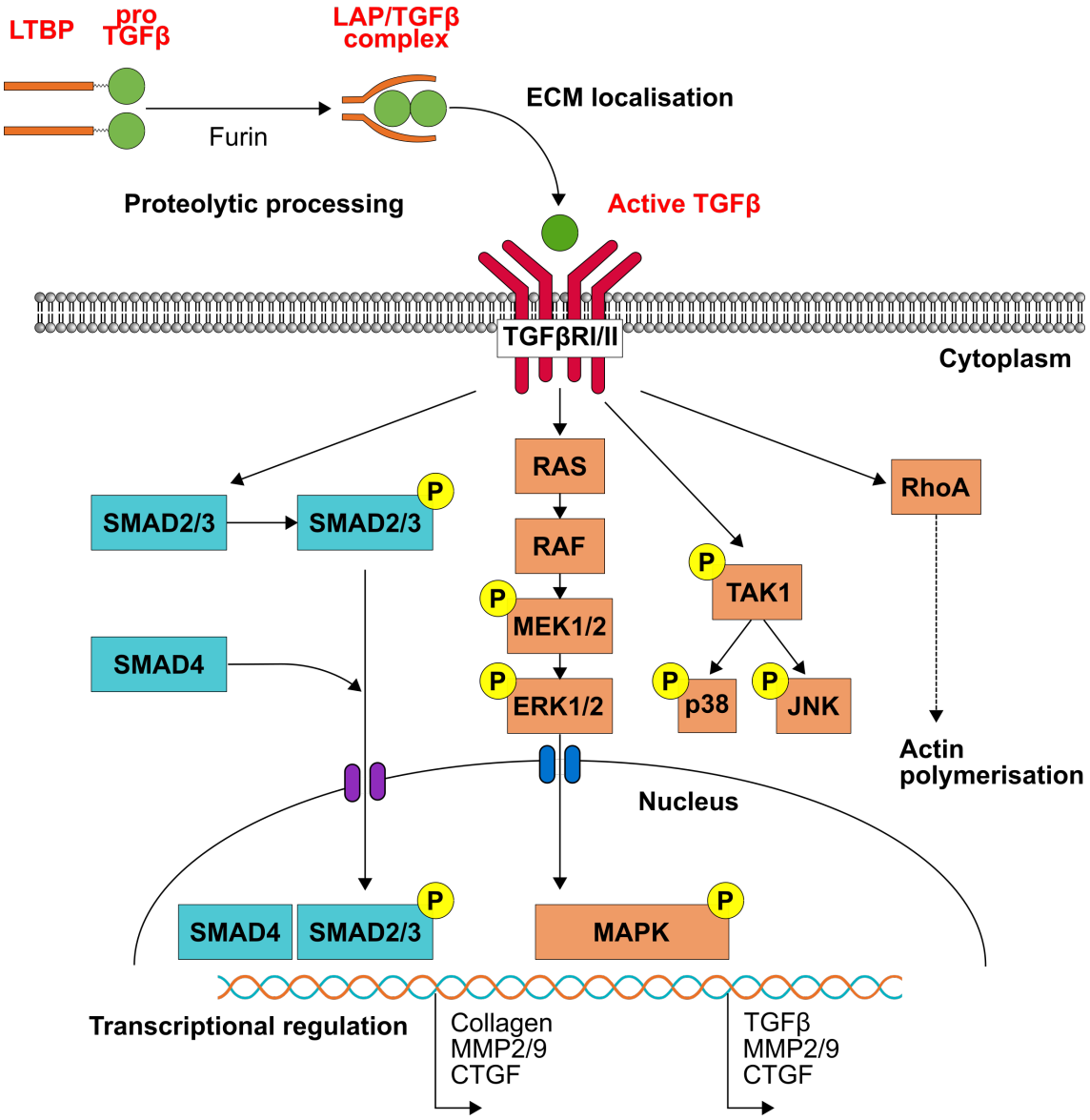

Figure 3.2: TGFβ activation and signal transduction. LAP is cleaved from mature TGFβ by proteases but remains bound to it non-covalently, conferring latency to TGFβ. Both canonical (blue) and non-canonical (orange) pathways influence gene expressions. CTGF; connective tissue growth factor, ERK; extracellular signal-regulated kinase, JNK; JUN N-terminal kinase, MAPK; mitogen-activated protein kinase, RAF; RAS-activated factor, TAK1; TGFβ-activated kinase 1

Whilst TGFβ is a crucial regulator of the ECM, its own activity and bioavailability are in turn regulated by components of the ECM. TGFβ is synthesised as a precursor molecule composed of a signal-peptide required for cell secretion, a latency-associated peptide (LAP) domain, and a C-terminal domain that becomes the mature cytokine following cleavage from the LAP domain. LAP remains non-covalently bound to TGFβ after proteolytic cleavage and together are secreted into the ECM bound to one of four latent TGFβ binding proteins (LTBPs 1-4) as part of a large latent complex

(LLC) [166]. LTBPs interact with fibrillin-1, heparin sulphate proteoglycans, and elastic microfibrils, serving to direct and store the latent TGFβ complex to specific sites within the ECM and to regulate the extracellular ligand activation process [167, 168]. Active TGFβ is eventually liberated from LAP either proteolytically by various ECM proteinases, via integrin-mediated conformational changes which allow cell-surface receptors to recognise mature TGFβ, or by integrin-mediated MMP cleavage of the latent complex [169].

LDS is caused by disruptions to TGFβ signalling due to loss-of-function mutations in different components of the pathway. Mutations in genes encoding for TGFβ receptors (*TGFBR1*, *TGFBR2*), TGFβ ligands (*TGFB2*, *TGFB3*) or the intracellular downstream effector (*SMAD3*), have been linked with the disease pathogenesis [154, 170–172]. Precise genotype-phenotype correlations are still lacking, but it is proposed that a mutation in any of these genes plus arterial aneurysm/dissection or a family history of LDS is sufficient for diagnosis [173]. LDS type 4 (LDS4) is caused by mutations in *TGFB2* and represents a milder end of the LDS spectrum compared to those of other LDS types, often with isolated aortic disease presenting in the mid-thirties [174]. Twenty mutations in *TGFB2* have been described in the literature to date (Table 3.1), mostly in the LAP domain of the protein, although the underlying pathogenic mechanisms remain unclear. While most of the mutations are predicted to be loss-of-function, their downstream effect appears to be a paradoxical activation of TGFβ signalling.

A new pedigree with LDS4 is reported here and it is confirmed that the causative variant p.(Arg320Cys) (NM_003238.3) causes striking up-regulation of TGFβ-1/2 and pSMAD2/3 expression within the aorta. This confirms that the variant is functional and corroborates previous reports of an enhanced aortic TGFβ 'tissue signature' in LDS and other TGFβ vasculopathies.

Table 3.1: Summary of *TGFB2* mutations reported in the literature

Exon	c-notation	p-notation	Domain	Reference
1	c.294_308del	p.Ala100_Tyr104del	LAP	[171]
1	c.297C>A	p.Tyr99*	LAP	[171]
1	c.304G>T	p.Glu102	LAP	[174]
3	c.475C>T	p.Arg159*	LAP	[175]
5	c.771C>A	p.Cys257	LAP	[174]
6	c.839-1G>A	p.Gly280Aspfs*41	LAP	[176]
6	c.958C>T	p.Arg320Cys	LAP	[177]
6	c.957_972dup	p.Asn325*	LAP	[174]
6	c.979C>T	p.Arg327Trp	LAP	[175,178]
6	c.980G>A	p.Arg327Gln	LAP	[175]
6	c.988C>T	p.Arg330Cys	LAP	[171]
6	c.995del	p.Leu332TrpfsTer27	LAP	[179]
7	c.1097C>A	p.Pro366His	Cyt	[171]
7	c.1106_1110del	p.Tyr369Cysfs*26	Cyt	[171,174]
7	c.1125del	p.Gly376Glufs*17	Cyt	[175]
7	c.116dupA	p.Ser389Lysfs*8	Cyt	[180]
Entire gene Chr1.hg19: g.(215,588,712)_(222,145,072)del				[171]
Entire gene Chr1.hg19: g.(215,963,393)_(220,705,991)del				[181]
Entire gene Chr1.hg19: g.(216,672,181)_(220,202,575)del				[171]
Entire gene Chr1.hg18: g.(212,338,589)_(217,573,448)del				[182]

LAP; latency-associated peptide, Cyt; *TGFB2* cytokine domain, *; translation termination codon, del; deletion, fs; frameshift.
Note: This list only includes variants identified as articles in PubMed and does not include variants from the ClinVar database since limited clinical information is available on these cases.

3.2.2 Case Report

A 27-year-old man presented with severe pain radiating down his back after lifting a lawn mower into a van. The family history revealed several family members with aortic aneurysms and dissections: his mother (III:6) died following an aortic dissection, a maternal uncle (III:1) had undergone an emergency repair of an aortic aneurysm, and his maternal grandfather (II:3) had a dissection of an abdominal aortic aneurysm and separate iliac artery aneurysms (Figure 3.3). On examination, the only symptom was an elevated BP of 240/100 mmHg. A CT scan with contrast showed a Stanford type-A dissection with an intimal flap extending the full length of the aorta from the aortic valve into both iliac arteries (Figure 3.4). The patient underwent open aortic repair and a surgical specimen was recovered for further examination. Histological examination showed fragmentation and disruption of the aortic elastic fibres and cystic medial necrosis (Figure 3.4).

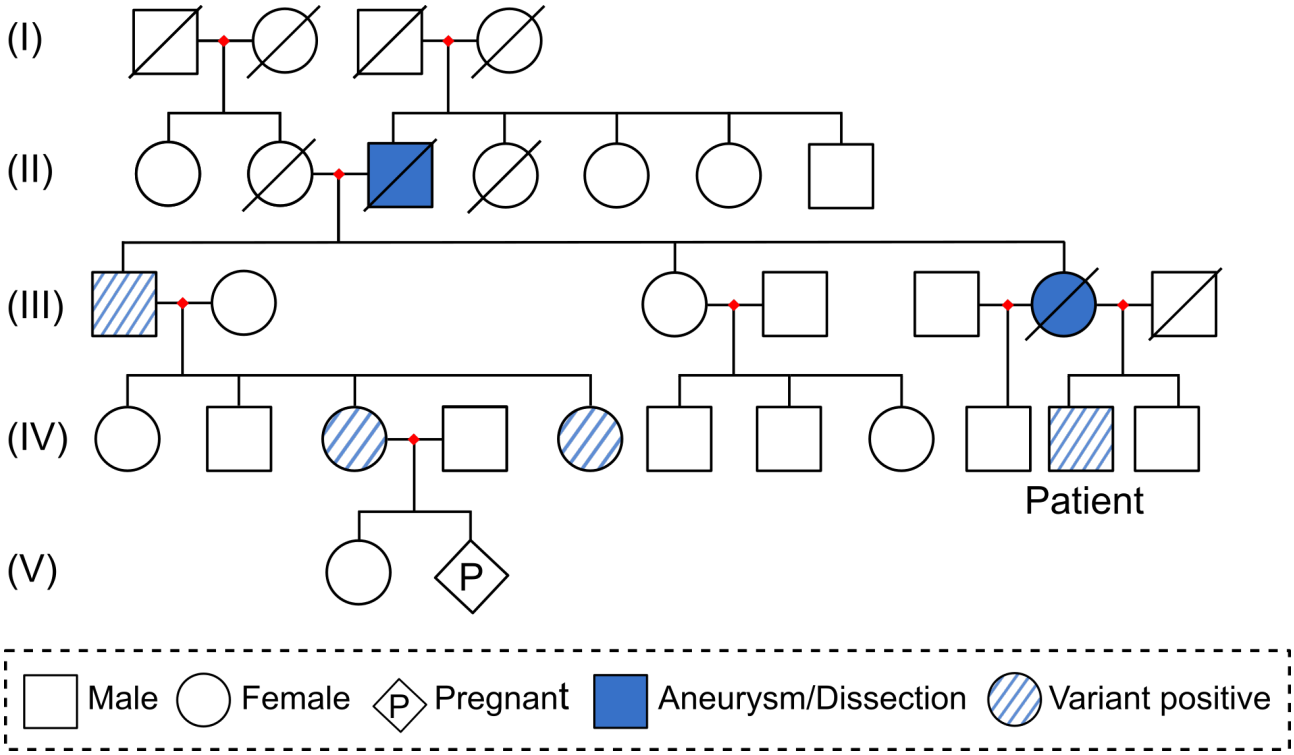

Figure 3.3: Family pedigree with multiple cases of aneurysms and dissections. Allele segregation suggests autosomal dominant inheritance. The variant was detected in the index case (IV:10), as well as in III:1, IV:3 and IV:5.

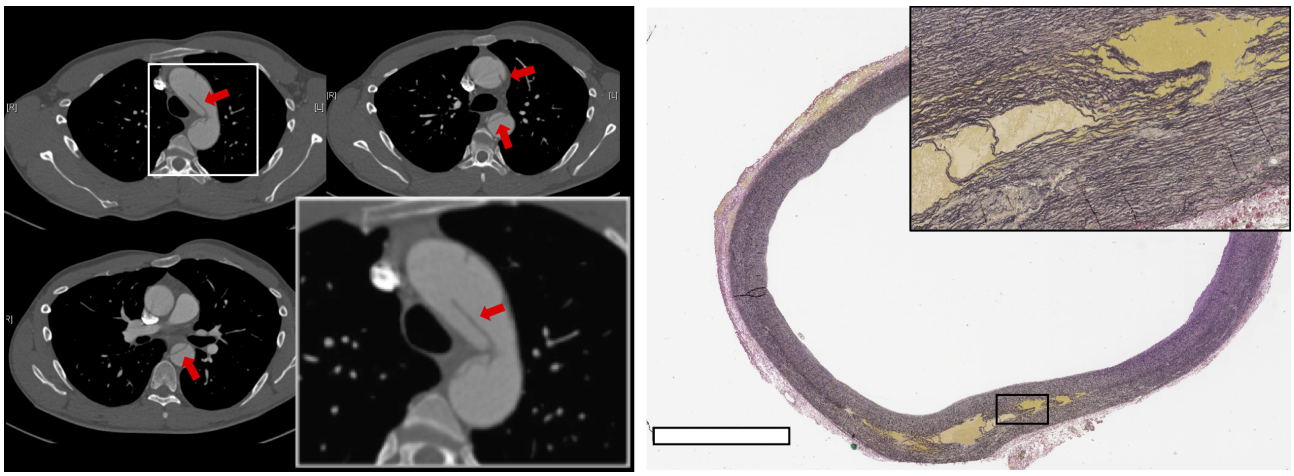

Figure 3.4: Clinical and histological findings. Left panel: CT images showing an intimal flap (red arrows) extending from the aortic valve into the thoracic aorta. Right panel: Elastin staining of IV:10 aorta showing extensive elastic fibre fragmentation at the site of dissection (scale bar = 6mm).

3.2.3 Sequencing and Variant Identification

DNA sequencing from the peripheral blood of the index case identified a missense variant (c.958C>T) (NM_003238.3) in exon 6 of the *TGFB2* gene (NG_027721.1). This variant causes a p.(Arg320Cys) substitution in a highly-conserved region of *TGFB2* (Figure 3.5). The variant was also detected in the

uncle (III:1) and two currently asymptomatic teenage family members (IV:3) and (IV:5) (Figure 3.5).

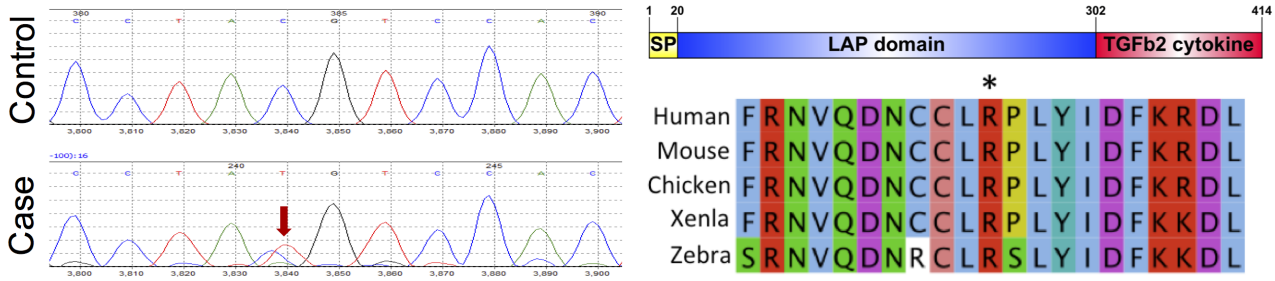

Figure 3.5: Molecular findings. Left panel: Sequencing chromatogram showing a missense mutation (c.958C>T) in exon 6 of *TGFB2*. Right panel: The mutation is within a region of *TGFB2* that is highly conserved across species. SP; signal peptide.

3.3 Methods

3.3.1 Data Submission

The phenotype and variant data were submitted into LOVD v.3.0 Build 16 (`http://medgen.ua.ac.be/LOVDv.3.0/individuals/00000322`).

3.3.2 Control Subjects

Formalin-fixed and paraffin embedded (FFPE) aortic tissue from age and gender matched donors (n=5) were obtained from the Transplant Service at Addenbrooke's Hospital (Cambridge, UK). All samples were handled in accordance with the policies and procedures of the Human Tissue Act and had local and regional ethical approval.

3.3.3 Protein Extraction from FFPE Sections

Western blotting for TGFB1 and TGFB2 was performed using aortic homogenates extracted from the FFPE sections of the surgical specimen and two controls. Three 15 µm FFPE sections of each tissue sample were deparaffinised in Histo-Clear II (National Diagnostics, USA) three times, and the procedure was serially repeated with 100%, 95% and 70% ethanol, washing twice for 10 min each. Pellets were air dried then re-suspended in Extraction Buffer EXB Plus (QIAGEN, Germany) containing β-mercaptoethanol, and incubated at 4°C for 5 min then at 100°C for 20 min followed by a 2 h incubation at 80°C with agitation, and a final incubation at 4°C for 1 min. Samples were then subjected to centrifugation at 16,000 $\times$ at 4°C for 15 min and the protein quantified using Pierce™ BCA protein assay (ThermoFisher Scientific, USA) and stored at -70°C until required.

3.3.4 Western Blotting

Western blotting was performed as described in Chapter 2. Immunoblotting for TGFB1 was performed under non-reducing conditions. Anti-TGFB2 rabbit polyclonal IgG antibody (ab66045, Abcam, UK) was used at 1:500 dilution, and β Actin mouse monoclonal IgG (MA5-15739, ThermoFisher Scientific, USA) was used as a loading control at 1:1000 dilution. Anti-TGFβ1 mouse monoclonal IgG antibody (ab64715, Abcam, UK) was used at 1:500 dilution and β Actin rabbit polyclonal IgG (A2066, Sigma-Aldrich, USA) was used as a loading control at 1:1000 dilution. Donkey anti-rabbit (925-32213, LI-COR Biotechnology UK Ltd, UK) IRDye® 800CW and goat anti-mouse (A-21058, ThermoFisher Scientific, USA) Alexa Fluor® 680 conjugated secondary antibodies were used at 1:5000 dilution.

3.3.5 Immunofluorescence and Immunohistochemical Staining

Antigen retrieval was performed in pH6 citrate buffer (Vector Laboratories Ltd, Peterborough, UK) for TGFB2 immunostaining and R-Universal buffer (Aptum Biologics Ltd) for TGFβ1 and pSMAD2/3 immunostaining. Sections were probed with a mouse monoclonal antibody specific for TGFB2 (ab36495, Abcam, Cambridge, UK) and a mouse monoclonal antibody specific for TGFB1 (ab64715, Abcam) for 16 h at 4°C at 1:200 dilution. Pre-absorbed goat IgG-conjugated Alexa Fluor® 633 secondary antibody (A21050, ThermoFisher Scientific, Waltham, MA, USA) was used at 1:200 dilution. Phosphorylated SMAD2/3 was probed using a rabbit polyclonal antibody specific for pSMAD2/3 (SC11769, Santa Cruz Biotechnology, USA) at 1:500 dilution using the HRP labelled polymer method described in Chapter 2.

3.4 Results

3.4.1 TGFB1 and TGFB2 Expression

Due to limited sample availability, transcript analysis of *TGFB1* and *TGFB2* was not conducted. Using the data from the Genotype-Tissue Expression (GTEx) project, both genes are shown to be expressed in the human aorta (`https://www.gtexportal.org/home/gene/TGFB1` and `https://www.gtexportal.org/home/gene/TGFB2`). However, the effect of the c.958C>T mutation on the transcript level of either genes is not known. At the protein level, immunofluorescent imaging showed markedly enhanced TGFB2 (Figure 3.6) and TGFB1 (Figure 3.7) expression in the aorta of the index case compared to age and gender-matched controls. This was confirmed by immunoblotting for both proteins in the aorta of IV:10, where compared to the controls, TGFB2 was nearly two-fold higher and TGFB1 15-fold higher (Figure 3.8).

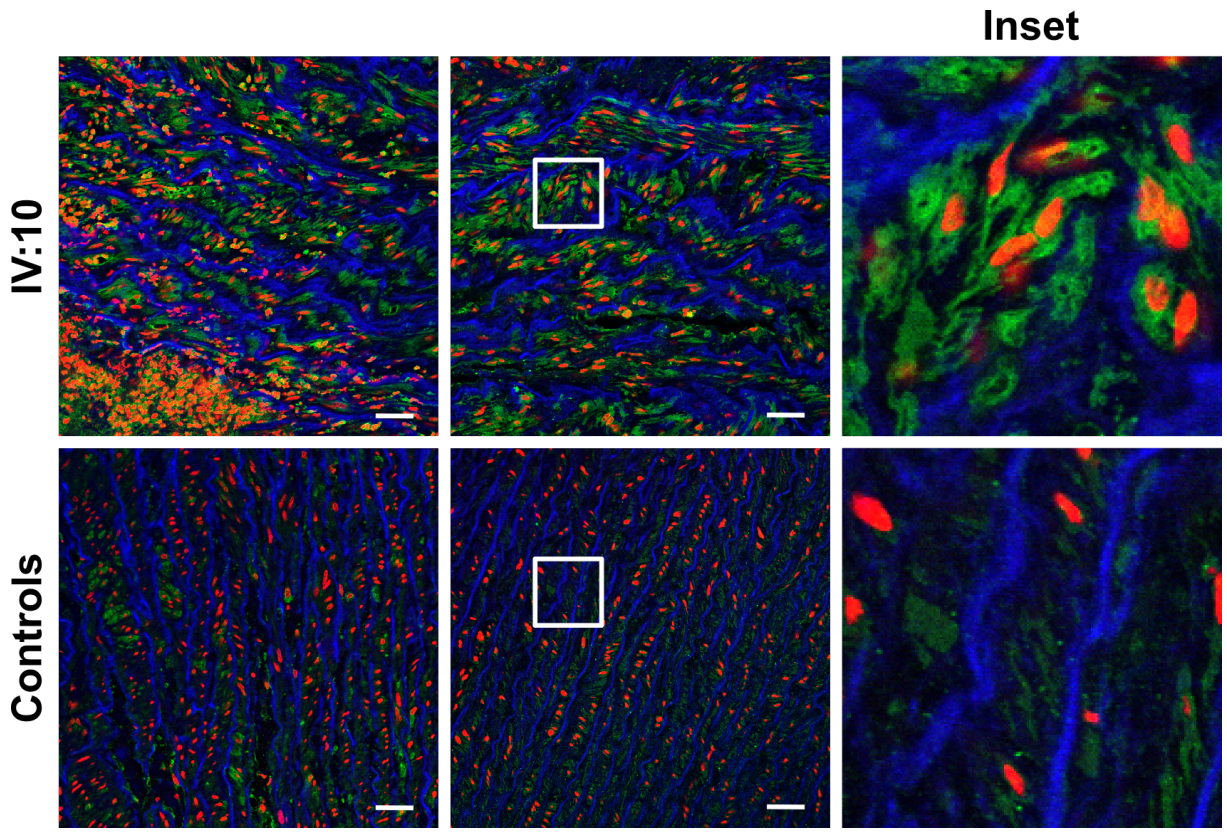

Figure 3.6: Aortic expression of TGFB2. Immunofluorescence staining of TGFB2 (green) shows increased expression in the aortic wall of IV:10 compared to age and gender-matched controls. Images are representative of (n=5) controls. Elastic fibres appear as blue (autofluorescence) and nuclei are counterstained red (scale bar = 50μM).

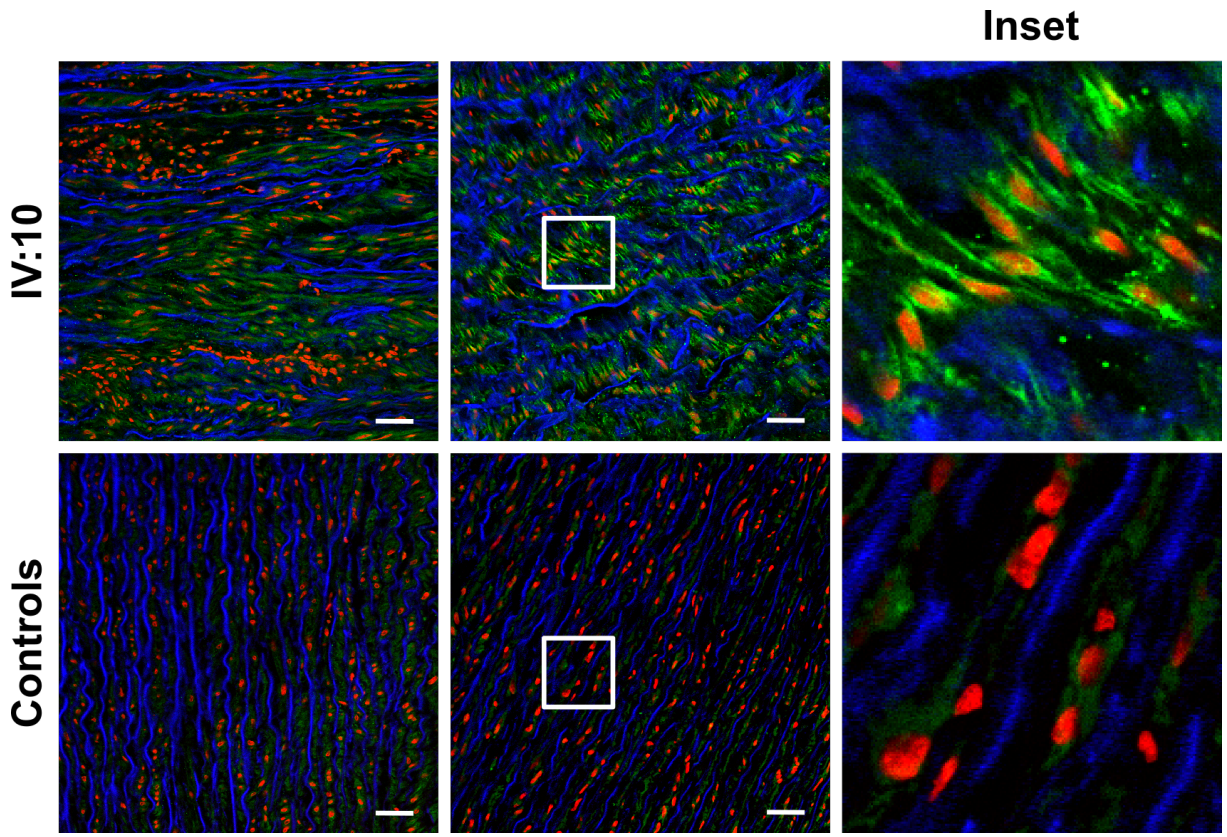

Figure 3.7: Aortic expression of TGFB1. Immunofluorescence staining of TGFB1 (green) shows increased expression in the aortic wall of IV:10 compared to age and gender-matched controls. Images are representative of (n=5) controls. Elastic fibres appear as blue (autofluorescence) and nuclei are counterstained red (scale bar = 50µM).

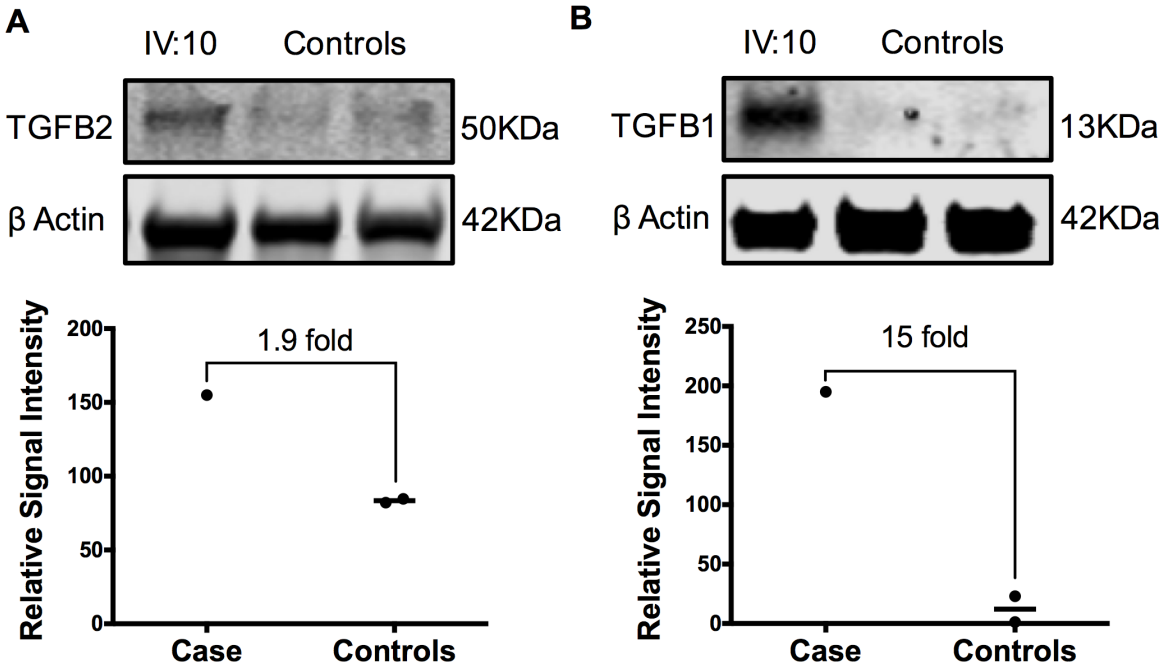

Figure 3.8: Western blotting of aortic TGFB2 and TGFB1 expression in IV:10 compared to age-matched controls. Signal intensities normalised against β Actin indicates a two-fold higher expression of TGFB2 and a 15-fold higher TGFB1 expression in the IV:10 sample.

3.4.2 Phosphorylated SMAD2/3 Expression

Immunohistochemical staining showed increased nuclear expression of pSMAD2/3 in the aorta of the index case compared to control subjects (Figure 3.9).

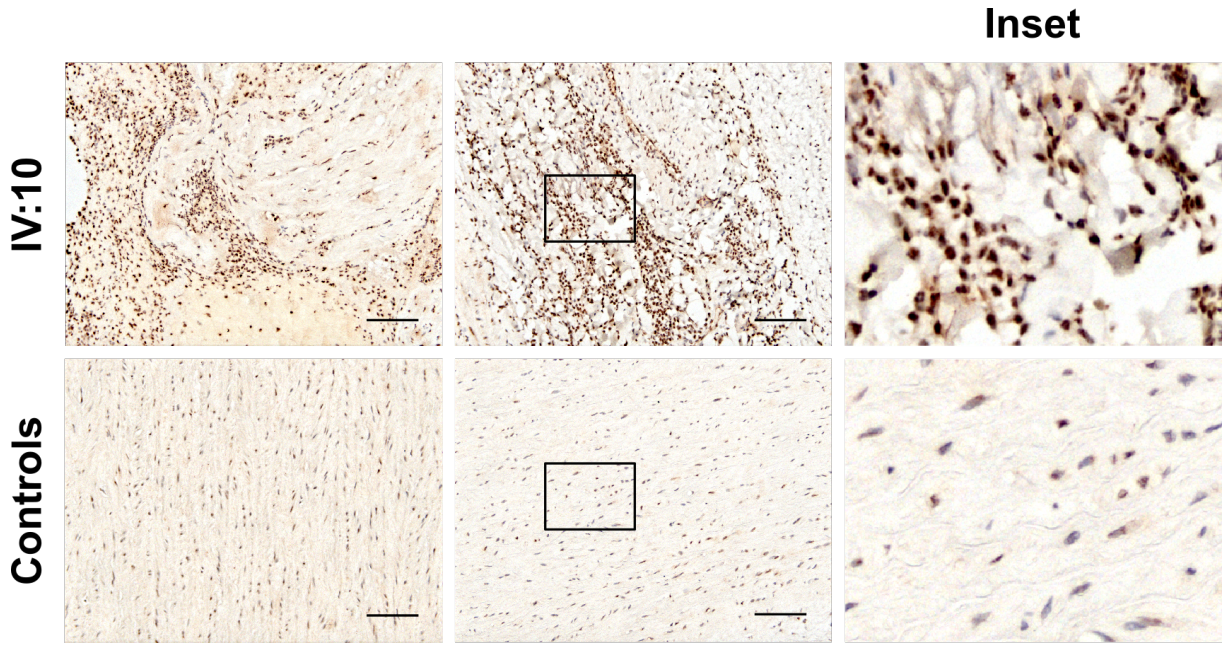

Figure 3.9: Aortic expression of pSMAD2/3. Immunohistochemical staining shows increased nuclear accumulation of pSMAD2/3 in the aorta of IV:10 compared to age and gender-matched controls. Images are representative of (n=5) controls (scale bar = 50µM).

3.5 Discussion

A new pedigree with a p.(Arg320Cys) substitution is reported here within a highly evolutionarily conserved region of *TGFB2* and a strong in silico prediction for pathogenicity [177]. Prior to this finding there had been no evidence to confirm its functional effects. This variant has been shown to induce significant up-regulation of TGFβ signalling, as demonstrated by increased immunostaining of TGFB1 and TGFB2 ligands and the canonical signal transducer pSMAD2/3 in the vessel wall of a subject with the variant. The outcomes of TGFβ signal transduction, and indeed consequences of its perturbation, are complex, diverse and not yet fully understood; however, the pathogenic effects of the observed TGFβ overdrive may be partly explained by the pathway's known roles in matrix synthesis, deposition and degradation. The TGFβ signalling pathway has been found to modulate aldosterone levels and sodium and water retention [183] which may, at least in part, explain the elevated BP seen in the index case. TGFβ promotes collagen synthesis and deposition [184], up-regulates transcriptional and post-translational elastogenesis [161], and stimulates the expression of connective tissue growth factor (CTGF), a matricellular protein with various roles in cell prolifera-

tion, adhesion and ECM synthesis [185]. Perturbations to this pathway are thus likely to disrupt the normal architecture of the vessel wall, predisposing to aneurysm and triggering dissection. Others have proposed a primary role for impaired mechanosensing caused by TGFβ signalopathy in the events leading to aortic dissection [186, 187]. This model is based on the observation that TGFβ, as well as other genes implicated in thoracic aortic aneurysms and aortic dissections, are involved in the regulation of microvascular tone [186, 188] and cellular mechanosensing and mechanoregulation of the ECM [187], coupled with the role of the ECM in controlling the level of interstitial fluid pressure on microvessels [189]. Accordingly, defective mechanoregulation caused by altered TGFβ signalling dampens the vascular tone in the aortic vasa vasorum, causing an increase in blood flow, fluid flux and pressure within the media, thus initiating the process of aortic dissection [186]. This process can be further exacerbated by dysregulations of interstitial fluid caused by any associated ECM remodelling, thereby further promoting and maintaining intraparietal oedema [186]. In support of this, pharmacological restoration of VSMCs contractility with rapamycin attenuates the incidence of aortic dissections in *Tgfbr2* mutant mice despite evidence of ECM dysregulation and VSMC explanted from Marfan patients undergo TGFβ-dependent phenotypic modulation characterised by a rise in their contractile machinery [190, 191].

The signature of enhanced TGFβ signalling is unexplained by the loss-of-function variant in *TGFB2*, but is thought to play a central role in the aortic dilatation and aneurysms seen in LDS, Marfan syndrome, arterial tortuosity syndrome and other inherited aortopathies [170, 171, 174]. Indeed, most LDS-related mutations are in evolutionarily conserved residues of the intracellular kinase domains of *TGFBR1/2*, and were originally suggested to impair TGFβ signalling. However, tissues from affected individuals consistently display signs of downstream pathway propagation, including increased pSMAD2 nuclear accumulation and enhanced CTGF expression [154, 192]. Several lines of evidence from experimental models also implicate high tgfβ signalling in aortic aneurysms. *Tgfb2*+/- haploinsufficiency in mice mirrors the classical features of LDS, causing aortic root dilatation and aneurysm, and triggering a higher expression of pSmad2/3 and extracellular signal-regulated kinases (Erk1/2), indicating up-regulation of both canonical and non-canonical pathways [171]. In addition, neutralisation of Tgfβ activity in Marfan and other murine models attenuates aortic wall abnormalities, diminishes aortic dilation, slows disease progression, and significantly improves animal survival [193–195]. One proposition to resolve this TGFβ paradox posits that other TGFβ ligands are overexpressed to compensate for the haploinsufficiency of a given TGFβ ligand. This shift in ligand usage is seen with higher Tgfb1 expression in *Tgfb2*+/- mice [171] and, indeed in the index case described here. Impaired sequestration of the latent TGFβ complexes in the ECM has also been

suggested [196]. Alternatively, driven by 1) the premise that aortic VSMCs originate from diverse progenitors [197], and 2) evidence of lineage-dependent disparities within the vessel wall in SMC responses to TGFβ [198], and 3) the observation of distinct cell populations with and without signs of TGFβ activation in aneurysmal tissue, Lindsay and Dietz [199] postulate that the TGFβ overshoot is a compensatory mechanism by cardiac neural crest-derived VSMCs for impaired signalling in neighbouring mesoderm second heart field-derived SMCs. While compelling, there is to date insufficient evidence to support this hypothesis, and at least in the index case reported here, a dichotomous pattern of nuclear pSMAD2/3 staining in the aorta was not observed.

Nonetheless, the longstanding view of TGFβ over-activity as the main driver of Marfan syndrome and related aortopathies has been frequently challenged. For example, selective abrogation of *Tgfbr2* in the SMCs of young wildtype and Marfan syndrome mice strains yields animals with classical features of inherited aortopathies, including elastin fragmentation, aortic dissection, dilation, macrophage and proteoglycan accumulation, without any evidence of aberrant canonical or non-canonical TGFβ signalling [200, 201]. Similarly, conditional disruption of the receptor in SMCs of postnatal LDS mice strains induces severe aortic dissection, dilatation and aortic wall thickening, together with diminished pSmad2 signalling [202]. As such, it remains debatable whether the enhanced TGFβ expression 'signature' observed in LDS and related syndromes is a trigger or a consequence of disease progression. Indeed, high TGFB1/2 expression may essentially reflect a repair process by mesenchymal cells following damage to the ECM [203] that becomes manifested at advanced stages of the disease. This view is supported by recent observations that aneurysmal progression is exacerbated with the early systemic neutralisation of TGFβ activity in experimental models of abdominal aortic aneurysms and Marfan syndrome [195, 204, 205]. More compelling is the finding that increased *Tgfb* gene expression in animal models of LDS that express mutant forms of Tgfb receptors are only detectable by 12 weeks, accentuating with the progression of vascular damage, despite evidence of aneurysms as early as 8 weeks of age [206]. Taken together, these observations add to the mounting evidence that TGFβ is a protective cytokine that plays a role in preserving vascular wall integrity and suggests that its enhanced expression is likely to be a late manifestation of the repair process and/or aneurysmal progression. Because the tissue recovered from the current study, and indeed all cases of aneurysms and dissections, represents late-stage disease, it is not possible to verify if the observed up-regulation is preceded by a phase of low or no TGFβ signalling.

In conclusion, the discovery of the genetic causes of aortic abnormalities found in inherited syndromes has played an important role in understanding aortic wall function and dysfunction. The

significance of TGFβ signalling in aortic ECM biology and pathophysiology has emerged via the identification of causal mutations underlying Marfan syndrome, LDS and related aortopathies. The finding of enhanced TGFβ signalling in the aortic wall of a case harbouring a p.(Arg320Cys) substitution in a highly-conserved region of *TGFB2* further corroborates the pathological implications of the TGFβ signalling overdrive. However, whether this is a feasible therapeutic target for inherited aortopathies remains questionable due to the contradictory outcome of neutralising Tgfβ activity in mice, and especially with the inadequate resolution of the TGFβ paradox. Specific targeting of the downstream effectors of the non-canonical pathway is providing promising outcomes [207, 208]. Thus, future work to further investigate the exact pathogenic sequence downstream of TGFβ during aneurysmal progression will be instrumental in yielding potential therapeutic strategies for these TGFβ signalopathies.

4

From Association to Function: Investigating the Role of 3'BCL11B Gene Desert Variants in Aortic Stiffness

4.1 Abstract

In recent years large scale association studies followed by functional characterisation have formed a paradigm for identifying genes and pathways of complex traits and diseases. The most recent genome wide analysis of carotid-femoral pulse wave velocity (cfPWV) identified a significant locus within the 14q32.2 gene desert. The region contains gene regulatory elements, with the transcriptional regulator B-cell CLL/lymphoma 11B (*BCL11B*) and long non-coding RNA (lncRNA) DB129663 representing potential targets for these enhancers. This chapter investigates the functional impact of gene desert single nucleotide polymorphisms (SNPs) on *BCL11B* and DB129663 transcripts in the human aorta in order to further characterise the role of this region in aortic stiffness.

The association of five lead SNPs from the genome-wide association studies (GWAS) meta-analysis was examined for *ex vivo* aortic stiffness and *BCL11B* and DB129663 aortic mRNA expression. Three of the five SNPs rs1381289, rs7152623 and rs10782490, associated significantly with PWV and showed allele-specific differences in *BCL11B* mRNA. The risk alleles associated with lower *BCL11B* expression suggesting a protective role for *BCL11B*. Despite the strong association, BCL11B protein was not detected in the human aorta; however, qPCR for CD markers showed that *BCL11B* transcript correlated strongly with markers for activated lymphocytes. In contrast, DB129663 transcripts were detected in 55% of the samples, and of the five SNPS only rs7152623 showed allele-specific differences in aortic DB129663 transcripts. No significant differences were observed in PWV between samples expressing or lacking DB129663, and therefore the implication of this lncRNA in aortic stiffness remains elusive.

This data confirms the significance of the 14q32.2 region as a risk locus for aortic stiffness and an upstream regulator of *BCL11B*. The *BCL11B* transcript detected in the human aorta may reflect lymphocyte infiltration, suggesting that immune mechanisms contribute to the observed association of *BCL11B* with aortic stiffness.

4.2 Introduction

4.2.1 Background

The last decade has seen a sharp surge in GWAS of complex physiological traits and diseases, which has been facilitated by the advent of high-throughput genotyping platforms. While these studies have been largely successful in identifying thousands of gene variants associated with complex traits, a gap remains in translating SNP associations into meaningful biological pathways. Correlating genetic variations with disease pathophysiology is particularly confounded by the observation that nearly 90% of SNPs are present within noncoding regions of the genome [209, 210]. This was also noted in the most recent genome wide analysis of cfPWV by the *AortaGen Consortium*, which identified a significant locus on chromosome 14 [72] (Figure 4.1). The top signals from this GWAS meta-analysis originate from a gene-poor region (14q32.2), although the region contains regulatory elements that may influence aortic stiffness via regulation of gene expression in a *trans* and tissue-specific manner. Previous studies in murine T cells suggest that the cfPWV region overlaps an enhancer for B-cell CLL/lymphoma 11B (*Bcl11b*), which resides 850kb upstream from the locus [88]. BCL11B, also known as *COUP-TF* interacting protein 2 (CTIP2), is a typical transcriptional regulator with six Cys2-His2-like zinc finger domains. It is highly expressed and crucial to the function of the cutaneous, immune and central nervous systems, and is a key regulator of odontogenesis and adipogenesis [211–214]. BCL11B also governs important aspects of the development, differentiation, recruitment and function of T lymphocytes and other immune cells [89]. The 14q32.2 enhancer cluster further maps to the promoter of DB129663, a primate-specific lncRNA expressed in aortic smooth muscle cells (SMCs) and cardiac fibroblasts but with a currently unidentified function [72]. In recent years, emerging evidence has underscored the role of variants in non-coding RNA regions in contributing to the risk of complex diseases [215–217]. The transcript profile of DB129663 in the human aorta and whether it is influenced by chromosome 14 variants remains to be explored.

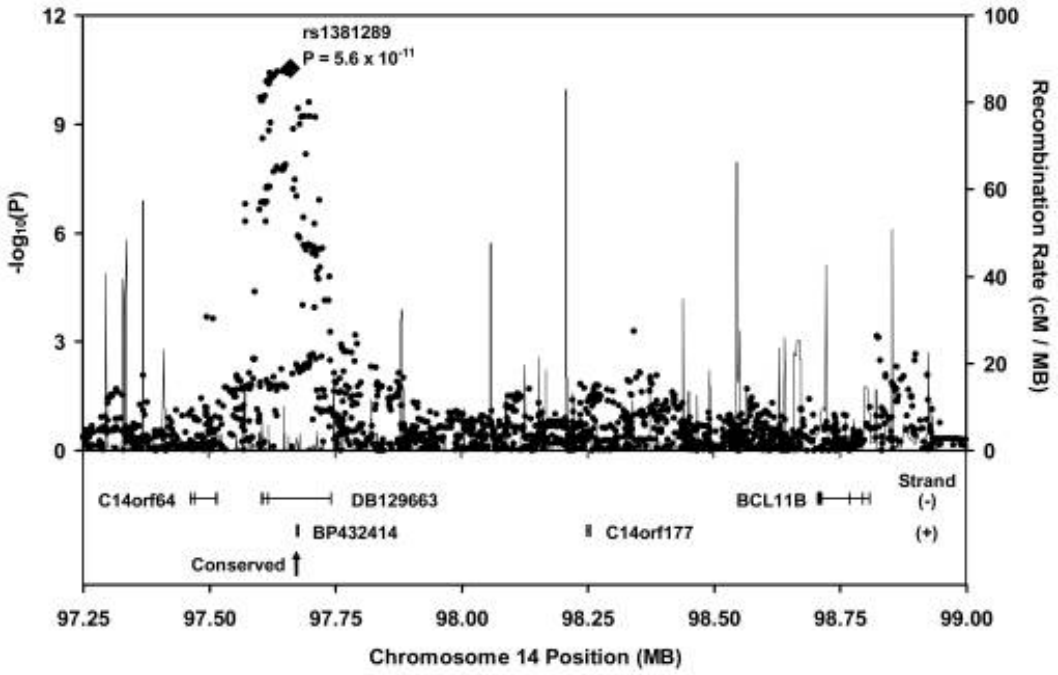

Figure 4.1: The chromosome 14q32.2 cfPWV GWAS association plot and surrounding genomic neighbourhood. Cited from Mitchell et al. [72].

To this end, the aim of this study was to examine the functional impact of the lead SNPs identified by the *AortaGen Consortium* on aortic *BCL11B* and DB129663 transcript levels and *ex vivo* measurements of aortic stiffness in a large sample of human aortic tissues, as well as determining the expression pattern of *BCL11B* in the human aorta. An understanding of how these genetic variations influence aortic stiffness will enhance understanding of the molecular mechanisms that contribute to alterations in PWV and may yield novel therapeutic targets. The aims of the literature review are to provide an overview of the multifaceted biological functions of BCL11B, to review the current knowledge on how alterations in its expression underscore a number of pathological conditions, and to summarise the evidence that links its functions to stiffening mechanisms.

4.2.2 BCL11B: Structure and Biological Functions

The *BCL11B* gene is located on human chromosome 14 (q32.2), is approximately 102 Kb in length and has a molecular weight of 95 kDa. Alternative splicing encodes two distinct but functionally analogous isoforms, alpha and beta, which are composed of 894 and 823 amino acid residues, respectively (Figure 4.2). Both isoforms contain the six C_2H_2 zinc finger binding domains critical to the functioning of *BCL11B* as a transcriptional regulator. The corresponding murine gene is 88% homologous to human *BCL11B* but is located on mouse chromosome 12 [218]. Mouse *Bcl11b* encodes three isoforms, alpha, beta and gamma, of which only the beta isoform resembles human BCL11B [219]. The encoded protein is largely nuclear but has also been detected in the mitochondria of mouse thy-

mocytes and human T cell lines [219]. BCL11B is a complex, multifaceted transcriptional factor with important roles in various cells and tissues and these will be discussed in the following sections.

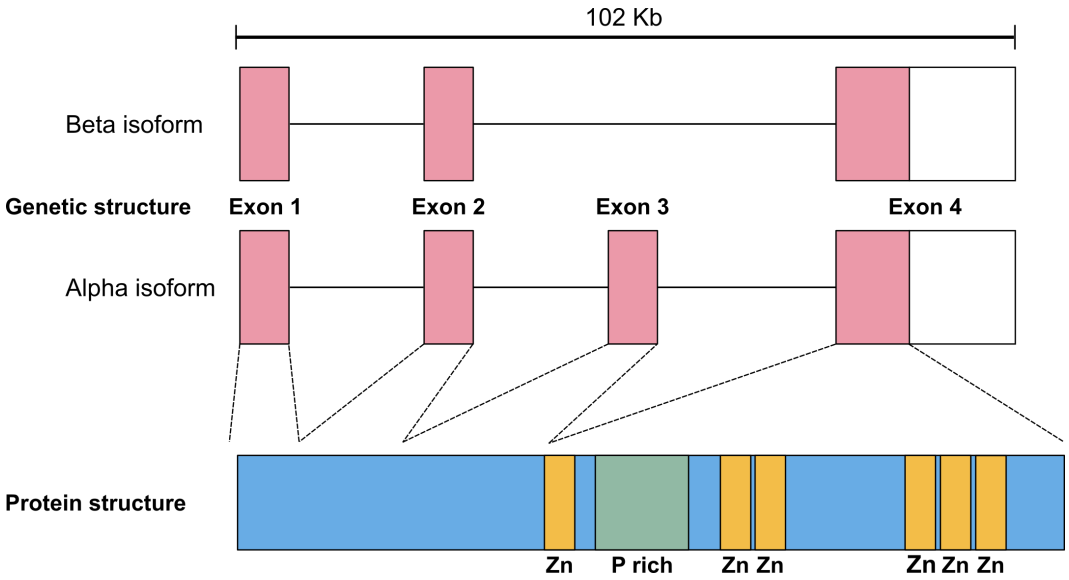

Figure 4.2: Schematic model of *BCL11B* isoforms and protein structure. The beta isoform lacks exon 3 but is functionally similar to the alpha isoform due to the presence of exon 4, which encodes the 6 zinc finger domains of BCL11B. Zn; zinc finger domain, P rich; proline-rich. Adapted from Lennon et al. [220].

4.2.2.1 Transcriptional Regulation

BCL11B was originally identified as a binding partner of the nuclear receptor chicken ovalbumin upstream promoter transcription factor (COUP-TF) group of orphan nuclear receptors (COUP-TFI, II and III) [221]. It was subsequently shown that BCL11B can regulate transcription independently of COUP-TF by directly binding to GC-rich motifs of target genes [222]. BCL11B-mediated transcriptional suppression is achieved primarily by recruiting proteins involved in chromatin modification and epigenetic regulation to the promoter template, most notably histone deacetylases (HDAC1 and HDAC2), histone methyltransferase (SUV39H1), heterochromatin protein 1 (HP1), members of the sirtuin family of proteins (SIRT1), transcription factor (SP1) and nucleosome remodelling and deacetylation (NuRD) complexes [223–226]. Mechanisms of transcriptional activation by BCL11B are only partly understood. The discovery of a small ubiquitin-like modifier (SUMO) and phosphorylation sites on BCL11B led to the identification of post-translational modification-driven regulation of *BCL11B* transcriptional activity in thymocytes. This process is regulated by MAP kinase and involves cyclical phosphorylation and sumoylation, which promotes the recruitment of p300, a histone acetyltransferase, to BCL11B-NuRD and targets the promoter complex, eventually leading to histone acetylation and transcriptional activation [227]. A large number of BCL11B molecular targets have been identified in various tissues and cell lines, including interleukin-2 (IL-2) [228], HIV-1 long ter-

minal repeats [226], and cyclin-dependent kinase inhibitors p21 and p57 [229]. Further gene targets will be discussed within the context of their tissue-specific functions in the following sections.

4.2.2.2 T Cell Commitment, Development and Survival

Intrathymic development of mature T cells from multipotent progenitor thymocytes occurs in distinct phases which are characterised by the serial loss and gain of key cell surface markers. The process of thymic differentiation and maturation is tightly regulated via major checkpoints involving a complex interplay of signal transduction, transcriptional regulation, and sequential rearrangement and assembling of the T cell receptor (TCR) from its pre-Tα and TCRβ subunits [219, 230]. BCL11B is known to regulate at least three checkpoints of this thymic development process (Figure 4.3): 1) T cell commitment at the double-negative DN2 stage; 2) the DN3 to DN4 transition, also known as β selection; and 3) the positive selection step, when double-positive (DP) cells differentiate into single-positive cells (SP).

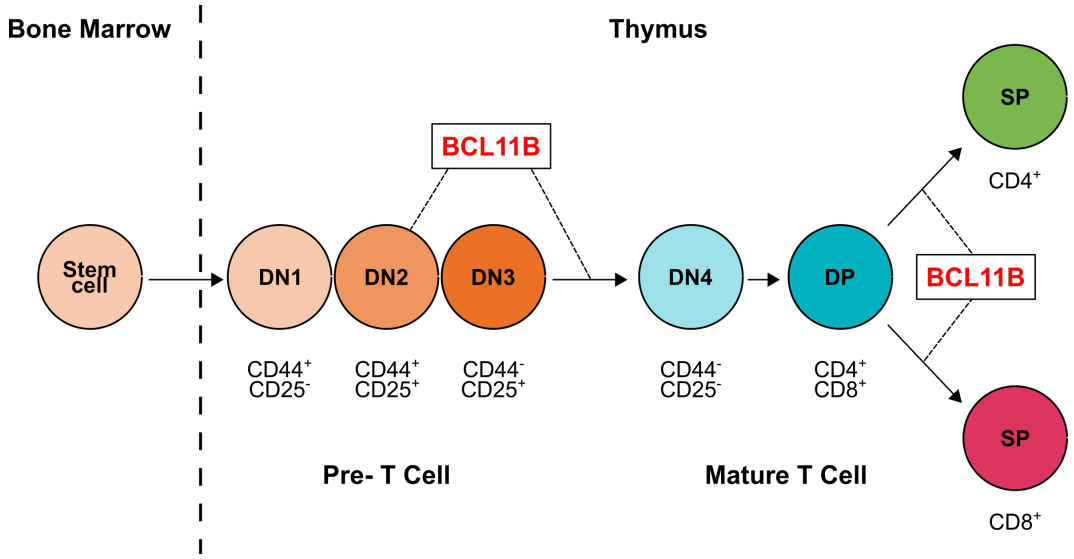

Figure 4.3: Role of BCL11B in thymopoiesis. BCL11B plays a critical role in regulating various stages of thymocyte development and differentiation. DN; double-negative, DP; double-positive, SP; single-positive.

The earliest fully-committed T cells appear at the early double-negative DN2 stage, when cells shed their alternative cellular identities [231]. It is at this stage that *BCL11B* expression is first induced in both human and murine cells [232, 233] through an activation process involving a collaborative machinery of four distinct regulatory elements: Notch signalling, GATA3, T-Cell Factor 1 (TCF1) and Runt-related Transcription Factor 1 (RUNX1) [234]. *Bcl11b* deletion in progenitor cells halts T cells multipotency and lineage commitment [231, 235, 236], impairs components of the TCR complex and its downstream signalling pathways [219], and impedes the expansion of pre-TCR cells [237]

leading to T lymphocyte development arrest. *Bcl11b* deletion at later stages reprograms DN2, DN3 and DP thymocytes into natural killer (NK)-like cells [238], blocks the differentiation of DP into SP cells [230], represses transcription factors involved in CD4 and CD8 lineage commitment [239], and yields defective DP thymocytes with increased glycolipid accumulation and enlarged lysosomal compartments [240]. In mature lymphocytes, BCL11B is expressed in, and is a crucial regulator of, cytotoxic, regulatory and helper T cells (CTL, Treg and Th, respectively), as well as type 2 innate lymphoid cells (ILC2) proper functioning and development [89, 240–242]. BCL11B is also important for thymocyte survival, and its deficiency enhances thymocyte susceptibility to apoptosis [219, 230, 243], possibly due to uncontrolled proliferation because of cell cycle and apoptotic pathway disturbances. For example, *BCL11B* depletion induces cyclin-dependent kinase 6 (CDK6), a regulator of G1/S phase transition, minichrome maintenance proteins, which are involved in establishing replication competence, and the highly regulated Ezrin, Radikin and Moesin (ERM) proteins, which crosslink the cortical actin cytoskeleton with the plasma membrane [244]. Conversely, ectopic expression of *BCL11B* leads to G1 arrest and up-regulation of cyclin dependent kinase inhibitors, *CDKN2C*, *CDKN1C* and *CDKN1B*, of which CDKN2C is a selective inhibitor of CDK6 [245]. Both intrinsic (BCL-2 family mediated) and extrinsic (TNF receptor mediated) apoptotic pathway signals are deregulated in *BCL11B*-deficient T cells. Most notably, the anti-apoptotic proteins BCL-2 and BCL-XL, which are required for mitochondrial integrity, are suppressed while tumour necrosis factor-related apoptosis-reducing ligand (TRAIL) is induced [219, 246]. BCL11B is evidently critical to thymocyte differentiation, proliferation and survival. Parallel functions have been observed in other cell types where BCL11B is expressed as discussed below.

4.2.2.3 Organ Development

4.2.2.3.1 Central Nervous System (CNS)

Bcl11b expression pattern in the CNS is well defined from the early stages of mouse embryonic development, and is maintained through adulthood in the cortex, hippocampus and basal ganglia [211]. Within these regions Bcl11b is highly expressed in several neuronal subtypes, including corticospinal motor neurons (CSMNs), vomeronasal sensory neurons (VSNs), a specific subset of striatal medium spiny neurons (MSNs), and granule neurons of the dentate gyrus, where it plays a vital role in the differentiation, specification and structural organisation of these cells [247–250]. Bcl11b acts as a downstream effector of the transcriptional repressor Fez Family Zinc Finer Protein 2 (FEZF2) in regulating cortical neuronal projection [251], and in its absence CSMNs fail to establish and maintain axonal connections to the spinal cord due to inadequate neuronal outgrowth and pathfinding [247].

Similarly, the loss of Bcl11b function impairs axonal projection of VSNs and innervation of striatal MSNs, resulting in severe abnormalities of the vomeronasal system and defective patterning of striatal compartments [248, 249]. Bcl11b also regulates the proliferation of progenitor cells in the hippocampal dentate gyrus, one of only two regions in the brain that undergoes continuous neurogenesis throughout the lifespan of mammals [250]. Hence, the ablation of *Bcl11b* impedes the functional integration of newly formed neurons into the hippocampal circuitry and diminishes progenitor cell proliferation, leading to impaired learning and memory [250, 252]. Over 240 Bcl11b gene targets have been identified in striatal cells, most of which encode components of the brain-derived neurotrophic factor (BDNF) signalling pathway, which is essential for the differentiation and survival of CNS cells, as well as for the development of high-order cortical functions [253]. Molecules involved in cell adhesion, most notably desmoplakin, have also been identified as Bcl11b targets in neuronal cells [250]. Together, these may explain the gross neurological defects elicited by *Bcl11b* depletion and underscore the critical functions of Bcl11b in the CNS.

4.2.2.3.2 Skin

Bcl11b is highly expressed within murine epidermal and dermal layers during early embryonic development, and is critical in maintaining skin homeostasis, establishing the epidermal permeability barrier and regulating epidermal proliferation and differentiation through inducing epidermal growth factor receptors (EGFR) and Notch1 transcription in keratinocytes [212, 254, 255]. BCL11B expression is markedly diminished in the adult skin, and in both humans and mice is restricted to the epidermal layer [212, 256] where its expression continues to play an important role in barrier function and epidermal homeostasis, as well as in regulating inflammation in the skin microenvironment [257].

4.2.2.3.3 Teeth

Tooth morphogenesis requires the differentiation and organisation of enamel-producing ameloblasts from epithelial precursor cells and dentine-producing odontoblasts from neural crest-derived mesenchymal cells via a series of coordinated epithelial-mesenchymal crosstalk involving multiple growth factors and signalling molecules [258]. The growth and repair of teeth is maintained throughout adulthood through the continuous proliferation and differentiation of epithelial and mesenchymal cells from progenitor and stem cells [258]. Bcl11b is highly expressed in both embryonic and adult teeth, and is a key regulator of ameloblast formation, dental epithelial differentiation and the maintenance of ameloblast progenitor cells [213, 259, 260]. These Bcl11b-mediated functions are under-

pinned by a large network of genes that are targeted by Bcl11b in ameloblasts and dental epithelial cells, including components of the TGFβ signalling pathway, fibroblast growth factors, sonic hedgehog, bone morphogenetic protein (BMP), matrix metallopeptidase 20, enamel-associated genes, β-catenin, and the osteogenic transcription factor MSX2 [213, 259–261].

4.2.2.3.4 Adipose Tissue

Bcl11b has recently been identified in murine white adipose tissue (WAT), where it regulates adipocyte differentiation by suppressing downstream targets of β-catenin/Wnt signalling pathways [214]. Despite a very low expression profile in WAT compared to the thymus, *Bcl11b* deficiency and heterozygosity results in animals with substantially reduced subcutaneous WAT and lower body weights [214, 262], suggesting profound physiological functions of Bcl11b even in tissues where it is lowly expressed.

4.2.3 BCL11B: Pathological Roles

4.2.3.1 Haematological and Intestinal Malignancies

BCL11B has been shown to be a haploinsufficient tumour suppressor gene in both mice [263]and humans [264]. Thus, *BCL11B* deficiency caused by a somatic mutation or allelic deletion is central to a spectrum of malignant transformations. Loss of at least one allele in mice significantly enhanced their susceptibility to thymic lymphoma [265], while in humans *BCL11B* mutations and deletions have been detected in a third of colorectal cancers [266] and 9-16% of T cell-acute lymphoblastic leukaemia (T-ALL) cases [264, 267, 268]. In addition, translocations in the chromosomal region harbouring *BCL11B* have been described in acute myeloid leukaemia (AML) [269, 270], acute mixed lineage leukaemia (AMLL) [271], and acute non-lymphoblastic leukaemia (ANLL) [272]. Targeted silencing of *BCL11B* using small interfering RNA in T cell lines suggests that perturbations of the mitochondrial and death receptor pathways may partly explain the mechanisms predisposing to these malignancies [243, 273].

4.2.3.2 Neurodegenerative Disorders

As a transcription factor that is highly enriched in regions of the brain critical to spatial learning and memory formation, it is unsurprising that *BCL11B* is associated with the pathogenesis of neurodegenerative disorders such as Alzheimer's disease and Huntington's disease (HD). A recent GWAS involving multiple families with hereditary late onset Alzheimer's disease identified *BCL11B* as a

novel causal gene [274], most likely attributable to its transcriptional regulation of BDNF whose levels are reduced in the brains of Alzheimer's patients [275]. In contrast, neural degeneration of the striatum in HD has been attributed to aberrant signalling of the inositol polyphosphate pathway, components of which are targets of BCL11B, which is depleted in HD patients, mouse models and HD cell lines due to mutant Huntington protein expansion [276, 277].

4.2.3.3 Inflammatory and Immune Diseases

BCL11B has been implicated in the pathogenesis of several immune-related disorders. For example, its expression is enhanced in atopic dermatitis (AD) and allergic contact dermatitis due to infiltrating lymphocytes, and is thought to contribute to the epidermal hyperproliferation phenotype of these inflammatory skin conditions possibly because of its role in maintaining cellular proliferation [256]. In fact, selective deletion of *Bcl11b* in mice keratinocytes recapitulates many of the defects observed in human AD and suggests that it is central to the disease aetiology; thymic stromal lymphopoietin (TSLP) is strongly induced in mutant mice which in turn enhances infiltration of chemokines and Th2 cytokines, thereby triggering further recruitment of lymphocytes to the inflammation site [255]. This inflammatory cascade, together with defective barrier functions, are suggested to promote a hyperproliferative response in the epidermis that is typically seen in AD [255]. Selective abrogation of *Bcl11b* in the epidermis elicits a similar exacerbated inflammatory response, with significant up-regulation of the inflammatory mediators IL4, IL6 and TSLP in the skin [257]. A similar manifestation was found in mice colons, where selective deletion of *Bcl11b* either at the T cell DP stage or in mature Treg cells triggered substantial leukocyte infiltration, accompanied by colon thickening, epithelial damage and disruption of the intestinal gland architecture, recapitulating key features of inflammatory bowel disease [241]. This phenotype appears to reflect a global alteration in the gut inflammatory profile, marked by a reduction of FOXP3 and IL10 suppressor functions, and increased proinflammatory cytokines TNF, IL17 and interferon γ (IFNγ), which together contribute to the infiltration of Th1 and Th17-producing CD4+ T cells, as well as neutrophils, dendritic cells and macrophages in the colons of mutant mice [241].

Finally, a heterozygous missense mutation in *BCL11B* yielding a dominant negative activity in the protein was recently discovered in a case of severe combined immunodeficiency (SCID) [278]. The mutant case displayed broad-spectrum abnormalities reflecting the multifaceted role of BCL11B in thymopoiesis and in organ development. These included the developmental arrest of immature T cells, severe craniofacial and dermal anomalies, an absent corpus callosum, intellectual impairment and pulmonary artery stenosis [278], substantiating the possibility of an important vasculature role

for BCL11B.

4.2.3.4 Potential Role in Aortic Stiffness

The multifaceted roles of BCL11B across diverse tissue types is well recognised, but its function in the aorta remains obscure despite accumulating evidence implicating it as a candidate gene for aortic stiffness. Indeed, *BCL11B* transcript levels measured in circulating leukocytes were recently correlated with PWV and decreased carotid distensibility in the Twins UK Cohort [95]. In view of the earlier described functions, the working hypothesis was that BCL11b may regulate the expression of genes that either directly regulate the architecture of the vessel wall or promote vascular calcification, inflammation and/or vascular SMC apoptosis. BCL11B interacts with COUP-TFII, a repressor of the notch signalling pathway which regulates arterial-venous blood vessel identity [221, 279]. In addition, the deletion or ectopic expression of *BCL11B* leads to perturbations of several genes and signalling pathways that have recognised roles in vascular calcification and extracellular matrix synthesis, deposition, turnover and assembly (Figure 4.4A and B). These include bone morphogenetic protein 4 (*BMP4*), IFNγ, nuclear factor kappa-light-chain-enhancer of activated B cells (*NFκB*), TGFβ signalling, heme oxygenase-1 (*HMOX-1*), fibronectin-1 (*FN1*), cadherin-10 (*CDH10*), collage type 1 alpha-1 (*COL1A1*), *SMAD1*, and the Wnt/β-catenin signalling pathway [214, 241, 243, 259, 280–282]. The role of BCL11B in thymopoiesis and in promoting the recruitment and infiltration of leukocytes, which has been extensively discussed earlier, suggests a possible inflammatory-mediated mechanism for BCL11B in promoting aortic stiffness (Figure 4.4C). Similar to its role in thymocyte survival, Bcl11b has recently been found to regulate genes involved in cell-cycle progression in murine mammary epithelial cells, including the cell-cycle repressors Foxo1/3&4, and cyclin-dependent kinase inhibitors Cdkn1a and Cdkn2a [283]. This suggests that the anti-apoptotic property of BCL11B may extend to other cell types, such as vascular SMCs, potentially contributing to the aetiology of aortic stiffness through this pathway (Figure 4.4D), especially as the anti-apoptotic proteins BCL-2 and BCL-XL, which are both effector targets of BCL11B in lymphocytes, are also key regulators of apoptosis within vascular SMCs [284].

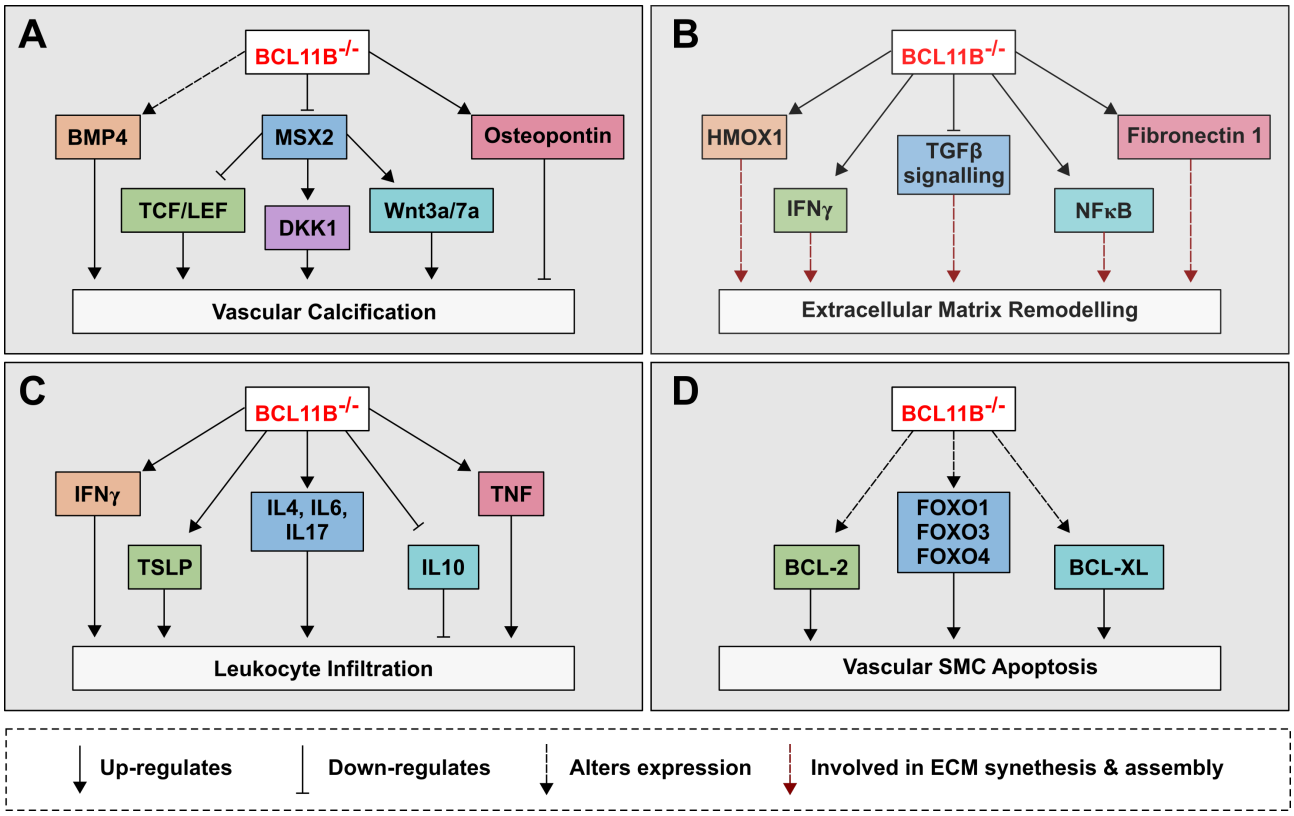

Figure 4.4: Potential pathways implicating BCL11B in aortic stiffness

4.2.4 DB129663: A Primate-Specific Long Non-Coding RNA

LncRNAs encompass a diverse group of non-protein-coding RNA species that are longer than 200 nucleotides. DB129663 (CCDS ID: AL163932.1 or RP11-6101.1) is a lncRNA lying directly within the region which has a significant association with cfPWV in the *AortaGen Consortium* GWAS meta-analysis. Specifically, the enhancer region maps to the promoter of DB129663, suggesting it may also be a target of the 14q32.2 enhancer elements. The DB129663 transcript is 542 bp in length and contains 3 non-coding exons (ENST00000555776.1). Mitchell et al. [72] reported the positive expression of DB129663 in the kidney and various cell lines, including aortic SMCs, umbilical vein endothelial cells, and cardiac fibroblasts. DB129662 is also reported to be expressed in the thymus, lung, temporal lobe and cerebral cortex (Ensembl database, version 89); however, the functional characteristics and expression patterns of DB129663 in the aorta remain undefined and therefore open to investigation. Despite the sharp rise of annotated lncRNAs over recent years, only a few have been functionally characterised [285], and therefore their precise role in human biology and disease risk and progression remains speculative. Notwithstanding, it is emerging that lncRNAs are essential actors in the transcriptional regulation of gene expression, either by recruiting various chromatin-modifying complexes [286], directly binding to RNA, DNA and proteins [287, 288], altering mRNA

stability [289], or altering chromatin conformation and sequestering its targets [290, 291]. LncRNAs are thus critical to a number of biological processes, including cellular proliferation [292], mitochondrial function [293], mammalian embryogenesis [287] and organ development [294]. Given these broad physiological functions, mutations in lncRNAs have been linked to a range of complex diseases and heritable conditions, including Alzheimer's disease [295], diabetes [296], HIV [297], various types of cancers [217, 298–300] and Coeliac disease [301] amongst many others. Several mechanisms for how lncRNAs may be impacted by genetic variants in regions involving their transcriptional control (e.g. enhancers or promoters) have been proposed. These include altering lncRNA transcript levels, inducing alternative splicing, and/or altering lncRNA function by modifying their secondary structures [210,302]. Identifying the influence of chromosome 14 SNPs on DB129663 transcripts in the aorta may provide important insights and possible therapeutic targets for aortic stiffness.

4.3 Methods

4.3.1 SNP Genotyping

The five SNPs selected for genotyping in this study are rs1381289, rs7152623, rs1461587, rs10782490 and rs17773233. These were the top SNPs from the *AortaGen Consortium* meta-analysis and are in a tight linkage disequilibrium (LD) block (D'=1). SNPs were genotyped by TaqMan® SNP genotyping assays as detailed in Chapter 2. The genetic information collected for each of the polymorphisms differed depending on gDNA quality and availability and/or genotyping assay failures.

4.3.2 Gene Expression

Gene expression levels of *BCL11B*, *CD45*, *CD25*, *CD8A* and *CD235A* were quantified using TaqMan® gene expression assays as detailed in Chapter 2.

4.3.3 PBMC RNA Extraction

cDNA generated from peripheral blood mononuclear cells (PBMCs) was used as a positive control for *BCL11B* and DB129663 gene expression experiments. Blood drawn from healthy donors was stored in PAXgene Blood RNA Tubes and total RNA was extracted using a PAXgene Blood RNA Validation Kit (PreAnalytix, Switzerland). Briefly, the PAXgene Blood RNA Tube was subjected to centrifugation at 3000 $\times$ g for 10 min and the supernatant discarded. The pellet was dissolved in RNase-free water by vortexing, followed by a second centrifugation step at 3000 $\times$ g for 10 min. The

pellet was dissolved in 350 µl resuspension buffer by vortexing and then transferred to a microcentrifuge tube. Next, 300 µl binding buffer and 40 µl proteinase K were added and the mixture was incubated at 55°C for 10 min in a shaking-incubator. The lysate was transferred to a PAXgene Shredder spin column, subjected to centrifugation at 18,000 $\times$ g for 3 min and the supernatant collected in a new microcentrifuge tube and mixed with 350 µl of 96-100% ethanol. The sample was transferred to a PAXgene RNA spin column, subjected to centrifugation at 18,000 $\times$ g for 1 min and the flow-through discarded. This was followed by a series of washes with wash buffers 1 and 2, and a final RNA elution in 40 µl nuclease-free water. On-column DNase treatment was performed prior to elution using PureLink® DNase Set (ThermoFisher Scientific, USA) to ensure digestion of all genomic DNA.

4.3.4 Preparation of Competent Cells

E. coli strain K-12 (New England Biolabs, UK) was pre-cultured and a single colony inoculated into 100 ml of LB medium and incubated at 37°C in a shaking-incubator. The optical density at 600nm (OD_{600}) was monitored at regular intervals to examine culture growth, and cells were harvested when an OD_{600} of 0.5-0.6 was reached. After briefly spinning, the cell pellet was re-suspended in 40 ml ice-cold 30 mM potassium acetate (pH 5.8), 50 mM $MnCl_2$, 100 mM KCl, 10 mM $CaCl_2$ and 15% glycerol, and stored on ice for 10 min. After briefly spinning the cell pellet was gently re-suspended in 4 ml ice-cold 10 mM MOPS-NaOH, 10 mM KCl, 75 mM $CaCl_2$ and 15% glycerol. Cells were snap frozen on dry ice and stored at -80°C. This protocol yielded a transformation efficiency of 6×10^7 colony forming units per µg of pUC19 DNA.

4.3.5 Plasmid Construct

The pcDNA3.1-FLAG-BCL11B plasmid was generated by PCR amplification using *BCL11B* expressed in the vector pORF (ORF016116, Applied Biological Materials Inc., Canada) as the template, and the following primers: 5'-CAAGGATGACGACG ATAAGGGATCCATGTCCCGCCGCAAACAG-3' and 5'-TTTAAACGGGCCCTCTA GACTCGAGCTCCTCTCGGCCTGCTC-3'. The PCR product was gel-purified and cloned into the BamHI/XhoI sites of pcDNA3.1(+)-FLAG mammalian expression vector (donated by Sumedha Garg, Cambridge, UK) using a NEBuilder® HiFi DNA Assembly Master Mix (New England BioLabs Inc., UK). Briefly, a 20 µl reaction mixture consisting of 60 fmol *BCL11B* insert DNA, 30 fmol vector DNA and 10 µl HiFi Assembley Master Mix were incubated for 60 min at 50°C then stored at 4°C.

4.3.6 Bacterial Transformation and Plasmid Purification

For transformation, 50 µl of competent cells and 2 µl of the assembled product were mixed and kept on ice for 30 min then heat-shocked in a 42°C water bath for 30 s before immediately chilling on ice for 2 min. Next, 550 µl of super optimal broth with catabolite repression (SOC) medium was added to the cells which were incubated at 37°C for 90 min with shaking at 250 rpm, before 100 µl was plated onto a LB agar plate supplemented with ampicillin and incubated at 37°C overnight. Single transformant colonies were inoculated into 5ml LB broth supplemented with ampicillin and incubated at 37°C overnight with shaking at 250 rpm. A High Pure Plasmid Isolation Kit (Roche, UK) was used to purify plasmid DNA for verification by Sanger sequencing (Source Bioscience, Cambridge, UK). A Qiagen Plasmid Plus Kit (QIAGEN, Germany) was used to purify plasmid DNA for cell transfection.

4.3.7 HEK293 Transfection

HEK293T cells were maintained in Dulbecco's modified Eagle's medium (DMEM) supplemented with 10% foetal bovine serum and 1% penicillin and streptomycin (ThermoFisher Scientific, USA). Cells were plated at a density of 1×10^5 per well in a 12-well plate and incubated for 24 h at 37°C in 5% CO_2. Cells were transfected with either FLAG-BCL11B or empty vector using the stable cationic polymer polyethylenimine (PEI). PEI condenses DNA into positively charged particles that bind to anionic cell surfaces; consequently, the PEI-DNA complex is endocytosed by a cell and the DNA is released into the cytoplasm [303]. For each well, 200 ng DNA was diluted in 100 µl of reduced serum media Opti-MEM (ThermoFisher Scientific, USA). PEI was added to the mixture at a 3:1 ratio of PEI (µg):DNA (µg) and incubated for 15 min, then gently added to the cells. Transfected cells were harvested after 48 h for Western blotting analysis or RNA extraction. Transfection was confirmed by qPCR and Western blotting analysis (Figure 4.5) using a rabbit polyclonal anti-FLAG antibody (F7425, Sigma-Aldrich, USA) and a mouse monoclonal anti-GAPDH (Sigma-Aldrich, USA) for the loading control.

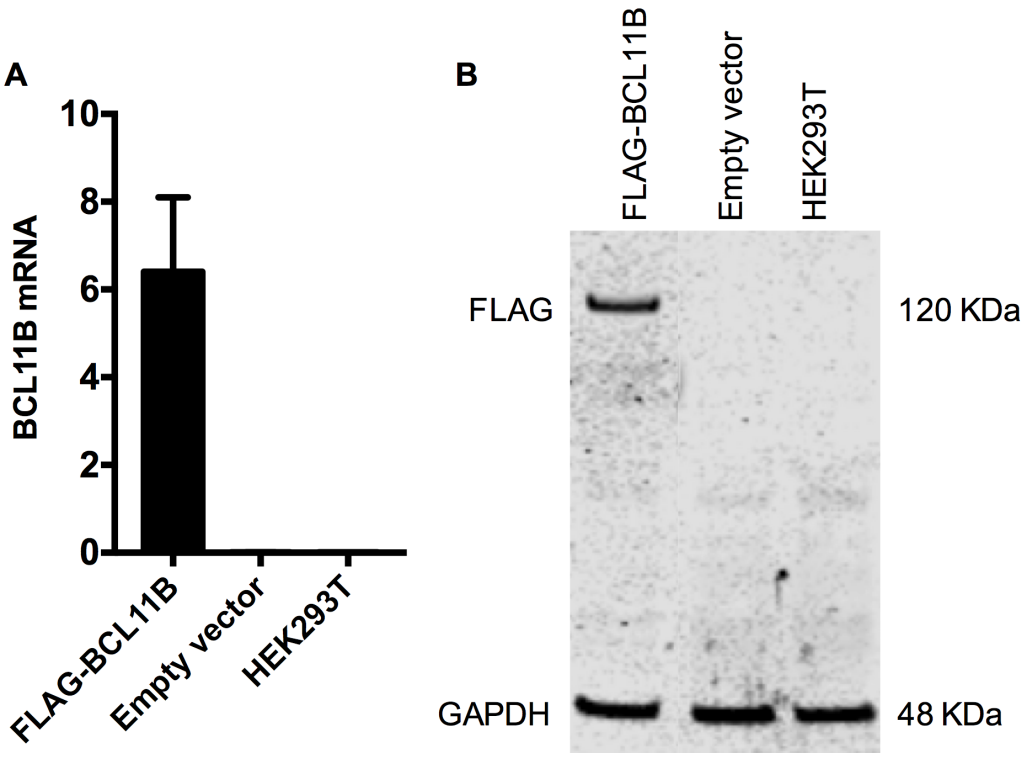

Figure 4.5: Confirmation of BCL11B transfection. (A) *BCL11B* mRNA detected in the transfected cells but not in the empty vector or HEK293T cells; (B) Western blot showing a positive band from BCL11B-transfected cells detected using anti-FLAG antibody

4.3.8 Antibodies

BCL11B expression in the aorta was probed using five antibodies that recognise different epitopes on BCL11B and are detailed in Table 4.1.

Table 4.1: List of antibodies used to probe BCL11B expression

Clonality	Catalog ID	Epitope	Dilution		
			WB	IHC	IF
Rat monoclonal	ab184565, Abcam	1-150	1:400	1:500	1:300
Rabbit monoclonal	12120, CST Signalling	300-450	1:200	1:500	1:200
Rabbit polyclonal	ab70452, Abcam	500-550	1:200	1:1000	1:200
Rabbit monoclonal	ab187668, Abcam	500-600	1:200	1:500	1:100
Rabbit polyclonal	ab28448, Abcam	850-950	1:400	1:1000	1:200

WB; Western blotting, IHC; immunohistochemistry, IF; immunofluorescence.

CD45 expression was probed with a rabbit polyclonal anti-CD45 antibody(ab10558, Abcam, UK), and a beta-actin rabbit polyclonal IgG (ThermoFisher Scientific, USA) antibody was used for the Western blotting loading control at a 1:1000 dilution. Donkey anti-rabbit (925-32213, LI-COR Biotechnology UK Ltd, UK) IRDye® 800CW and goat anti-rat Alexa Fluor® 680 (A21096, ThermoFisher Scientific, USA) conjugated secondary antibodies were both used at a 1:5000 dilution for Western

blotting analysis.

4.3.9 Bcl11b Expression in Mice

Brain, thymus, spleen and whole aortic tissues were harvested from 10-week-old wild-type mice (n=9) and preserved in either RNAlater® for gene expression and Western blotting analysis then stored at -80°C, or in 4% (v/v) paraformaldehyde overnight for immunohistochemical staining. The aortae were perfused 3 times with RNA-free PBS immediately after harvesting to remove blood contamination. Adipose tissue was trimmed from aortic samples used for Western blotting analysis and gene expression. RNA was extracted using a RNeasy Mini Kit (QIAGEN, Germany) and cDNA generated using GoScriptTM Reverse Transcription (Promega, USA). *Bcl11b* mRNA was probed using a TaqMan® gene expression assay (Mm00480516_m1) and a Eukaryotic 18S rRNA Endogenous Control (ThermoFisher Scientific, USA) for normalisation. Protein was extracted from tissues using RIPA buffer supplemented with Calbiochem® protease inhibitors (Merck, USA). Bcl11b was probed using a rabbit polyclonal anti-Bcl11b (ab70452, Abcam, UK) antibody at a 1:200 dilution for Western blotting analysis as described earlier. The EnVision™ + Dual Link system (Dako, UK) was used for immunohistochemical detection with a rabbit polyclonal anti-Bcl11b (ab70452, Abcam, UK) antibody at a 1:1000 dilution. Bcl11b was further probed in tissues harvested from 10-week-old Bcl11b-tdTomato reporter mice (a gift from Dr Pentao Liu, Wellcome Trust Sanger Institute, Cambridge, UK). The reporter mice were on a C57BL/6 background and the tdTomato cassette was targeted to the 3'UTR of *Bcl11b*. To generate conditional knockouts mice were injected with tamoxifen 1 week prior to tissue harvesting, resulting in the deletion of exon 4 of *Bcl11b*. A rabbit polyclonal anti-RFP (600-401-379, Rockland Immunochemicals, USA) antibody was used at a 1:2000 dilution for Western blotting analysis. Human colorectal cells expressing tdTomato (a gift from Fatima Junaid, Cancer Research UK Cambridge Institute) were lysed using RIPA buffer and the protein lysate used as a positive control for RFP.

4.3.10 DB129663 Transcript Detection

4.3.10.1 Real-Time qPCR

The DB129663 transcript was examined in 50 randomly selected aortic samples using three custom gene expression assays as detailed in Table 4.2. The assays yielded a positive signal in PBMCs but failed to amplify DB129663 in all the aortic samples tested, potentially due to low transcript abundance in these samples.

Table 4.2: DB129663 gene expression assays

	Forward Primer/ Reverse Primer (5′-3′)	Probe (5′-3′)
1	CAGAGGAGCAGATAAGGAAGCAA/ TCATTTCCTTGCCATCCACAGT	ATAGCTCCCGACAAATC
2	CATTTCCTTGCCATCCACAG/ GTTTACACATGCGGACAAGC	TAACCCACTCACCATCCCTGACCA
3	information withheld by manufacturer	TCACTCCAGGCTTTTAATTTCAGTC

4.3.10.2 PCR Amplification

As RT-qPCR lacked the sensitivity to detect the DB129663 transcript in the samples tested, the presence of the transcript was explored by PCR amplification using five different primer combinations, which are listed in Table 4.3. Sequences were evaluated using the BLAST search algorithm and primers were subsequently synthesised by Sigma-Aldrich (USA).

Table 4.3: DB129663 PCR combinations

	Forward Primer (5′-3′)	Reverse Primer (5′-3′)	Exons
1	GCTATGACAAGTTCCACTGTGG	CACTGGGTGGAGTTAGCAGGTT	1-2
2	CAACAACCTTCTTCTCCATGC	AGGGTGCCTGAGGATGGTGA	1-3
3	CAACAACCTTCTTCTCCATGC	CAACAACCTTCTTCTCCATGC	1-2
4	TTCAAGTCAGCAGCATAGGG	TACACTGCAGCCACTTCTCA	2-3
5	CAACAACCTTCTTCTCCATGC	TACACTGCAGCCACTTCTCA	1-3

The PCR reaction consisted of 2 µl stock cDNA, 1$\times$ PCR buffer (BioGene, UK), 2.5 mM MgCl2, 1 U Taq DNA Polymerase Gold (BioGene, UK), 0.25 µM of each primer and 100 µM dNTP mix (Promega, USA) in a final volume of 20 µl. The PCR thermal cycling conditions consisted of an initial denaturing step at 95°C for 10 min followed by a touchdown procedure of 15 cycles of denaturing at 95°C for 30 s, annealing at 75°C for 45 s decreasing by 1°C per cycle and extension at 72°C for 60 s. The touchdown procedure was followed by 25 cycles of denaturing at 95°C for 30 s, annealing at 60°C for 45 s and extension at 72°C for 60 s, with a final extension of 72°C for 10 min. Amplified PCR products were separated on a 2% (w/v) agarose gel stained with ethidium bromide at 100 V for 40 min. Products were gel purified using a Wizard SV Gel and PCR Clean Up System (Promega, USA) and the samples verified by Sanger Sequencing (Source Bioscience, Cambridge, UK). This protocol yielded non-specific products for primer combinations 1 and 2, and less than a 5% detection rate in 100 randomly selected aortic samples with primer combinations 3-5.

PCR amplification was further attempted with primer combinations 3-5 using a high-fidelity polymerase. The PCR reaction consisted of 2 µl stock cDNA, 2.5 U Q5 High-Fidelity DNA Polymerase

(New England BioLabs, USA), 1× Q5 Reaction Buffer, 1× Q5 High GC Enhancer, 0.25 µM of each primer and 200 µM dNTP mix (Promega, USA) in a final volume of 25 µl. The thermocycling conditions consisted of an initial denaturation at 98°C for 30 s, followed by 35 cycles of denaturing at 98°C for 10 s, annealing for 20 s and extension at 72°C for 20 s, with a final extension at 72°C for 2 min. Optimal annealing temperatures for each primer combination was determined using the NEB Tm calculator tool (New England BioLabs, USA). PCR products were separated on an agarose gel and purified before being verified by Sanger Sequencing. While this protocol improved product specificity, the detection rate remained below 5% in 50 randomly selected aortic samples.

4.3.10.3 ExiLERATE LNA Real-Time PCR

Locked nucleic acid (LNA™) oligonucleotides are modified nucleic acids in which the ribose sugar is conformationally locked by connecting the 2' oxygen to the 4' carbon position [304]. The resultant oligonucleotides have enhanced hybridisation stability to complementary nucleic acids, making them useful for detecting low abundance transcripts. The following LNA primers were synthesised by EXIQON (Denmark): 5'-GCTATGACAAGTTCCACTG-3' and 5'-GTGCCTGAGGATGGTG-3'. Real-time PCR was carried out using the ExiLERATE SYBRGreen Master Mix (EXIQON, Denmark) with a final concentration of 200 nM for each primer and 0.8 µl cDNA template in a final reaction volume of 10 µl. The thermocycling conditions consisted of an initial denaturation at 95°C for 10 min followed by 40 amplification cycles at 95°C for 10 s and 60°C for 1 min. Transcripts were below detection limits for quantification and the presence or absence of DB129663 was therefore verified by agarose gel electrophoresis.

4.3.11 Statistical Analysis

Non-normally distributed variables were log-transformed for statistical analyses. Pearson's correlation coefficients were used to determine correlations between age and aortic measurements, and deviations from the Hardy-Weinberg equilibrium were tested using the χ^2 test. For each SNP Student's t-tests with Welch's correction were used to compare *BCL11B* mRNA differences between the two homozygous allele carriers. As the thoracic section of the aorta differs histologically and embryologically from the abdominal segment, regression models were constructed using samples from the ascending aorta, arch and thoracic aorta only (n=185). Associations between SNPs and log normalised PWV were tested assuming an additive inheritance pattern in multiple linear regression models, and adjusting for confounders such as age, age^2, gender, height and weight, which are known to influence aortic PWV. Pearson's correlation coefficients were used to determine bivariate

correlations between *BCL11B* and *CD* markers. Associations between SNP genotypes and the presence or absence of DB129663 transcripts were tested using Pearson's χ^2 test (df=2). In all statistical tests a p-value of <0.05 was considered significant.

4.4 Results

4.4.1 Study Sample Characteristics

4.4.1.1 Clinical and Demographic

The clinical and demographic features of the donor samples are provided in Table 4.4. The majority of the samples were obtained from healthy Caucasian donors, 57% of which were male. Less than 10% had a documented history of cardiovascular disease, although nearly 30% were recorded to be hypertensive and 17% had an inflammatory condition. In total, 87% of the specimens were retrieved from the thoracic and ascending aorta, and nearly all had a grossly normal internal appearance except for a minority that had visible plaques or calcification. PWV derived from *ex vivo* elastic modulus measurements were comparable to *in vivo* values in the literature for PWV [305]. No significant differences were observed in mean PWV between genders (P=0.57, Student's t test).

Table 4.4: Baseline characteristics of the study cohort

	All Subjects (n=214)	**Range (Min-Max)**
Male/Female	125/89	
Age (years)	57 (19)	17-83
Height (m)	1.7 (0.2)	1.45-2.0
Weight (Kg)	80 (20)	47-160
BMI (Kg/m^3)	27.04 (6)	16-69
SBP (mmHg)	120 (32)	40-260
DBP (mmHg)	68±14	20-120
Elastic Modulus (MPa)	0.14 (0.09)	0.05-0.63
PWV (m/s)	3.53 (0.97)	2.4-9.49

Data are mean± SD or median (IQR)

4.4.1.2 Age and Aortic Dimensions

In agreement with the published literature [306–308], aortic wall thickness (r=0.48, P<0.0001), radius (r=0.61, P<0.0001) and stiffness measurements (r=0.39, P<0.0001 for elastic modulus and r=0.42, P<0.0001 for PWV) correlated strongly with age (Figure 4.6) and PWV was significantly higher in donors with a reported history of hypertension (P<0.001, Student's t test). Age correlations across all parameters were strong for both genders (Male vs. female: r=0.57, P<0.0001 vs. r=0.35, p=0.001

for aortic wall thickness, r= 0.74, P<0.0001 vs. r=0.46, P<0.0001 for aortic radius, r=0.38, P<0.0001 vs. r=0.46, P<0.0001 for elastic modulus and r=0.39, P<0.0001 vs. r=0.48, P<0.0001 for PWV).

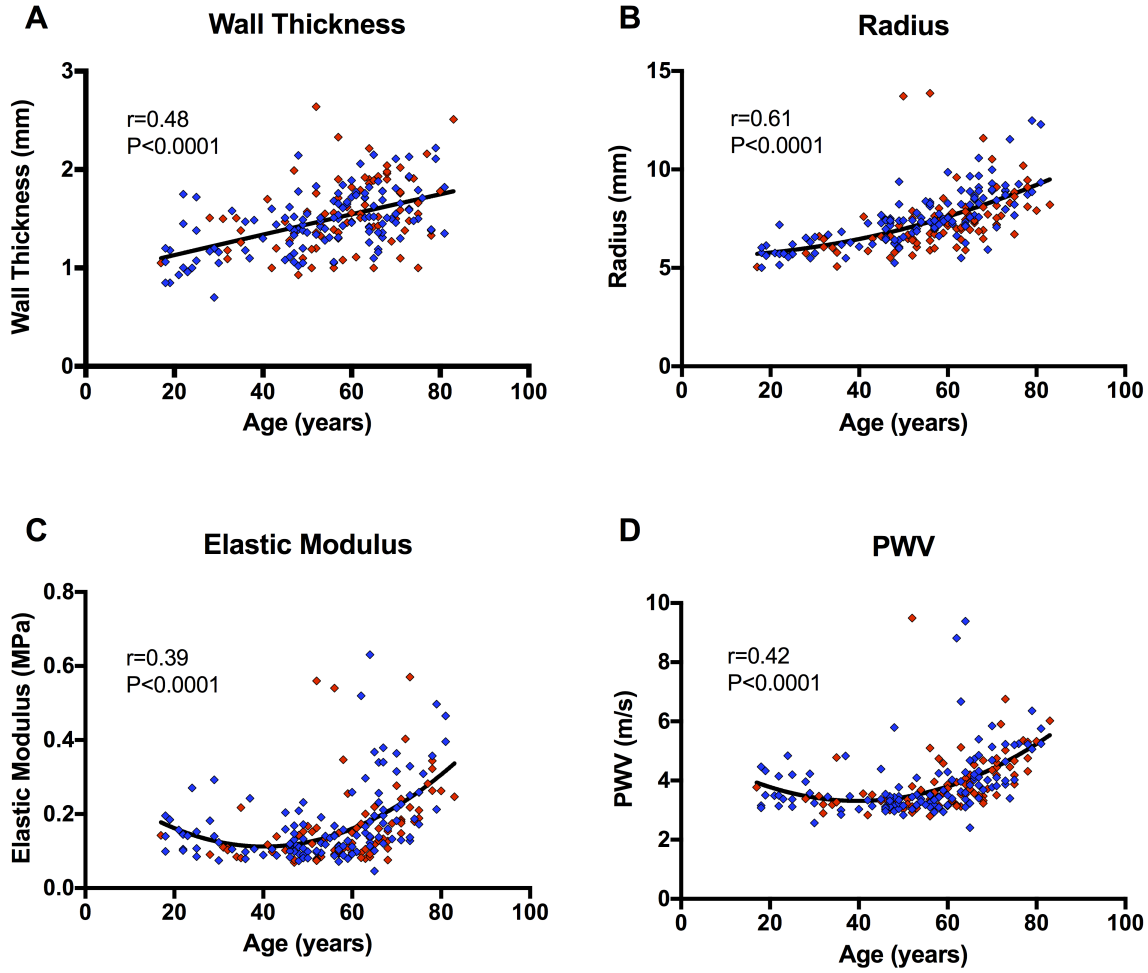

Figure 4.6: Correlation plots of age against aortic dimensions and stiffness measures. Aortic wall thickness, radius, elastic modulus and PWV increases with increasing age. The trend is similar between genders (Blue data points represent males and red data points represent females).

4.4.2 Association of 3'*BCL11B* Gene Desert SNPs with Aortic Stiffness

The association of PWV in donor aortas (n=209) was investigated against the lead SNPs from the *AortaGen Consortium* meta-analysis. Details of the five SNPs, including minor allele frequency and genotype percentages, are provided in (Table 4.5), and the Hardy-Weinberg equilibrium was found to be satisfied for all the SNPs tested.

Table 4.5: Chromosome 14 polymorphisms with genotype and allele frequencies

SNPs	Genotypes	N(%)	Hardy-Weinberg Test	Alleles	N(%)	Global MAF
rs1381289	CC	60 (29.1)	χ^2=0.312	C	226 (54.9)	T=40.1%
	CT	106 (51.5)	P=0.576	T	186 (45.1)	
	TT	40 (19.4)				
rs7152623	AA	73 (35.4)	χ^2=1.024	A	251 (60.9)	A=28.5%
	AG	105 (51.0)	P=0.312	G	161 (39.1)	
	GG	28 (13.6)				
rs1461587	GG	11 (5.3)	χ^2=0.495	G	88 (21.2)	G=21.8%
	GT	66 (31.7)	P=0.482	T	328 (78.8)	
	TT	131 (62.9)				
rs10782490	CC	49 (23.9)	χ^2=0.395	C	205 (50)	T=48.7%
	CT	107(52.2)	P=0.530	T	205 (50)	
	TT	49 (23.9)				
rs17773233	GG	138 (66.4)	χ^2=0.098	G	338 (81.2)	T=11.6%
	GT	62 (29.8)	P=0.754	T	78 (18.8)	
	TT	8 (3.8)				

Global minor allele frequency (MAF) is derived from the 1000Genome data, retrieved from dbSNP (`https://www.ncbi.nlm.nih.gov/snp/`).

Allele frequencies of the 5 SNPs investigated in this aortic tissue resource were comparable to those observed in the GWAS meta-analysis. The minor allele frequencies were 0.45 vs. 0.44 for rs1381289, 0.39 vs. 0.42 for rs7152623, 0.21 vs. 0.26 for rs1461587, 0.50 vs. 0.47 for rs10782490 and 0.19 vs. 0.19 for rs17773233; donor aortae vs. *AortaGen Consortium*, respectively.

All the SNPs from the GWAS meta-analysis showed an allele-dose trend with the calculated PWV in the aortic tissue resource (Figure 4.7A). Multiple linear regression models, including traditional confounders for PWV, such as age, age^2, gender, height and weight, were constructed, and this analysis showed that only two SNPs, rs1381289 and rs7152623, were associated significantly and independently with PWV (Table 4.6). These two associations remained significant in the subsequent multiple regression analysis which excluded abdominal aorta and iliac segments (n=185) although a third SNP, rs10782490 was also found to reach statistical significance in this analysis. No evidence of a significant PWV association was seen with rs17773233 and rs1461587 in either analyses but the results pointed towards a protective effect for their minor alleles.

Table 4.6: Multiple regression analysis showing parameters associated with PWV

Model	Predictors	Primary Analysis*			Secondary Analysis**		
		β	P	Adj R^2	β	P	Adj R^2
1	Age	2.110	<0.001	0.41	1.967	<0.001	0.45
	Age^2	-2.592	<0.001		-2.495	<0.001	
	Gender	0.008	0.913		-0.009	0.899	
	Height	0.063	0.395		0.063	0.441	
	Weight	-0.079	0.184		-0.049	0.445	
	rs1381289	-0.136	**0.015**		-0.157	**0.007**	
2	Age	2.104	<0.001	0.41	1.964	<0.001	0.44
	Age^2	-2.572	<0.001		-2.475	<0.001	
	Gender	0.015	0.832		-0.001	0.988	
	Height	0.067	0.368		0.069	0.393	
	Weight	-0.075	0.213		-0.046	0.473	
	rs7152623	0.118	**0.035**		0.139	**0.017**	
3	Age	2.063	<0.001	0.40	1.887	<0.001	0.43
	Age^2	-2.536	<0.001		-2.409	<0.001	
	Gender	0.019	0.786		0.003	0.966	
	Height	0.070	0.349		0.073	0.374	
	Weight	-0.081	0.182		-0.053	0.417	
	rs10782490	-0.098	0.083		-0.120	**0.039**	
4	Age	2.046	<0.001	0.40	1.900	<0.001	0.43
	Age^2	-2.526	<0.001		-2.428	<0.001	
	Gender	0.032	0.653		0.023	0.751	
	Height	0.073	0.330		0.079	0.333	
	Weight	-0.076	0.204		-0.047	0.468	
	rs17773233	-0.095	0.087		-0.098	0.090	
5	Age	2.059	<0.001	0.42	1.898	<0.001	0.43
	Age^2	-2.532	<0.001		-2.420	<0.001	
	Gender	0.032	0.648		0.024	0.738	
	Height	0.069	0.356		0.075	0.358	
	Weight	-0.075	0.215		-0.046	0.475	
	rs1461587	-0.070	0.216		-0.080	0.171	

*regression analysis for PWV, adjusted for age, age^2, gender, height and weight using an additive gene-dose model;

**regression analysis for PWV, adjusted for age, age^2, gender, height and weight using an additive gene-dose model and excluding abdominal and iliac samples ;

The parameter β is the estimated effect on PWV per minor allele in the additive model.

4.4.3 3'*BCL11B* Gene Desert SNPs and Aortic *BCL11B* Gene Expression

Because the SNPs investigated reside within a region harbouring gene regulatory elements, evidence that these variants had distal regulatory effects on *BCL11B* transcript, the nearest known gene of this locus on the minus strand was sought. Allelic effects were estimated by comparing the mean expres-

sion of *BCL11B* mRNA in the two homozygote classes for each SNP (Figure 4.7B). The homozygous risk allele (T) of the lead SNP rs1381289 showed 3-fold lower *BCL11B* expression compared to the homozygous C-allele (P=0.0005); heterozygous individuals displayed an intermediate phenotype. The association was weakened but remained significant in the secondary analysis that excluded abdominal and iliac aortic rings (P=0.005). Similarly, the homozygous risk (A) allele of rs7152623 showed 2.3-fold lower *BCL11B* expression compared to the homozygous G-allele (P=0.004) and remained significant in the secondary analysis (P=0.040). Consistent with this, the homozygous risk (C) allele of rs10782490 also showed lower *BCL11B* transcript expression compared to the homozygous T-allele (1.8-fold, P=0.05); however, the association was no longer significant in the secondary analysis. *BCL11B* transcript levels were not influenced by the rs1461587 or rs17773233 genotypes in both the primary and secondary analyses, although there was a trend towards lower *BCL11B* mRNA expression among carriers of the risk allele. Together, this data demonstrates that three of the risk SNPs are associated with lower *BCL11B* expression and behave as expression-associated SNPs (e-SNPs).

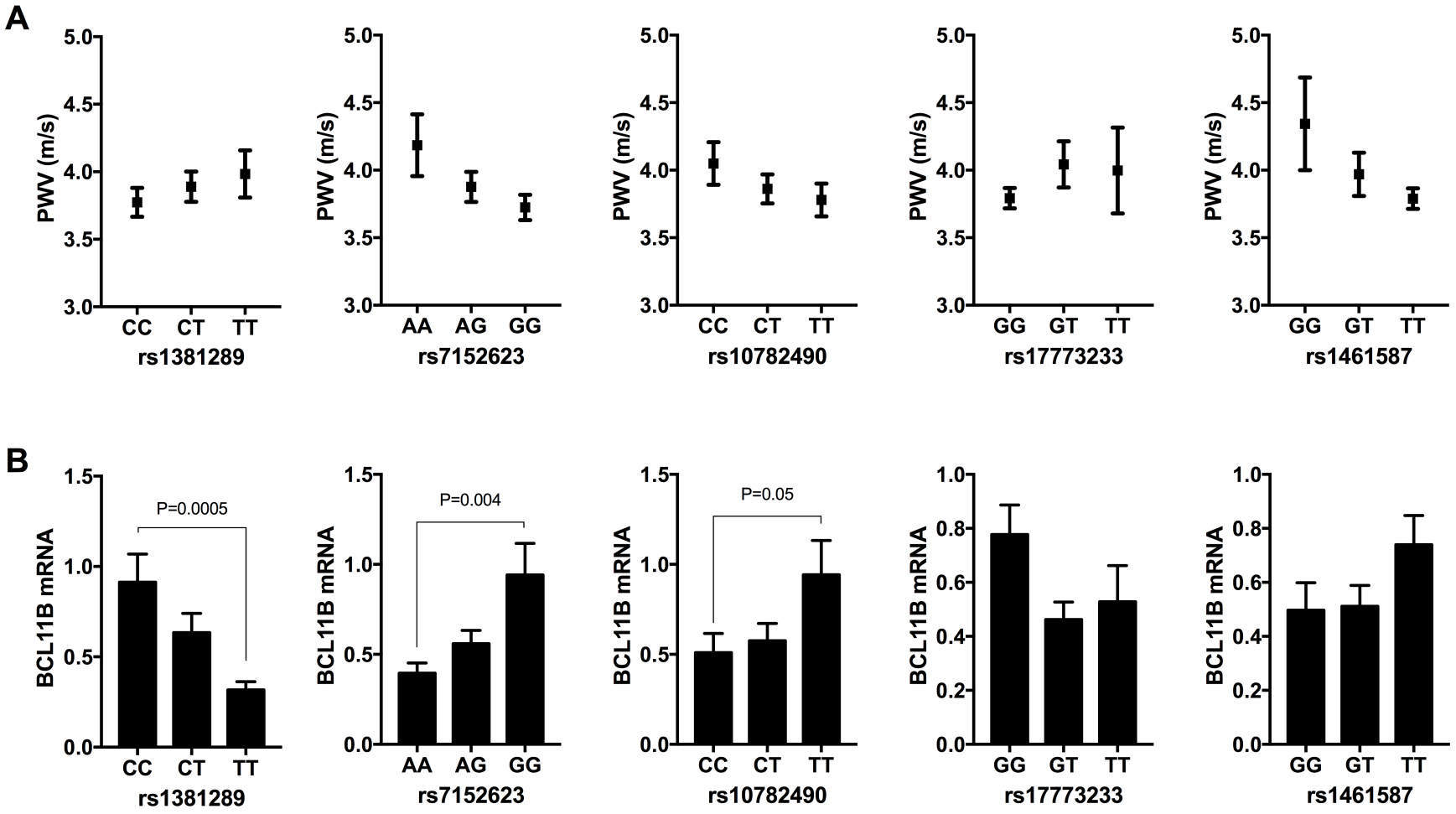

Figure 4.7: Association of 3'*BCL11B* gene desert SNPs with PWV and *BCL11B* gene expression in human aortic tissue. (A) PWV stratified by genotype, data are mean±SEM; (B) *BCL11B* mRNA stratified by genotype, data are mean±SEM.

4.4.4 *BCL11B* Aortic Distribution

The expression pattern of *BCL11B* was further examined across the length of the aorta and it was found that *BCL11B* transcript was mostly abundant in the ascending aorta, followed by the thoracic, abdominal and iliac arteries (Figure 4.8).

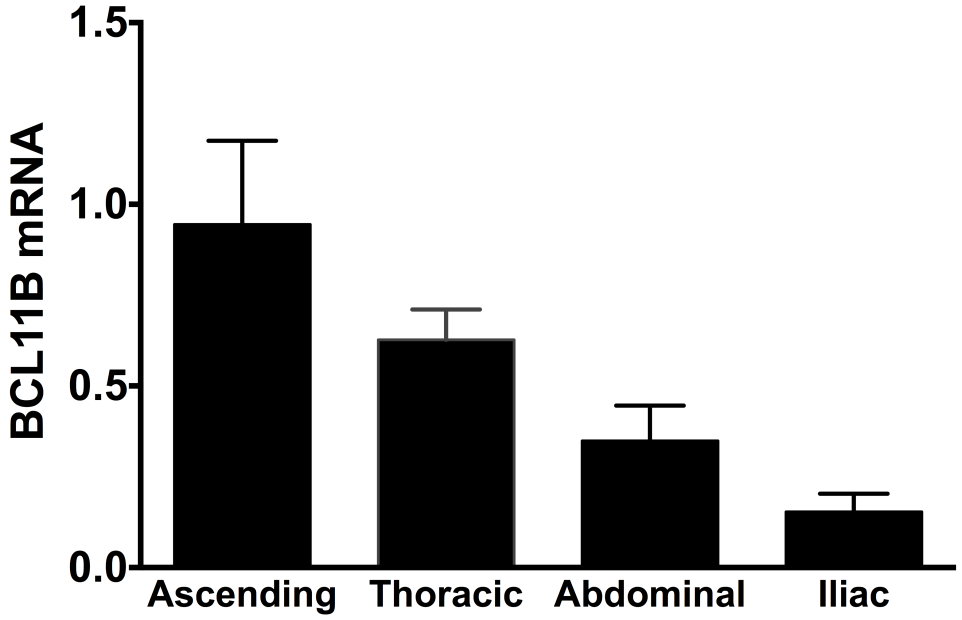

Figure 4.8: Expression of *BCL11B* mRNA in different segments of the human aorta indicating a reduction in *BCL11B* moving distally along the aorta. Data are mean±SEM *BCL11B* transcript normalised against *GAPDH*.

4.4.5 No Evidence of BCL11B Protein Expression in the Human Aorta

To examine the functional significance of BCL11B in the aorta, its expression was probed using antibodies that target different epitopes on the protein. Samples were selected from the extreme ends of the PWV spectrum (n=15 low PWV and n=15 high PWV), as well as an additional (n=15) samples that exhibited the highest levels of *BCL11B* gene expression. BCL11B expression was detected in adult tonsil sections, where it is highly expressed, and in adult skin, where BCL11B expression is much lower, confirming the sensitivity of the immunohistochemical protocol (Figure 4.9). BCL11B expression was not detected in any of the aortic samples either by Western blot immunodetection of aortic homogenates (Figure 4.10) or immunohistochemical staining of formalin-fixed paraffin-embedded sections (Figure 4.11). Tyramide signal amplification was employed to increase the detection sensitivity of the immunohistochemistry, but this still failed to identify BCL11B expression in human aortae (Figure 4.12).

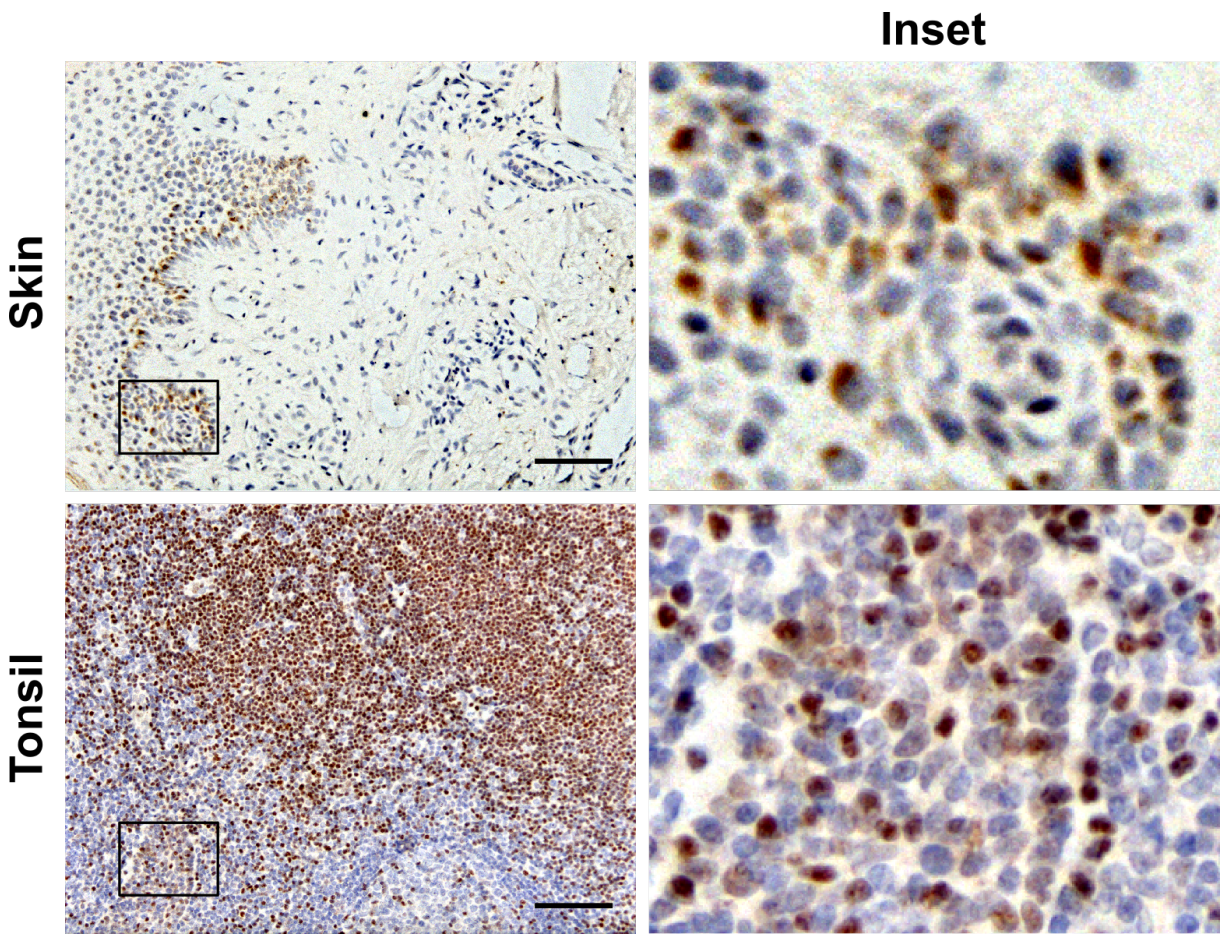

Figure 4.9: Expression of BCL11B in the skin and tonsil. Immunohistochemical staining of adult skin and tonsil sections showing nuclei positively stained for BCL11B expression (scale bar=50µm).

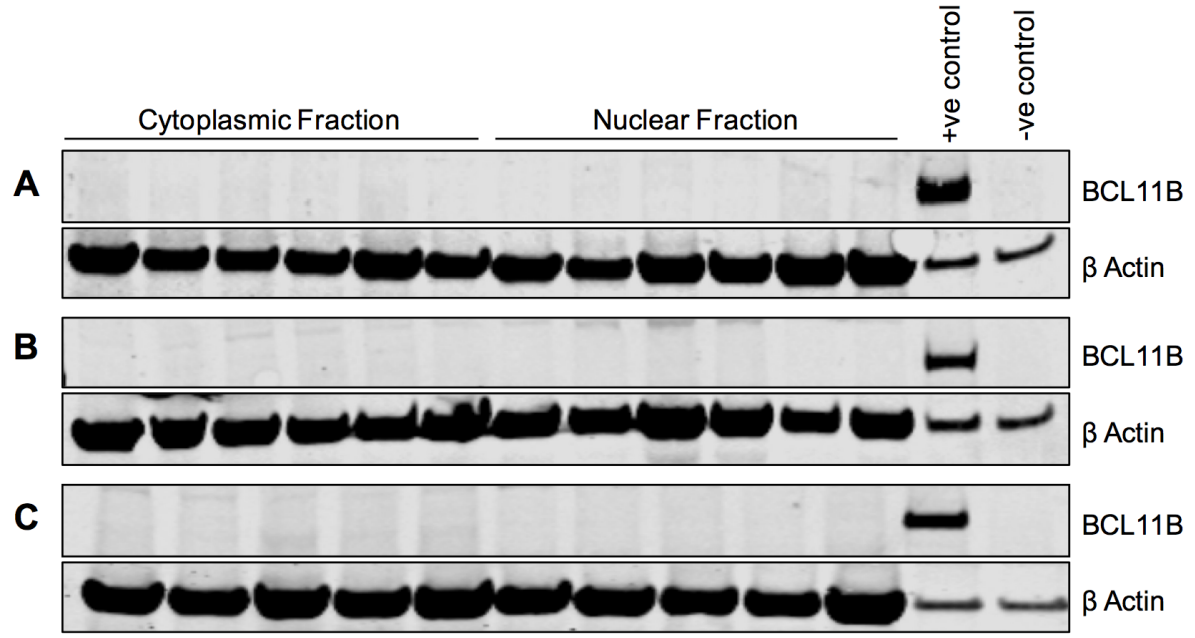

Figure 4.10: Representative Western blot of aortic BCL11B expression. Blot shows negative staining across nuclear and cytoplasmic homogenates of (A) Low PWV samples, (B) High PWV samples and (C) Samples with the highest *BCL11B* mRNA levels. The positive control is a protein lysate of HEK293T expressing full length BCL11B and the negative control is a protein lysate of HEK293T expressing an empty vector control.

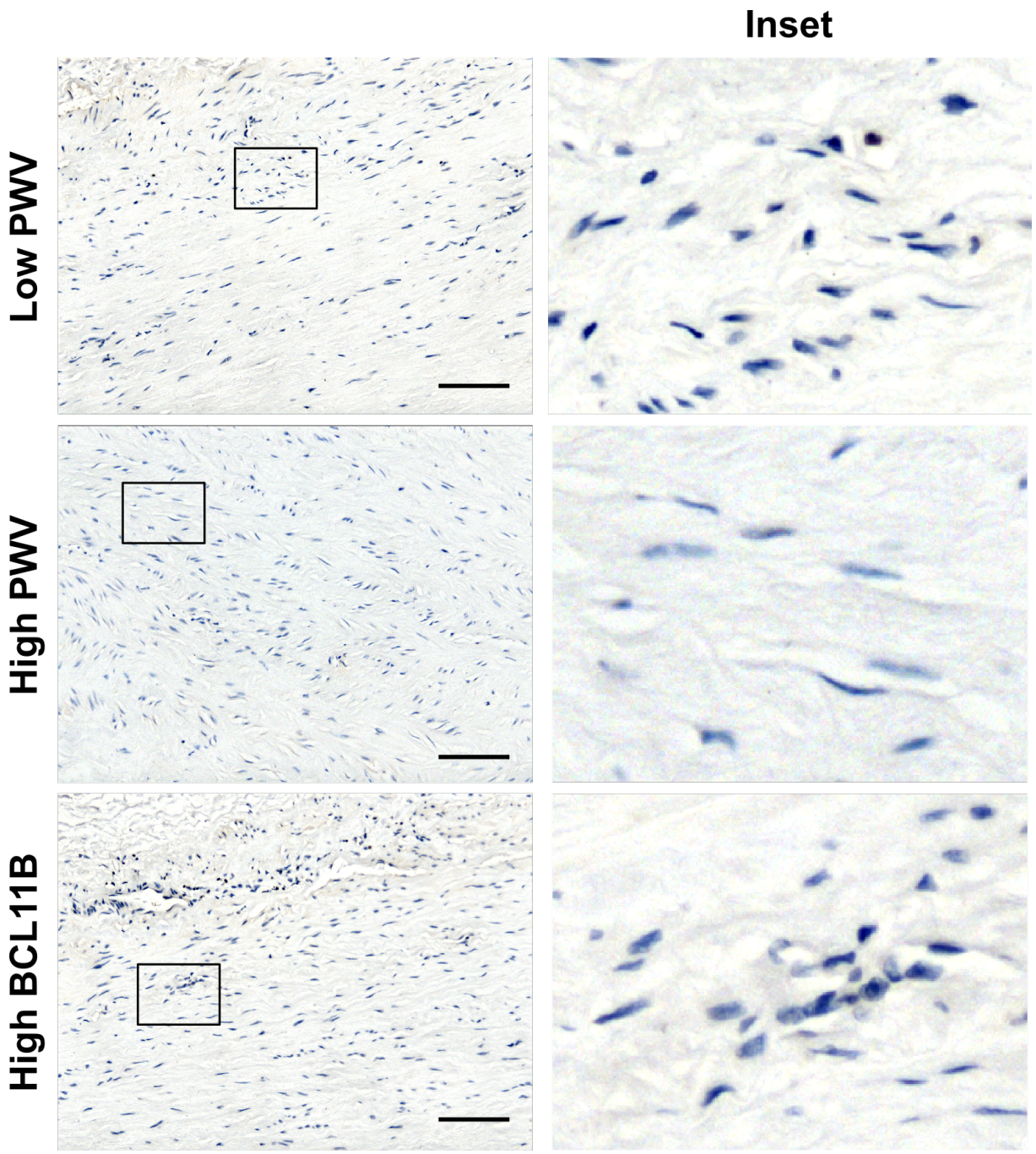

Figure 4.11: Expression of BCL11B in the aorta. Representative immunohistochemical staining of aortic samples showing a lack of BCL11B expression in the aorta including those with the highest *BCL11B* transcript levels (scale bar=50µm).

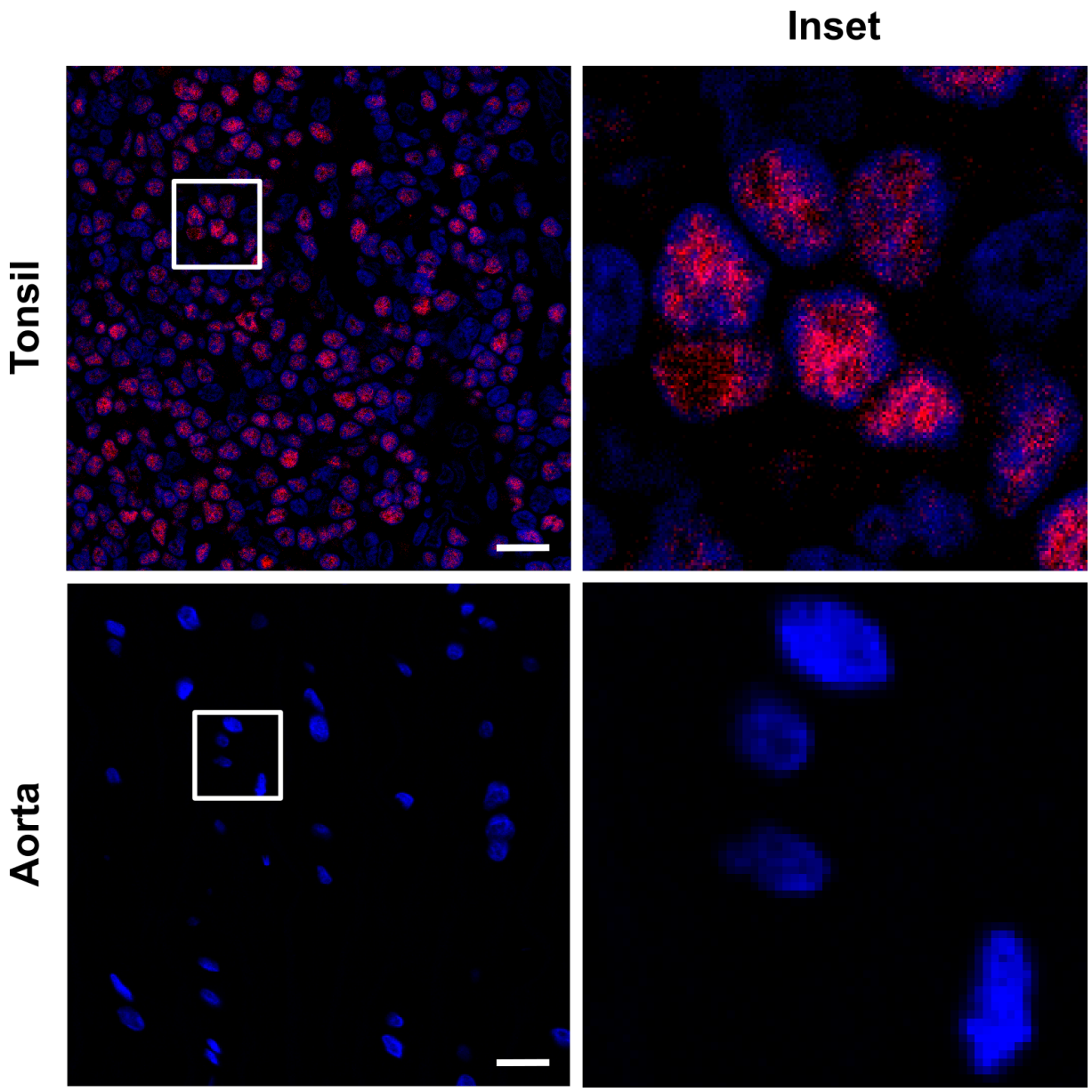

Figure 4.12: Immunofluorescence with tyramide signal amplification of BCL11B in the tonsil and aorta. The tonsil section shows nuclei (blue) positively stained for BCL11B expression (red), while no signal is detected in the aortic section (scale bar=20µm).

This led to questioning whether *BCL11B* is constitutively expressed in aortic SMCs or if the levels detected in the aortic tissue samples simply reflected underlying infiltration from circulating leukocytes. Corroborating the lack of BCL11B protein detection in the aorta, *BCL11B* gene expression quantified using real-time quantitative PCR in cultured primary human aortic SMCs was negligible ($2^{-\Delta Ct}$ =0.003 $\pm$ 0.0005, n=2) compared to that in PBMCs (724.4 $\pm$ 10.09, n=2) or HEK293T cells (5.5 $\pm$ 0.16, n=2), which have been reported in the literature to lack BCL11B expression (Figure 4.13).

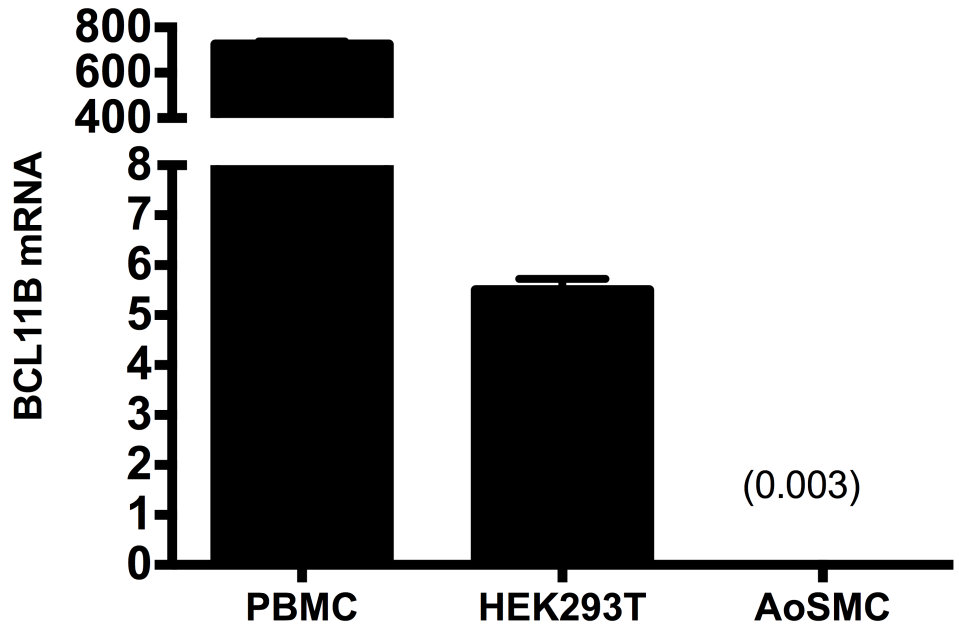

Figure 4.13: Comparison of *BCL11B* mRNA expression across cell types. A reduction in *BCL11B* mRNA expression in cultured human aortic vascular smooth muscle cells compared to PBMCs and HEK293T cells. Data are mean±SEM *BCL11B* transcripts normalised against *GAPDH*.

4.4.6 No Evidence of Bcl11b Protein Expression in the Mouse Aorta

The expression pattern of Bcl11b was examined in wild-type 10-week-old mice, with the thymus, spleen and brain serving as positive controls (Figure 4.14). Similar to the patterns observed in human tissues, *Bcl11b* gene expression was detected in the aorta but in negligible quantities ($2^{-\Delta Ct}$=0.0003 $\pm$ 0.00001, n=3) compared to the thymus (0.31 $\pm$ 0.006, n=3) and spleen (0.029 $\pm$ 0.002, n=3). Bcl11b expression was below detection limits in Western blot analyses of aortic homogenates and immunohistochemical staining of formalin-fixed paraffin-embedded sections (n=3). Similarly, Bcl11b expression was below detection limits in Western blot analyses of aortic homogenates from *Bcl11b*-tdTomato expressing reporter mice using an anti-RFP antibody (Figure 4.15).

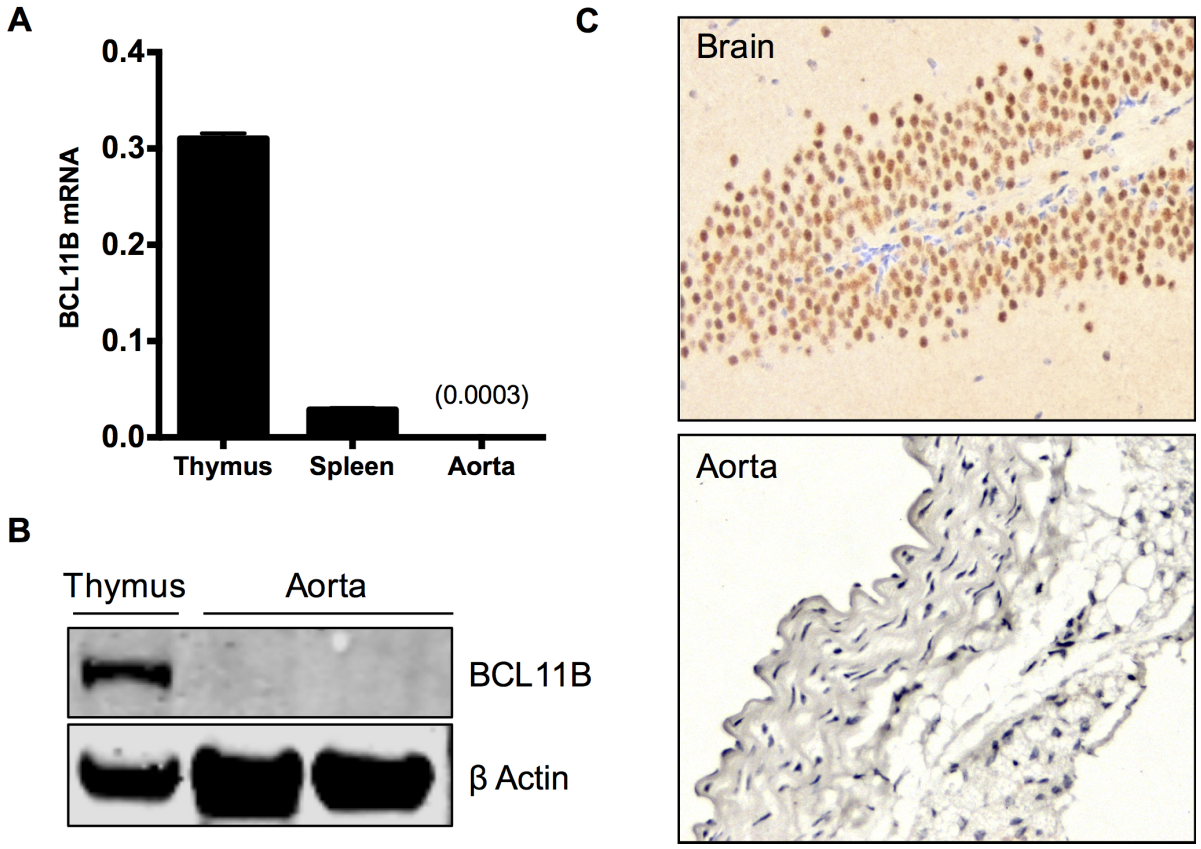

Figure 4.14: Expression of Bcl11b in wild-type 10-week old mice. (A) *Bcl11b* signal detected from mice aorta using qPCR is small compared to that from the thymus and spleen. Data are mean±SEM *Bcl11b* transcript normalised against *r18S*. (B) Immunoblot detection of Bcl11b shows a positive signal from the mouse thymus homogenate but not the aorta. (C) Bcl11b expression is detected in immunohistochemical staining of the mouse brain but not the aorta. Images are representative of (n=3) samples.

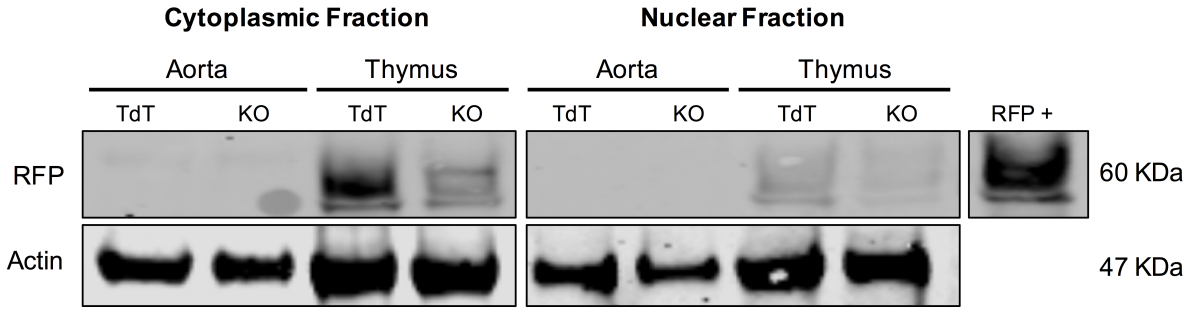

Figure 4.15: Expression of *Bcl11b*/TdTomato reporter construct in 10-week-old mice. The aortic and thymus protein extracts were fractionated before immunoblotting to show the relative distribution between the nucleus and cytosol. TdT= Bcl11b-Tdtomato reporter mice (Bcl11bTd/flox), KO= TdTomato reporter mice treated with Tamoxifen (conditionally knocks out the TdTomato cassette and exon 4 of *Bcl11b*). RFP+ is a protein lysate of human colorectal cancer cells expressing tdTomato.

4.4.7 BCL11B Expression in the Aorta Reflects T Cell Infiltration

Having obtained these results the possibility that aortic *BCL11B* gene expression is a manifestation of leukocyte infiltration was explored. *BCL11B* transcript levels were examined to see if they correlated

with those of specific lymphocyte markers in (n=85) randomly selected aortic samples (Figure 4.16A-C). Transcript levels of the leukocyte common antigen *CD45*, the cytotoxic T-lymphocyte marker *CD8A*, and the activated T-lymphocyte marker *CD25* were all quantified. The *BCL11B* transcript correlated strongly with the detection of *CD45* (r=0.90, P<0.0001), *CD8*α (r=0.83, P<0.0001) and *CD25* (r=0.77, P<0.0001). This was further supported by immunohistochemical staining for CD45 in the aorta (n=8), which showed higher levels of staining in aortas with high *BCL11B* mRNA expression (Figure 4.17). It was also considered whether these positive associations were due to inadequate removal of residual blood from the tissue samples by quantifying the expression of the specific erythrocyte marker *CD235A*. However, *BCL11B* gene expression was found not to correlate with *CD235A* gene expression (r=-0.043, P=0.71, Figure 4.16D).

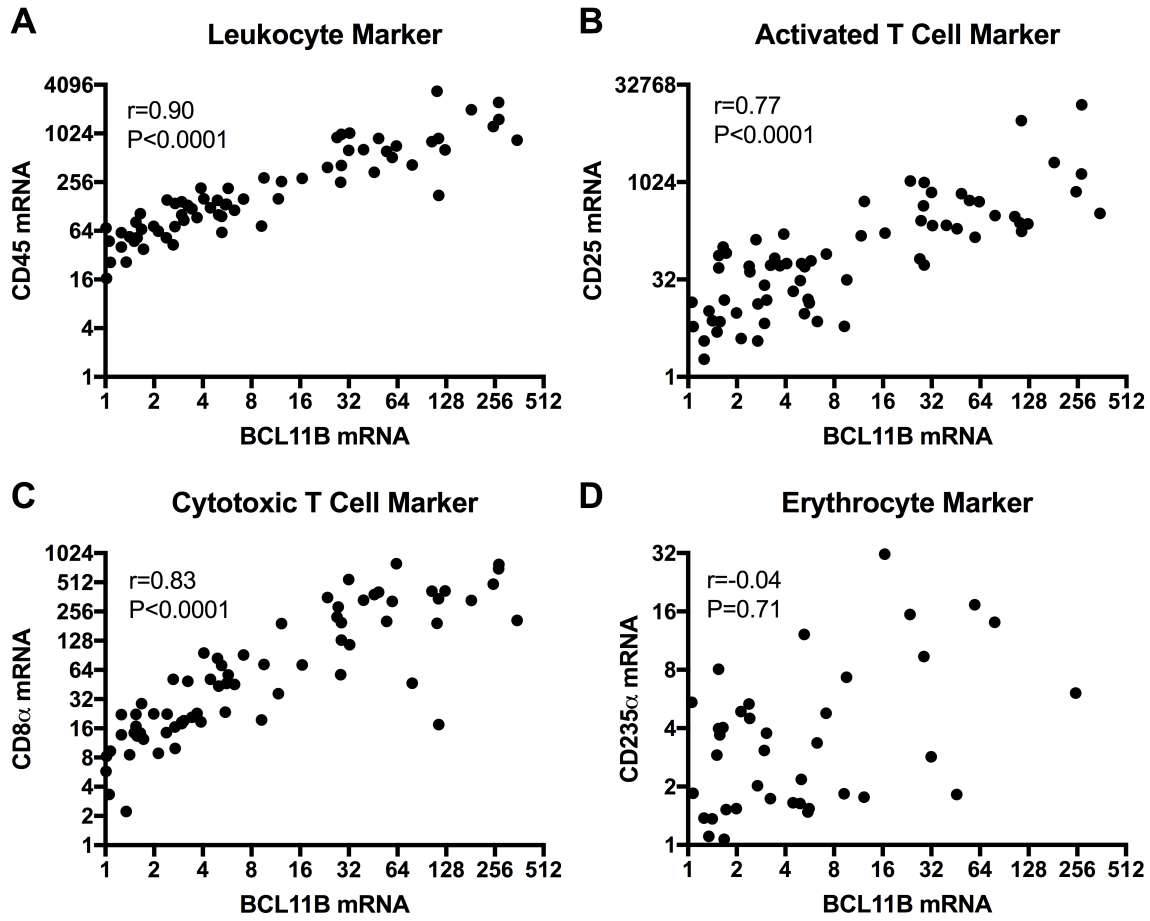

Figure 4.16: Aortic *BCL11B* expression correlates with the detection of leukocyte markers. Plots of *BCL11B* mRNA against (A) *CD45* mRNA, (B) *CD25* mRNA and (C) *CD8*α mRNA (n=85) show a strong positive correlation between *BCL11B* and these leukocyte markers but not with (D) the erythrocyte marker *CD235*α mRNA. Data points are expressed on the Log2 scale.

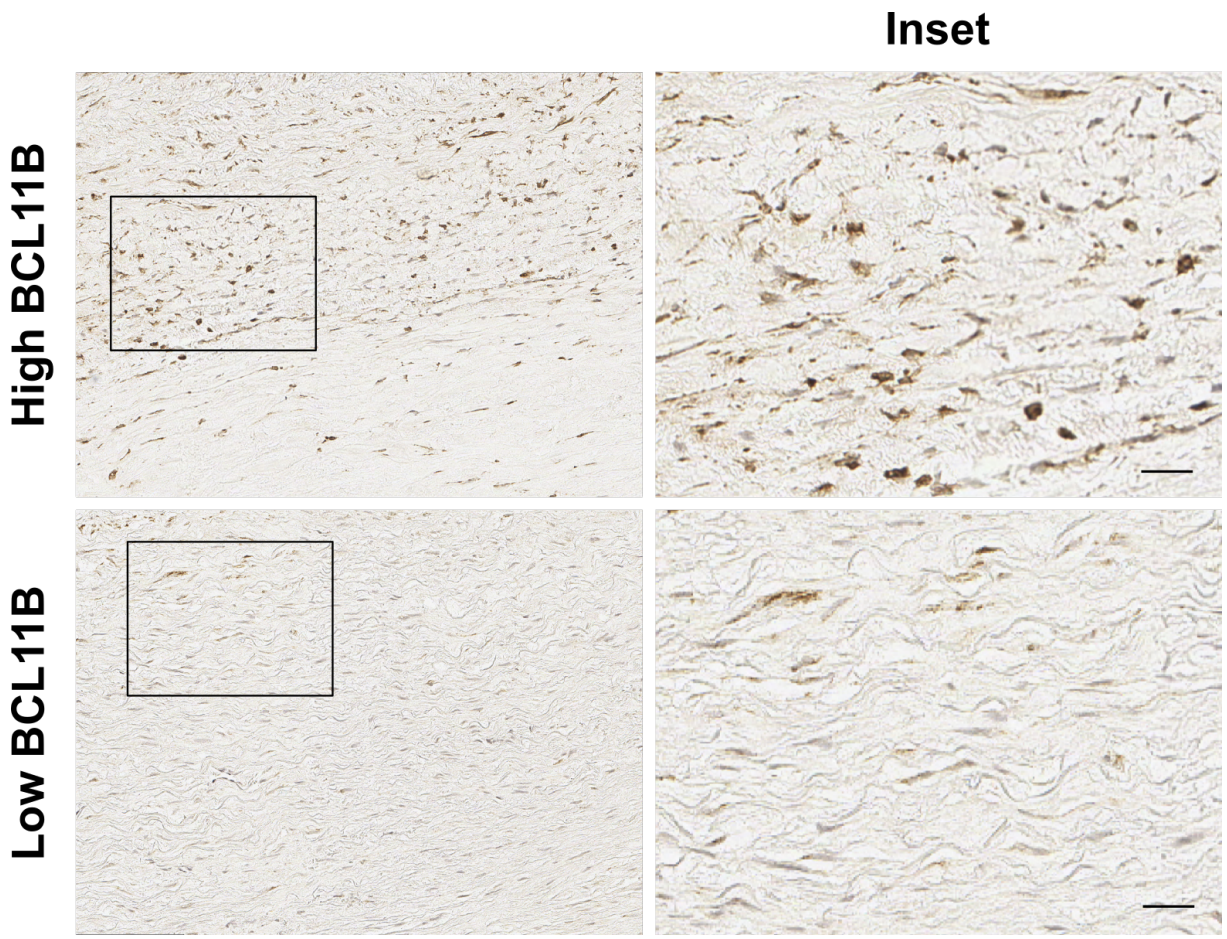

Figure 4.17: Aortic CD45 expression. Representative immunohistochemical staining for the antigen CD45 on human aortic sections expressing either high (n=4) or low (n=4) levels of *BCL11B* mRNA. Samples with high *BCL11B* mRNA showed strikingly higher CD45 staining compared to those with low *BCL11B* mRNA (scale bar=20µm).

4.4.8 DB129663 Expression in the Aorta

Out of the aortic samples (n=159) that were screened for lncRNA DB129663, 55% (n=88) were positive for the transcript. Age, gender distribution, BMI and blood pressure measurements were comparable between samples expressing DB129663 to those that did not express the transcript (Table 4.7).

Table 4.7: Characteristics of donors expressing DB129663

	DB129663		
	+ (n=71)	**- (n=87)**	**P value**
Age (years)	57±13	56±15	0.513
Gender (% male)	52%	48%	0.336
BMI (Kg/m^3)	28.2±6	27.9±6	0.703
SBP(mmHg)	125±28	128±34	0.609
DBP (mmHg)	68±15	68±13	0.842

Data are mean±SD

It was examined whether aortic expression of DB129663 was associated with increased stiffness. No

significant differences in PWV between samples expressing or lacking DB129663 expression were found in either the primary analysis which included all samples (n=159) (Figure 4.18A) or the secondary analysis which included only thoracic specimens (n=136) (Figure 4.18B).

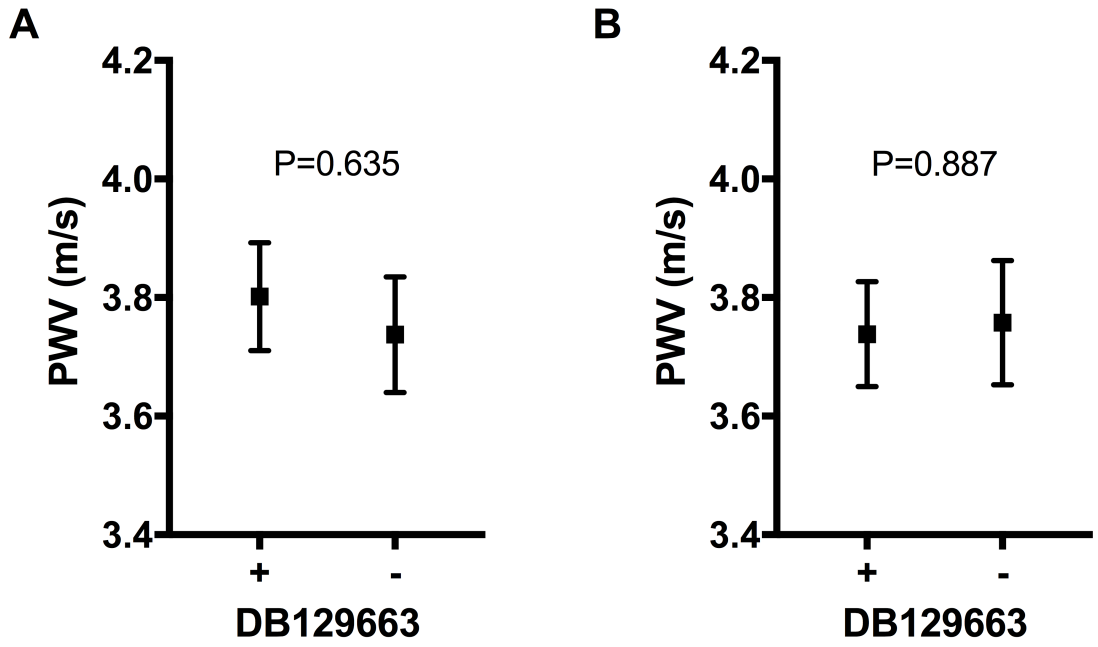

Figure 4.18: Association of aortic DB129663 transcript expression with PWV. (A) Primary analysis of all samples and (B) secondary analysis of only thoracic specimens did not show any differences in PWV between samples expressing or lacking DB129663. P values derived using the Student's t test.

It was then examined whether DB129663 expression in the aorta was impacted by the 3'*BCL11B* gene desert SNPs. As DB129663 mRNA was not quantifiable in the aortic samples, this was accomplished by calculating the percentage of samples positive for DB129663 within each SNP genotype (Figure 4.19). Of the five SNPs rs7152623 showed marginally-significant genotype differences in DB129663 transcript presence: 76% of the homozygous risk allele (A) carriers were DB129663 positive compared to 59% of the homozygous (G) carriers (P=0.042). None of the other polymorphisms showed a significant association with DB129663 expression.

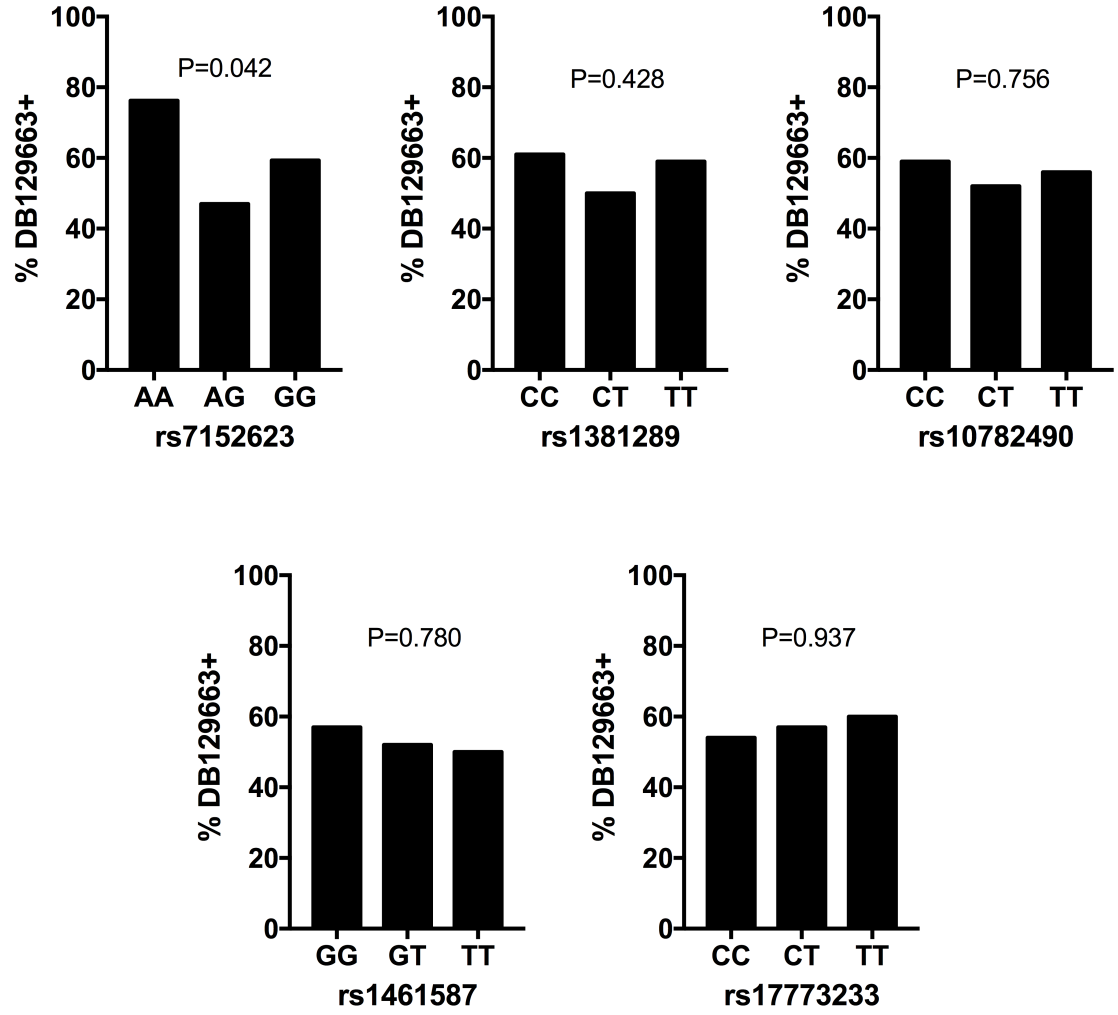

Figure 4.19: Association of *3'BCL11B* gene desert SNPs with the presence or absence of the DB129663 transcript in human aortic tissue. Bar charts represent the percentage of samples positive for DB129663 within each SNP genotype. P values derived using Pearson's χ^2 test test.

Because DB129663 is known to be expressed in the thymus it was questioned whether the transcripts detected in the aortic tissues were potentially a reflection of transcripts present in leukocytes that have infiltrated the aorta. DB129663 mRNA in cDNA generated from aortic SMCs was compared to that in PBMCs and two different leukocyte cell lines; Jurkat cells and the human monocytic cell line THP1 (Figure 4.20). Similar to the aortic tissue specimens, DB129663 transcript levels in aortic SMCs was below the quantifiable threshold but was highly expressed in PBMCs, Jurkat and THP1 cells. To probe this further, transcript levels of the leukocyte common antigen *CD45* were quantified in the samples that were positive or negative for DB129663 expression, with the hypothesis that if DB129663 presence in the aorta originates from infiltrating leukocytes, then *CD45* levels will be higher in the samples expressing DB129663. However, *CD45* mRNA levels did not differ significantly between the two groups (Figure 4.21A), suggesting that DB129663 may be constitutively expressed in the aorta, albeit at very low levels. Finally, given the role of lncRNAs in transcriptional

regulation and also the close proximity of DB129663 to *BCL11B*, it was investigated whether *BCL11B* mRNA expression levels in the aorta were driven by DB129663 regulatory mechanisms. Transcript levels of *BCL11B* in samples expressing DB129663 were compared to those lacking DB129663, but no statistically significant differences were found between the two groups (Figure 4.21B).

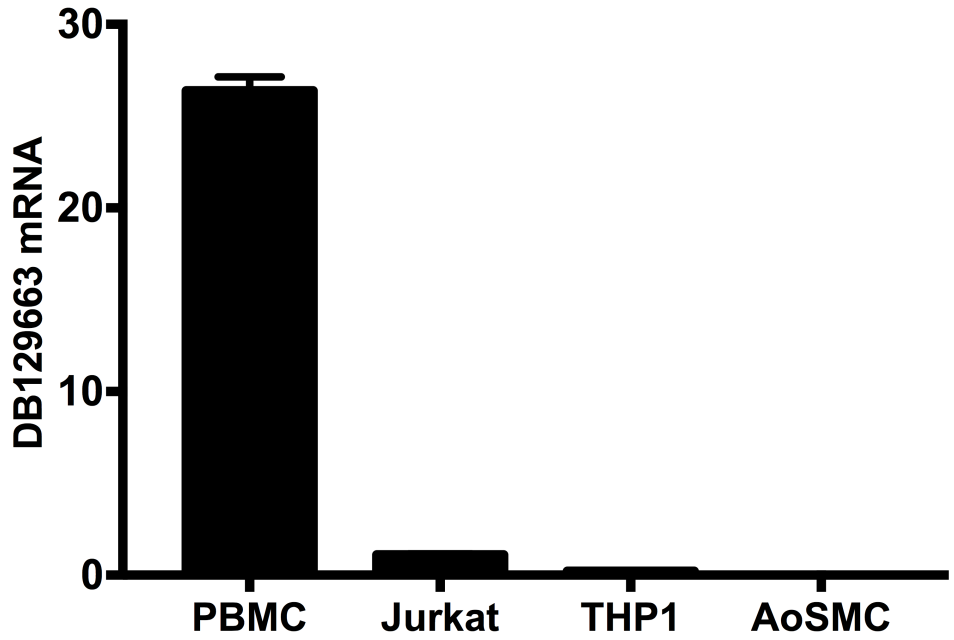

Figure 4.20: Comparison of DB129663 transcript expression across several cell lines. DB129663 is highly expressed in PBMCs and moderately expressed in Jurkat cells and the human monocytic cell, THP1, but is below detection limits in human aortic vascular smooth muscle cells. Data are mean±SEM DB129663 transcript normalised against *GAPDH*.

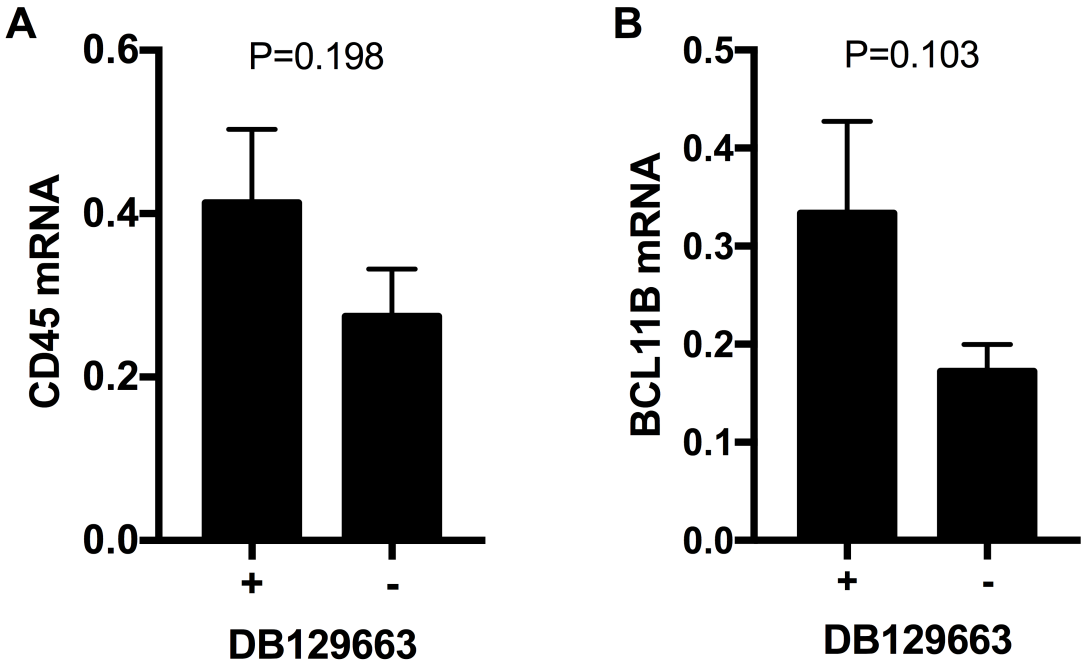

Figure 4.21: Association of aortic DB129663 expression with *CD45* and *BCL11B* mRNA levels. (A) *CD45* and (B) *BCL11B* transcript levels did not differ significantly between samples that expressed or lacked DB129663. P values derived using the Student's t test.

4.5 Discussion

The most recent GWAS meta-analysis and multi-centre study of over 20,000 individuals identified a number of candidate functional SNPs that showed significant associations with cfPWV. As with most complex traits, translating these variants to biological function remains a challenge, especially given that the risk locus lies in a non-coding, gene-poor genomic region. A growing body of evidence supports tissue-specific, long-range regulatory mechanisms for GWAS-identified risk SNPs [309–311]. The GWAS region of association harbours gene enhancer elements, such as DNAse-I hypersensitive sites, transcription factor binding sites, and signatures of chromatin modification and is able to drive T cell specific *Bcl11b* expression in a reporter system [72, 88]. The lncRNA, DB129663, lies in the immediate vicinity of the GWAS locus, and is therefore a putative target for these enhancer elements. The GWAS SNPs were therefore examined to see if they drive the transcription of *BCL11B* and DB129663. An understanding of how these genetic variations influence aortic stiffness is key to a better understanding of the molecular mechanisms that modify PWV.

Using a resource of over 200 human aortic samples, it was found that rs1381289, rs7152623 and rs10782490 are eQTL SNPs, as *BCL11B* mRNA levels were significantly influenced by the genotype of these SNPs. However, as the three SNPs are in tight LD, it is difficult to ascertain which of the

three is the causal SNP. It was also shown that at least one of the SNPs, rs7152623, potentially drives DB129663 transcription in the aorta, thereby strengthening the evidence for the functionality of this SNP. This finding is supported by the GTEx database (`https://gtexportal.org/home/`) which shows rs7152623 to display significant *trans*-association with DB129663 transcript levels in the testes ($P= 9.4 \times 10^{-10}$) in the same direction of effect observed in the donor aortas. Notwithstanding these findings, the poor reproducibility of many strong eQTLs reported in the literature [312] warrant replication of the identified eQTLs in external cohorts to ensure reproducibility and robustness of these data.

Further evidence was provided of the biological importance of the 14q32.2 locus by demonstrating associations for the three SNPs with PWV measured *ex vivo* in the proximal aorta and the results suggest an inverse relationship between *BCL11B* transcript levels and PWV. As PWV varies along the whole length of the aorta, it was important to distinguish the molecular contributors of aortic stiffness in the elastin-rich proximal aorta from the embryologically distinct and collagen-rich distal aorta. This is highlighted by the finding of regional differences in *BCL11B* expression along the arterial tree, being more pronounced in the ascending and thoracic aorta compared to the distal abdominal aorta and iliac arteries.

Despite strong evidence for its association with aortic stiffness, no evidence of BCL11B protein expression in the adult human aorta samples was found. Moreover, *BCL11B* mRNA was not detected in aortic vascular SMCs using conventional quantitative real-time PCR. In view of this, and given that BCL11B is highly expressed in human T lymphocytes, it was questioned whether it is constitutively expressed in the aorta or whether the transcripts from infiltrating leukocytes had been detected. *BCL11B* gene expression was found to strongly correlate with markers for total leukocytes and both activated and cytotoxic T lymphocytes, implying that inflammatory mechanisms may underlie the association of *BCL11B* with aortic stiffness. Lymphocytes have been speculated to have an important role in hypertension and the pathophysiological changes that result in the vessel wall. The role of BCL11B in determining T lymphocyte fate may involve it in these processes as well [313], while loss of BCL11B signalling can also be a powerful proinflammatory stimulus. The colons of mice lacking *Bcl11b* display significant levels of infiltrated proinflammatory Th1 and Th17 CD4+ T cells, neutrophils and macrophages, and consequently develop inflammatory bowel disease [241]. This has been partly attributed to a profile of enhanced proinflammatory transcripts in *Bcl11b*-deficient T reg cells, including tumour necrosis factor (*TNF*), *IFN*γ and *IL-17*, combined with the down-regulation of the immunosuppressive cytokine *IL-10* [241]. A similar BCL11B-dependent

perturbation of the inflammatory system and inflammasome has been reported in other cell types. For example, abolishing *BCL11B* from innate type 2 lymphoid cells (ILC2s) alters their functional and genetic profiles, leading to *GATA3* and *ROR-*α down-regulation and increased neutrophil infiltration in the airways [89]. Similarly, enhanced inflammatory cell infiltration has been reported in the mouse epidermis, where selective silencing of *Bcl11b* in keratinocytes increased the infiltration of eosinophils, monocytes, CD3+ and CD4+ T lymphocytes and CD45+ leukocytes in the skin [255]. In contrast, increased levels of BCL11B detected in the brain of patients with latent HIV infections appears to trigger a neuroinflammatory cascade by deregulating the expression of IL-6 and TNFα in neurons and microglial cells [314]. It is worth noting that the silencing and ectopic expression of BCL11B does not necessarily lead to the activation and suppression of transcripts vis-à-vis. This is highlighted by a largely diverse set of genes that are up-regulated or down-regulated in response to *BCL11B* silencing and overexpression in naive T cells [282]. In these cells BCL11B regulates the expression of several interleukins, as well as chemokine (C-X-C motif) ligands 10 and 11, which play a role in T cell recruitment and infiltration [282]. Overall, the evidence indicates that BCL11B regulates a number of elements in the inflammatory pathway and it accomplishes this in a cell-specific manner. It can be speculated that differential expression of *BCL11B* amongst the SNP haplotypes modulates the lymphocytee infiltration signal identified.

An obvious paradox stemming from these observations is how *BCL11B* transcript abundance can be protective (associating inversely with PWV) if expression of *BCL11B* is proinflammatory. The current data makes this difficult to determine, as it reflects a single time point in what is otherwise a long-term and highly dynamic process. The *BCL11B* transcript in the aorta is a marker of a complex interaction of circulating leukocytes, vascular endothelial cells, and the cellular and matrix components of the vessel wall. The lack of *BCL11B* expression in vascular SMCs, in addition to a high expression in PBMCs, suggests that endothelial and leukocyte cell lines may be more relevant cell types to functionally characterise how BCL11B influences aortic stiffness.

BCL11B may not be the only effector gene controlled by the 14q32.2 locus, and this GWAS signal may modulate aortic stiffness as part of a larger interplay of transcriptional regulation involving other targets flanking the 14q32.2 gene desert. For example, human vaccinia-related kinase 1 (*VRK1*) lies 1.1 Mb centromeric to the locus. This is the most prominent type of serine-threonine kinase within the nucleus and it has been shown to complex-with and promote the stabilisation and accumulation of p53 [315, 316]. p53 is a transcription factor that has been associated with aneurysmal vascular SMCs, and its accumulation has been implicated in the pathogenesis of aortic cystic medial degen-

eration [317, 318]. Importantly, p53 is tightly regulated via the TGFβ signalling cascade, a common pathway that underlies inherited aortopathies, such as Marfan and Loeys-Dietz syndromes, and familial thoracic aortic aneurysms and dissections. Several lines of evidence indicate that p53 may be a target of BCL11B transcriptional control [246], presenting a shared downstream target where independent effects on *VKR1* and *BCL11B* transcription potentially converge and potentiate aortic stiffness.

Also within close vicinity of the locus is the primate-specific lncRNA DB129663, which was hypothesised to be a target of the enhancer elements of the 14q32.2 gene desert [72]. As lncRNAs are emerging as key players in transcriptional regulation, post-transcriptional modification and epigenetic modulation, it was speculated that DB129663 may be central to the association of this region with aortic stiffness. However, no indication of its association with PWV, nor with other cardiovascular risk factors, such as age, blood pressure and BMI, were identified. Similarly, no suggestion of its influence on the transcriptional regulation of its neighbouring gene, *BCL11B*, was found. The small sample size and lack of a sensitive assay for quantitating DB129663 transcript is likely to have precluded such findings. Its presence in the aortae of only half the samples thus remains obscure and warrants further investigation.

To conclude, this study has investigated the role of 3'*BCL11B* gene desert SNPs on *BCL11B* and DB129663 mRNA expression and PWV measured *ex vivo* in a large sample of human aortic tissue. It has been demonstrated that rs1381289, rs7152623 and rs10782490 are significantly associated with PWV and *BCL11B* expression. In addition, rs7152623 also showed allele-specific differences in DB129663 transcript presence in the samples. However, detection of BCL11B at the protein level was not achieved, but the results suggest that the *BCL11B* transcripts detected in the human aorta reflect lymphocyte infiltration. Therefore it is hypothesised that it is immune mechanisms that largely govern the association of *BCL11B* with aortic stiffness.

4.6 Limitations and Future Work

This study has several limitations, the first being that it only utilised one approach to functionally characterise the GWAS locus using the human aortic resource. Additional approaches could be used to consolidate findings from this work. A combination of bioinformatics strategies, such as annotating the SNPs with ENCODE and other publically available data, in addition to genome editing of the SNPs followed by an assessment of target gene expression, would further validate the conclusions drawn. Second, the signal from the GWAS meta-analysis resides within a particularly large

topologically associating domain (TAD) [319]. Whereas this study examined only two targets within this region, it is conceivable that any of the other genes or non-coding RNAs residing in the corresponding TAD could be the actual effector target. Amongst those, in addition to the earlier mentioned *VKR1*, are histone methyltransferase SET Domain Containing 3 (*SETD3*), Coiled-Coil Domain Containing 85C (*CCDC85C*), the cyclin transcription regulator Cyclin K (*CCNK*), microRNA 320, Cytochrome P450 Subfamily 46 (*CYP46A1*), Echinoderm Microtubule Associated Protein Like 1 (*EML1*), and Y RNA. Future work should incorporate these putative targets to delineate the precise molecular mechanisms through which this locus underlies aortic stiffness. A third limitation of this work pertains to the inadequate exploitation of the *Bcl11b*-TdTomato reporter mice in answering some of the fundamental questions of this work. Proper *in vivo* cardiovascular phenotyping of the conditional knockouts combined with a histological examination of the aortic rings for signs of leukocyte infiltration may have provided additional support for the postulation of an inflammatory-mediated role of BCL11B in promoting aortic stiffness.

Despite its lack of association with PWV, the exact function of DB129663 in the human aorta and why it is expressed in approximately half of the samples remains vague and open to further investigation. This study could have been expanded by incorporating RNA fluorescence in situ hybridisation (RNA-FISH) experiments to identify the specific localisation and distribution of DB129663 within the aortic wall. Unquestionably, attempting to identify some of its functions by comparing *BCL11B* and *CD45* in a small set of heterogeneous samples is rather rudimentary. Gain and loss of function experiments followed by global gene expression analysis would provide a more comprehensive overview of its targets and effector pathways. In addition, a variety of pull-down experiments [320, 321] to identify interacting RNA, DNA and protein could provide further mechanistic insights into its precise functions. With the increasing biological roles and pathophysiological implications being assigned to lncRNAs, functional characterisation of DB129663 and further investigation into its role in the aorta may be worthwhile.

5

Candidate Gene Study: The Matrix Proteins Aggrecan and Fibulin-1 are Key Players in Aortic Stiffness

5.1 Abstract

A candidate-gene based association study using tagging single nucleotide polymorphisms (tagSNPs) was performed on young healthy ENIGMA study participants selected for high and low aortic pulse wave velocity (aPWV) values. Significantly associated tagSNPs in the genes coding for the ECM proteins aggrecan and fibulin-1 were subsequently validated in the remaining ENIGMA individuals. The association of four lead SNPs was then examined for *ex vivo* aortic stiffness in human donor aortas, and tissue expression of these SNPs and their encoded proteins was also explored .

Neither the aggrecan nor the fibulin-1 SNPs showed any significant associations with *ex vivo* PWV in the study cohort. While the aggrecan tagSNP rs2882676 displayed differential transcript abundance between homozygous allele carriers, this did not translate at the protein level. Both aggrecan and fibulin-1 were found to be present in the aortic wall, but with marked differences in the distribution and glycation of aggrecan, reflecting the loss of chondroitin-sulphate binding domains. Although these differences were age-dependent, the striking finding was the acceleration of this process in stiff versus elastic young aortas. These findings suggest that aggrecan and fibulin-1 play critical roles in determining the biomechanics of the aorta, and their modification with age could underpin age-related aortic stiffening.

5.2 Introduction

5.2.1 Background

The pursuit of aortic stiffness susceptibility genes has relied on several approaches, including Mendelian forms of aortic pathologies, genome-wide association studies (GWAS), linkage mapping, gene expression profiling and candidate gene studies. Mendelian aortopathies have been instrumental in recognising the impact of TGFβ signalling dysregulation on aortic wall integrity, which predisposes mutation carriers to aortic dilatation and rupture. This was highlighted in Chapter 3 with the functional validation of a novel missense variant within *TGFB2* in a Loeys-Dietz pedigree. A meta-analysis of GWAS from the AortaGen Consortium cohorts identified multiple SNPs that were strongly associated with cfPWV, which map to the 3'*BCL11B* gene desert. While the GWAS approach affords an unbiased method for examining the association of a large array of SNPs with aortic stiffness, as shown in the previous chapter, extracting biologically relevant information from these signal loci remains a challenge, and the mechanism underlying the association of the gene desert locus with PWV points towards immune-mediated mechanisms although this remains speculative. Linkage mapping and candidate gene based studies have identified a number of susceptibility genes for aortic stiffness, which can be broadly categorised into three main themes: genes involved in blood pressure regulation; genes modulating signalling pathways; and genes regulating the ECM and structural integrity of the aortic wall (as reviewed in Chapter 1). The significance of ECM regulation in the genomic landscape of arterial stiffness was corroborated in Durier and colleague's transcriptomic profiling of human aortas, which identified integrins and proteoglycans amongst the transcripts that were differentially expressed between distensible and stiff aortas [75]. However, the precise mechanisms by which these proteoglycans promote arterial stiffness remains to date unexplained.

Most genetic studies conducted to date have been based on older cohorts (>45 years) [72], with environmental exposures, such as smoking, hypertensive burden, and atherosclerosis potentially confounding the observed associations. Arterial stiffness is also impacted by age-related alterations to the arterial wall, including ECM remodelling, elastin fragmentation, vascular smooth muscle cell apoptosis, inflammation and oxidative stress [322]. One way to overcome these issues is to investigate younger subjects in order to minimise the confounding influence of cardiovascular burden and hence identify the 'pure' genetic contribution [77]. To this end, a candidate-gene based association study was conducted using the phenotypic extremes from a cohort of young healthy adults (the

ENIGMA cohort) with a low cardiovascular risk. Subjects were chosen from the opposite ends of the PWV spectrum and compared using tagSNPs to capture genetic information from the linkage disequilibrium (LD) blocks of the genes of interest [323]. Significantly associated tagSNPs in the genes encoding ECM proteoglycans, aggrecan and fibulin-1, were subsequently validated in the remaining ENIGMA individuals [Publication 3].

The aim of this study was to examine the functional impact of the validated SNPs from the ENIGMA cohort against *ex vivo* aortic stiffness in donor aortic tissues and to determine the expression patterns of their encoded proteins, aggrecan and fibulin-1, within the vasculature. A better characterisation of the expression profiles of these proteoglycans in the human aorta would provide mechanistic insight into their association with aortic stiffness, and may facilitate the goal of pharmacologically reversing the process. The aim of the review of the literature is to provide context for understanding the potential roles of aggrecan and fibulin-1 in the stiffening process by underscoring their key molecular features and their currently known biological and pathological functions.

5.2.2 Aggrecan: Structure, Domains and Degradation

Aggrecan is a 250 kDa extracellular chondroitin sulphate proteoglycan (CSPG) encoded by the *ACAN* gene on chromosome 15q (26.1). As suggested by its name, aggrecan has a tendency to form large supramolecular complexes with hyaluronan and the link protein which are in excess of 200 MDa in size [324], thereby supporting its retention and assembly within the ECM [325, 326]. The protein itself is composed of three functionally distinct globular domains; the N terminus G1 and G2 domains, and a C terminus G3 domain, each of which are encoded by different exons (Figure 5.1). The largest component of aggrecan is its central glycosaminoglycan (GAG) attachment region which carries keratin sulphate (KS) and chondroitin sulphate (CS) chains, and is encoded by a single large large exon (12) [327]. Aggrecan is highly expressed in the cartilage, and is also present in significant amounts in minisci, tendons, muscles and brain tissue [328]. It has also been described in the aorta of the chicken embryo [329], but its distribution and expression patterns in the human aorta have not yet been explored.

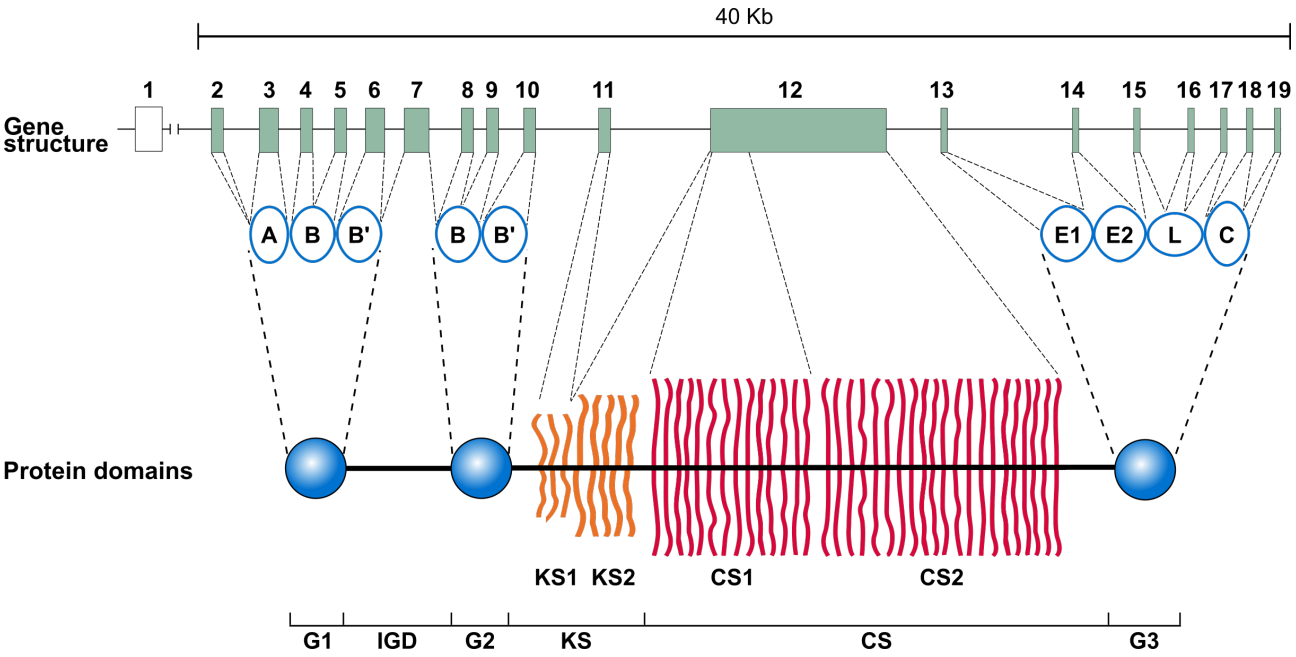

Figure 5.1: Schematic model of *ACAN* exon and their corresponding protein domains. Solid shaded boxed denote the coding regions. G1, globular domain 1; IGD, interglobular domain; G2, globular domain 2; KS, keratin sulphate chains; CS, chondroitin sulphate chains; G3 globular domain 3.

5.2.2.1 The Globular Domains

The G1 domain is composed of an immunoglobulin-like repeat (A subdomain) and two proteoglycan tandem repeats (B and B' subdomains). These latter subdomains jointly mediate the the interaction of the G1 domain with hyaluronan, while the A motif enhances this binding interaction and also mediates the interaction of the G1 domain with the link protein [330, 331]. Thus, the G1 domain is critical for anchoring aggrecan to the ECM. In contrast, no biological functions have been assigned to the G2 domain, despite its relative structural similarity to the G1 domain. Although lacking an immunoglobulin-like repeat, it consists of similar B-B' motifs but these do not appear to have similar interaction properties with hyaluronan [330] nor with any other molecules reported to date. This domain is unique to aggrecan compared to other CSPG and is highly conserved between species, leading to the suggestion that it is involved in the secretion of aggrecan following its biosynthesis [332].

The C-terminus G3 domain is structurally different to the N-terminus G1 and G2 domains and is composed of four distinct motifs: an EGF module (EGF1), a calcium-binding EGF module (EGF2), a C-type lectin domain (CLD) and a complement regulatory protein (CRP) domain. The specific functions of these motifs in aggrecan have primarily been derived from functional work in lecticans and vesrican which express similar motifs. The CLD motif mediates calcium-dependent interactions

with other ECM proteins including tensican-R [333], fibulin-1 [334], fibulin-2 [335], fibrillin-1 [336] as well with carbohydrates [337] and cell surface sulphated glycolipids [338]. Less is known about the functions of the other G3 subdomains, but unlike CLD which is constitutively expressed in humans, the EGFs and CRP are subject to alternative splicing [339, 340]. Different splice variants modify the binding affinities of the G3 domain with its ligands, suggesting their importance in regulating aggrecan's interactions with the structural proteins of the ECM [340]. The G3 domain has also been shown to promote GAG chain attachment, an essential component of the structural and functional properties of aggrecan [332]. Taken together, the C-terminal G3 domain bridges components of the cell surface with various proteins of the ECM, thus mediating the structural organisation of aggrecan within the matrix, as well as the overall assembly and organisation of the ECM.

5.2.2.2 The Interglobular Domain

The interglobular domain (IGD) is a rod-shaped structure which is flanked by the G1 and G2 domains of aggrecan. To date, no biological functions have been ascribed to the IGD but it is highly susceptibile to proteolytic degradation by a number of proteases such as MMPs, plasmin and leukocyte elastases and cathepsin B (Figure 5.3) [341, 342]. This degradation is detrimental to the tissues within which aggrecan is expressed, and compared to the other aggrecan cleavage sites which are present, cleavage of the IGD is the most detrimental as it releases the entire GAG-containing segment of aggrecan [343].

5.2.2.3 The Glycosaminoglycan Side Chains

A mature aggrecan molecule possesses 30 KS and 100 CS chains covalently attached to its central core, together resulting in the largest domain of aggrecan [344]. CS is a linear polysaccharide composed of alternating chains of glucuronic acid and N-acetyl galactosamine, with sulphated groups being present on the galactosamine moiety (Figure 5.2) [345]. In contrast, KS is composed of alternating disaccharide units of galactose and N-acetyl glucosamine. Sulphation commonly occurs at the N-acetyl glucosamine moiety but galactose can also be sulphated (Figure 5.2) [345] .

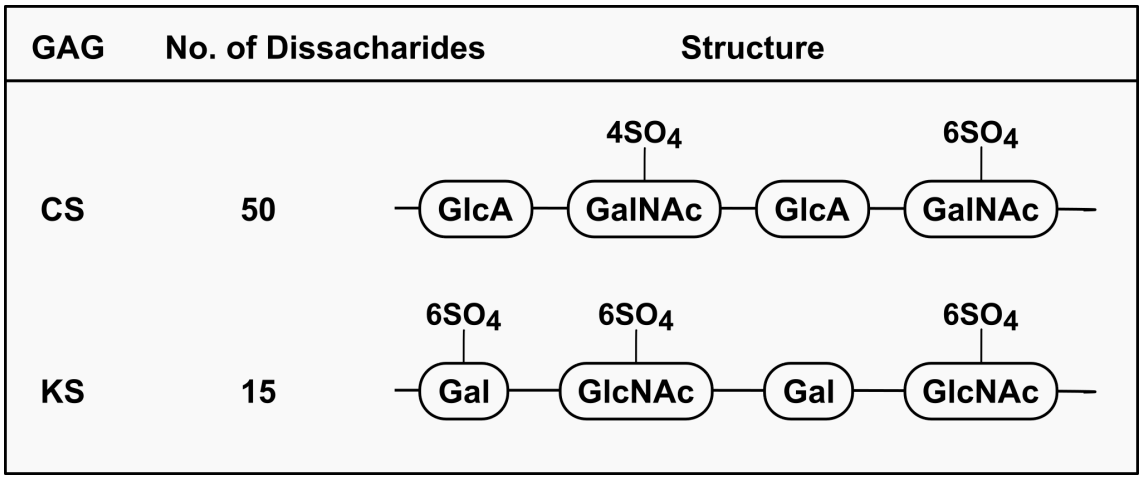

Figure 5.2: Structure of the chondroitin sulphate and keratin sulphate chains. A representative disaccharide sequence is indicated along with the common sulphation position and typical number of disaccharide units per chain. GalNAc; N-acetyl galactosamine, GlcA; glucuronic acid, Gal; galactosamine, GlcNAc; N-acetyl glucosamine. Figure modified from Roughley and Lee [345].

The sulphation patterns of the chains play an essential role in the stability of aggrecan and protection against enzymatic degradation [346]. Together, these GAG chains make up 80% of the molecular mass of aggrecan and endow the molecule with one of its most important functional features, a high concentration of anionic charge, and there are estimated to be 80,000 to 10,000 negatively charged groups per molecule thus creating an osmotic pressure that draws water into the ECM [328, 345]. Along with the structural and spacial organisation of aggrecan as an aggregating molecule, this distinctive osmotic activity of aggrecan accords compressive resilience to the tissues within which it is expressed and is a major contributor to their load-bearing and viscoelastic properties [328, 345]. In addition, KS chains associate weakly with collagen fibrils in the cornea [347] and in cartilage [348], which has been suggested to help maintain the spatial organisation and structural integrity of the proteoglycan aggregates [347, 348]. Both CS and KS chains are subject to continuous changes throughout life, with changes to the structure, length and sulphation patterns of CS chains commencing during the foetal stage and continuing through young adulthood [349]. With increasing age, these chains, along with the main core and globular domains of the protein, also undergo degradative changes.

5.2.2.4 Degradation and Age-Related Modifications

An intact aggrecan monomer is estimated to have a half-life of 3.5 - 5.5 years in human articular cartilage and intervertebral disks but 21.5 - 23.5 years for its G1 domain within the same tissues [350, 351]. This contrast in residence time reflects age-related alterations in the synthesis and enzymatic and non-enzymatic degradation of aggrecan. Increasing age is associated with a significant decline in

aggrecan transcript abundance, biosynthesis and the capacity to form large molecular size aggregates in the ECM [352–354], resulting in a 50% drop in synthesis by the fourth decade compared to the second decade [353]. This regression has partly been accounted for by the accumulation of advanced glycation end-products (AGEs) in the ECM, which inhibit aggrecan synthesis at the transcriptional and post-translational levels [355]. Glycation end-products also induce changes to lysine residues in the G1 domain, preventing the assembly of aggrecan aggregates and facilitating their dissociation from hyaluronan [356]. However, the most notable age-related changes pertain to the predisposition of aggrecan to considerable proteolytic degradation at a number of sites along its length, resulting in the detachment of heterogenous fragments from the assembled aggregate (Figure 5.3).

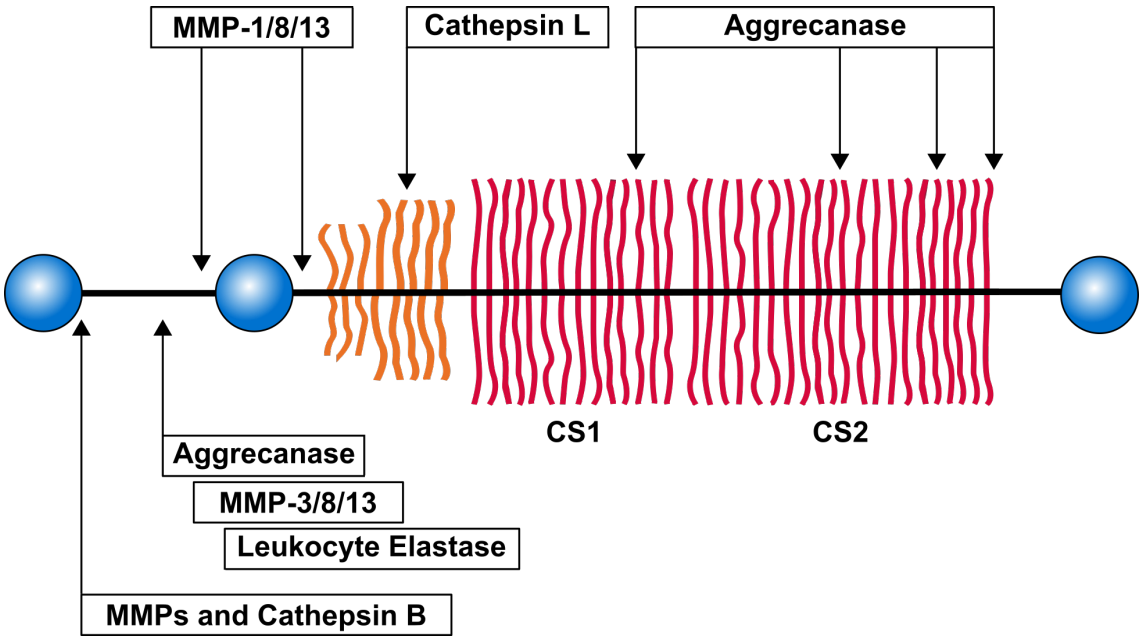

Figure 5.3: Currently identified sites of aggrecan core protein cleavage by tissue proteinases

Matrix metalloproteinases (MMP-1,2,3,7,8,9 and 13) have been traditionally recognised as the primary drivers of aggrecan degradation [357–361], but a crucial role for disintegrin and metalloproteinase with thrombospondin motifs (ADAMTS-1,8,9,15,16,18 and in particular ADAMTS-4 and 5), also known as aggrecanases, was later established [362–365]. Cleavage by leukocyte elastase, cysteine and serine proteases has also been described at various sites within the protein [342, 366, 367]. These cleavage events separate the GAG-rich region from the G1 domain, which is then termed 'free G1' and remains affixed to the hyaluronan filament via the link protein, thus explaining its longer residence time and its accumulation in the ECM with increasing age [350, 368, 369]. In contrast, the fragmented peptides lose their binding affinity for hyaluronan and face two outcomes; small fragments rapidly diffuse out of a tissue [369, 370], while larger fragments are usually retained but may undergo further degradation by lysosomal exocytosis [369–371]. Enzymatic degradation

is a dynamic process that is subject to large inter-individual variability with regards to the extent of degradation, as well as in the combination of enzymes that generate the pool of fragments [372]. Work in mice resistant to aggrecan proteolysis suggests that aggrecan loss from the tissue can also occur independently of proteolytic degradation via unidentified mechanisms [373].

In addition to the the degradative changes, aggrecan undergoes age-dependent stoichiometric modifications, most notably the elongation of KS chains and a concomitant shortening of CS chains [374, 375]. Collectively, these alterations compromise the functional properties of aggrecan and the stability of the aggregate assembly, predisposing to ECM degeneration, loss of viscoelasticity and therefore the ability of the tissue to withstand compressive loads [328]. In contrast to these observations, aggrecan shows a significant increase in transcript and protein abundance with age in the meniscus [376], indicating that the age-dependent modifications described are site and tissue-dependent.

5.2.3 Aggrecan: Biological Functions

5.2.3.1 Cartilaginous Tissue Viscoelasticity

The function of aggrecan is best understood from its role in cartilaginous tissues, mainly articular cartilage, intervertebral disk and meniscus, where it has been extensively characterised across several species. Aggrecan is a key structural component of the articular cartilage ECM, where it imparts structural and mechanical stability to the tissue [345], as well as the narrow pericellular matrix (PCM) surrounding chondrocytes, where it is thought to regulate biomechanical and biochemical signal transduction to this population of cells [377]. The load-bearing capacity of cartilage is attained through a fine balance of hydration imparted which is due to the polyanionic nature of GAG chains which imbibe water into the matrix, and resistance is imparted by the tensile forces of collagen fibrils within which the aggrecan assembly is enmeshed [378]; a high aggrecan concentration is required to achieve this equilibrium for proper cartilage functioning [378]. Because of the avascular nature of cartilage, the absorption of water into the the cartilage is also believed to aid nutrient delivery and waste dispersion between the synovial fluid and chondrocytes [328, 378]. Recent evidence from *ACAN* knockout cell lines further suggests a role for aggrecan in a range of cellular functions. *ACAN* depletion in chondrocytes triggers changes to the expression of genes that are involved in mineralisation, apoptosis, mitosis, cell membrane transportation, transcriptional regulation and cell matrix interactions, potentially as a compensatory mechanism for the changes in the local cellular milieu [379]. In a similar fashion, the intervertebral disc and knee joint meniscus are required to

withstand compressive forces, which is made possible as a result of a swelling equilibrium due to a high content of aggrecan in their inner zones which is resisted by collagen fibrils in the surrounding outer compartment [380]. In addition to these functions, aggrecan has inhibitory functions in endothelial cell adhesion, migration and nerve growth and is suggested to underlie the avascular and aneural nature of cartilaginous tissues [381–383].

5.2.3.2 Bone Formation and Skeletal Development

Most mammalian bones develop from chondrocyte precursors in a complex and tightly regulated process known as endochondral ossification [384]. During this process chondrocytes undergo several cycles of differentiation, proliferation, maturation and spatial organisation in order to establish a cartilage model, the mechanical template from which bone is ultimately made. Mature chondrocytes subsequently become enclosed in the ECM and ultimately stop dividing, are subject to hypertrophy and are apoptosised. At this stage the constructed cartilage is invaded by blood vessels, osteoclasts and osteoblasts, and bone mineralisation commences [384]. Amongst the many growth regulators, transcription factors and signalling pathways involved in regulating this process, ECM components, including aggrecan, are elemental in providing chondrocytes with structural support and the means necessary for the transmission of growth factors and signalling molecules [384–386]. Aggrecan is highly expressed during the early stages of bone formation and the abundance and sulphation patterns of its GAG chains change to accommodate the various requirements of each phase. Importantly, aggrecan and other proteoglycans inhibit the formation of calcium phosphate and hydroxyapatite crystals, and it is only following the cessation of *ACAN* mRNA and alterations to its structure that the mineralisation step proceeds [385, 386].

5.2.3.3 Pleiotropic Actions in the Brain

Aggrecan is an important constituent of the ECM of the central nervous system (CNS) where it is predominantly found in the perineuronal net (PNN) surrounding specific subpopulations of neurons [387], including the dentate gyrus, brainstem nuclei, hippocampus, cerebellum, reticular nucleus of the thalamus, optic nerve and at lower levels in the frontal lobe [388, 389]. *ACAN* transcripts and protein expression in the brain are undetectable during early embryonic development, become more prominent postnatally, and are maintained throughout adulthood [390, 391]. Despite being encoded by the same gene, aggrecan in the brain lacks KS chains, has fewer CS chains and exhibits different sulphation patterns compared to the homologue found in cartilage [392], suggesting substantial tissue-specific post-translational modifications, which may yield diverse functions across

tissues. The biological significance of aggrecan in the brain is not well defined, but may involve protection against neurodegeneration [393, 394], reducing oxidative stress by scavenging redox-active iron ions [395], regulating activity-dependent cortical plasticity and neuronal migration [396, 397], sustaining the activity of fast-firing neurons by acting as a buffering system for cations in the microenvironment of PN-associated neurons [398], and supporting glial cell maturation by regulating genes involved in astrocyte differentiation potentially through ECM signalling mechanisms [399].

5.2.4 Aggrecan: Pathological Roles

5.2.4.1 Arthritis and Disc Degeneration

Aggrecan degradation is a leading cause of degenerative diseases of cartilaginous tissues, most notably osteoarthritis (OA), rheumatoid arthritis (RA) and intervertebral disc degeneration (IVDD) [378, 380]. As has been described, the structural organisation of aggrecan with ECM components, together with the high degree of sulphated GAG chain substitution in its core protein, provides cartilage tissues with the ability to withstand compressive loads. The proteolytic cleavage of aggrecan decreases the distinctive anionic charge of the molecule, compromising its ability to resist compression, thereby predisposing cartilaginous tissues to erosion and weakening [378]. While the gradual proteolytic cleavage of aggrecan occurs as part of the normal ageing process, the rate of tissue erosion is accelerated in OA, RA and IVDD [378, 380, 400]. Subjects demonstrate atypical and enhanced enzyme-generated neopeptides within damaged regions of the cartilage, as well as in the synovial fluid, signifying extensive proteolytic degradation; some neopeptides are retained, while others are lost from the tissue [370, 401]. The accumulated aggrecan fragments have a slow turnover rate within the matrix, which is thought to hinder the regeneration of aggrecan molecules and to impede the repair process [378, 380]. The molecular mechanisms driving the accelerated degradation of aggrecan are complex, involving a complex cross-talk of pathways that regulate the transcription of aggrecan, MMPs and aggrecanases in chondrocytes (Figure 5.4) [402, 403]. Accumulating evidence also implicates epitopes on aggrecan moieties in the initiation of an inflammatory cascade, further exacerbating cartilage degeneration [404, 405]. Both T cell and B cell epitopes have been described, the former mostly being present on the G1 domain, while the latter are on the CS attachment region; however, initial exposure to the immune system is believed to involve a G3 epitope that is released upon proteolytic cleavage [405–407]. The inflammatory response is sustained by further degradation of the aggrecan molecule, which exposes additional epitopes within the CS attachment region and releases G3 fragments, and the CLD motif is a potent activator of the classical and alternative complement pathways [407, 408]. In concert, these observations provide clues to possible pathological

implications for aggrecan in the aortic wall, as the signalling pathways implicated in accelerating aggrecan degradation in the cartilage are those that are also intimately involved in maintaining vascular ECM homeostasis.

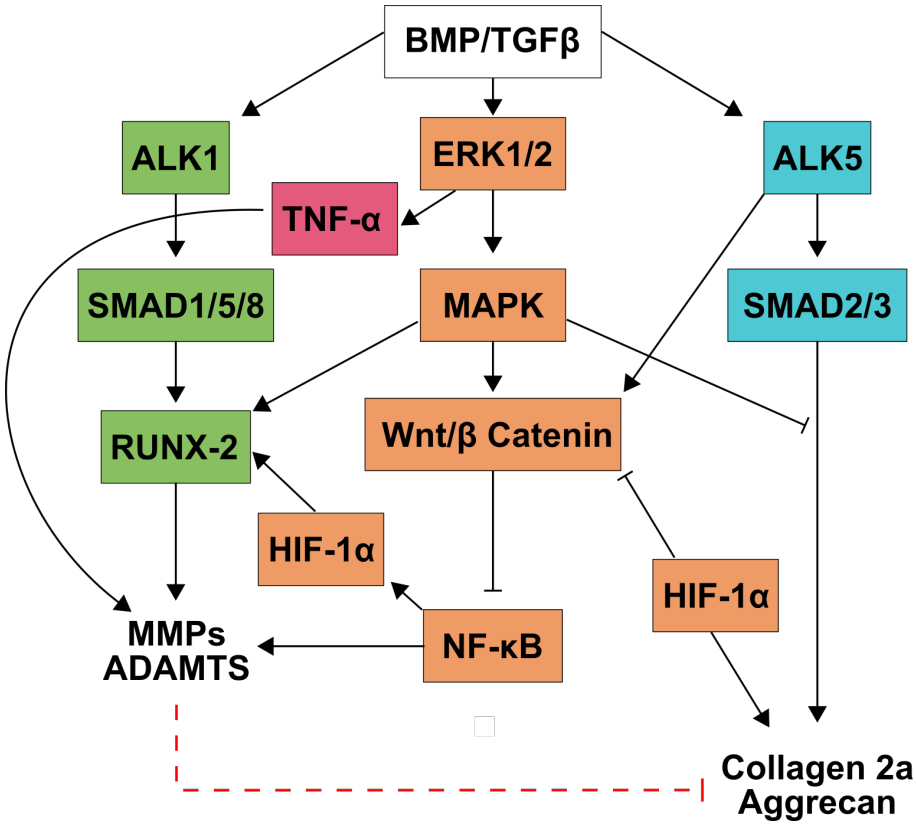

Figure 5.4: Schematic overview of signalling cross-talk between pathways involved in regulating the expression of aggrecan and its proteolytic enzymes in chondrocytes. ALK; activin-like kinase, BMP; bone morphogenic proteins, HIF; hypoxia-related factors, NF-κB; nuclear factor kappa B; TGFβ; transforming growth factor β. Image modified from Mariani et al. [403].

5.2.4.2 Cerebral Vascular Pathology

Hereditary Cystatin C Amyloid Angiopathy (HCCAA) is an autosomal dominant disorder caused by a mutation in the cystatin C gene and is characterised by amyloid accumulation in small and medium-sized arteries of the CNS and lethal intracerebral haemorrhages in young adults [409]. The leptomeningeal arteries in patients with HCCAA typically display extensive elastin fragmentation, endothelial degeneration, progressive loss of VSMCs, the thickening of basement membranes, and enhanced ECM matrix deposition [409, 410]. The arteries further show striking accumulation of collagen IV and aggrecan, a finding which is suggested to be the primary driver of aortic amyloid deposition and the arterial manifestation in these patients [409]. The overlapping features with aortic stiffness (e.g. elastin fragmentation, collagen accumulation and ECM deposition), justifies exploring the role of this proteoglycan in the stiffening of large vessels.

5.2.4.3 Aortic Stiffness and Atherosclerosis

Aggrecan is detected within all aortic layers during early and late embryonic development of the chick and mouse, and persists into adulthood but decreases with increasing age [329, 411]. Whilst its physiological and pathological roles are yet to be clarified, the distribution of proteoglycans is believed to contribute to the residual stress of a healthy aorta [412]. The specific role of aggrecan in aortic stiffness was first highlighted by Durier et al., who reported its transcript to be up-regulated in subjects with stiff aortas [75]. Other proteoglycans, such as small leucine-rich repeat proteoglycans, were subsequently found to correlate with aortic stiffness but their protein levels were mostly down-regulated in subjects with stiff aortas [76]. In contrast, elastin haploinsufficient mice, which display phenotypic features that mirror human thoracic aortic aneurysms, show extensive aggrecan deposition in the aorto-pulmonary septum (APS) region of the proximal aorta [413]; crucially, the APS region also show substantial VSMC hyperplasia and are stiffer than the non-APS region [413]. The mechanisms underlying these associations are unclear, but a degenerative impact of GAG accumulation within the aortic media has been evoked. Aneurysmal aortas typically show extensive elastin fragmentation with parallel collagen accumulation and GAG deposition [414]. The pool of negatively charged GAGs have been demonstrated to increase Donnan swelling pressures within aortic media predisposing to intra-lamellar delamination which, together with the loss of tensile strength due to elastin fragmentation, renders the aortic wall susceptible to dissection [415].

Aggrecan and other proteoglycans are enriched at sites of intimal hyperplasia and have been implicated in the progression of atherosclerosis and formation of atherosclerotic plaques [416, 417]. The negatively charged KS and CS display a high affinity for lipoproteins, potentially instigating atherogenesis by stimulating the uptake and retention of low-density and other atherogenic lipoproteins in the vascular intima [416]. In contrast, *ACAN* transcript in VSMCs has recently been shown to be stimulated by apatite crystals and alkaline phosphatase, indicating that aggrecan accumulation during atherogenesis may be an adaptive response to the presence of calcific deposits in plaques [417]. Aggrecan may also be involved in the transdifferentiation of VSMC into chondrocytes, further exacerbating the calcification of intimal plaques and promoting medial calcification [417, 418]. Taken together, it appears that an even distribution of aggrecan is elemental to vascular integrity and that its dysregulation may impact the biochemical and mechanical properties of the aorta. Hence, a comprehensive characterisation of its expression and functions in the vasculature is vital to appreciating its involvement in these and other aortic pathologies.

5.2.4.4 Phenotypes Linked to *ACAN* Mutations and Common Polymorphisms

At least 25 different pathological *ACAN* mutations have been described to date, predominantly missense or nonsense mutations within the three globular domains resulting in *ACAN* haploinsufficiency [419–426]. Mutated molecules appear to impair ECM assembly, function and interaction with other matrix proteins, giving rise to a wide phenotypic spectrum [420]. Although there are no clear genotype-phenotype correlations the most common feature is short stature, while other anatomical abnormalities, such as early onset osteoarthritis, advanced bone maturation, osteochondritis dissecans, degenerative disk disease, and craniofacial abnormalities are also noted.

A variable number of tandem repeat (VNTR) polymorphism occurring within a highly conserved region of CS1 has been linked with an increased risk of osteoarthritis and premature lumbar disk degeneration [427, 428]. It is suggested that the VNTR results in variation in the length of the core protein and the degree of CS attachment, impacting the water-reserving function of aggrecan and thus enhancing susceptibility to tissue degeneration [428–430]. A number of common SNPs within *ACAN* have similarly been associated with lumbar disc degeneration and herniation [431–433].

Similar to *ACAN* pathological mutations, homozygous cartilage matrix deficiency (cmd) mice harbouring a 7-bp deletion in exon 5 of the *Acan* gene present with dwarfism, a cleft palate and succumb immediately after birth due to respiratory failure [434]. In contrast, heterozygous animals appear normal at birth but develop slight dwarfism and age-associated spinal misalignment with abnormal collagen fibril morphology within cartilage [435].

5.2.5 Fibulin-1: Structure, Domains and Binding Partners

The fibulins are ubiquitously expressed ECM glycoproteins, and there are currently eight identified family members based on homologies at the gene and protein level. Fibulins range in size between 50-600 KDa and are characterised by a modular structure containing an epidermal growth factor (EGF)-like motif, followed by a series of calcium-binding (cb)-EGF-like motifs, and a C-terminal fibulin (FC) domain. Fibulin-1 is a 90 KDa protein encoded by the *FBLN1* gene which maps to chromosome 22(q13.3) [436]. Alternative splicing yields four variants: fibulin-1A-D, which differ in amino acid sequence, length of the FC domain, and binding partners (Figure 5.5) [437]. Fibulin-1 is detected during early embryonic stages and plays an important role in organogenesis [438, 439]. It predominantly localises to basement membranes, microfibrils and elastic fibres of the skin, kidney, lung, liver and cardiovascular tissues, where it interacts with several structural proteins and growth factors, and is also found in association with coagulation factors in the blood [334, 438–442].

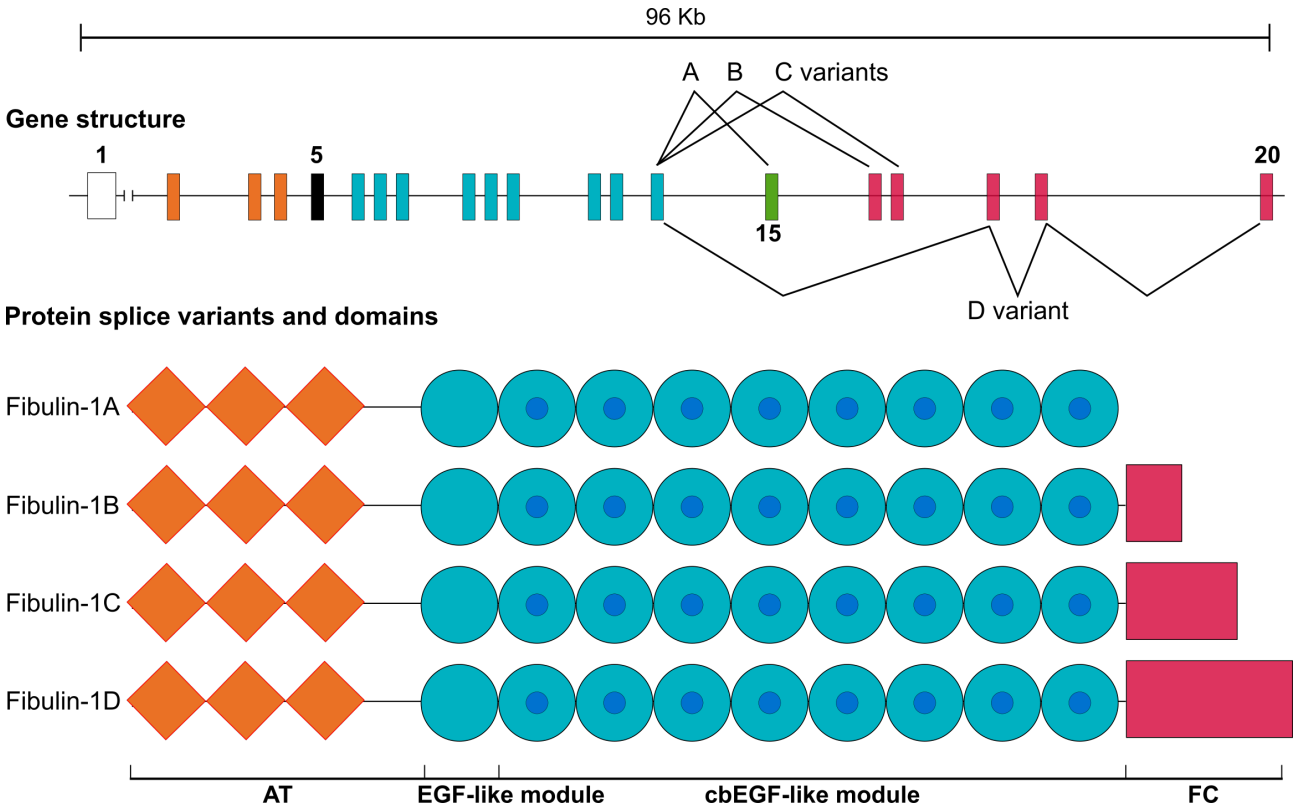

Figure 5.5: Schematic model of *FBLN1* exons and their corresponding protein domains and splice variants. Exons colours reflect those of the protein motifs that they encode. Exon 1 is the translation start and signal peptide, exon 5 encodes the short junctional segment between the AT and EGF-like module, and exon 15 starts with a stop codon and therefore doesn't encode an extra domain for variant A. AT; anaphylatoxin-like domain. Image modified from Timpl et al. [443].

5.2.5.1 Anaphylatoxin-like Domain

All four fibulin-1 isoforms contain three anaphylatoxin-like (AT) repeats at the N-terminal, which are rich in cysteine and disulphide groups [444]. These motifs are unique to fibulin-1 and fibulin-2 amongst all fibulins, and do not appear to impact on ligand affinity, however their specific contribution to the functions of these fibulins is not well defined [444].

5.2.5.2 Calcium Binding Domains

Many ECM proteins, including fibulin-1, contain moieties that are capable of binding calcium with various degrees of affinities [443, 445]. Calcium ions confer important properties to the proteins with which they are bound, such as enhancing their thermal stability, protecting against proteolytic degradation, and providing structural stabilisation to the protein [445]. Calcium ions ligate to fibulin-1 through its cbEGF-like motifs, which have been shown to protect fibulin-1 against MMP, plasmin and thrombin degradation [446], and mediate the interaction of fibulin-1 with self-association sites present on fibulin-1 molecules to form dimers and with other basement membrane ligands [447–449].

5.2.5.3 C-terminal Fibulin Domain

The fibulin family of proteins are defined by the presence of the carboxy-terminal FC globular domain. Variations in the amino acid sequence and length of the FC domain results in the four distinct isoforms of fibulin-1. While the precise function of this domain is not clear, it is potentially important in conferring functional specificity to the different fibulin-1 isoforms. The splice variants display differential tissue expression and affinities to their binding partners, and have distinct roles in health and diseases [437, 450, 451]. For example, fibulin-1C binds nidogen at a 30-fold higher affinity than fibulin-1D [444], and in nematodes the former is required for organ morphology while the latter is required for the assembly of hemicentin polymers [450]. Fibulin-1A and fibubulin-1B, are expressed predominantly during development and not in adult tissues [452].

5.2.5.4 Binding Partners

Much of the understanding of fibulin-1 functions originates from its tissue localisation and from the identification of the proteins that it interacts with. A list of currently known fibulin-1 binding partners and their functions are summarised in Table 5.1.

Table 5.1: Molecular interactions of fibulin-1

Interacting Protein	Summary of Functions	References
ADAMTS-1/5	Aggrecanase with anti-angiogenic activity; associated with several inflammatory processes.	[453, 454]
Aggrecan	Imparts viscoelasticity to tissues.	[334]
Angiogenin	Mediates new blood vessel formation.	[455]
β-amyloid precursor protein	Cell surface receptor, cleaved into peptides that promote transcription. May form amyloid plaques associated with Alzheimer's disease	[456]
ECMI	Ossification, skin hoemostasis, angiogenesis and tumour biology.	[457]
Fibrinogen	Blood coagulation, cell adhesion and chemotaxis.	[458]
Fibronectin	Blood coagulation, cell adhesion and chemotaxis.	[459]
Fibulin-7	Unknown	[460]
HB-EGF	Cell adhesion and migration; involved in cardiac valve development, atherogenesis and intimal hyperplasia.	[461]
Laminin	Associate with structural proteins of the ECM; involved in cell attachment and differentiation.	[462]
Nidogen	Organogenesis and embryonic development.	[447]
SHBG	Androgen and oestrogen transport in the blood.	[463]
Tropoelastin	Elastin precursor.	[441]
Versican	Chondroitin sulphate proteoglycan; involved in cell adhesion, proliferation, migration and angiogenesis.	[334]

ECMI; Extracellular matrix protein 1, HB-EGF; Heparin binding-EGF, SHBG; sex-hormone binding globulin.

Fibulin-1 appears to serve different functions contingent on the tissue-specific interactions with its binding partner. Its interaction with ADAMTS-1 and 5 mediates the cleavage of aggrecan and versican, while its interaction with β-amyloid precursor protein blocks neural stem cell proliferation [454, 456, 464]. Although the biological significance of these interactions are not clear, they point towards important functions for fibulin-1 in matrix assembly and remodelling, cell adhesion and mobility and blood coagulation.

5.2.6 Fibulin-1: Biological Functions

5.2.6.1 Organ and Vessel Wall Development

Fibulin-1 expression is detected during early human and mouse embryonic development, and is notably prominent in the heart valve, in the aorta preceding elastin fibre formation, and in zones undergoing epithelial-mesenchymal conversion, including neural crest cells and the developing tooth and hair follicles [438, 439, 465]. In the aortas of human embryos of gestational weeks (gw) 4-10, fibulin-1 is detected as early as gw4 in the endothelial basement membrane and perivascular mesenchyme, in the tunica adventitia by gw6, and is completely absent from the endothelium and tunica media [438]. Fibulin-1 expression persists into adulthood in most tissues, and its aortic distribution patterns are most visible in association with the internal elastic membrane and the adventitia, and mildly present in the medial layer surrounding VSMC [456, 466]. Fibulin-1 null animals generally succumb by the second day postpartum due to a combination of haemorrhage and significant respiratory, cranial nerve, renal, cardiac, microvessel and aortic arch malformations [465, 467]. Haemorrhage occurs mostly in skin, muscle and perineurial tissues, and is presumed to be due to the abnormal endothelial lining of microvessels which results in disrupted vessel walls. Moreover, the capillaries of the heart, lungs, kidneys and abdominal cavity organs appear widened and irregular, supporting a specific role for fibulin-1 in angiogenesis [465]. Its specific localisation within the amorphous core of elastin fibres also suggests its contribution to the elasticity of the tissues within which it is expressed [440]. The mechanisms underlying fibulin-1 mediated heart development have partially been elucidated, and appear to involve the suppression of ventricular cardiomyocyte proliferation by mediating ADAMTS-1 cleavage of versican [464].

5.2.6.2 Circulating Fibulin-1

Fibulin-1 is present in the circulation at concentrations (30-50µg) exceeding those of other ECM proteins commonly found in the blood, including laminin and type IV collagen [458]. In addition to its association with the blood coagulation factors fibronectin and fibrinogen, fibulin-1 is also found

incorporated into *in vivo* and *in vitro* formed fibrin clots, as it promotes platelet adhesion by bridging fibrinogen to the platelet integrin $\alpha_{IIb}\beta_3$, and is heavily present in human coronary artery atherosclerotic lesions [458,468,469]. Previous studies have strongly supported a role for circulating fibulin-1 in haemostasis and thrombogenesis but these are challenged by the observation that fibulin-1 knockout mice do not display abnormal coagulation [465]. The function of circulating fibulin-1 in plasma is thus not conclusive, but a crucial observation is that it fluctuates in association with several conditions indicating a pleiotropy of important physiological and pathological functions. For example, it's levels correlate with markers of renal and kidney function, diabetes, atrial fibrillation, aortic valve stenosis, as well as with PWV and Augmentation Index [470–474].

5.2.7 Fibulin-1: Pathological Roles

5.2.7.1 Aortic Stiffness and Dissections

The strong overlap of fibulin-1 expression with elastic fibres support its role in imparting elasticity to the tissues within which it is present. It is therefore not surprising that it has been implicated in aortic stiffness and dissections. Durier et al. first identified its transcript to be up-regulated in subjects with increased arterial stiffness, and it was subsequently found to be up-regulated in non-atherosclerotic aortic specimens of type 2 diabetic subjects [75,466]. The differential transcript expression in this group was also evident at the protein level, where fibulin-1 expression in external elastin membranes was more pronounced in diabetic subjects compared to non-diabetic subjects [466]. Consequently, fibulin-1 was suggested to be involved in diabetes-associated arterial stiffness and ECM alterations. Fibulin-1 is also differentially expressed in mineralising compared to non-mineralising VSMC, further supporting its pathological role in altering normal arterial wall architecture by promoting vascular calcification [475]. Moreover, the association of fibulin-1 with atherosclerotic lesions is specifically pronounced in regions rich in macrophages [469], suggesting inflammatory-mediated mechanisms are associated with arterial stiffness. The strong correlation of circulating fibulin-1 levels with stiffness indexes further substantiates these observations, and further characterisation of fibulin-1 in the vasculature may aid in understanding the mechanisms that drive its association with arterial stiffness.

In contrast to these findings aortic tissues recovered from Stanford type A dissections display a significant down-regulation of fibulin-1 transcript and protein abundance, despite overlapping aetiologies with arterial stiffness [476,477]. Importantly, concomitant with the down-regulation of fibulin-1 is the profile of increased MMPs and diminished elastin and collagen IV, both at the transcript and

protein levels. The altered expression of fibulin-1 in these patients may be a consequence of elastin loss from the aorta triggered by the increased expression of elastinolytic MMPs. Alternatively, given the association of fibulin-1 with structural components of the ECM and the role of the ECM in cellular signal transduction, its loss from the aorta may compromise the structural framework of the aortic wall and modulate its signalling activities, collectively impairing aortic connective tissue and predisposing to dissection. Fibulin-1 expression is altered in other connective tissues of the cardiovascular system in association with disease status; it is down-regulated in atrial tissues of patients with atrial fibrillation and in the mitral valve of animal models with mitral regurgitation, but is up-regulated in myocardial tissues from patients with coronary artery disease and those with dilated cardiomyopathy [478–480].

5.2.7.2 Respiratory Diseases

Fibulin-1 is a major contributor of several respiratory conditions, and is upregulated in primary bronchoepithelial cells and the sera of patients with chronic obstructive pulmonary disease (COPD) [452], in the sera and airway smooth muscle cells of asthamtic patients [481], and in the sera and lungs of subjects with idiopathic pulmonary fibrosis [482]. In accordance with these findings, *Fbln-1c* deletion in mice protects against COPD progression, diminishes airway collagen deposition and promotes the infiltration of pro-inflammatory cytokines Tnf-α, IL-33, Tgf-β and the chemokine Cxcl1 in lung tissues [452]. These effects are potentially mediated by a specific bioactive peptide within the FC module of fibulin-1C, which was shown to enhance fibroblast proliferation and attachment, and the deposition of several glycoproteins in COPD derived fibroblasts [483]. These findings support a strong role for fibulin-1 in collagen assembly, ECM remodelling and inflammation.

5.2.7.3 Phenotypes Linked to *FBLN1* Mutations

Mutations within *FBLN1* have not been widely identified in association with human genetic diseases. A chromosomal translocation occurring in intron 19 of *FBLN1* has been reported in a pedigree with complex synplydactyly [484], where the phenotypic manifestation of the mutations carriers, mainly limb deformations, was attributed to haploinsufficiency of the *FBLN-1D* isoform caused by the translocation. This interpretation is in agreement with the role of fibulin-1 in organogenesis described earlier. More recently, a missense mutation p.(Cys397Phe) corresponding to the cbEGF domain has been described in a family displaying similar symptoms of digit fusion, in addition to brain atrophy and mental retardation [485]. To date, no other pathogenic mutations or common variants in *FBLN1* have been reported.

5.3 Methods

5.3.1 Study Design and Phenotype Definitions

A multi-stage candidate gene-based design was adopted for this study (Figure 5.6), and the data reported in this chapter reflects the work executed for stages III and IV of the study.

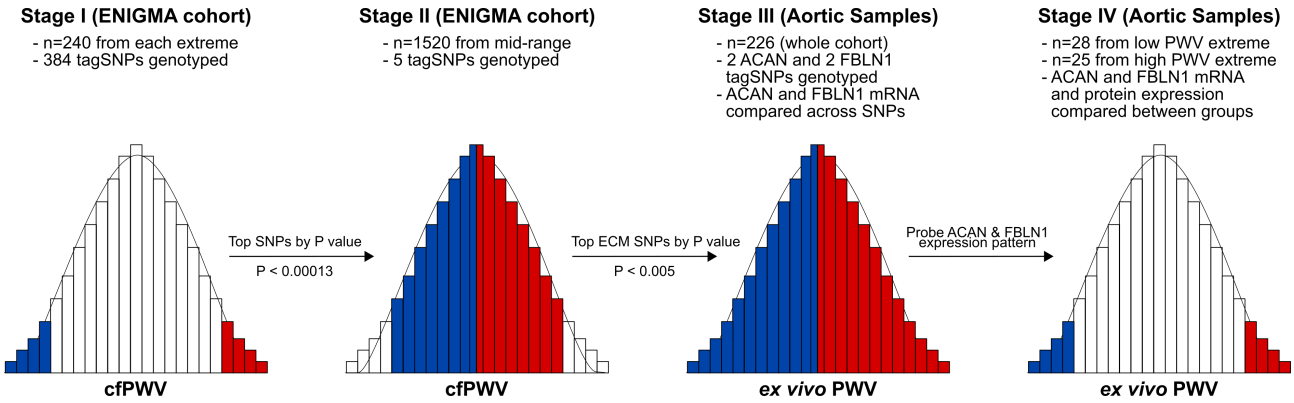

Figure 5.6: Study design. During stage I genotyping of 384 tagSNPs was performed on 240 samples from each extreme of PWV in the ENIGMA cohort. In stage II, 5 SNPs were replicated in the remainder of the ENIGMA participants with mid-range PWV values (n=1520), and then the SNPs that were associated most significantly with PWV were validated in the donor aortic samples (stage III) and further correlated with transcript levels of their respective genes. During stage IV the transcript and protein expression patterns of aggrecan and fibulin-1 were investigated in samples from the extreme ends of the *ex vivo* PWV distribution.

Briefly, in the first stage of the study (Stage I, Figure 5.6), a total of 384 tagSNPs were selected on the basis of gene expression profiling work undertaken by Durier et al. [75], in addition to other genes known to be associated with PWV or arterial wall properties [486]. The SNPs were generated from either the International HapMap project, SeattleSNPs database or intronic/exonic or promoter SNPs from previously published association studies. SNPs were genotyped in 240 samples below the age of 25 from each extreme of PWV within the ENIGMA cohort [487], adjusting for mean arterial pressure as a confounder. Highly significant SNPs (P<0.00013) which were related to the ECM were selected for replication in the remaining participants of the ENIGMA cohort with mid-range PWV values (Stage II). In total, five SNPs were validated in this stage, three in *ACAN* (rs3743399, rs2882676 and rs2293087) and two in *FBLN1* (rs2018279, rs2238823). The P-values of the five tag-SNPs with PWV and further details on SNP selection and gene assignment to these SNPs are described by Yasmin et al. [Publication 3]. Because significant associations were observed between PWV and *ACAN* and *FBLN1* in the primary and replication studies [Publication 3], the actual role of these proteins was investigated in human donor aortic tissues in stages III and IV of the study. SNPs that associated significantly in the ENIGMA replication cohort were tested for their association with *ex*

vivo aortic stiffness in the tissue samples (n=226), as well as with *ACAN* and *FBLN1* mRNA and protein levels. To further define a functional role for aggrecan and fibulin-1, transcript abundance and protein distribution were examined in the extremes of the *ex vivo* PWV distribution (Stage IV, Figure 5.6). This 'extreme selection' strategy [488] allows for the greatest phenotypic separation between 'cases' (i.e. high PWV) and 'controls' (i.e. low PWV), thus maximising the power to detect possible differential expression of these genes and their respective protein distribution in the aorta. Age-associated changes to the expression patterns of aggrecan and fibulin-1 were also examined, with individuals <32 years (n=10) being classified as 'young' and those >60 years (n=10) as 'old'.

5.3.2 SNP Genotyping

Two exonic tagSNPs in *ACAN* (rs2293087 and rs2882676) located within exons 3 and 13, respectively, and two intronic tagSNPs in *FBLN1* (rs2018279 and rs2238823) were genotyped using TaqMan® SNP Genotyping assays (ThermoFisher Scientific, USA) as described in Chapter 2. The genetic information collected for each of the polymorphisms differed depending on DNA quality and availability, and/or genotyping assay failures. SNP genotyping was carried out by Sarah Cleary (Cambridge University, UK).

5.3.3 *ACAN* and *FBLN1* Gene Expression

ACAN and *FBLN1* gene expression was quantified using TaqMan® gene expression assays as detailed in Chapter 2. The *ACAN* assay overlaps exon boundaries 11-12, which code for KS and CS regions of human aggrecan core protein (NP_001126.3). The fold difference in *ACAN* and *FBLN1* gene expression between low and high EM samples was calculated using the $2^{-\Delta Ct}$ method (Eq. 2.2).

5.3.4 Antibodies

The aggrecan G1 domain was probed with an anti-aggrecan (ab36861, Abcam, UK) rabbit polyclonal IgG antibody that recognises residues 50-150 of aggrecan, which was used at a 1:200 dilution. The CS region was probed with an anti-aggrecan antibody (MCA145T, Bio-Rad, USA) that recognises an epitope within the N-terminal CS-binding region at a 1:400 dilution, while the aggrecan G3 domain was probed with an anti-aggrecan antibody H-300 (sc25674, Santa Cruz Biotechnology, USA) that recognises residues 1911-1962 of aggrecan corresponding to the G3 domain at a 1:100 dilution. Anti fibulin-1 (sc20818, Santa Cruz Biotechnology, USA) rabbit polyclonal IgG antibody was used at 1:200 dilution, while an anti-β Actin mouse monoclonal IgG (MA5-15739, ThermoFisher Scientific, USA) was used at 1:1000 dilution. Donkey anti-rabbit (925-32213, LI-COR, USA) IRDye® 800CW and

goat anti-mouse (A-21058, ThermoFisher Scientific, USA) Alexa Fluor® 680 conjugated secondary antibodies were used for Western blots at 1:5000 dilution. Pre-absorbed goat IgG-conjugated Alexa Fluor® 633 secondary antibody (A21050, ThermoFisher Scientific, USA) was used for immunofluorescent staining at 1:200 dilution.

5.3.5 Statistical Analysis

Deviations from the Hardy-Weinberg equilibrium were tested using the χ^2 test, and skewed data were log-transformed for statistical analyses. To assess the independent contribution of the tagSNP genotypes on PWV, multiple regression analysis was performed adjusting for known determinants of PWV (age, age^2, gender, height and weight) and following an additive model of inheritance. A secondary multiple regression analysis excluding all abdominal and iliac specimen was also performed adjusting for the same factors. An unpaired Student's t test with Welch's correction was used to compare differences between the two homozygous allele carriers of tagSNPs and their transcript levels. Statistical significance between low PWV and high PWV samples was determined using a two-tailed Student's t-test. A post hoc ANCOVA analysis was performed to account for the confounding effect of age between the two groups. For Western blot quantification statistical significance between groups was determined using the non-parametric Mann Whitney U test. In all tests a P value of <0.05 was considered significant.

5.4 Results

5.4.1 Study Sample Characteristics

The clinical and demographic features of the entire study cohort are provided in Table 4.4 (Chapter 4). The baseline characteristics of the samples with the lowest and highest *ex vivo* PWV values are described in Table 5.2; donors in the stiffer, high PWV group were older and had higher systolic blood pressure compared to the low PWV group.

Table 5.2: Baseline characteristics of the study cohort

	Low PWV (n=28)	**High PWV (n=25)**	**P value**
Male/Female	19/9	15/10	0.502
Age (years)	48±10	71±9	<0.001
PWV (m/s)	2.95±0.16	5.99±1.32	<0.001
BMI (Kg/m^3)	27.6±3.1	28.1±5.6	0.699
SBP (mmHg)	125±29	131±25	0.388
DBP (mmHg)	70±16	65±14	0.210

Data are mean±SD

5.4.2 Genetic Association Analysis

The two *ACAN* SNPs (rs2882676 and rs2293087) were found to significantly deviate from the Hardy-Weinberg equilibrium (P<0.001 and P=0.006, respectively; Table 5.3). However, visual inspection of the genotyping data did not indicate genotyping errors or signs of sub-optimal separation, and both SNPs were therefore retained in the analysis. Hardy-Weinberg equilibrium was satisfied for the two *FBLN1* SNPs, rs2018279 and rs2238823 (Table 5.3).

Table 5.3: *ACAN* and *FBLN1* polymorphisms with genotype and allele frequencies

SNPs	**Genotypes**	**N(%)**	**Hardy-Weinberg Test**	**Alleles**	**N(%)**	**Global MAF**
rs2882676	AA	30 (13.9)	χ^2=18.39	A	122 (27.7)	C=42.4%
	AC	62 (28.7)	P<0.001	C	310 (72.3)	
	CC	124 (57.4)				
rs2293087	GG	72 (39.3)	χ^2=7.29	G	215 (58.7)	G=44.5%
	GT	71 (38.8)	P=0.006	T	151 (41.3)	
	TT	40 (21.9)				
rs2018279	AA	66 (30.3)	χ^2=0.018	A	239 (54.8)	T=47.5%
	AT	107 (49.1)	P=0.893	T	197 (45.2)	
	TT	45 (20.6)				
rs2238823	AA	126 (57.5)	χ^2=0.776	A	329 (75.1)	G=19.2%
	AG	77(35.2)	P=0.378	G	109 (24.9)	
	GG	16 (7.3)				

Global minor allele frequency (MAF) is derived from the 1000Genome data, retrieved from dbSNP (`https://www.ncbi.nlm.nih.gov/snp/`).

5.4.2.1 *ACAN* tagSNPs

No significant differences were observed in PWV among either rs2882676 or rs2293087 genotypes (Figures 5.7A and 5.8A). Multiple regression analyses correcting for known confounders of PWV further did not show a significant association with PWV for these SNPs, both in the primary analysis

including all samples and the secondary analysis that excluded all abdominal and iliac specimens (Table 5.4). Next, it was investigated if the variants modulated the expression of aggrecan in the donor aorta. Donors homozygous for the rs2882676/A allele were found to have significantly higher *ACAN* mRNA expression compared to those who were homozygous for the A allele (P=0.04; Figure 5.7B), with the difference remaining significant even after correcting for age as a confounder (P=0.05, ANCOVA). This was further examined at the protein level in donor aortic homogenates. Because of the age-associated changes in aggrecan, only subjects below the age of 45 from each genotype were selected for the analysis. Despite the correlation with *ACAN* mRNA, genotypes for rs2882676 did not show any correlations with aggrecan protein expression (Figure 5.7C-D). In contrast, donors with rs2293087 genotypes did not show any significant correlation with *ACAN* transcript levels (Figure 5.8B) and the difference remained below the significance threshold after correcting for age as a confounder (P=0.130, ANCOVA). Protein expression was therefore not explored further for this SNP.

Table 5.4: Multiple regression analyses of the *ACAN* tagSNPs

Model	Predictors	Primary Analysis*			Secondary Analysis**		
		β	P	Adj R^2	β	P	Adj R^2
1	Age	-2.305	<0.001	0.43	-2.065	<0.001	0.46
	Age^2	2.782	<0.001		2.591	<0.001	
	Gender	-0.003	0.967		0.037	0.610	
	Height	-0.088	0.228		-0.069	0.391	
	Weight	0.097	0.102		0.095	0.140	
	rs2882676	-0.016	0.776		-0.001	0.989	
2	Age	-2.467	<0.001	0.47	-2.191	<0.001	0.50
	Age^2	2.956	<0.001		2.745	<0.001	
	Gender	-0.082	0.258		-0.038	0.619	
	Height	-0.104	0.168		-0.071	0.398	
	Weight	0.029	0.630		0.012	0.849	
	rs2293087	0.051	0.376		0.051	0.399	

*regression analysis for PWV, adjusted for age, age^2, gender, height and weight using an additive gene-dose model;

**regression analysis for PWV, adjusted for age, age^2, gender, height and weight using an additive gene-dose model and excluding abdominal and iliac samples ;

The parameter β is the estimated effect on PWV per minor allele in the additive model.

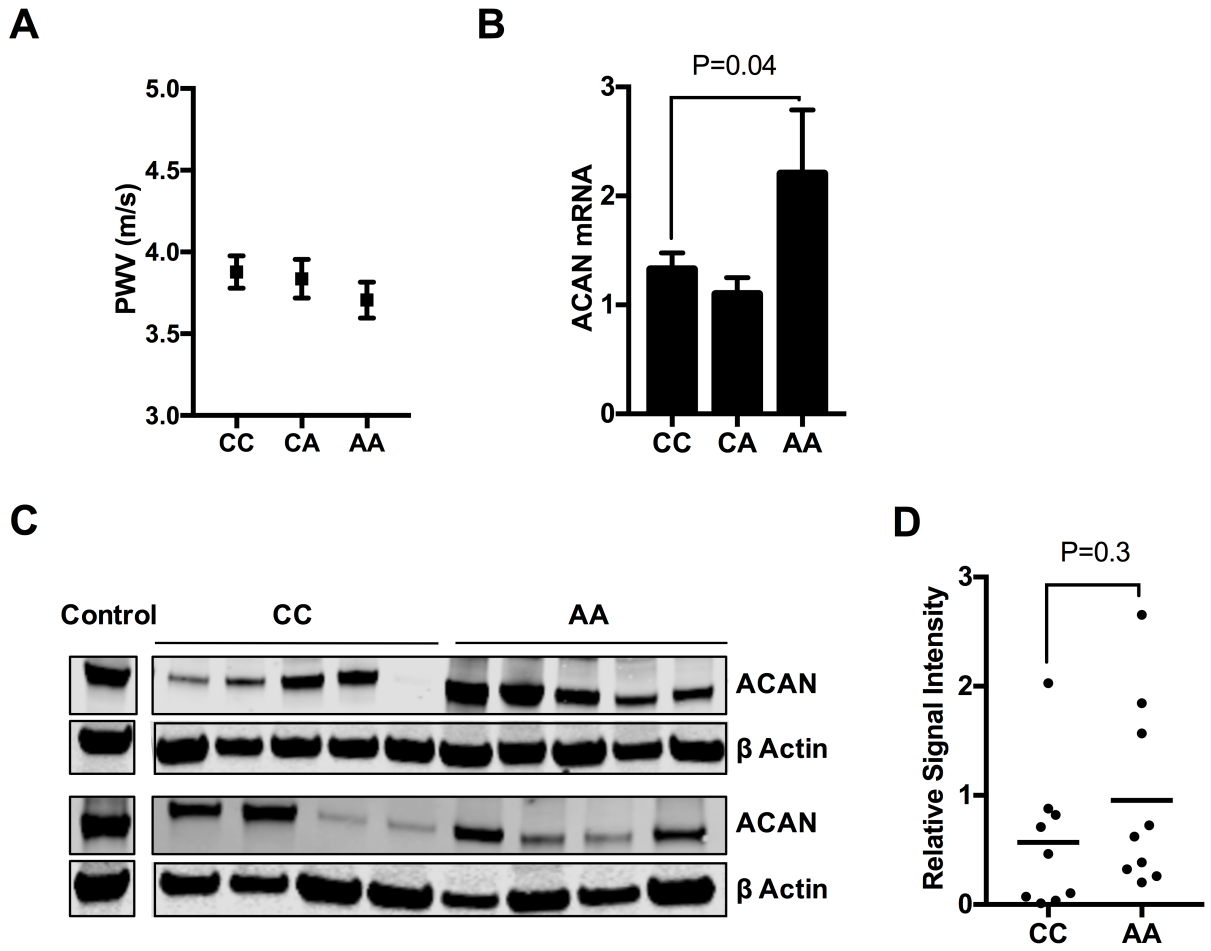

Figure 5.7: rs2882676 polymorphism correlations with PWV, *ACAN* transcript and protein expression. (A) PWV stratified by genotype. (B) Transcript expression pattern of *ACAN* in the three genotypes; bars represent the mean±SEM of *ACAN* transcript, normalised against *GAPDH*. P value derived using the Student's t test. (C) Western blot of the CS region in the two homozygous allele donors (n=18). The control sample is a homogenate of all samples used in the experiment to normalise between blots. (D) quantification of aggrecan Western blot signal intensities normalised against β Actin. Horizontal line indicates mean signal intensity.

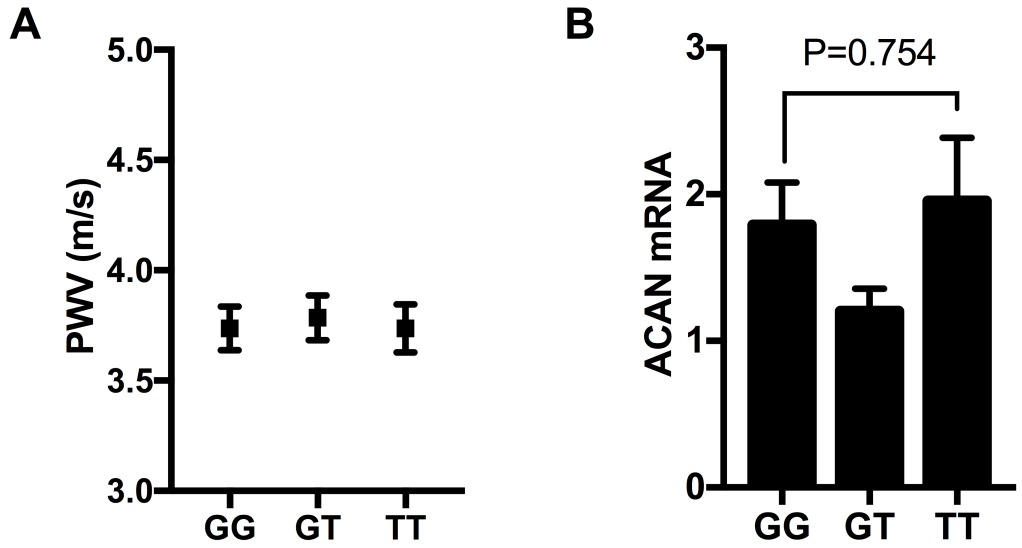

Figure 5.8: rs2293087 polymorphism correlations with PWV and *ACAN* transcript (A) PWV stratified by genotype. (B) Transcript expression pattern of *ACAN* in the three genotypes; bars represent the mean±SEM of *ACAN* transcript, normalised against *GAPDH*. P value derived using the Student's t test.

5.4.2.2 *FBLN1* tagSNPs

Similar to the *ACAN* tagSNPs, no differences were observed in PWV among genotypes of the *FBLN1* SNPs, rs2018279 or rs223823 (Figures 5.9A and 5.10A). The lack of association persisted in both the primary and secondary multiple regression analyses accounting for the known confounders (Table 5.5). These SNPs were further tested for their association with aortic *FBLN1* transcripts, but no association between the SNPs respective genotypes and *FBLN1* mRNA were identified (Figures 5.9B and 5.10B). The protein level was further explored for rs2018279 but the Western blot quantitation did not indicate any differences between its genotypes (Figure 5.9C-D).

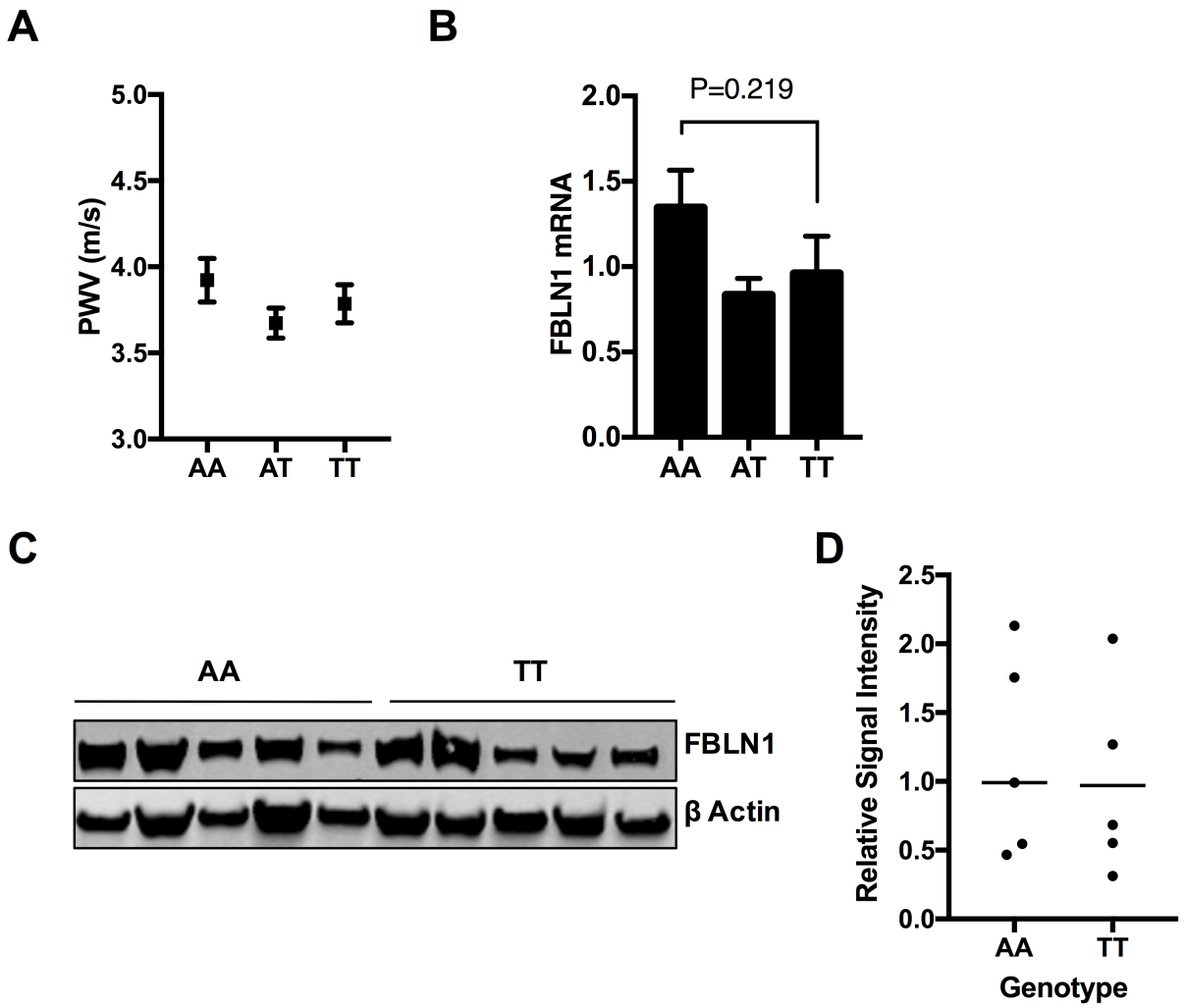

Figure 5.9: PWV and *FBLN1* mRNA and protein stratified by rs2018279. (A) PWV stratified by genotype; data points are mean±SEM of PWV. (B) Transcript expression levels of *FBLN1* across the three genotypes; bars represent the mean±SEM of *FBLN1* transcript, normalised against *GAPDH*. P value derived using the Student's t test. (C) Protein expression levels of fibulin-1 between the two homozygous allele donors, showing no genotype differences in aortic fibulin-1 content. (D) Quantification of fibulin-1 signal intensities normalised against β Actin of the Western blot in panel (C).

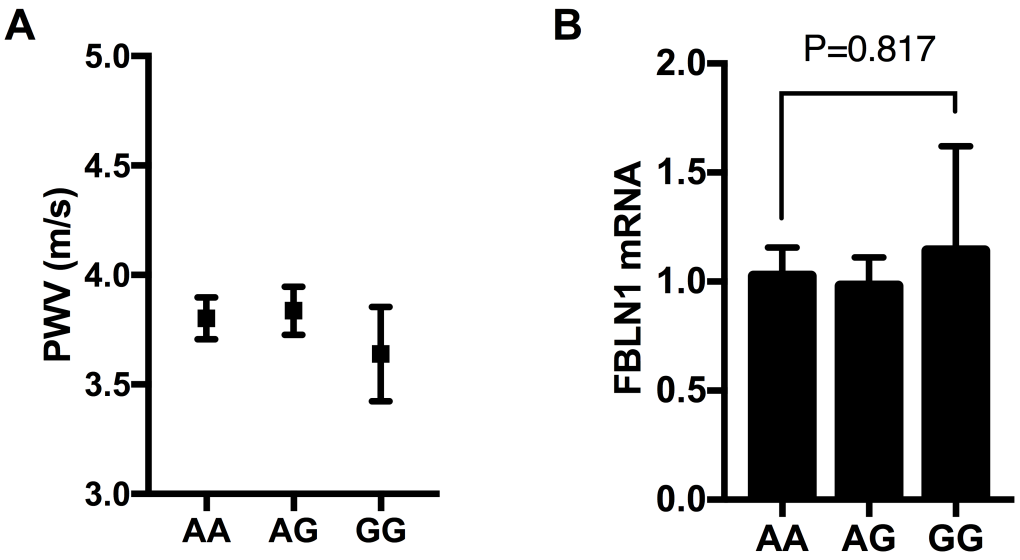

Figure 5.10: PWV and *FBLN1* mRNA stratified by rs2238823 genotypes. (A) PWV stratified by genotypes; data points are mean±SEM of PWV. (B) Transcript expression levels of *FBLN1* in the three genotypes; bars represent the mean±SEM of *FBLN1* mRNA, normalised against *GAPDH*. P value derived using the Student's t test.

Table 5.5: Multiple regression analyses of the *FBLN1* tagSNPs

Model	Predictors	Primary Analysis*			Secondary Analysis**		
		β	P	Adj R^2	β	P	Adj R^2
1	Age	-1.974	<0.001	0.37	-1.888	<0.001	0.40
	Age^2	2.438	<0.001		2.397	<0.001	
	Gender	-0.038	0.606		0.002	0.982	
	Height	-0.074	0.337		-0.080	0.336	
	Weight	0.087	0.159		0.067	0.316	
	rs2018279	-0.039	0.505		-0.051	0.402	
2	Age	-1.994	<0.001	0.35	-1.892	<0.001	0.40
	Age^2	2.445	<0.001		2.402	<0.001	
	Gender	-0.035	0.632		-0.013	0.864	
	Height	-0.082	0.289		-0.090	0.227	
	Weight	0.090	0.149		0.074	0.270	
	rs2238823	0.008	0.891		-0.005	0.937	

*regression analysis for PWV, adjusted for age, age^2, gender, heigh and weight using an additive gene-dose model;
**regression analysis for PWV, adjusted for age, age^2, gender, heigh and weight using an additive gene-dose model and excluding abdominal and iliac samples;
The parameter β is the estimated effect on PWV per minor allele in the additive model.

5.4.3 Patterns of Aggrecan and Fibulin-1 Aortic Expression

To further define the functional role of aggrecan and fibulin-1 in the vasculature, their transcript and protein expression patterns were examined in subjects from the extreme ends of the PWV dis-

tribution (respectively low PWV and high PWV). Because many ECM proteins are altered or degraded with age, the expression patterns were further compared between young (<32 years) and old (>60years) subjects. Data from the GTEx Consortium [489] was used to compare the gene expression of *ACAN* and *FBLN1* in the aorta relative to other tissue types. The GTEx Project provides whole transcriptome RNA-sequencing profiles of over 40 tissues (e.g aorta, skin, brain, skeletal muscle, whole blood) from hundreds of human donors of various ages.

5.4.3.1 *ACAN* Expression Across Tissue Types

Data obtained from the GTEx portal (GTEx Analysis Release V7) shows a striking difference in the tissue-specific expression profile of *ACAN*, being most highly expressed in the tibial (n=441), aorta (n=299) and coronary (n=173) arteries compared to other tissue types (Figure 5.11).

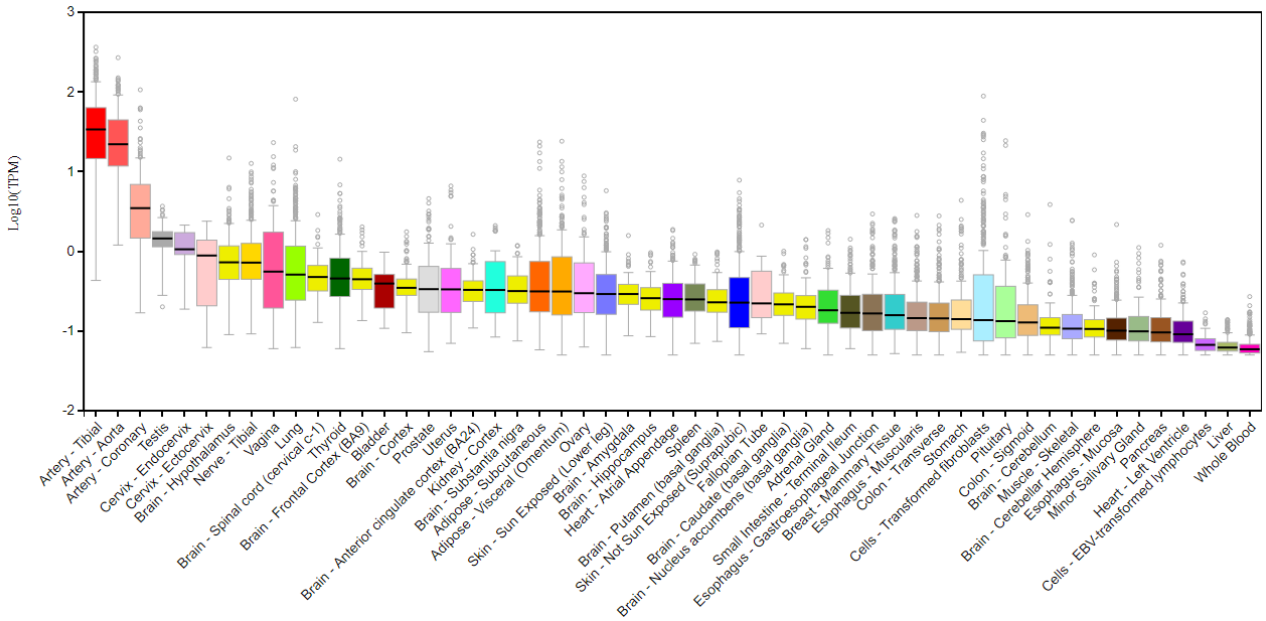

Figure 5.11: Expression pattern of *ACAN* across tissue types (`https://gtexportal.org/home/gene/ACAN`). TPM; transcripts per million reads.

5.4.3.2 Transcript and Protein Distribution of Aggrecan with Age and PWV

Aggrecan protein expression patterns in the aortic wall were investigated using antibodies that recognise epitopes on the three main domains of the protein; the N-terminal G1-G2 domain, the CS middle region and the C-terminal G3 domain. Aggrecan G1-G2 and G3 domains were found to be present throughout the vessel wall layers of young subjects (Figure 5.12A and C). However, in older subjects a striking deposition of G1-G2 domain staining was seen across the medial layer with a marked loss of immunofluorescent intensity for G3 domain staining (Figure 5.12C). This in-

dicates an age-dependent loss of the C-terminal and accumulation of N-terminal fragments in the aortic wall. CS fragments are necessary for viscoelasticity and their loss was confirmed by Western blotting aortic wall homogenates, which confirmed a 3.5-fold reduction (Figure 5.12B and D) in CS detected by immunoblotting in the older group (n=5) compared to the younger group (n=5). To examine if this loss in CS from the aortas of older donors was driven by changes to transcription levels, *ACAN* transcript abundance in aortic tissue was measured and the levels stratified by age decade (Figure 5.12F), which showed an incremental decline in ACAN transcript after the fifth decade.

Aggrecan protein expression patterns were then compared in young and old donor aortas based on their *ex vivo* elasticity (extreme ends of PWV values). Strikingly, it was found that young subjects with stiff aortas had a G1-G2 staining pattern that was more typical of the older aortas ($P<0.05$, Figure 5.13A). Conversely, young subjects with more distensible aortas expressed strikingly higher G3 compared to both older subjects and subjects with stiffer aortas (high PWV) (Figure 5.13B). It was also found that aggrecan expression of the CS attachment region was significantly compromised in both young and old aortas with high PWV compared to the low PWV counterparts (Figure5.13C-D). At the transcript level, high PWV donors had a significantly lower expression of *ACAN* mRNA (2.5-fold) compared to the low PWV group (Figure 5.13 D), which was measured using an assay for the overlapping exon boundaries 11-12, which encode the CS region. The difference persisted after correcting for age as a confounder (ANCOVA, $P<0.05$).

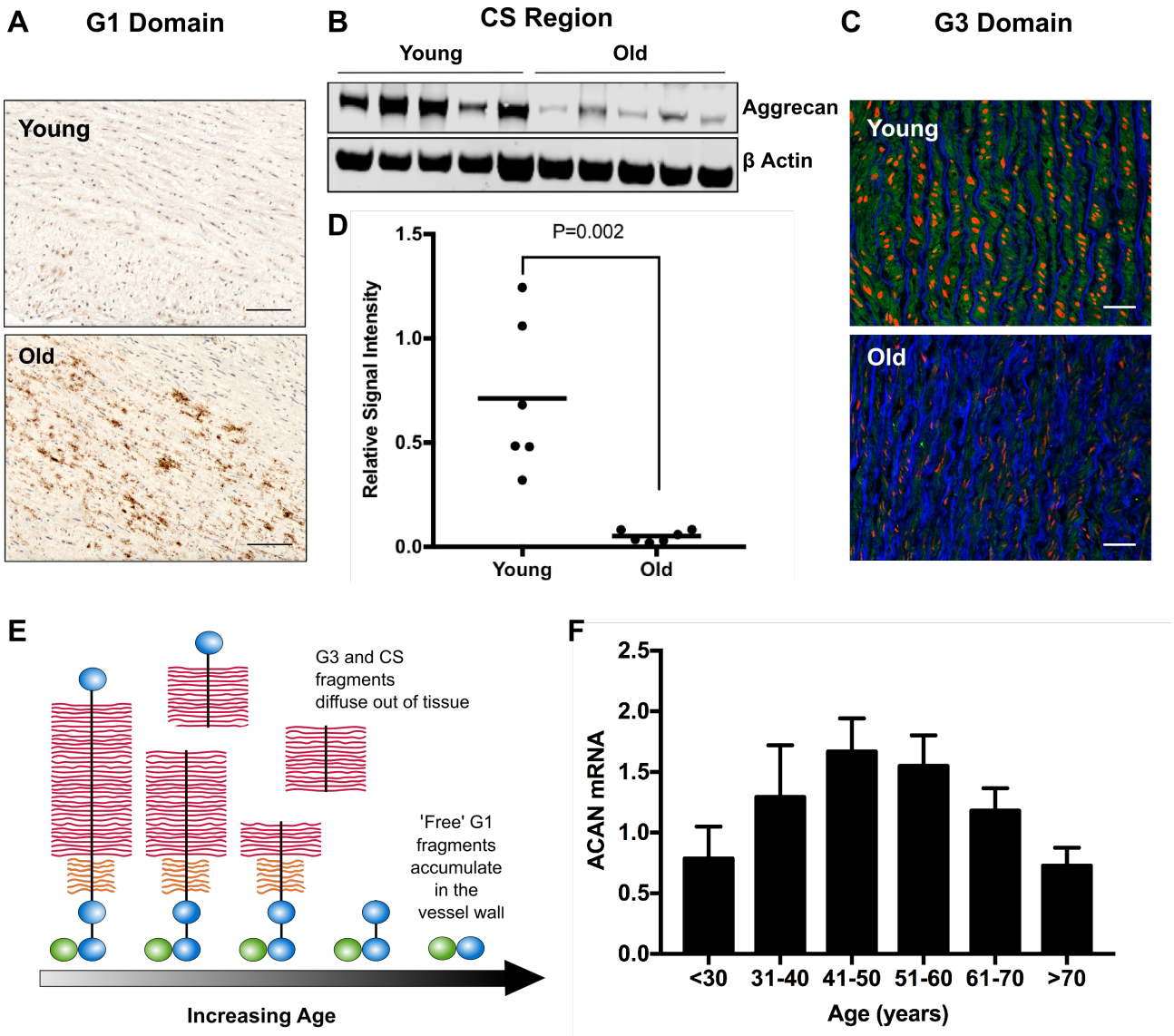

Figure 5.12: Age-associated changes in aggrecan expression patterns. (A) Representative sections showing immunohistochemical staining for the G1-G2 domain of aggrecan in the medial layer (Scale bar, 50µm). (B) Western blots showing the expression of the CS attachment region in young vs. older donors. (C) Representative immunofluorescence staining showing the uniform expression of aggrecan G3 domain (green) across the vessel wall of younger donors that is largely absent from older donors; elastic fibres are blue (autofluorescence) and nuclei are counterstained red (Scale bar, 50µm). (D) Quantification of aggrecan-CS signal intensities in young vs. older subjects, showing a significant difference in protein abundance between the two groups. P value derived using the Mann Whitney U test. (E) Schematic diagram of the degradation of C-terminal aggrecan fragments and their diffusion out of the vessel wall with increasing age, accompanied by an accumulation of G1 fragments. (F) *ACAN* transcript expression across age decades; bars represent mean±SEM normalised against *GAPDH*.

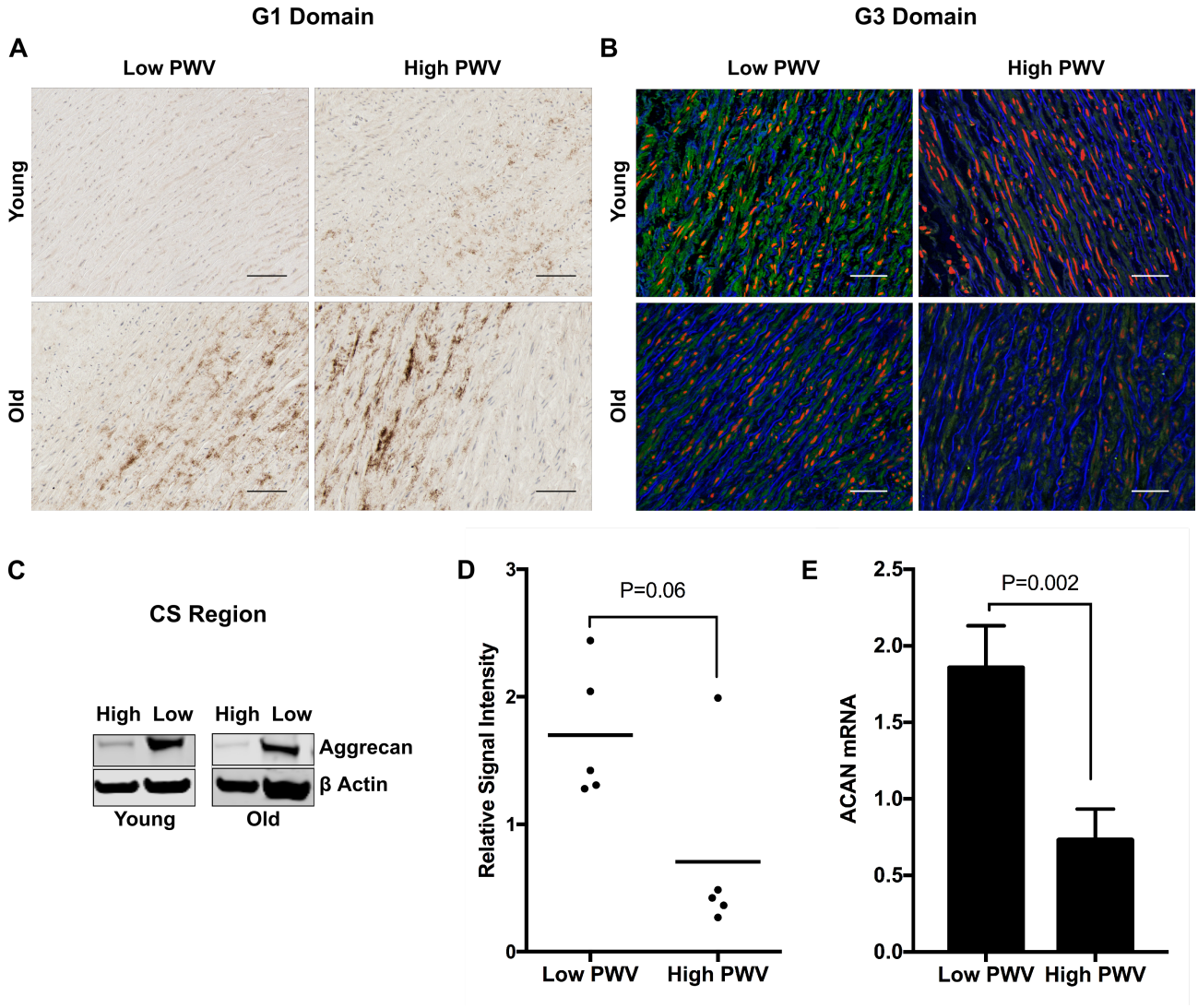

Figure 5.13: Aggrecan protein and transcript distribution in donors with low and high PWV. (A) Representative immunohistochemical staining comparing young and old samples with low PWV and high PWV. Young samples with high PWV show higher G1 deposits compared to young samples with low PWV (Scale bar 50µm). (B) Representative immunofluorescence staining of G3 domain showing higher G3 expression in young aortas with low PWV compared to high PWV samples (Scale bar 50µm). (C) Representative Western blot of aggrecan-CS region showing markedly higher levels in the aortas of low PWV subjects compared to high PWV subjects in both age groups. (D) Quantitation of aggrecan-CS signal intensities, normalised against β Actin; scatter plot represents individual values on the blot with the mean signal intensity and statistical significance determined by the Mann Whitney U test. (E) Transcript levels of *ACAN* showing lower levels of the transcript in high PWV samples compared to low PWV samples; bars represent mean±SEM *ACAN* transcript normalised against *GAPDH*. P value derived using the Student's t test.

5.4.3.3 *FBLN1* Expression Across Tissue Types

While not markedly high, the GTEx portal (GTEx Analysis Release V7) shows *FBLN1* transcript to be present across the tibial, coronary and aorta arteries (Figure 5.14). *FBLN1* transcript abundance in the aorta is comparable to that in the lung where fibulin-1 is a major contributor of several respiratory diseases (Section 5.2.7) and much higher than in whole blood where fibulin-1 is known to circulate

in high concentrations (Section 5.2.6).

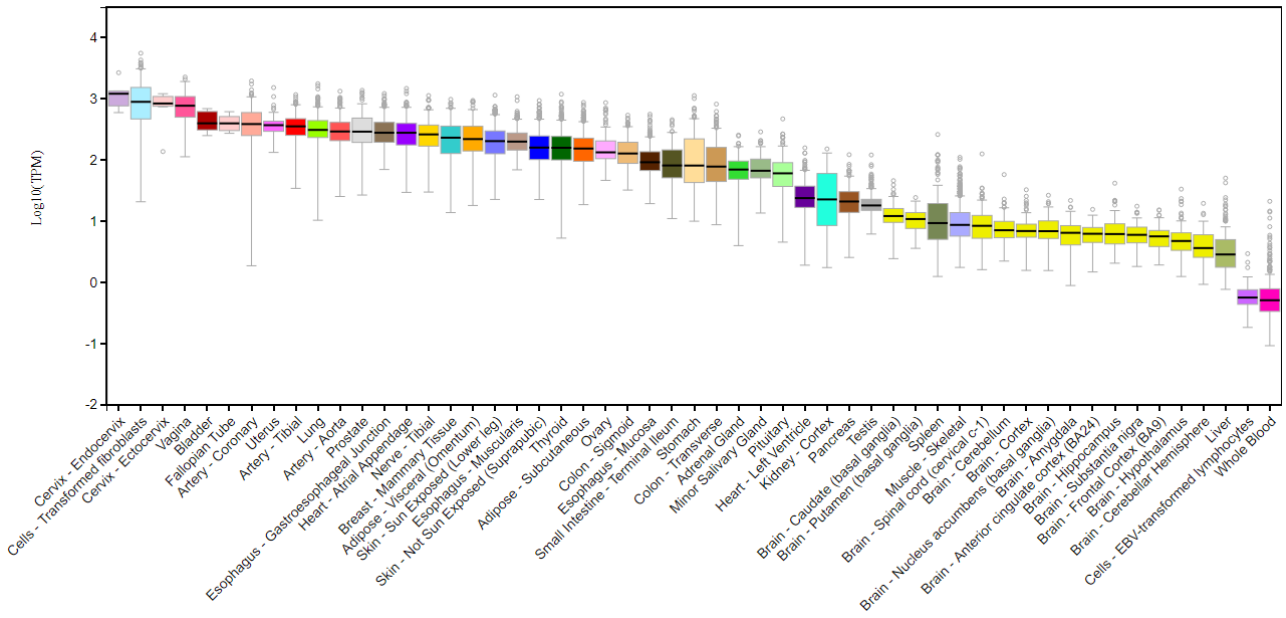

Figure 5.14: Expression pattern of *FBLN1* across tissue types (`https://gtexportal.org/home/gene/FBLN1`). TPM; transcripts per million reads.

5.4.3.4 Transcript and Protein Distribution of Fibulin-1 with Age and PWV

Fibulin-1 protein expression patterns were similarly examined in tissues from younger and older donor aortas. This protein was evident across all layers of the vessel wall in both age groups (Figure 5.15A) but was more prominent in the tunica intima and adventitia of the younger donors. Immunoblotting of whole aortic lysates also showed that total fibulin-1 was actually higher in the younger subjects compared to the older donors (P=0.008, Figure 5.15B-C), indicating age-related changes. *FBLN1* transcript was measured across the whole cohort and stratified by age decades to examine if the decrease in fibulin-1 content in the older subjects was a reflection of a decrease in *FBLN1* transcript abundance; however, no indication of age-associated changes to *FBLN1* transcript was observed (Figure 5.15D). The difference in fibulin-1 protein and transcript abundance between low and high PWV samples was also assessed, and the high PWV group showed a trend towards lower fibulin-1 expression compared to the low PWV group both at both the protein and transcript levels (Figure 5.16). The difference in *FBLN1* transcript levels between the groups persisted even after adjusting for age (P=0.01, ANCOVA).

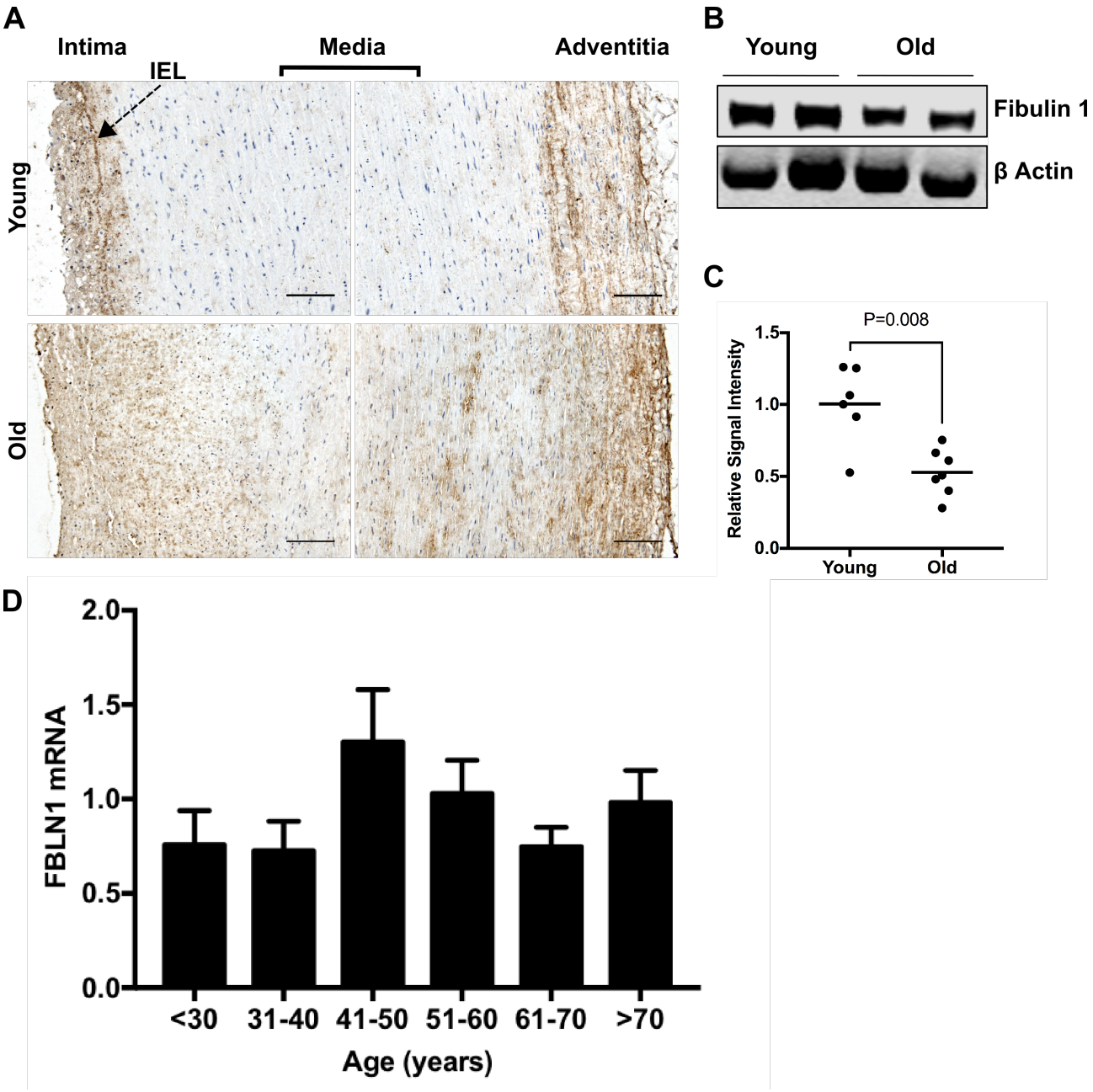

Figure 5.15: Fibulin-1 aortic distribution and gene expression levels in young and old subjects. (A) Representative immunohistochemical staining showing the pattern of fibulin-1 distribution in aortic sections from a young vs. an old donor; fibulin-1 is expressed throughout the vessel wall but appears denser in the intima and medial layers of young subjects compared to the more even distribution in the older aorta (scale bar, 50µm); IEL, internal elastic lamina. (B) Representative Western blot comparing fibulin-1 protein expression in young and old subjects. (C) Quantitative analysis of fibulin-1 signal intensities, normalised against β Actin in young (n=6) vs. old donor tissues (n=7); solid bar is the mean intensity and the P value is derived using a Mann Whitney U test. (D) *FBLN1* transcript levels stratified by age decade; bars represent mean±SEM, *FBLN1* transcript normalised against *GAPDH*.

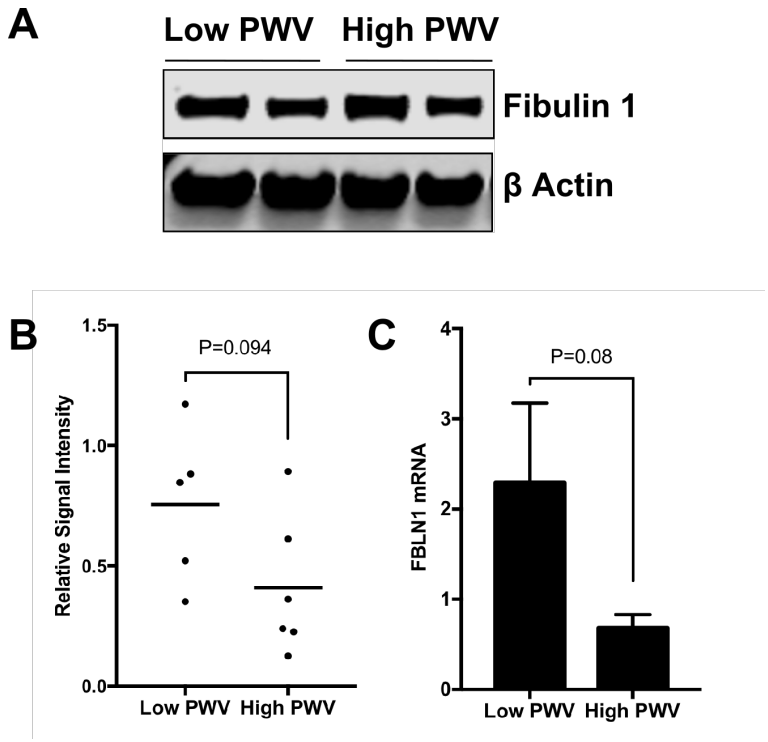

Figure 5.16: Fibulin-1 protein and transcript levels in donors with high and low PWV. (A) Representative Western blot of fibulin-1 in subjects with high and low PWV. (B) Quantification plot shows fibulin-1 protein levels are lower in the high PWV group compared to the low PWV donors (P=0.094); bars represent the mean signal intensity normalised against β Actin. P value derived using a Mann Whitney U test. (C) Transcript levels of *FBLN1* in donor aortas are significantly lower in high PWV samples compared to low PWV samples; bars represent mean$\pm$SEM *FBLN1* transcript normalised against *GAPDH*. P value derived using a Student's t test.

5.5 Discussion

The extracellular matrix (ECM) is a key player in age-related remodelling of the aortic wall and its response to hypertension or injury. Proteoglycans are key components of the ECM and are strongly correlated with PWV [75, 76], yet the underlying mechanisms by which they impact aortic stiffness remain poorly defined. This candidate-gene based study utilised tagging SNPs to capture the genetic information from linkage disequilibrium and haplotype blocks of the ECM proteoglycans, aggrecan and fibulin-1. The exonic (rs2882676/C) and intronic (rs2293087/G) *ACAN* tagSNPs were found to be significantly associated with higher PWV values in the discovery (extreme ends of PWV) and replication (mid-range PWV) ENIGMA cohorts [Publication 3]. A similar association was not found with *ex vivo* PWV in human donor aortic tissues which may reflect an underpowered study arising from the modest sample size compared to the ENIGMA cohort. However, the significant deviation of these SNPs from the Hardy-Weinberg equilibrium may itself be an indicator of a disease-susceptibility locus [490], suggesting that these SNPs may still be relevant markers for aortic stiffness. The *ACAN* rs2882676 SNP alters a codon at amino acid position 1508, resulting in amino acid

substitution from glutamine to alanine at position 1508 (E1508A), possibly altering the expression of *ACAN*. Non-synonymous SNPs are often assumed to be functional especially in cases where the substitution changes resides in an important domain or motif in a protein. This may be the case for the rs2882676 on exon 13 encoding the EGF-like motif of the G3 domain. The pathogenicity of this SNP is supported by its association with late-onset Alzheimer's disease [491], and more recently, with lumbar disk herniation [433]. It is shown here that while this SNP does alter *ACAN* transcript in the aorta protein levels are not altered. Notwithstanding, the latter was probed using an antibody that targeted the CS-attachment region, presenting a flawed experimental design for this arm of the study and warranting further investigations of its specific effect on the G3 domain. The E1508A substitution potentially alters not only the aggrecan content in the tissue but also aspects of its functionality. A missense mutation in the CLD motif of the G3 domain yielding a V2303M amino acid substitution, for instance, has been shown to disrupt ECM interactions, with the mutated protein showing a loss of interactions with fibulin-1, fibulin-2 and tenascin-R [420]. The E1508A substitution is in the EGF motif which has no definitive function in aggrecan but has been suggested to alter its binding affinities with ECM proteins [340]. In versican the EGF motif has been shown to promote cell proliferation [492], inhibit mesenchymal cell differentiation [493], mediate actin-filament assembly, and regulate aggrecan and collagen expression [494]. Of note, aggrecan protein levels were highly variable between the different genotype carriers of rs2882676 which may be explained by genotype variations within aggrecan-degrading enzymes that were not investigated in this work. Genes encoding MMPs, for instance, have been shown to harbour SNPs which alter their enzymatic activity [495, 496]. Hence, individuals carrying either of the rs2882676 genotypes may also be carriers of diverse *MMP* SNP genotypes with either increased or decreased proteolytic activity thus ultimately influencing the levels of aggrecan detected in the samples.

The precise role of the various domains of aggrecan in the vasculature is not known, but evidence is provided here that the protein abundance of the CS-region and the G3 domain is diminished in subjects with stiffer aortas. This reduced expression is potentially a reflection of compromised aggrecan synthesis, as indicated by the lower *ACAN* transcript levels in subjects with stiff aortas. As *ACAN* transcription is regulated by several pathways (Figure 5.4), reduced *ACAN* levels in stiff aortas may be the final outcome of a combination of perturbations to the upstream elements of these pathways. The enhanced accumulation of G1 fragments in both young and old subjects with stiff aortas also suggests contemporaneous degradation of aggrecan domains. The N terminal G1 domain of aggrecan interacts with hyaluronan and a link protein, forming a stable complex which anchors the aggrecan molecule to the tissue. However, the proteolytic degradation of aggrecan core protein yields

high concentrations of G1 fragments, which are retained in tissues because of their attachment to hyaluronan [497], impacting the stabilising capacity of the link protein in forming this proteoglycan complex and impeding the regeneration of aggrecan molecules [369]. The large central domain of aggrecan typically carries >100 KS and CS chains per molecule, and the negative charges provided by these sulphate groups attracts counter ions and draws water into the ECM; aggrecan thus imparts viscoelasticity and loadbearing properties to tissues in which it is expressed. Consequently, the heterogeneous distribution of aggrecan across the aortic wall is probably crucial in regulating the residual stress of the aorta and its loss therefore mitigates the biomechanical properties of the aorta [412].

Aggrecan expression and structure does not remain constant at other sites throughout life. For instance, transcript abundance of aggrecan and other related proteoglycans is significantly diminished in articular chondrocytes isolated from adult cartilage compared to those extracted from neonatal donors [498]. In addition, in human articular cartilage, intervertebral disc and sclera, aggrecan undergoes age-dependent proteolysis resulting in the progressive loss of its C-terminal and the accumulation of N-terminal G1 fragments [380, 499–501]. For the first time, it has been shown here that a similar age-dependent process of aggrecan degradation occurs in the human aortic vessel wall, together with *ACAN* transcript abundance declining with age. In line with these findings, transcript and protein abundance of aggrecan and other proteoglycan core proteins falls in the aortas of adult mice compared to late stage embryos [413, 502]. The total GAG content in human thoracic aorta also decreases after the age of 40 [503], and is lower in non-atherosclerotic ascending aortas of old subjects compared to younger ones [504]. Intriguingly, Manley et al. [504] observed a higher number of amino acids associated with CS chains in old aortic samples compared to younger one; approximately 2 serine molecules per GAG chain in older subjects and 1 serine molecule per GAG chain in younger subjects. It is suspected that the fragmentation of aortic aggrecan exposes additional sites on CS chains for attachment with serine residues. Conversely, the data from this study is in conflict with previous findings by Durier et al. [75], who reported increased *ACAN* transcript abundance in association with increased aortic PWV, although this discrepancy may reflect their small sample size (n=9) and heterogeneity of the sample taken from coronary artery bypass grafting patients (>50yrs). The age-dependent loss of aortic aggrecan may partly be explained by reduced synthesis of the protein from reduced transcript levels, as suggested by a notable decline in transcript levels after the fifth decade. However, the accumulation of G1 fragments in the medial layer of older subjects implicates post-translational modifications of ECM components. Aggrecan is degraded by a number of proteases, including ADAMTS-4,5, MMP-1,2,3,8,9,13, cathepsins and calpains [505], and the CS and

IGD regions are particularly susceptible to proteolytic cleavage [380]. In the aorta, aggrecan degradation is likely to be due to an increase in the activity and expression of aortic MMP-2, MMP-9 and calpain-1 with advancing age [506–509].

The proteolytic degradation of aggrecan and reduced *ACAN* expression could contribute to the stiffening of aorta in several ways. Firstly, GAGs such as aggrecan, are involved in the load-bearing properties of tissues, and to achieve this aggrecan forms large complexes with other matrix proteins such as fibulin, tenascin and lumican, which are restrained in the tissue by a scaffold of collagen fibrils that contributes to the ECM organisation [501, 510, 511]. Loss of aggrecan functionality could therefore impact on viscoelasticity, medial ECM disorganisation, and collagen fibril redistribution, all leading to increased stiffness. Secondly, the concomitant accumulation of G1 fragments in the medial layer may further promote its degeneration and pathological ECM remodelling. In addition, the degradation of aggrecan weakens its intrinsic ability to suppress calcium phosphate formation [512], and it is highly likely that aortic wall mineralisation, a strong determinant of aortic stiffness, is facilitated by aggrecan fragmentation. Furthermore, the gradual cleavage of aggrecan exposes highly immunogenic epitopes of the protein [407], thus potentially inducing an inflammatory cascade in the aortic wall and exacerbating the stiffening process. *ACAN* gene depletion in cells has been shown to trigger transcriptional changes to a number of genes with possible implications to aortic stiffness. Amongst those are a number of leucine-rich proteoglycans (SLRP) known to regulate collagen fibrillogenesis [379, 513], in addition to several genes involved in vascular calcification, most prominently alkaline phosphatase and carbonic anhydrase [379, 514, 515]. Given the association of aggrecan with amyloid deposition described in HHCAA, it is further possible that the changes to aggrecan composition in the aortic wall underpin senile aortic amyloid accumulation, which is estimated to be present in 97-100% of subjects > 55 years old [516]. PWV strongly associates with β amyloid plaque deposition in the brain [517], but a similar association in the aorta is yet to be established. Taken together, the loss of aggrecan from the vessel wall and the concurrent accumulation of N terminus fragments is likely to induce extracellular matrix perturbations, trigger vascular inflammation and promote calcification, thereby creating a milieu that is conducive to aortic wall stiffening.

The fate of cleaved G3 and CS fragments in the aorta is yet to be established but is potentially important. These may be released into the circulation, where they could provide a novel biomarker for aortic stiffness, although this signal may be difficult to distinguish from that caused by fragments exiting joint cartilage with age. This hypothesis is supported by the presence of GAGs in old aortas that have been proteolytically digested *ex vivo* [504]. A better understanding of the precise mech-

anisms regulating aggrecan decline could also identify novel therapeutic targets, which could be aimed at either restoring aortic aggrecan content or preventing its proteolytic degradation. Aggrecan analogues resistant to proteolysis have been tested in articular cartilage repair [518, 519], presenting a potentially attractive therapeutic option for aortic stiffness. Mutant mice strains resistant to aggrecanolysis display a high level of aggrecan preservation in the cartilage, are protected against cartilage erosion, and have accelerated cartilage repair following inflammation [343]. Thus, therapies targeting aggrecanases, of which there are currently at least 36 patented compounds specific for ADAMTS-4 and -5 [520], may be viable therapeutic options in the future. A selective monoclonal antibody to ADAMS-5 has recently been shown to suppress the release of aggrecan fragments from human knee cartilage explants, justifying its clinical development as a disease-modifying osteoarthritis drug [521].

Fibulin-1 is an ECM protein which is present throughout the arterial wall, but its expression is highest in the outermost layer of the tunica media in association with external elastic lamina [440]. However, the clinical significance of fibulin-1 in the vasculature remains unclear and there are no definite associations of fibulin-1 with human disease. Besides being an ECM protein, fibulin-1 circulates in high concentrations in plasma and is a cardiovascular disease biomarker reflecting elastolysis [466, 471]. It is also associated with heart failure [522], severe aortic valve stenosis [470], vascular calcification [475], is up-regulated in non-atherosclerotic diabetic tissues [466], and is affected by arterial wall mechanics [75]. Moreover, fibulin-1 up-regulation is linked with increased stiffness [474, 523] and kidney disease [471], whilst its down-regulation is related to aortic dissection [476, 477]. Fibulin-1 levels are also affected by interventions, so patients treated with spironolactone show reduced levels in parallel with regression of vascular remodelling [524].

Given the relation of fibulin-1 with elastic fibres in the vessel wall, it is perhaps not surprising that aPWV associated with the intronic *FBLN1* polymorphisms (rs2018279, rs2238823) in the ENIGMA cohorts [Publication 3]. However, these SNPs showed no significant association with *ex vivo* PWV in the human donor tissues and showed no significant effects on *FBLN1* transcript or fibulin-1 protein levels in the aorta. These SNPs potentially regulate the expression of neighbouring genes in *trans* or are in LD with other functional SNPs.

The expression of fibulin-1 transcript and protein was down-regulated in donors with stiff aortas and aortas from older donors had significantly lower fibulin-1 protein expression compared to younger ones. This is the same pattern observed with aggrecan, but may not be coincidental. Fibulin-1 is a high affinity ligand for the G3 domain of aggrecan [334], so a reduction in fibulin-1 expression may

be explained by the loss of aggrecan from the vessel walls. Of crucial note, fibulin-1 transcript and protein levels have been shown to be regulated by TGFβ in the airway smooth muscle cells [481]. Conversely, fibulin-1 is a potent suppressor TGFβ2 in the cardiac outflow tract of mice embryos [525], suggesting a possible role for fibulin-1 in the feedback loop regulating TGFβ latency and sequestration in the ECM. In view of these observations, the differential abundance of fibulin-1 may either be secondary to or may be a primary driver of perturbations to the TGFβ signalling pathway, which in return contributes to the disruption the aortic wall and the progression of aortic stiffness. The data presented here are in accord with the observations found in tissues recovered from acute aortic and Stanford type A dissections, where fibulin-1 is down-regulated [476, 477]. Age-related elastin fragmentation and medial degeneration are the hallmarks of aortic stiffness leading to aortic dissection, which presumably explains the parallel loss of fibulin-1. Fibulin-1 is thought to interact with elastin and microfibrils, and therefore plays a role in elastic fibrogenesis and contributes to the visco-elastic nature of the vessel wall [440]. Currently, it is not clear whether the observed decline in fibulin-1 expression contributes to the age-related fraying and fragmentation of elastin fibres or is a consequence of it. The expression patterns of fibulin-1 in the young and old from the extreme ends of PWV was not examined, and further studies are needed to address these important points.

To conclude, the *ACAN* and *FBLN1* tagSNPs did not associate with *ex vivo* PWV in human donor aortic samples. However, the assessment of the expression patterns of aggrecan and fibulin-1 in the aortic walls of young and old donors from the extreme ends of the PWV spectrum suggests a significant role for these ECM proteins within the vasculature. It has been shown that young donors with stiff aortas exhibit distribution patterns of these proteins that are more typical of the old donors with stiff aortas; hence, age-related degradation of aggrecan and loss of fibulin-1 in the human aorta may be key early events predisposing to age-related aortic stiffening. These findings challenge the prevailing view that stiffness simply reflects age-related calcification and elastin fibre fragmentation, and this work may facilitate the development of novel biomarkers for aortic stiffness, as well as generate pharmacological therapies that halt or reverse the stiffening process.

5.6 Limitations and Future Work

This is the first study that has examined the transcript and protein expression patterns of the three main domains of aggrecan in the aortic wall in association with age and aortic stiffness, but it is not without its limitations. First, the downstream effect of the variants was merely investigated quantitatively, in terms of their effect on total fibulin-1 and aggrecan transcript and protein content in the

aortic wall. Particularly with the missense mutation in *ACAN*, alterations in transcript or protein abundance may not be the only manifestation of the rs2882676 SNP yielding the E1508A amino acid substitution, and further qualitative examination of specimens harbouring this substitution may provide additional evidence on the pathological impact of this SNP. Because of the suggested role of the EGF motif in regulating the binding affinities of aggrecan with fibulin-1, fibulin-2 and tenisecan-R, and the prominent role of these proteins in preserving the structural integrity of the aortic wall, it is worth investigating the effect of the E1508A substitution on the histological expression patterns of these proteins in the aortas of individuals carrying the missense variant. This may be supplemented with quantitative analysis of their total content amongst different allele carriers. Furthermore, the alterations in aggrecan content between the SNPs respective genotypes were probed using an antibody that targeted the CS-attachment region and this therefore needs to be examined using an antibody targeting the G3 domain.

Aggrecan undergoes heavy tissue-specific, post-translational modifications and it is not clear whether similar to the form found in the brain, the protein expressed in the aorta contains KS chains. The *ACAN* gene also has eight known protein coding splice variants (Ensembl database, version 89), some of which entirely lack the EGF and CRP motifs. It is not known if the transcript is alternatively spliced in the aorta, or which of the splice variants is the prevalent form. It is therefore imperative to identify the specific enzymes responsible for the degradation of aggrecan in the aorta and to identify the the fate of the cleaved products; whether they remain or are released from the aortic wall. Probing aortic specimen from healthy, young and old donors with antibodies targeted against specific enzyme- generated cleavage products (e.g. MMP generated cleavage fragments and aggrecanase generated cleavage fragments [526]) will be the first step towards answering these questions. Importantly, it will be crucial to ascertain the localisation of these neopeptides within the aortic wall and to determine whether their expression co-localises with histological manifestations of aortic stiffness, such as elastin fragmentation, collagen accumulation, and medial calcification, and whether this differs in individuals with stiffer aortas. In addition, a few hypotheses were generated regarding the mechanisms linking the degradation of aggrecan with aortic stiffness which could be examined in donor samples. This includes co-staining aggrecan with calcium, β-ameyloid and markers of inflammation. In concert, addressing these fundamental aspects of aggrecan expression and degradation in the human aortic wall will be crucial in determining its tissue-specific functions, providing further mechanistic insights, and formulating further inferences concerning its role in the aetiology of aortic stiffness.

With regards to fibulin-1, its expression patterns in the aortas of young and old individuals from the extremes of PWV was not explored, presenting a major caveat of the current work. Investigating the expression patterns in these subjects will provide vital clues as to whether the observed changes in distribution patterns with age are secondary to increased stiffness or a cause of it. It will also be crucial to establish which of the four isoforms is the most relevant to the vascular wall, as this will have implications on its tissue-specific functions and binding partners. Finally, when selecting the subjects for the high and low PWV categories, the high abundance of fibulin-1 in atherosclerotic lesions and its up-regulation in aortas of diabetic subjects was not taken into consideration, which may have confounded the conclusions drawn from this work. Subjects with visible lesions and those reported to have diabetes need to be excluded to ensure that the observed patterns reflect changes to fibulin-1 independently of these factors.

6

Conclusion and Future Directions

Aortic stiffness has emerged over the last decade as an important predictor of cardiovascular endpoints. As with most cardiovascular traits, aortic stiffness has a multi-factorial aetiology, is moderately heritable, and its genetic architecture is diverse, including many common variants with subtle effects. However, unlike many cardiovascular conditions there are currently no direct therapeutic treatments specifically aimed at arresting or reversing this trait, despite evidence to support the potential for its pharmacological modulation.

In recent years a combination of genomic and transcriptomic investigations have laid the foundations for elucidating some of the key molecular determinants that underlie aortic stiffness. Most of the genetic associations, which were reviewed in Chapter 1, can be assigned to one of three broad categories: blood pressure regulation, signalling pathways and aortic wall structural integrity/ECM homeostasis. Inconsistencies in replication across populations, coupled with the failure of the largest published GWAS meta-analysis to confirm the associations for variants identified from earlier studies, has emphasised the need to further investigate the molecular underpinnings of this trait.

The aim of this thesis was to expand the existing knowledge of the genetic landscape that governs aortic stiffness. The study employed multiple approaches to identify the genetic basis of the stiffening mechanism in a large repository of human aortas that had undergone biomechanical phenotyping, permitting the genetic, transcript and protein associations to be interrogated within the tissue most relevant to the trait. It was hoped that would result in a clearer understanding of the molecular pathways that underpin the stiffening mechanisms and help uncover novel targets that may be amenable to pharmacological interventions.

The first part of the study examined the molecular basis of Loeys-Dietz type 4 in a pedigree with multiple cases of aortic aneurysms and dissections, and the identified mutation p.(Arg320Cys) was

found to be within a highly evolutionary conserved consensus of the *TGFB2* cytokine domain. Despite the missense nature of this mutation, immunocytochemical analyses demonstrated a striking and paradoxical up-regulation of TGFB1/2 ligands, as well as the canonical signal transducer pSMAD2/3 in the mutant case compared to age and gender-matched controls. This was in keeping with the enhanced TGBβ "tissue signature" typically observed in aortic tissues recovered from Loeys-Dietz and other Marfan-related cases. This case study underscores the pathological implications of TGFβ signalling overdrive in the disruption of the normal architecture of the vessel wall.

The second part of the study attempted to provide a biological basis for the genetic GWAS signal identified by Mitchell and colleagues in 2012 [72]. This is the largest GWAS meta-analysis of cfPWV yet reported and constituted a consortium of 11 cohorts with over 20,000 participants. The locus lies within a 2 Mb region that contains no known genes but is known to harbour gene enhancer elements and is flanked at its telomeric end by *BCL11B*; the hypothesised target for the enhancer cluster. This is a nuclear transcription factor which controls the embryologic fate of blood vessels, is a potent regulator of T cell fate and identity, and has been shown to modulate the expression of genes relevant to aortic function, including those that promote vascular calcification, ECM remodelling and VSMC apoptosis. The current work confirmed the association of three SNPs from the GWAS meta-analysis with PWV predicted from *ex vivo* aortic stiffness and with mRNA levels of *BCL11B*. Despite the expression of *BCL11B* transcript within the aortas, the protein was not found to be present in the vessel itself. Instead, strong correlations with leukocyte markers suggest that the mRNA signals originate from infiltrating leukocytes in the aortic wall; hence the expression of protein levels is below the detection sensitivities for Western blotting and immunocytochemical methods. These findings indicate that the effects of BCL11B on aortic stiffness in the adult aorta are mediated via inflammatory mechanisms, which is supported by evidence from the literature illustrating that the loss of BCL11B is a powerful proinflammatory stimulus. The expression of DB129663, a long non-coding RNA in close vicinity to the GWAS locus, was also investigated in the aortas but was not found to correlate with *ex vivo* PWV. The negative findings of this work emphasise the need to investigate other targets in the topologically association domain (TAD) within which the GWAS locus resides, and to define the functions of DB129663 which was detected in nearly 50% of the aortas but has currently no known functions. Indeed, until other genes in the TAD are explored for their association with the GWAS SNPs, the conclusions drawn from these results cannot be fully substantiated.

In the final part of the study genetic associations with aortic stiffness were explored from a candidate-gene perspective utilising tagSNPs that effectively capture the genetic information from linkage dis-

equilibrium blocks. SNPs in the ECM genes, *ACAN* and *FBLN1*, were found to modulate cfPWV in young, healthy adults from the ENIGMA cohort. Although the SNPs failed to associate with *ex vivo* PWV measurements in the donor aortas, a comprehensive assessment of the transcript abundance and protein expression patterns of aggrecan and fibulin-1 in young and old subjects from extreme ends of the *ex vivo* PWV spectrum shed important light on their role in the stiffening process. The most novel aspect of this work was the discovery that aggrecan undergoes the same process in the aorta that occurs in cartilaginous tissues, where there is a decline in synthesis coupled with a progressive loss of the C-terminal and binding sites for GAG side chains due to proteolytic degradation. The resulting alteration in the biomechanical properties of the aorta can therefore be explained by the ageing of aggrecan, as not only are the GAG chains, which are responsible for imparting viscoelasticity by imbibing water into the ECM, lost from the tissue, but the concomitant accumulation of N-terminal G1 domain impedes the regeneration of new aggrecan molecules and contributes to further degeneration of the tissue. The degradation of aggrecan from the vessel wall provides a compelling interpretation for many of the age-related changes observed in the arterial wall matrix. For example, the loss of affinity with other structural elements of the ECM leads to medial disorganisation, as well as the exposure of highly immunogenic epitopes along its length thereby contributing to a proinflammatory profile. Furthermore, the ablation of its intrinsic capacity to suppress calcium phosphate formation and its role in chondro-osseous VSMC programming potentially triggers and/or promotes the process of medial calcification. Fibulin-1 similarly showed changes in its transcript abundance, protein levels and expression patterns which were associated with age. However, it is difficult to ascertain whether these changes to fibulin-1 expression are primary drivers of the age-related structural changes to the aortic wall or a secondary effect due to elastin fraying and fragmentation given its specific localisation within the amorphous core of elastin fibres.

A central theme emerging from this work is the role of TGFβ signalling in the regulation of various components of the ECM, and its deregulation is potentially at the root of the pathophysiological manifestations of aortic stiffness. Indeed, this was first highlighted with the overshoot in signalling reported in the Loeys-Dietz case study. While its downstream effectors regulate genes involved ECM synthesis and homeostasis, in contrast its own activity and bioavailability are regulated by components of the ECM. It later became apparent that components of the TGFβ pathway are targets of BCL11B transcription and that its downstream effectors not only regulate the expression of aggrecan, but also the major proteolytic enzymes, MMPs and aggrecanases, responsible for its degradation. TGFβ was yet again seen to be intertwined with fibulin-1, which is a potent suppressor of TGFβ while its own transcription and protein expression are regulated by TGFβ. These observations

underscore the complexity of factors regulating aortic function and cautions against the inclination to presume that its molecular determinants act autonomously. The polygenicity of aortic stiffness is indeed incontrovertible, and one parsimonious model is that at least one or more biological pathways unite many of the empirical findings for aortic stiffness, and there is compelling evidence that in this case it is the TGFβ signalling pathway. Thus, a major task in future investigations would be to determine this 'chicken-or-egg' conundrum: which comes first, ECM remodelling or TGFβ signalling perturbation?

To conclude, the work detailed in this thesis reinforces the difficulties of defining a biological context for susceptibility loci identified in GWAS. The identification of aggrecan as an important player in the aortic wall matrix may pave the way for the development of pharmacological agents that can restore its content in the vessel wall or arrest its degradation, thereby preserving its viscoelastic properties. However, the current findings reflect only a proportion of what is otherwise a complex interaction between multiple genes, signalling pathways and environmental factors that simultaneously impact aortic function. While this work attempted to investigate the molecular basis of aortic stiffness from different angles, it was conducted with a rudimentary approach, testing the association of one polymorphism independently of the other. The mechanism of susceptibility to aortic stiffening is complex and is more realistically impacted by a cumulative effect of these variations. Indeed, an often-cited basis for the failure to detect significant associations in complex diseases is the presence of epistasis between loci [527]. Furthermore, it is becoming evident that polymorphisms could exert their function by regulating gene expression in unsuspected cell types or under specific environmental conditions [528]. Thus, discerning the biologically and pathogenically relevant cell type underlying the genetic association signal remains a major challenge for GWAS follow-up studies. Taken together, future work should aim to explore this trait at the "systems biology" level by integrating gene-gene interactions, genomic, metabolomic, transcriptomic, epigenomic and proteomic analyses to comprehensively capture the complex mechanisms and pathways that underpin the stiffening process.

Bibliography

[1] G. A. Roth, C. Johnson, A. Abajobir, F. Abd-Allah, S. F. Abera, G. Abyu, M. Ahmed, B. Aksut, T. Alam, K. Alam, F. Alla, N. Alvis-Guzman, S. Amrock, H. Ansari, J. Ärnlöv, H. Asayesh, T. M. Atey, L. Avila-Burgos, A. Awasthi, A. Banerjee, A. Barac, T. Bärnighausen, L. Barregard, N. Bedi, E. Belay Ketema, D. Bennett, G. Berhe, Z. Bhutta, S. Bitew, J. Carapetis, J. J. Carrero, D. C. Malta, C. A. Castañeda-Orjuela, J. Castillo-Rivas, F. Catalá-López, J. Y. Choi, H. Christensen, M. Cirillo, L. Cooper, M. Criqui, D. Cundiff, A. Damasceno, L. Dandona, R. Dandona, K. Davletov, S. Dharmaratne, P. Dorairaj, M. Dubey, R. Ehrenkranz, M. El Sayed Zaki, E. J. A. Faraon, A. Esteghamati, T. Farid, M. Farvid, V. Feigin, E. L. Ding, G. Fowkes, T. Gebrehiwot, R. Gillum, A. Gold, P. Gona, R. Gupta, T. D. Habtewold, N. Hafezi-Nejad, T. Hailu, G. B. Hailu, G. Hankey, H. Y. Hassen, K. H. Abate, R. Havmoeller, S. I. Hay, M. Horino, P. J. Hotez, K. Jacobsen, S. James, M. Javanbakht, P. Jeemon, D. John, J. Jonas, Y. Kalkonde, C. Karimkhani, A. Kasaeian, Y. Khader, A. Khan, Y. H. Khang, S. Khera, A. T. Khoja, J. Khubchandani, D. Kim, D. Kolte, S. Kosen, K. J. Krohn, G. A. Kumar, G. Kwan, D. K. Lal, A. Larsson, S. Linn, A. Lopez, P. A. Lotufo, H. M. A. El Razek, and Others, "Global, Regional, and National Burden of Cardiovascular Diseases for 10 Causes, 1990 to 2015," *Journal of the American College of Cardiology*, 2017.

[2] J. D. Schwalm, M. McKee, M. D. Huffman, and S. Yusuf, "Resource effective strategies to prevent and treat cardiovascular disease," *Circulation*, vol. 133, no. 8, pp. 742–755, 2016.

[3] I. S. Okwuosa, S. C. Lewsey, T. Adesiyun, R. S. Blumenthal, and C. W. Yancy, "Worldwide disparities in cardiovascular disease: Challenges and solutions," *International Journal of Cardiology*, vol. 202, pp. 433–440, 2016.

[4] R. L. Sacco, G. A. Roth, K. S. Reddy, D. K. Arnett, R. Bonita, T. A. Gaziano, P. A. Heidenreich, M. D. Huffman, B. M. Mayosi, S. Mendis, C. J. Murray, P. Perel, D. J. Piñeiro, S. C. Smith, K. A. Taubert, D. A. Wood, D. Zhao, and W. A. Zoghbi, "The heart of 25 by 25: Achieving the goal of reducing global and regional premature deaths from cardiovascular diseases and

stroke: A modeling study from the American Heart Association and World Heart Federation," *Circulation*, vol. 133, no. 23, pp. e674–e690, 2016.

[5] S. Laurent, J. Cockcroft, L. Van Bortel, P. Boutouyrie, C. Giannattasio, D. Hayoz, B. Pannier, C. Vlachopoulos, I. Wilkinson, H. Struijker-Boudier, and E. N. f. N.-i. I. o. L. Arteries, "Expert consensus document on arterial stiffness: Methodological issues and clinical applications," *European Heart Journal*, vol. 27, no. 21, pp. 2588–2605, 2006.

[6] P. V. Vaitkevicius, M. Lane, H. Spurgeon, D. K. Ingram, G. S. Roth, J. J. Egan, S. Vasan, D. R. Wagle, P. Ulrich, M. Brines, J. P. Wuerth, A. Cerami, and E. G. Lakatta, "A cross-link breaker has sustained effects on arterial and ventricular properties in older rhesus monkeys," *Proceedings of the National Academy of Sciences*, vol. 98, no. 3, pp. 1171–1175, 2001.

[7] J. A. Chirinos, J. G. Kips, D. R. Jacobs, L. Brumback, D. A. Duprez, R. Kronmal, D. A. Bluemke, R. R. Townsend, S. Vermeersch, and P. Segers, "Arterial wave reflections and incident cardiovascular events and heart failure: MESA (Multiethnic Study of Atherosclerosis)," *Journal of the American College of Cardiology*, vol. 60, no. 21, pp. 2170–2177, 2012.

[8] A. Toprak, J. Reddy, W. Chen, S. Srinivasan, and G. Berenson, "Relation of pulse pressure and arterial stiffness to concentric left ventricular hypertrophy in young men (from the Bogalusa Heart Study)," *The American Journal of Cardiology*, vol. 103, no. 7, pp. 978–84, 2009.

[9] U. Raaz, A. M. Zöllner, I. N. Schellinger, R. Toh, F. Nakagami, M. Brandt, F. C. Emrich, Y. Kayama, S. Eken, M. Adam, L. Maegdefessel, T. Hertel, A. Deng, A. Jagger, M. Buerke, R. L. Dalman, J. M. Spin, E. Kuhl, and P. S. Tsao, "Segmental aortic stiffening contributes to experimental abdominal aortic aneurysm development," *Circulation*, vol. 131, no. 20, pp. 1783–1795, 2015.

[10] S. R. Waldstein, S. C. Rice, J. F. Thayer, S. S. Najjar, A. Scuteri, and A. B. Zonderman, "Pulse pressure and pulse wave velocity are related to cognitive decline in the Baltimore Longitudinal Study of Aging," *Hypertension*, vol. 51, no. 1, pp. 99–104, 2008.

[11] M. P. Pase, J. J. Himali, G. F. Mitchell, A. Beiser, P. Maillard, C. Tsao, M. G. Larson, C. Decarli, R. S. Vasan, and S. Seshadri, "Association of aortic stiffness with cognition and brain aging in young and middle-aged adults: The Framingham Third Generation Cohort Study," *Hypertension*, vol. 67, no. 3, pp. 513–519, 2016.

[12] J. Ding, G. F. Mitchell, M. L. Bots, S. Sigurdsson, T. B. Harris, M. Garcia, G. Eiriksdottir, M. A. Van Buchem, V. Gudnason, and L. J. Launer, "Carotid arterial stiffness and risk of incident

cerebral microbleeds in older people: The Age, Gene/Environment Susceptibility (AGES)-Reykjavik study," *Arteriosclerosis, Thrombosis, and Vascular Biology*, vol. 35, no. 8, pp. 1889–1895, 2015.

[13] G. F. Mitchell, "Effects of central arterial aging on the structure and function of the peripheral vasculature: implications for end-organ damage," *Journal of Applied Physiology (1985)*, vol. 105, no. 5, pp. 1652–1660, 2008.

[14] A. Karras, J. P. Haymann, E. Bozec, M. Metzger, C. Jacquot, G. Maruani, P. Houillier, M. Froissart, B. Stengel, P. Guardiola, S. Laurent, P. Boutouyrie, M. Briet, and N. T. S. Group, "Large artery stiffening and remodeling are independently associated with all-cause mortality and cardiovascular events in chronic kidney disease," *Hypertension*, vol. 60, no. 6, pp. 1451–1457, 2012.

[15] S. Zoungas and R. P. Asmar, "Arterial stiffness and cardiovascular outcome," *Clin Exp Pharmacol Physiol*, vol. 34, no. 7, pp. 647–651, 2007.

[16] C. Vlachopoulos, K. Aznaouridis, and C. Stefanadis, "Prediction of cardiovascular events and all-cause mortality with arterial stiffness: a systematic review and meta-analysis," *Journal of the American College of Cardiology*, vol. 55, no. 13, pp. 1318–1327, 2010.

[17] G. F. Mitchell, A. L. DeStefano, M. G. Larson, E. J. Benjamin, M. H. Chen, R. S. Vasan, J. A. Vita, and D. Levy, "Heritability and a genome-wide linkage scan for arterial stiffness, wave reflection, and mean arterial pressure: the Framingham Heart Study," *Circulation*, vol. 112, no. 2, pp. 194–199, 2005.

[18] M. Cecelja, B. Jiang, L. Bevan, M. L. Frost, T. D. Spector, and P. J. Chowienczyk, "Arterial stiffening relates to arterial calcification but not to noncalcified atheroma in women. A twin study," *Journal of the American College of Cardiology*, vol. 57, no. 13, pp. 1480–1486, 2011.

[19] M. Cecelja and P. Chowienczyk, "Molecular Mechanisms of Arterial Stiffening," *Pulse*, vol. 4, no. 1, pp. 43–48, 2016.

[20] J. A. Collins, J. V. Munoz, T. R. Patel, M. Loukas, and R. S. Tubbs, "The anatomy of the aging aorta," *Clinical Anatomy*, vol. 27, no. 3, pp. 463–466, 2014.

[21] H. Järveläinen, A. Sainio, M. Koulu, T. N. Wight, and R. Penttinen, "Extracellular matrix molecules: potential targets in pharmacotherapy," *Pharmacological Reviews*, vol. 61, no. 2, pp. 198–223, 2009.

[22] J. M. Ruddy, J. A. Jones, F. G. Spinale, and J. S. Ikonomidis, "Regional heterogeneity within the aorta: Relevance to aneurysm disease," *Journal of Thoracic and Cardiovascular Surgery*, vol. 136, no. 5, pp. 1123–1130, 2008.

[23] R. Grant, "Content and distribution of aortic collagen, elastin and carbohydrate in different species," *Journal of Atherosclerosis Research*, vol. 7, no. 4, pp. 463–472, 1967.

[24] W. J. Rogers, Y.-L. Hu, D. Coast, D. A. Vido, C. M. Kramer, R. E. Pyeritz, and N. Reichek, "Age-associated changes in regional aortic pulse wave velocity," *Journal of the American College of Cardiology*, vol. 38, no. 4, pp. 1123–1129, 2001.

[25] N. Westerhof, J. W. Lankhaar, and B. E. Westerhof, "The arterial windkessel," 2009.

[26] M. F. O'Rourke and J. Hashimoto, "Mechanical factors in arterial aging: a clinical perspective," *Journal of the American College of Cardiology*, vol. 50, no. 1, pp. 1–13, 2007.

[27] P. B. Dobrin, *Elastin, collagen and the pathophysiology of arterial aneurysms*, book section 4, pp. 42–73. Intelligence Unit, Georgetown, Texas: Landes Bioscience, 2000.

[28] M. R. Roach and A. C. Burton, "The reason for the shape of the distensibility curves of arteries," *Canadian Journal of Biochemistry and Physiology*, vol. 35, no. 8, pp. 681–690, 1957.

[29] M. O'Rourke, "Mechanical Principles in Arterial Disease," *Hypertension*, vol. 26, no. 1, pp. 2–9, 1995.

[30] W. W. Nichols, M. F. O'Rourke, and C. Vlachopoulos, *McDonald's blood flow in arteries: Theoretical, experimental and clinical principles*, book section 411-446. UK: Hodder Arnold, 6th ed., 2011.

[31] D. C. Paik, W. G. Ramey, J. Dillon, and M. D. Tilson, "The nitrite/elastin reaction: implications for in vivo degenerative effects.," *Connective Tissue Research*, vol. 36, no. 3, pp. 241–51, 1997.

[32] A. Brüel and H. Oxlund, "Changes in biomechanical properties, composition of collagen and elastin, and advanced glycation endproducts of the rat aorta in relation to age," *Atherosclerosis*, vol. 127, no. 2, pp. 155–165, 1996.

[33] J. Atkinson, "Age-related medial elastocalcinosis in arteries: mechanisms, animal models, and physiological consequences," *Journal of Applied Physiology*, vol. 105, no. 5, pp. 1643–1651, 2008.

[34] S. Park and E. G. Lakatta, "Role of inflammation in the pathogenesis of arterial stiffness," *Yonsei Medical Journal*, vol. 53, no. 2, pp. 258–261, 2012.

[35] M. Alghatrif and E. G. Lakatta, "The reality of aging viewed from the arterial wall," in *Blood Pressure and Arterial Wall Mechanics in Cardiovascular Diseases* (M. Safar, M. O'Rourke, and E. Frohlich, eds.), pp. 137–153, London: Springer, 2014.

[36] a. P. Avolio, F. Q. Deng, W. Q. Li, Y. F. Luo, Z. D. Huang, L. F. Xing, and M. F. O'Rourke, "Effects of aging on arterial distensibility in populations with high and low prevalence of hypertension: comparison between urban and rural communities in China," *Circulation*, vol. 71, no. 2, pp. 202–210, 1985.

[37] D. Lemogoum, W. Ngatchou, C. Janssen, M. Leeman, L. Van Bortel, P. Boutouyrie, J. P. Degaute, and P. Van De Borne, "Effects of hunter-gatherer subsistence mode on arterial distensibility in cameroonian pygmies," *Hypertension*, vol. 60, no. 1, pp. 123–128, 2012.

[38] M. T. Schram, P. J. Kostense, R. A. Van Dijk, J. M. Dekker, G. Nijpels, L. M. Bouter, R. J. Heine, and C. D. Stehouwer, "Diabetes, pulse pressure and cardiovascular mortality: the Hoorn Study," *Journal of Hypertension*, vol. 20, no. 9, pp. 1743–1751, 2002.

[39] M. Cecelja and P. Chowienczyk, "Dissociation of aortic pulse wave velocity with risk factors for cardiovascular disease other than hypertension: A systematic review," *Hypertension*, vol. 54, no. 6, pp. 1328–1336, 2009.

[40] T. Horvath, J. Osztovits, A. Pinter, L. Littvay, D. Cseh, A. D. Tarnoki, D. L. Tarnoki, A. L. Jermendy, R. Steinbach, J. Metneki, G. Schillaci, M. Kollai, and G. Jermendy, "Genetic impact dominates over environmental effects in development of carotid artery stiffness: a twin study," *Hypertension Research*, vol. 37, no. 1, pp. 88–93, 2014.

[41] C. M. McEniery, I. B. Wilkinson, N. B. Johansen, D. R. Witte, A. Singh-Manoux, M. Kivimaki, A. G. Tabak, E. J. Brunner, and M. J. Shipley, "Nondiabetic glucometabolic status and progression of aortic stiffness: The whitehall II study," *Diabetes Care*, vol. 40, no. 4, pp. 599–606, 2017.

[42] Yasmin, C. M. McEniery, S. Wallace, I. S. Mackenzie, J. R. Cockcroft, and I. B. Wilkinson, "C-reactive protein is associated with arterial stiffness in apparently healthy individuals," *Arteriosclerosis, Thrombosis, and Vascular Biology*, vol. 24, no. 1524-4636 (Electronic), pp. 969–974, 2004.

[43] L. Tomlinson, Y. Ben-Shlomo, B. Caplin, C. Delles, C. J. Ferro, J. Goddard, R. Hoefield, S. G. Holt, P. A. Kalra, C. M. Mceniery, C. W. Mcintyre, E. P. Mcquarrie, C. Rajkumar, T. Savage, M. W. Taal, C. R. Tomson, J. N. Townend, D. J. Webb, D. C. Wheeler, and I. B. Wilkinson, "Renal disease is associated with accelerated vascular ageing: Initial results of the UK Research

Alliance into Kidney Disease and Arterial Stiffness (Ureka) Collaboration," *Journal of Hypertension*, vol. 28, p. 1, 2010.

[44] I. B. Wilkinson and C. M. McEniery, "Arteriosclerosis: Inevitable or self-inflicted?," *Hypertension*, vol. 60, no. 1, pp. 3–5, 2012.

[45] M. Briet, P. Boutouyrie, S. Laurent, and G. M. London, "Arterial stiffness and pulse pressure in CKD and ESRD," *Kidney International*, vol. 82, no. 4, pp. 388–400, 2012.

[46] J. C. Bramwell and A. V. Hill, "Velocity of transmission of the pulse-wave: and elasticity of arteries," *The Lancet*, vol. 199, no. 5149, pp. 891–892, 1922.

[47] K. H. Parker, "A brief history of arterial wave mechanics," *Medical and Biological Engineering and Computing*, vol. 47, no. 2, pp. 111–118, 2009.

[48] R. Skalak, S. R. Keller, and T. W. Secomb, "Mechanics of blood flow," *Journal of Biomechanical Engineering*, vol. 103, no. 2, pp. 102–115, 1981.

[49] Y. Ben-Shlomo, M. Spears, C. Boustred, M. May, S. G. Anderson, E. J. Benjamin, P. Boutouyrie, J. Cameron, C. H. Chen, J. K. Cruickshank, S. J. Hwang, E. G. Lakatta, S. Laurent, J. Maldonado, G. F. Mitchell, S. S. Najjar, A. B. Newman, M. Ohishi, B. Pannier, T. Pereira, R. S. Vasan, T. Shokawa, K. Sutton-Tyrell, F. Verbeke, K. L. Wang, D. J. Webb, T. Willum Hansen, S. Zoungas, C. M. McEniery, J. R. Cockcroft, and I. B. Wilkinson, "Aortic pulse wave velocity improves cardiovascular event prediction: an individual participant meta-analysis of prospective observational data from 17,635 subjects," *Journal of the American College of Cardiology*, vol. 63, no. 7, pp. 636–646, 2014.

[50] A. Adji, M. F. O'Rourke, and M. Namasivayam, "Arterial stiffness, its assessment, prognostic value, and implications for treatment," *American Journal of Hypertension*, vol. 24, no. 1, pp. 5–17, 2011.

[51] S. S. Franklin, S. A. Khan, N. D. Wong, M. G. Larson, and D. Levy, "Is pulse pressure useful in predicting risk for coronary heart Disease? The Framingham heart study," *Circulation*, vol. 100, no. 4, pp. 354–360, 1999.

[52] E. J. Kim, C. G. Park, J. S. Park, S. Y. Suh, C. U. Choi, J. W. Kim, S. H. Kim, H. E. Lim, S. W. Rha, H. S. Seo, and D. J. Oh, "Relationship between blood pressure parameters and pulse wave velocity in normotensive and hypertensive subjects: invasive study," *Journal of Human Hypertension*, vol. 21, no. 2, pp. 141–148, 2007.

[53] K. A. Groth, H. Hove, K. Kyhl, L. Folkestad, M. Gaustadnes, N. Vejlstrup, K. Stochholm, J. R. Østergaard, N. H. Andersen, and C. H. Gravholt, "Prevalence, incidence, and age at diagnosis in Marfan Syndrome," *Orphanet Journal of Rare Diseases*, vol. 10, p. 153, 2015.

[54] C. J. A. Ramachandra, A. Mehta, K. W. Q. Guo, P. Wong, J. L. Tan, and W. Shim, "Molecular pathogenesis of Marfan syndrome," *International Journal of Cardiology*, vol. 187, no. 1, pp. 585–591, 2015.

[55] T. Morisaki and H. Morisaki, "Genetics of hereditary large vessel diseases," *Human Genetics*, vol. 16, pp. 21–26, 2016.

[56] J. T. Powell, R. J. Turner, M. Sian, R. Debasso, and T. Lanne, "Influence of fibrillin-1 genotype on the aortic stiffness in men," *Journal of Applied Physiology (1985)*, vol. 99, no. 3, pp. 1036–1040, 2005.

[57] T. L. Medley, T. J. Cole, C. D. Gatzka, W. Y. Wang, A. M. Dart, and B. A. Kingwell, "Fibrillin-1 genotype is associated with aortic stiffness and disease severity in patients with coronary artery disease," *Circulation*, vol. 105, no. 7, pp. 810–815, 2002.

[58] Yasmin, K. M. O'Shaughnessy, C. M. McEniery, J. R. Cockcroft, and I. B. Wilkinson, "Genetic variation in fibrillin-1 gene is not associated with arterial stiffness in apparently healthy individuals," *Journal of Hypertension*, vol. 24, no. 3, pp. 499–502, 2006.

[59] M. P. Sie, F. U. Mattace-Raso, A. G. Uitterlinden, P. P. Arp, A. Hofman, A. P. Hoeks, R. S. Reneman, R. Asmar, C. M. van Duijn, and J. C. Witteman, "TGF-beta1 polymorphisms and arterial stiffness; the Rotterdam Study," *Journal of Human Hypertension*, vol. 21, no. 6, pp. 431–437, 2007.

[60] C. A. Morris, "Introduction: Williams syndrome," *American Journal of Medical Genetics, Part C: Seminars in Medical Genetics*, vol. 154C, no. 2, pp. 203–208, 2010.

[61] Y. Aggoun, D. Sidi, B. I. Levy, S. Lyonnet, J. Kachaner, and D. Bonnet, "Mechanical properties of the common carotid artery in Williams syndrome," *Heart*, vol. 84, no. 3, pp. 290–293, 2000.

[62] P. Lacolley, P. Boutouyrie, M. Glukhova, J. M. Daniel Lamaziere, P. F. Plouin, P. Bruneval, P. Vuong, P. Corvol, and S. Laurent, "Disruption of the elastin gene in adult Williams syndrome is accompanied by a paradoxical reduction in arterial stiffness," *Clinical Science*, vol. 103, no. 1, pp. 21–29, 2002.

[63] O. Hanon, V. Luong, J. J. Mourad, L. A. Bortolotto, X. Jeunemaitre, and X. Girerd, "Aging, carotid artery distensibility, and the Ser422Gly elastin gene polymorphism in humans," *Hypertension*, vol. 38, no. 5, pp. 1185–1189, 2001.

[64] L. Deng, R. Huang, Z. Chen, L. Wu, and D. L. Xu, "A study on polymorphisms of elastin gene in Chinese Han patients with isolated systolic hypertension," *American Journal of Hypertension*, vol. 22, no. 6, pp. 656–662, 2009.

[65] N. Iwai, K. Kajimoto, Y. Kokubo, and H. Tomoike, "Extensive genetic analysis of 10 candidate genes for hypertension in Japanese," *Hypertension*, vol. 48, no. 5, pp. 901–907, 2006.

[66] N. Beridze and W. H. Frishman, "Vascular Ehlers-Danlos syndrome: pathophysiology, diagnosis, and prevention and treatment of its complications," *Cardiology in Review*, vol. 20, no. 1, pp. 4–7, 2012.

[67] M. J. Eagleton, "Arterial complications of vascular Ehlers-Danlos syndrome," 2016.

[68] M. J. Barnes and R. W. Farndale, "Collagens and atherosclerosis," *Experimental Gerontology*, vol. 34, no. 4, pp. 513–525, 1999.

[69] D. J. Brull, L. J. Murray, C. A. Boreham, S. H. Ralston, H. E. Montgomery, A. M. Gallagher, F. E. McGuigan, G. Davey Smith, M. Savage, S. E. Humphries, and I. S. Young, "Effect of a COL1A1 Sp1 binding site polymorphism on arterial pulse wave velocity: an index of compliance," *Hypertension*, vol. 38, no. 3, pp. 444–448, 2001.

[70] D. Levy, M. G. Larson, E. J. Benjamin, C. Newton-Cheh, T. J. Wang, S. J. Hwang, R. S. Vasan, and G. F. Mitchell, "Framingham Heart Study 100K Project: genome-wide associations for blood pressure and arterial stiffness," *BMC Medical Genetics*, vol. 8 Suppl 1, p. S3, 2007.

[71] K. V. Tarasov, S. Sanna, A. Scuteri, J. B. Strait, M. Orru, A. Parsa, P. I. Lin, A. Maschio, S. Lai, M. G. Piras, M. Masala, T. Tanaka, W. Post, J. R. O'Connell, D. Schlessinger, A. Cao, R. Nagaraja, B. D. Mitchell, G. R. Abecasis, A. R. Shuldiner, M. Uda, E. G. Lakatta, and S. S. Najjar, "COL4A1 is associated with arterial stiffness by genome-wide association scan," *Circulation: Cardiovascular Genetics*, vol. 2, no. 2, pp. 151–158, 2009.

[72] G. F. Mitchell, G. C. Verwoert, K. V. Tarasov, A. Isaacs, A. V. Smith, Yasmin, E. R. Rietzschel, T. Tanaka, Y. Liu, A. Parsa, S. S. Najjar, K. M. O'Shaughnessy, S. Sigurdsson, M. L. De Buyzere, M. G. Larson, M. P. Sie, J. S. Andrews, W. S. Post, F. U. Mattace-Raso, C. M. McEniery, G. Eiriksdottir, P. Segers, R. S. Vasan, M. J. van Rijn, T. D. Howard, P. F. McArdle, A. Dehghan, E. S. Jew-

ell, S. J. Newhouse, S. Bekaert, N. M. Hamburg, A. B. Newman, A. Hofman, A. Scuteri, D. De Bacquer, M. A. Ikram, B. M. Psaty, C. Fuchsberger, M. Olden, L. V. Wain, P. Elliott, N. L. Smith, J. F. Felix, J. Erdmann, J. A. Vita, K. Sutton-Tyrrell, E. J. Sijbrands, S. Sanna, L. J. Launer, T. De Meyer, A. D. Johnson, A. F. Schut, D. M. Herrington, F. Rivadeneira, M. Uda, I. B. Wilkinson, T. Aspelund, T. C. Gillebert, L. Van Bortel, E. J. Benjamin, B. A. Oostra, J. Ding, Q. Gibson, A. G. Uitterlinden, G. R. Abecasis, J. R. Cockcroft, V. Gudnason, G. G. De Backer, L. Ferrucci, T. B. Harris, A. R. Shuldiner, C. M. van Duijn, D. Levy, E. G. Lakatta, and J. C. Witteman, "Common genetic variation in the 3'-BCL11B gene desert is associated with carotid-femoral pulse wave velocity and excess cardiovascular disease risk: the AortaGen Consortium," *Circulation: Cardiovascular Genetics*, vol. 5, no. 1, pp. 81–90, 2012.

[73] M. P. Sie, F. U. Mattace-Raso, A. G. Uitterlinden, P. P. Arp, A. Hofman, H. A. Pols, A. P. Hoeks, R. S. Reneman, R. Asmar, C. M. van Duijn, and J. C. Witteman, "The interleukin-6-174 G/C promoter polymorphism and arterial stiffness; the Rotterdam Study," *Vascular Health and Risk Management*, vol. 4, no. 4, pp. 863–869, 2008.

[74] J. Díez, "Structural alterations in arterial stiffness: Role of arterial fibrosis," in *Blood Pressure and Arterial Wall Mechanics in Cardiovascular Diseases* (M. Safar, M. O'Rourke, and E. Frohlich, eds.), pp. 205–213, London: Springer, 2014.

[75] S. Durier, C. Fassot, S. Laurent, P. Boutouyrie, J. P. Couetil, E. Fine, P. Lacolley, V. J. Dzau, and R. E. Pratt, "Physiological genomics of human arteries: quantitative relationship between gene expression and arterial stiffness," *Circulation*, vol. 108, no. 15, pp. 1845–1851, 2003.

[76] M. Lyck Hansen, H. C. Beck, A. Irmukhamedov, P. S. Jensen, M. H. Olsen, and L. M. Rasmussen, "Proteome analysis of human arterial tissue discloses associations between the vascular content of small leucine-rich repeat proteoglycans and pulse wave velocity," *Arteriosclerosis, Thrombosis, and Vascular Biology*, vol. 35, no. 8, pp. 1896–1903, 2015.

[77] Yasmin, C. M. McEniery, S. Wallace, Z. Dakham, P. Pulsalkar, K. Maki-Petaja, M. J. Ashby, J. R. Cockcroft, and I. B. Wilkinson, "Matrix metalloproteinase-9 (MMP-9), MMP-2, and serum elastase activity are associated with systolic hypertension and arterial stiffness," *Arteriosclerosis, Thrombosis, and Vascular Biology*, vol. 25, no. 2, p. 372, 2005.

[78] Yasmin, C. M. McEniery, K. M. O'Shaughnessy, P. Harnett, A. Arshad, S. Wallace, K. Maki-Petaja, B. McDonnell, M. J. Ashby, J. Brown, J. R. Cockcroft, and I. B. Wilkinson, "Variation in the human matrix metalloproteinase-9 gene is associated with arterial stiffness in healthy

individuals," *Arteriosclerosis, Thrombosis, and Vascular Biology*, vol. 26, no. 8, pp. 1799–1805, 2006.

[79] S. Zhou, J. Feely, J. P. Spiers, and A. Mahmud, "Matrix metalloproteinase-9 polymorphism contributes to blood pressure and arterial stiffness in essential hypertension," *Journal of Human Hypertension*, vol. 21, no. 11, pp. 861–867, 2007.

[80] T. L. Medley, B. A. Kingwell, C. D. Gatzka, P. Pillay, and T. J. Cole, "Matrix metalloproteinase-3 genotype contributes to age-related aortic stiffening through modulation of gene and protein expression," *Circulation Research*, vol. 92, no. 11, pp. 1254–1261, 2003.

[81] R. Huang, L. Deng, A. Shen, J. Liu, H. Ren, and D. L. Xu, "Associations of MMP1, 3, 9 and TIMP3 genes polymorphism with isolated systolic hypertension in Chinese Han population," *International Journal of Medical Sciences*, vol. 10, no. 7, pp. 840–847, 2013.

[82] M. Wang, L. Jiang, R. E. Monticone, and E. G. Lakatta, "Proinflammation: the key to arterial aging," *Trends in Endocrinology and Metabolism*, vol. 25, no. 2, pp. 72–79, 2014.

[83] M. Wang, J. Zhang, L. Q. Jiang, G. Spinetti, G. Pintus, R. Monticone, F. D. Kolodgie, R. Virmani, and E. G. Lakatta, "Proinflammatory profile within the grossly normal aged human aortic wall," *Hypertension*, vol. 50, no. 1, pp. 219–227, 2007.

[84] C. M. McEniery, M. Spratt, M. Munnery, J. Yarnell, G. D. Lowe, A. Rumley, J. Gallacher, Y. Ben-Shlomo, J. R. Cockcroft, and I. B. Wilkinson, "An analysis of prospective risk factors for aortic stiffness in men: 20-year follow-up from the Caerphilly prospective study," *Hypertension*, vol. 56, no. 1, pp. 36–43, 2010.

[85] W. Schumacher, J. Cockcroft, N. J. Timpson, C. M. McEniery, J. Gallacher, A. Rumley, G. Lowe, G. D. Smith, I. B. Wilkinson, and Y. Ben-Shlomo, "Association between C-reactive protein genotype, circulating levels, and aortic pulse wave velocity," *Hypertension*, vol. 53, no. 2, pp. 150–157, 2009.

[86] H. Zhu, W. Yan, Y. Tan, K. Li, G. Kapuku, F. A. Treiber, S. Su, G. A. Harshfield, H. Snieder, and Y. Dong, "Adhesion molecule polymorphisms and pulse wave velocity in American youth," *Twin Research and Human Genetics*, vol. 11, no. 5, pp. 517–523, 2008.

[87] R. Schnabel, M. G. Larson, J. Dupuis, K. L. Lunetta, I. Lipinska, J. B. Meigs, X. Yin, J. Rong, J. A. Vita, C. Newton-Cheh, D. Levy, J. Keaney J. F., R. S. Vasan, G. F. Mitchell, and E. J. Benjamin,

"Relations of inflammatory biomarkers and common genetic variants with arterial stiffness and wave reflection," *Hypertension*, vol. 51, no. 6, pp. 1651–1657, 2008.

[88] L. Li, J. A. Zhang, M. Dose, H. Y. Kueh, R. Mosadeghi, F. Gounari, and E. V. Rothenberg, "A far downstream enhancer for murine Bcl11b controls its T-cell specific expression," *Blood*, vol. 122, no. 6, pp. 902–911, 2013.

[89] D. Califano, J. J. Cho, M. N. Uddin, K. J. Lorentsen, Q. Yang, A. Bhandoola, H. Li, and D. Avram, "Transcription Factor Bcl11b Controls Identity and Function of Mature Type 2 Innate Lymphoid Cells," *Immunity*, vol. 43, no. 2, pp. 354–368, 2015.

[90] C. M. McEniery, B. J. McDonnell, A. So, S. Aitken, C. E. Bolton, M. Munnery, S. S. Hickson, Yasmin, K. M. Maki-Petaja, J. R. Cockcroft, A. K. Dixon, I. B. Wilkinson, and A.-C. C. T. Investigators, "Aortic calcification is associated with aortic stiffness and isolated systolic hypertension in healthy individuals," *Hypertension*, vol. 53, no. 3, pp. 524–531, 2009.

[91] J. Blacher, A. P. Guerin, B. Pannier, S. J. Marchais, and G. M. London, "Arterial calcifications, arterial stiffness, and cardiovascular risk in end-stage renal disease," *Hypertension*, vol. 38, pp. 938–942, 2001.

[92] Y. Wang, Y. Zhang, Y. Li, X. Zhou, X. Wang, P. Gao, L. Jin, X. Zhang, and D. Zhu, "Common variants in the ATP2B1 gene are associated with hypertension and arterial stiffness in Chinese population," *Molecular Biology Reports*, vol. 40, no. 2, pp. 1867–1873, 2013.

[93] M. Roos, T. Richart, T. Kouznetsova, M. von Eynatten, J. Lutz, U. Heemann, M. Baumann, and J. A. Staessen, "Fetuin-A and arterial stiffness in patients with normal kidney function," *Regulatory Peptides*, vol. 154, no. 1-3, pp. 39–43, 2009.

[94] P. Eller, K. Hochegger, G. M. Feuchtner, E. Zitt, I. Tancevski, A. Ritsch, F. Kronenberg, A. R. Rosenkranz, J. R. Patsch, and G. Mayer, "Impact of ENPP1 genotype on arterial calcification in patients with end-stage renal failure," *Nephrology Dialysis Transplantation*, vol. 23, no. 1, pp. 321–327, 2008.

[95] M. Cecelja, B. Jiang, M. Mangino, T. D. Spector, and P. J. Chowienczyk, "Association of cross-sectional and longitudinal change in arterial stiffness with gene expression in the Twins UK Cohort," *Hypertension*, vol. 67, no. 1, pp. 70–76, 2016.

[96] M. Bailey, S. Pillarisetti, P. Jones, H. Xiao, D. Simionescu, and N. Vyavahare, "Involvement of matrix metalloproteinases and tenascin-C in elastin calcification," *Cardiovascular Pathology*, vol. 13, no. 3, pp. 146–155, 2004.

[97] M. Mangino, M. Cecelja, C. Menni, P.-C. Tsai, W. Yuan, K. Small, J. Bell, G. F. Mitchell, P. Chowienczyk, and T. D. Spector, "Integrated multiomics approach identifies calcium and integrin-binding protein-2 as a novel gene for pulse wave velocity.," *Journal of Hypertension*, vol. 34, no. 1, pp. 79–87, 2016.

[98] S. S. Najjar, A. Scuteri, V. Shetty, J. G. Wright, D. C. Muller, J. L. Fleg, H. P. Spurgeon, L. Ferrucci, and E. G. Lakatta, "Pulse wave velocity is an independent predictor of the longitudinal increase in systolic blood pressure and of incident hypertension in the Baltimore Longitudinal Study of Aging," *Journal of the American College of Cardiology*, vol. 51, no. 14, pp. 1377–1383, 2008.

[99] C. A. Peralta, K. L. Adeney, M. G. Shlipak, D. Jacobs, D. Duprez, D. Bluemke, J. Polak, B. Psaty, and B. R. Kestenbaum, "Structural and functional vascular alterations and incident hypertension in normotensive adults," *American Journal of Epidemiology*, vol. 171, no. 1, pp. 63–71, 2010.

[100] P. Boutouyrie, S. Laurent, and M. Briet, "Importance of arterial stiffness as cardiovascular risk factor for future development of new type of drugs," *Fundamental and Clinical Pharmacology*, vol. 22, no. 3, pp. 241–246, 2008.

[101] M. AlGhatrif and E. G. Lakatta, "The conundrum of arterial stiffness, elevated blood pressure, and aging," *Current Hypertension Reports*, vol. 17, no. 2, p. 12, 2015.

[102] A. R. Aroor, V. G. Demarco, G. Jia, Z. Sun, R. Nistala, G. A. Meininger, and J. R. Sowers, "The role of tissue Renin-Angiotensin-aldosterone system in the development of endothelial dysfunction and arterial stiffness," *Frontiers in Endocrinology*, vol. 4, p. 161, 2013.

[103] M. Wang, B. Khazan, and E. G. Lakatta, "Central Arterial Aging and Angiotensin II Signaling," *Current Hypertension Reviews*, vol. 6, no. 4, pp. 266–281, 2010.

[104] M. Safar, O. Henry, and J. Blacher, "Vascular Aging: Biology and Implications," *Current Cardiovascular Risk Reports*, vol. 5, no. 5, pp. 450–456, 2011.

[105] M. E. Safar, S. Millasseau, A. Mahmud, and J. Blacher, "Relations between large artery structure and function and aldosterone," *Journal of Hypertension*, vol. 29, no. 9, pp. 1676–1683, 2011.

[106] M. Lajemi, C. Labat, S. Gautier, P. Lacolley, M. Safar, R. Asmar, F. Cambien, and A. Benetos, "Angiotensin II type 1 receptor-153A/G and 1166A/C gene polymorphisms and increase in aortic stiffness with age in hypertensive subjects," *Journal of Hypertension*, vol. 19, no. 3, pp. 407–413, 2001.

[107] D. Tousoulis, E. Androulakis, N. Papageorgiou, E. Chatzistamatiou, A. Miliou, G. Moustakas, G. Latsios, A. M. Kampoli, K. Toutouzas, E. Oikonomou, M. Zaromytidou, I. Kallikazaros, and C. Stefanadis, "Genetic polymorphism M235T of angiotensinogen: effects on endothelial function and arterial stiffness in hypertensives," *International Journal of Cardiology*, vol. 155, no. 3, pp. 501–503, 2012.

[108] A. Benetos, F. Cambien, S. Gautier, S. Ricard, M. Safar, S. Laurent, P. Lacolley, O. Poirier, J. Topouchian, and R. Asmar, "Influence of the angiotensin II type 1 receptor gene polymorphism on the effects of perindopril and nitrendipine on arterial stiffness in hypertensive individuals," *Hypertension*, vol. 28, no. 6, pp. 1081–1084, 1996.

[109] H. Taniwaki, T. Kawagishi, M. Emoto, T. Shoji, M. Hosoi, K. Kogawa, Y. Nishizawa, and H. Morii, "Association of ACE gene polymorphism with arterial stiffness in patients with type 2 diabetes," *Diabetes Care*, vol. 22, no. 11, pp. 1858–1864, 1999.

[110] S. Gardier, M. Vincent, P. Lantelme, M. O. Rial, G. Bricca, and H. Milon, "A1166C polymorphism of angiotensin II type 1 receptor, blood pressure and arterial stiffness in hypertension," *Journal of Hypertension*, vol. 22, no. 11, pp. 2135–2142, 2004.

[111] A. Benetos, A. Giron, L. Joly, M. Temmar, R. Nzietchueng, B. Pannier, K. Bean, F. Thomas, C. Labat, and P. Lacolley, "Influence of the AGTR1 A1166C genotype on the progression of arterial stiffness: A 16-year longitudinal study," *American Journal of Hypertension*, vol. 26, no. 12, pp. 1421–1427, 2013.

[112] M. E. Safar, V. Cattan, P. Lacolley, R. Nzietchueng, C. Labat, M. Lajemi, N. de Luca, and A. Bénétos, "Aldosterone synthase gene polymorphism, stroke volume and age-related changes in aortic pulse wave velocity in subjects with hypertension," *Journal of Hypertension*, vol. 23, no. 6, pp. 1159–1166, 2005.

[113] J. Blacher, A. Kakou, J. M. Lacombe, and M. E. Safar, "Preferential association of aldosterone synthase gene polymorphism with central blood pressure and wave reflections in hypertensive individuals," *Journal of Human Hypertension*, vol. 24, no. 4, pp. 291–299, 2010.

[114] K. Sudhir, W. L. Mullen, D. Hausmann, P. J. Fitzgerald, T. M. Chou, P. G. Yock, and K. Chatterjee, "Contribution of endothelium-derived nitric oxide to coronary arterial distensibility: An in vivo two-dimensional intravascular ultrasound study," *American Heart Journal*, vol. 129, no. 4, pp. 726–732, 1995.

[115] T. J. Vuurmans, P. Boer, and H. A. Koomans, "Effects of endothelin-1 and endothelin-1 receptor blockade on cardiac output, aortic pressure, and pulse wave velocity in humans," *Hypertension*, vol. 41, no. 6, pp. 1253–1258, 2003.

[116] J. Mayer O., J. Filipovsky, M. Pesta, R. Cifkova, M. Dolejsova, and J. Simon, "Synergistic effect of angiotensin II type 1 receptor and endothelial nitric oxide synthase gene polymorphisms on arterial stiffness," *Journal of Human Hypertension*, vol. 22, no. 2, pp. 111–118, 2008.

[117] I. B. Wilkinson, S. S. Franklin, and J. R. Cockcroft, "Nitric oxide and the regulation of large artery stiffness: from physiology to pharmacology," *Hypertension*, vol. 44, no. 2, pp. 112–116, 2004.

[118] W. Chen, S. R. Srinivasan, M. G. Bond, R. Tang, E. M. Urbina, S. Li, E. Boerwinkle, and G. S. Berenson, "Nitric oxide synthase gene polymorphism (G894T) influences arterial stiffness in adults: The Bogalusa Heart Study," *American Journal of Hypertension*, vol. 17, no. 7, pp. 553–559, 2004.

[119] G. F. Mitchell, C. Y. Guo, S. Kathiresan, R. S. Vasan, M. G. Larson, J. A. Vita, M. J. Keyes, M. Vyas, C. Newton-Cheh, S. L. Musone, A. L. Camargo, J. A. Drake, D. Levy, C. J. O'Donnell, J. N. Hirschhorn, and E. J. Benjamin, "Vascular stiffness and genetic variation at the endothelial nitric oxide synthase locus: the Framingham Heart study," *Hypertension*, vol. 49, no. 6, pp. 1285–1290, 2007.

[120] J. J. Mourad, G. Ducailar, A. Rudnicki, M. Lajemi, A. Mimran, and M. E. Safar, "Age-related increase of pulse pressure and gene polymorphisms in essential hypertension: a preliminary study," *Journal of Renin Angiotensin Aldosterone System*, vol. 3, no. 2, pp. 109–115, 2002.

[121] P. Lacolley, S. Gautier, O. Poirier, B. Pannier, F. Cambien, and A. Benetos, "Nitric oxide synthase gene polymorphisms, blood pressure and aortic stiffness in normotensive and hypertensive subjects," *Journal of Hypertension*, vol. 16, no. 1, pp. 31–35, 1998.

[122] J. Mayer O., J. Filipovsky, M. Pesta, R. Cifkova, M. Dolejsova, and J. Simon, "The interaction of endothelial nitric oxide synthase polymorphism and current smoking in terms of increased arterial stiffness," *Physiol Res*, vol. 59, no. 4, pp. 529–536, 2010.

[123] M. Lajemi, S. Gautier, O. Poirier, J. P. Baguet, A. Mimran, P. Gosse, O. Hanon, C. Labat, F. Cambien, and A. Benetos, "Endothelin gene variants and aortic and cardiac structure in never-treated hypertensives," *American Journal of Hypertension*, vol. 14, no. 8 (Pt 1), pp. 755–760, 2001.

[124] J. Goddard, C. Eckhart, N. R. Johnston, A. D. Cumming, A. J. Rankin, and D. J. Webb, "Endothelin A receptor antagonism and angiotensin-converting enzyme inhibition are synergistic via an endothelin B receptor-mediated and nitric oxide-dependent mechanism," *Journal of the American Society of Nephrology*, vol. 15, no. 10, pp. 2601–2610, 2004.

[125] N. Dhaun, I. M. MacIntyre, D. Kerr, V. Melville, N. R. Johnston, S. Haughie, J. Goddard, and D. J. Webb, "Selective endothelin-A receptor antagonism reduces proteinuria, blood pressure, and arterial stiffness in chronic proteinuric kidney disease," *Hypertension*, vol. 57, no. 4, pp. 772–779, 2011.

[126] M. Iemitsu, S. Maeda, T. Otsuki, J. Sugawara, T. Tanabe, S. Jesmin, S. Kuno, R. Ajisaka, T. Miyauchi, and M. Matsuda, "Polymorphism in endothelin-related genes limits exercise-induced decreases in arterial stiffness in older subjects," *Hypertension*, vol. 47, no. 5, pp. 928–936, 2006.

[127] P. Palatini, E. Casiglia, J. Gąsowski, J. Głuszek, P. Jankowski, K. Narkiewicz, F. Saladini, K. Stolarz-Skrzypek, V. Tikhonoff, L. Van Bortel, W. Wojciechowska, and K. Kawecka-Jaszcz, "Arterial stiffness, central hemodynamics, and cardiovascular risk in hypertension," *Vascular Health and Risk Management*, vol. 7, pp. 725–739, 2011.

[128] W. Chen, S. R. Srinivasan, E. Boerwinkle, and G. S. Berenson, "Beta-adrenergic receptor genes are associated with arterial stiffness in black and white adults: the Bogalusa Heart Study," *American Journal of Hypertension*, vol. 20, no. 12, pp. 1251–1257, 2007.

[129] K. M. Mäki-Petäjä and I. B. Wilkinson, "Anti-inflammatory drugs and statins for arterial stiffness reduction," *Current Pharmaceutical Design*, vol. 15, no. 3, pp. 290–303, 2009.

[130] M. F. O'Rourke, A. Adji, M. Namasivayam, and J. Mok, "Arterial aging: a review of the pathophysiology and potential for pharmacological intervention," *Drugs & Aging*, vol. 28, no. 10, pp. 779–795, 2011.

[131] D. a. Kass, E. P. Shapiro, M. Kawaguchi, a. R. Capriotti, a. Scuteri, R. C. DeGroof, and E. G. Lakatta, "Improved arterial compliance by a novel advanced glycation end-product crosslink breaker.," *Circulation*, vol. 104, no. 13, pp. 1464–1470, 2001.

[132] P. Boutouyrie, P. Lacolley, M. Briet, V. Regnault, A. Stanton, S. Laurent, and A. Mahmud, "Pharmacological modulation of arterial stiffness," *Drugs*, vol. 71, no. 13, pp. 1689–1701, 2011.

[133] J. Topouchian, R. El Feghali, B. Pannier, S. Wang, F. Zhao, K. Smetana, K. Teo, and R. Asmar, "Arterial stiffness and pharmacological interventions–the TRanscend arterial stiffNess Substudy (TRANS study)," *Vascular Health and Risk Management*, vol. 3, no. 4, pp. 381–387, 2007.

[134] H. Ait-Oufella, C. Collin, E. Bozec, B. Laloux, K. T. Ong, C. Dufouil, P. Boutouyrie, and S. Laurent, "Long-term reduction in aortic stiffness: a 5.3-year follow-up in routine clinical practice," *Journal of Hypertension*, vol. 28, no. 11, pp. 2336–2341, 2010.

[135] K. T. Ong, S. Delerme, B. Pannier, M. E. Safar, A. Benetos, S. Laurent, P. Boutouyrie, and Investigators, "Aortic stiffness is reduced beyond blood pressure lowering by short-term and long-term antihypertensive treatment: a meta-analysis of individual data in 294 patients," *Journal of Hypertension*, vol. 29, no. 6, pp. 1034–1042, 2011.

[136] T. Dudenbostel and S. P. Glasser, "Effects of antihypertensive drugs on arterial stiffness," *Cardiology in Review*, vol. 20, no. 5, pp. 259–263, 2012.

[137] A. Mahmud, "Reducing arterial stiffness and wave reflection âĂŞ Quest for the Holy Grail?," *Artery Research*, vol. 1, no. 1, pp. 13–19, 2007.

[138] K. M. Maki-Petaja, F. C. Hall, A. D. Booth, S. M. Wallace, Yasmin, P. W. Bearcroft, S. Harish, A. Furlong, C. M. McEniery, J. Brown, and I. B. Wilkinson, "Rheumatoid arthritis is associated with increased aortic pulse-wave velocity, which is reduced by anti-tumor necrosis factor-alpha therapy," *Circulation*, vol. 114, no. 11, pp. 1185–1192, 2006.

[139] C. H. Wang, R. W. Chang, Y. H. Ko, P. R. Tsai, S. S. Wang, Y. S. Chen, W. J. Ko, C. Y. Chang, T. H. Young, and K. C. Chang, "Prevention of arterial stiffening by using low-dose atorvastatin in diabetes is associated with decreased malondialdehyde," *PLoS ONE*, vol. 9, no. 3, p. e90471, 2014.

[140] A. I. Kanaki, P. A. Sarafidis, P. I. Georgianos, K. Kanavos, I. M. Tziolas, P. E. Zebekakis, and A. N. Lasaridis, "Effects of low-dose atorvastatin on arterial stiffness and central aortic pressure augmentation in patients with hypertension and hypercholesterolemia," *American Journal of Hypertension*, vol. 26, no. 5, pp. 608–616, 2013.

[141] A. M. Briones, N. Rodríguez-Criado, R. Hernanz, A. B. García-Redondo, R. R. Rodrigues-Díez, M. J. Alonso, J. Egido, M. Ruiz-Ortega, and M. Salaices, "Atorvastatin prevents angiotensin

II-induced vascular remodeling and oxidative stress," *Hypertension*, vol. 54, no. 1, pp. 142–149, 2009.

[142] T. Fukui, K. H. Parker, and T. Yamaguchi, "Pulse wave propagation in large blood vessels based on fluid-solid interactions methods," *Single and Two-Phase Flows on Chemical and Biomedical Engineering*, pp. 460–471, 2012.

[143] D. Shahmirzadi, E. E. Konofagou, and R. X. Li, "Pulse-Wave Propagation in Straight-Geometry Vessels for Stiffness Estimation: Theory, Simulations, Phantoms and In Vitro Findings," *Journal of Biomechanical Engineering*, vol. 134, no. 11, pp. 1145021–1145026, 2012.

[144] S. Bustin, H. S. Dhillon, S. Kirvell, C. Greenwood, M. Parker, G. L. Shipley, and T. Nolan, "Variability of the reverse transcription step: practical implications," *Clinical Chemistry*, vol. 61, no. 1, pp. 202–212, 2015.

[145] S. Broeders, I. Huber, L. Grohmann, G. Berben, I. Taverniers, M. Mazzara, N. Roosens, and D. Morisset, "Guidelines for validation of qualitative real-time PCR methods," *Trends in Food Science and Technology*, vol. 37, no. 2, pp. 115–126, 2014.

[146] K. J. Livak and T. D. Schmittgen, "Analysis of relative gene expression data using real-time quantitative PCR and the 2(-Delta Delta C(T)) Method," *Methods*, vol. 25, no. 4, pp. 402–408, 2001.

[147] J. Vandesompele, K. De Preter, F. Pattyn, B. Poppe, N. Van Roy, A. De Paepe, and F. Speleman, "Accurate normalization of real-time quantitative RT-PCR data by geometric averaging of multiple internal control genes," *Genome Biology*, vol. 3, no. 7, pp. research0034.1–research0034.11, 2002.

[148] G. L. Bratthauer, "The peroxidase-antiperoxidase (PAP) method and other all-immunologic detection methods," *Methods in Molecular Biology*, vol. 588, pp. 243–255, 2010.

[149] G. L. Bratthauer, "The avidin-biotin complex (ABC) method and other avidin-biotin binding methods," *Methods in Molecular Biology*, vol. 588, pp. 257–270, 2010.

[150] L. Faget and T. S. Hnasko, "Tyramide Signal Amplification for Immunofluorescent Enhancement," *Methods in Molecular Biology*, vol. 1318, pp. 161–172, 2015.

[151] S. Padmanabhan, M. Caulfield, and A. F. Dominiczak, "Genetic and molecular aspects of hypertension," *Circulation Research*, vol. 116, no. 6, pp. 937–959, 2015.

[152] P. Tsipouras, R. Del Mastro, M. Sarfarazi, B. Lee, E. Vitale, A. H. Child, M. Godfrey, R. B. Devereux, D. Hewett, and B. Steinmann, "Genetic linkage of the Marfan syndrome, ectopia lentis, and congenital contractural arachnodactyly to the fibrillin genes on chromosomes 15 and 5. The International Marfan Syndrome Collaborative Study," *New England Journal of Medicine*, vol. 326, no. 14, pp. 905–909, 1992.

[153] P. Beighton, A. De Paepe, B. Steinmann, P. Tsipouras, and R. J. Wenstrup, "Ehlers-Danlos syndromes: revised nosology, Villefranche, 1997. Ehlers-Danlos National Foundation (USA) and Ehlers-Danlos Support Group (UK)," *American Journal of Medical Genetics*, vol. 77, no. 1, pp. 31–37, 1998.

[154] B. L. Loeys, J. Chen, E. R. Neptune, D. P. Judge, M. Podowski, T. Holm, J. Meyers, C. C. Leitch, N. Katsanis, N. Sharifi, F. L. Xu, L. A. Myers, P. J. Spevak, D. E. Cameron, J. De Backer, J. Hellemans, Y. Chen, E. C. Davis, C. L. Webb, W. Kress, P. Coucke, D. B. Rifkin, A. M. De Paepe, and H. C. Dietz, "A syndrome of altered cardiovascular, craniofacial, neurocognitive and skeletal development caused by mutations in TGFBR1 or TGFBR2," *Nature Genetics*, vol. 37, no. 3, pp. 275–281, 2005.

[155] L. Van Laer, H. Dietz, and B. Loeys, "Loeys-Dietz syndrome," *Advances in Experimental Medicine and Biology*, vol. 802, pp. 95–105, 2014.

[156] D. Wu, Y. H. Shen, L. Russell, J. S. Coselli, and S. A. LeMaire, "Molecular mechanisms of thoracic aortic dissection," *Journal of Surgical Research*, vol. 184, no. 2, pp. 907–924, 2013.

[157] C. A. Nienaber, R. E. Clough, N. Sakalihasan, T. Suzuki, R. Gibbs, F. Mussa, M. P. Jenkins, M. M. Thompson, A. Evangelista, J. S. Yeh, N. Cheshire, U. Rosendahl, and J. Pepper, "Aortic dissection," *Nature Reviews Disease Primers*, vol. 2, p. 16071, 2016.

[158] A. Weiss and L. Attisano, "The TGFbeta superfamily signaling pathway," *Wiley Interdisciplinary Reviews: Developmental Biology*, vol. 2, no. 1, pp. 47–63, 2013.

[159] R. A. Ignotz and J. Massagué, "Transforming growth factor-beta stimulates the expression of fibronectin and collagen and their incorporation into the extracellular matrix," *The Journal of Biological Chemistry*, vol. 261, no. 9, pp. 4337–4345, 1986.

[160] D. R. Edwards, G. Murphy, J. J. Reynolds, S. E. Whitham, A. J. Docherty, P. Angel, and J. K. Heath, "Transforming growth factor beta modulates the expression of collagenase and metalloproteinase inhibitor," *The EMBO Journal*, vol. 6, no. 7, pp. 1899–1904, 1987.

[161] V. M. Kähäri, D. R. Olsen, R. W. Rhudy, P. Carrillo, Y. Q. Chen, and J. Uitto, "Transforming growth factor-beta up-regulates elastin gene expression in human skin fibroblasts. Evidence for post-transcriptional modulation," *Laboratory Investigation*, vol. 66, no. 5, pp. 580–588, 1992.

[162] F. Verrecchia, M. L. Chu, and A. Mauviel, "Identification of novel TGF-beta /Smad gene targets in dermal fibroblasts using a combined cDNA microarray/promoter transactivation approach," *The Journal of Biological Chemistry*, vol. 276, no. 20, pp. 17058–17062, 2001.

[163] E. S. Kim, M. S. Kim, and A. Moon, "TGF-beta-induced upregulation of MMP-2 and MMP-9 depends on p38 MAPK, but not ERK signaling in MCF10A human breast epithelial cells," *International Journal of Oncology*, vol. 25, no. 5, pp. 1375–1382, 2004.

[164] H. Dadlani, M. L. Ballinger, N. Osman, R. Getachew, and P. J. Little, "Smad and p38 MAP kinase-mediated signaling of proteoglycan synthesis in vascular smooth muscle," *Journal of Biological Chemistry*, vol. 283, no. 12, pp. 7844–7852, 2008.

[165] M. L. Burch, S. N. Yang, M. L. Ballinger, R. Getachew, N. Osman, and P. J. Little, "TGF-beta stimulates biglycan synthesis via p38 and ERK phosphorylation of the linker region of Smad2," *Cellular and Molecular Life Sciences*, vol. 67, no. 12, pp. 2077–2090, 2010.

[166] J. J. Doyle, E. E. Gerber, and H. C. Dietz, "Matrix-dependent perturbation of TGFβ signaling and disease," *FEBS Letters*, vol. 586, no. 14, pp. 2003–2015, 2012.

[167] D. B. Rifkin, "Latent transforming growth factor-beta (TGF-beta) binding proteins: orchestrators of TGF-beta availability," *The Journal of Biological Chemistry*, vol. 280, no. 9, pp. 7409–7412, 2005.

[168] R. Flaumenhaft, M. Abe, Y. Sato, K. Miyazono, J. Harpel, C. H. Heldin, and D. B. Rifkin, "Role of the latent TGF-beta binding protein in the activation of latent TGF-beta by co-cultures of endothelial and smooth muscle cells," *Journal of Cell Biology*, vol. 120, no. 4, pp. 995–1002, 1993.

[169] P. J. Wipff and B. Hinz, "Integrins and the activation of latent transforming growth factor beta1 - an intimate relationship," *European Journal of Cell Biology*, vol. 87, no. 8-9, pp. 601–615, 2008.

[170] I. M. van de Laar, R. A. Oldenburg, G. Pals, J. W. Roos-Hesselink, B. M. de Graaf, J. M. Verhagen, Y. M. Hoedemaekers, R. Willemsen, L. A. Severijnen, H. Venselaar, G. Vriend, P. M. Pattynama, M. Collee, D. Majoor-Krakauer, D. Poldermans, I. M. Frohn-Mulder, D. Micha, J. Timmermans, Y. Hilhorst-Hofstee, S. M. Bierma-Zeinstra, P. J. Willems, J. M. Kros, E. H. Oei, B. A. Oostra, M. W. Wessels, and A. M. Bertoli-Avella, "Mutations in SMAD3 cause a

syndromic form of aortic aneurysms and dissections with early-onset osteoarthritis," *Nature Genetics*, vol. 43, no. 2, pp. 121–126, 2011.

[171] M. E. Lindsay, D. Schepers, N. A. Bolar, J. J. Doyle, E. Gallo, J. Fert-Bober, M. J. Kempers, E. K. Fishman, Y. Chen, L. Myers, D. Bjeda, G. Oswald, A. F. Elias, H. P. Levy, B. M. Anderlid, M. H. Yang, E. M. Bongers, J. Timmermans, A. C. Braverman, N. Canham, G. R. Mortier, H. G. Brunner, P. H. Byers, J. Van Eyk, L. Van Laer, H. C. Dietz, and B. L. Loeys, "Loss-of-function mutations in TGFB2 cause a syndromic presentation of thoracic aortic aneurysm," *Nature Genetics*, vol. 44, no. 8, pp. 922–927, 2012.

[172] A. M. Bertoli-Avella, E. Gillis, H. Morisaki, J. M. Verhagen, B. M. de Graaf, G. van de Beek, E. Gallo, B. P. Kruithof, H. Venselaar, L. A. Myers, S. Laga, A. J. Doyle, G. Oswald, G. W. van Cappellen, I. Yamanaka, R. M. van der Helm, B. Beverloo, A. de Klein, L. Pardo, M. Lammens, C. Evers, K. Devriendt, M. Dumoulein, J. Timmermans, H. T. Bruggenwirth, F. Verheijen, I. Rodrigus, G. Baynam, M. Kempers, J. Saenen, E. M. Van Craenenbroeck, K. Minatoya, R. Matsukawa, T. Tsukube, N. Kubo, R. Hofstra, M. J. Goumans, J. A. Bekkers, J. W. Roos-Hesselink, I. M. van de Laar, H. C. Dietz, L. Van Laer, T. Morisaki, M. W. Wessels, and B. L. Loeys, "Mutations in a TGF-beta ligand, TGFB3, cause syndromic aortic aneurysms and dissections," *Journal of the American College of Cardiology*, vol. 65, no. 13, pp. 1324–1336, 2015.

[173] G. MacCarrick, r. Black J. H., S. Bowdin, I. El-Hamamsy, P. A. Frischmeyer-Guerrerio, A. L. Guerrerio, P. D. Sponseller, B. Loeys, and r. Dietz H. C., "Loeys-Dietz syndrome: a primer for diagnosis and management," *Genetics in Medicine*, vol. 16, no. 8, pp. 576–587, 2014.

[174] C. Boileau, D. C. Guo, N. Hanna, E. S. Regalado, D. Detaint, L. Gong, M. Varret, S. K. Prakash, A. H. Li, H. D'Indy, A. C. Braverman, B. Grandchamp, C. S. Kwartler, L. Gouya, R. L. Santos-Cortez, M. Abifadel, S. M. Leal, C. Muti, J. Shendure, M. S. Gross, M. J. Rieder, A. Vahanian, D. A. Nickerson, J. B. Michel, G. Jondeau, and D. M. Milewicz, "TGFB2 mutations cause familial thoracic aortic aneurysms and dissections associated with mild systemic features of Marfan syndrome," *Nature Genetics*, vol. 44, no. 8, pp. 916–921, 2012.

[175] M. Renard, Marjolijn.Renard@ugent.be, G. B. for Medical Genetics Ghent University Hospital, B. Callewaert, G. B. for Medical Genetics Ghent University Hospital, F. Malfait, G. B. for Medical Genetics Ghent University Hospital, L. Campens, G. B. for Medical Genetics Ghent University Hospital, S. Sharif, B. U. K. Clinical Genetics Unit Birmingham Women's Hospital, M. del Campo, S. de Salut Barcelona, I. Valenzuela, S. de Salut Barcelona, C. Mcwilliam, A. U. K.

Clinical Genetics Centre Forester Hill, P. Coucke, G. B. for Medical Genetics Ghent University Hospital, A. D. Paepe, G. B. for Medical Genetics Ghent University Hospital, J. D. Backer, and G. B. for Medical Genetics Ghent University Hospital, "Thoracic aortic-aneurysm and dissection in association with significant mitral valve disease caused by mutations in TGFB2," *International Journal of Cardiology*, vol. 165, no. 3, pp. 584–587, 2013.

[176] M. Ritelli, N. Chiarelli, C. Dordoni, S. Quinzani, M. Venturini, R. Maroldi, P. Calzavara-Pinton, and M. Colombi, "Further delineation of Loeys-Dietz syndrome type 4 in a family with mild vascular involvement and a TGFB2 splicing mutation," *BMC Medical Genetics*, vol. 15, p. 91, 2014.

[177] M. Gago-Diaz, A. Blanco-Verea, G. Teixido-Tura, I. Valenzuela, M. Del Campo, M. Borregan, B. Sobrino, J. Amigo, D. Garcia-Dorado, A. Evangelista, A. Carracedo, and M. Brion, "Whole exome sequencing for the identification of a new mutation in TGFB2 involved in a familial case of non-syndromic aortic disease," *Clinica Chimica Acta*, vol. 437, pp. 88–92, 2014.

[178] J. A. Schubert, B. J. Landis, A. R. Shikany, R. B. Hinton, and S. M. Ware, "Clinically relevant variants identified in thoracic aortic aneurysm patients by research exome sequencing," *American Journal of Medical Genetics Part A*, vol. 170A, no. 5, pp. 1288–1294, 2016.

[179] J. M. Mazzella, M. Frank, P. Collignon, M. Langeois, A. Legrand, X. Jeunemaitre, and J. Albuisson, "Phenotypic variability and diffuse arterial lesions in a family with Loeys-Dietz syndrome type 4," *Clinical Genetics*, vol. 91, no. 3, pp. 458–462, 2017.

[180] R. Leutermann, S. Sheikhzadeh, L. Brockstadt, M. Rybczynski, V. van Rahden, K. Kutsche, Y. von Kodolitsch, and G. Rosenberger, "A 1-bp duplication in TGFB2 in three family members with a syndromic form of thoracic aortic aneurysm," *European Journal of Human Genetics*, vol. 22, no. 7, pp. 944–948, 2014.

[181] H. Gaspar, B. Lutz, K. Reicherter, S. Lühl, R. Taurman, H. Gabriel, R. E. Brenner, and G. Borck, "4.7 Mb deletion encompassing TGFB2 associated with features of Loeys-Dietz syndrome and osteoporosis in adulthood," *American Journal of Medical Genetics Part A*, vol. 173, no. 8, pp. 2289–2292, 2017.

[182] P. Fontana, R. Genesio, A. Casertano, G. Cappuccio, A. Mormile, L. Nitsch, A. Iolascon, G. Andria, and D. Melis, "Loeys-Dietz syndrome type 4, caused by chromothripsis, involving the TGFB2 gene," *Gene*, vol. 538, no. 1, pp. 69–73, 2014.

[183] M. Kakoki, O. M. Pochynyuk, C. M. Hathaway, H. Tomita, J. R. Hagaman, H.-S. Kim, O. L. Zaika, M. Mamenko, Y. Kayashima, K. Matsuki, S. Hiller, F. Li, L. Xu, R. Grant, A. M. Bertorello, and O. Smithies, "Primary aldosteronism and impaired natriuresis in mice underexpressing TGFβ1," *Proceedings of the National Academy of Sciences*, vol. 110, no. 14, pp. 5600–5, 2013.

[184] J. Varga and S. A. Jimenez, "Stimulation of normal human fibroblast collagen production and processing by transforming growth factor-beta," *Biochemical and Biophysical Research Communications*, vol. 138, no. 2, pp. 974–980, 1986.

[185] M. M. Chen, A. Lam, J. A. Abraham, G. F. Schreiner, and A. H. Joly, "CTGF expression is induced by TGF- beta in cardiac fibroblasts and cardiac myocytes: a potential role in heart fibrosis.," *Journal of Molecular and Cellular Cardiology*, vol. 32, pp. 1805–1819, 2000.

[186] Z. Mallat, A. Tedgui, and D. Henrion, "Role of microvascular tone and extracellular matrix contraction in the regulation of interstitial fluid: Implications for aortic dissection," *Arteriosclerosis, Thrombosis, and Vascular Biology*, vol. 36, no. 9, pp. 1742–1747, 2016.

[187] J. D. Humphrey, M. A. Schwartz, G. Tellides, and D. M. Milewicz, "Role of mechanotransduction in vascular biology: Focus on thoracic aortic aneurysms and dissections," *Circulation Research*, vol. 116, no. 8, pp. 1448–1461, 2015.

[188] G. Litteri, D. Carnevale, A. D'Urso, G. Cifelli, P. Braghetta, A. Damato, D. Bizzotto, A. Landolfi, F. D. Ros, P. Sabatelli, N. Facchinello, A. Maffei, D. Volpin, A. Colombatti, G. M. Bressan, and G. Lembo, "Vascular smooth muscle emilin-1 is a regulator of arteriolar myogenic response and blood pressure," *Arteriosclerosis, Thrombosis, and Vascular Biology*, vol. 32, no. 9, pp. 2178–2184, 2012.

[189] R. K. Reed and K. Rubin, "Transcapillary exchange: Role and importance of the interstitial fluid pressure and the extracellular matrix," *Cardiovascular Research*, vol. 87, no. 2, pp. 211–217, 2010.

[190] J. Ferruzzi, S. I. Murtada, G. Li, Y. Jiao, S. Uman, M. Y. Ting, G. Tellides, and J. D. Humphrey, "Pharmacologically improved contractility protects against aortic dissection in mice with disrupted transforming growth factor-β signaling despite compromised extracellular matrix properties," *Arteriosclerosis, Thrombosis, and Vascular Biology*, vol. 36, no. 5, pp. 919–927, 2016.

[191] E. Crosas-Molist, T. Meirelles, J. López-Luque, C. Serra-Peinado, J. Selva, L. Caja, D. Gorbenko Del Blanco, J. J. Uriarte, E. Bertran, Y. Mendizábal, V. Hernández, C. García-Calero, O. Bus-

nadiego, E. Condom, D. Toral, M. Castellà, A. Forteza, D. Navajas, E. Sarri, F. Rodríguez-Pascual, H. C. Dietz, I. Fabregat, and G. Egea, "Vascular smooth muscle cell phenotypic changes in patients with marfan syndrome," *Arteriosclerosis, Thrombosis, and Vascular Biology*, vol. 35, no. 4, pp. 960–972, 2015.

[192] S. Inamoto, C. S. Kwartler, A. L. Lafont, Y. Y. Liang, V. T. Fadulu, S. Duraisamy, M. Willing, A. Estrera, H. Safi, M. C. Hannibal, J. Carey, J. Wiktorowicz, F. K. Tan, X. H. Feng, H. Pannu, and D. M. Milewicz, "TGFBR2 mutations alter smooth muscle cell phenotype and predispose to thoracic aortic aneurysms and dissections," *Cardiovascular Research*, vol. 88, no. 3, pp. 520–529, 2010.

[193] J. P. Habashi, D. P. Judge, T. M. Holm, R. D. Cohn, B. L. Loeys, T. K. Cooper, L. Myers, E. C. Klein, G. Liu, C. Calvi, M. Podowski, E. R. Neptune, M. K. Halushka, D. Bedja, K. Gabrielson, D. B. Rifkin, L. Carta, F. Ramirez, D. L. Huso, and H. C. Dietz, "Losartan, an AT1 antagonist, prevents aortic aneurysm in a mouse model of Marfan syndrome," *Science*, vol. 312, no. 5770, pp. 117–121, 2006.

[194] V. L. King, A. Y. Lin, F. Kristo, T. J. Anderson, N. Ahluwalia, G. J. Hardy, A. P. Owens, D. A. Howatt, D. Shen, A. M. Tager, A. D. Luster, A. Daugherty, and R. E. Gerszten, "Interferon-gamma and the interferon-inducible chemokine CXCL10 protect against aneurysm formation and rupture," *Circulation*, vol. 119, no. 3, pp. 426–435, 2009.

[195] J. R. Cook, N. P. Clayton, L. Carta, J. Galatioto, E. Chiu, S. Smaldone, C. A. Nelson, S. H. Cheng, B. M. Wentworth, and F. Ramirez, "Dimorphic effects of transforming growth factor-β signaling during aortic aneurysm progression in mice suggest a combinatorial therapy for Marfan syndrome," *Arteriosclerosis, Thrombosis, and Vascular Biology*, vol. 35, no. 4, pp. 911–917, 2015.

[196] E. R. Neptune, P. a. Frischmeyer, D. E. Arking, L. Myers, T. E. Bunton, B. Gayraud, F. Ramirez, L. Y. Sakai, and H. C. Dietz, "Dysregulation of TGF-beta activation contributes to pathogenesis in Marfan syndrome," *Nature Genetics*, vol. 33, no. 3, pp. 407–11, 2003.

[197] M. W. Majesky, "Developmental basis of vascular smooth muscle diversity," *Arteriosclerosis, Thrombosis, and Vascular Biology*, vol. 27, no. 6, pp. 1248–1258, 2007.

[198] S. Topouzis and M. W. Majesky, "Smooth muscle lineage diversity in the chick embryo. Two types of aortic smooth muscle cell differ in growth and receptor-mediated transcriptional re-

sponses to transforming growth factor-beta," *Developmental Biology*, vol. 178, no. 2, pp. 430–445, 1996.

[199] M. E. Lindsay and H. C. Dietz, "Lessons on the pathogenesis of aneurysm from heritable conditions," *Nature*, vol. 473, no. 7347, pp. 308–316, 2011.

[200] J. H. Hu, H. Wei, M. Jaffe, N. Airhart, L. Du, S. N. Angelov, J. Yan, J. K. Allen, I. Kang, T. N. Wight, K. Fox, A. Smith, R. Enstrom, and D. A. Dichek, "Postnatal Deletion of the Type II Transforming Growth Factor-β Receptor in Smooth Muscle Cells Causes Severe Aortopathy in Mice," *Arteriosclerosis, Thrombosis, and Vascular Biology*, vol. 35, no. 12, pp. 2647–2656, 2015.

[201] H. Wei, J. H. Hu, S. N. Angelov, K. Fox, J. Yan, R. Enstrom, A. Smith, and D. A. Dichek, "Aortopathy in a mouse model of Marfan syndrome is not mediated by altered transforming growth factor β signaling," *Journal of the American Heart Association*, vol. 6, no. 1, 2017.

[202] W. Li, Q. Li, Y. Jiao, L. Qin, R. Ali, J. Zhou, J. Ferruzzi, R. W. Kim, A. Geirsson, H. C. Dietz, S. Offermanns, J. D. Humphrey, and G. Tellides, "Tgfbr2 disruption in postnatal smooth muscle impairs aortic wall homeostasis," *Journal of Clinical Investigation*, vol. 124, no. 2, pp. 755–767, 2014.

[203] M. Horiguchi, M. Ota, and D. B. Rifkin, "Matrix control of transforming growth factor-beta function," *Biochemical Journal*, vol. 152, no. 4, pp. 321–329, 2012.

[204] Y. Wang, H. Ait-Oufella, O. Herbin, P. Bonnin, B. Ramkhelawon, S. Taleb, J. Huang, G. Offenstadt, C. Combadière, L. Rénia, J. L. Johnson, P. L. Tharaux, A. Tedgui, and Z. Mallat, "TGF-beta activity protects against inflammatory aortic aneurysm progression and complications in angiotensin II-infused mice," *Journal of Clinical Investigation*, vol. 120, no. 2, pp. 422–432, 2010.

[205] X. Chen, D. L. Rateri, D. A. Howatt, A. Balakrishnan, J. J. Moorleghen, L. A. Cassis, and A. Daugherty, "TGF-β neutralization enhances AngII-induced aortic rupture and aneurysm in both thoracic and abdominal regions," *PLoS ONE*, vol. 11, no. 4, p. e0153811, 2016.

[206] E. M. Gallo, D. C. Loch, J. P. Habashi, J. F. Calderon, Y. Chen, D. Bedja, C. van Erp, E. E. Gerber, S. J. Parker, K. Sauls, D. P. Judge, S. K. Cooke, M. E. Lindsay, R. Rouf, L. Myers, C. M. ap Rhys, K. C. Kent, R. A. Norris, D. L. Huso, and H. C. Dietz, "Angiotensin II-dependent TGF-β signaling contributes to Loeys-Dietz syndrome vascular pathogenesis," *Journal of Clinical Investigation*, vol. 124, no. 1, pp. 448–460, 2014.

[207] T. M. Holm, J. P. Habashi, J. J. Doyle, D. Bedja, Y. Chen, C. van Erp, M. E. Lindsay, D. Kim, F. Schoenhoff, R. D. Cohn, B. L. Loeys, C. J. Thomas, S. Patnaik, J. J. Marugan, D. P. Judge, and H. C. Dietz, "Noncanonical TGFβ signaling contributes to aortic aneurysm progression in Marfan syndrome mice," *Science*, vol. 332, no. 6027, pp. 358–361, 2011.

[208] J. P. Habashi, J. J. Doyle, T. M. Holm, H. Aziz, F. Schoenhoff, D. Bedja, Y. Chen, A. N. Modiri, D. P. Judge, and H. C. Dietz, "Angiotensin II type 2 receptor signaling attenuates aortic aneurysm in mice through ERK antagonism," *Science*, vol. 332, no. 6027, pp. 361–365, 2011.

[209] L. A. Hindorff, P. Sethupathy, H. A. Junkins, E. M. Ramos, J. P. Mehta, F. S. Collins, and T. A. Manolio, "Potential etiologic and functional implications of genome-wide association loci for human diseases and traits," *Proceedings of the National Academy of Sciences*, vol. 106, no. 23, pp. 9362–9367, 2009.

[210] B. Hrdlickova, R. C. de Almeida, Z. Borek, and S. Withoff, "Genetic variation in the non-coding genome: Involvement of micro-RNAs and long non-coding RNAs in disease," *Biochimica et Biophysica Acta*, vol. 1842, no. 10, pp. 1910–1922, 2014.

[211] M. Leid, J. E. Ishmael, D. Avram, D. Shepherd, V. Fraulob, and P. Dollé, "CTIP1 and CTIP2 are differentially expressed during mouse embryogenesis," *Gene Expression Patterns*, vol. 4, no. 6, pp. 733–739, 2004.

[212] O. Golonzhka, M. Leid, G. Indra, and A. K. Indra, "Expression of COUP-TF-interacting protein 2 (CTIP2) in mouse skin during development and in adulthood," *Gene Expression Patterns*, vol. 7, no. 7, pp. 754–760, 2007.

[213] O. Golonzhka, D. Metzger, J. M. Bornert, B. K. Bay, M. K. Gross, C. Kioussi, and M. Leid, "Ctip2/Bcl11b controls ameloblast formation during mammalian odontogenesis," *Proceedings of the National Academy of Sciences*, vol. 106, no. 11, pp. 4278–4283, 2009.

[214] J. Inoue, Y. Ihara, D. Tsukamoto, K. Yasumoto, T. Hashidume, K. Kamimura, Y. Nakai, S. Hirano, M. Shimizu, R. Kominami, and R. Sato, "Identification of BCL11B as a regulator of adipogenesis," *Science Reports*, vol. 6, p. 32750, 2016.

[215] M. S. Cunnington, M. Santibanez Koref, B. M. Mayosi, J. Burn, and B. Keavney, "Chromosome 9p21 SNPs Associated with Multiple Disease Phenotypes Correlate with ANRIL Expression," *PLoS Genetics*, vol. 6, no. 4, p. e1000899, 2010.

[216] G. Jin, J. Sun, S. D. Isaacs, K. E. Wiley, S. T. Kim, L. W. Chu, Z. Zhang, H. Zhao, S. L. Zheng, W. B. Isaacs, and J. Xu, "Human polymorphisms at long non-coding RNAs (lncRNAs) and association with prostate cancer risk," *Carcinogenesis*, vol. 32, no. 11, pp. 1655–1659, 2011.

[217] W. Pan, L. Liu, J. Wei, Y. Ge, J. Zhang, H. Chen, L. Zhou, Q. Yuan, C. Zhou, and M. Yang, "A functional lncRNA HOTAIR genetic variant contributes to gastric cancer susceptibility," *Molecular Carcinogenesis*, vol. 55, no. 1, pp. 90–96, 2016.

[218] X. Huang, X. Du, and Y. Li, "The role of BCL11B in hematological malignancy," *Experimental Hematology and Oncology*, vol. 1, no. 1, p. 22, 2012.

[219] Y. Wakabayashi, H. Watanabe, J. Inoue, N. Takeda, J. Sakata, Y. Mishima, J. Hitomi, T. Yamamoto, M. Utsuyama, O. Niwa, S. Aizawa, and R. Kominami, "Bcl11b is required for differentiation and survival of alphabeta T lymphocytes," *Nature Immunology*, vol. 4, no. 6, pp. 533–539, 2003.

[220] M. J. Lennon, S. P. Jones, M. D. Lovelace, G. J. Guillemin, and B. J. Brew, "Bcl11b: A New Piece to the Complex Puzzle of Amyotrophic Lateral Sclerosis Neuropathogenesis?," *Neurotoxicity Research*, vol. 29, no. 2, pp. 201–207, 2016.

[221] D. Avram, A. Fields, K. Pretty On Top, D. J. Nevrivy, J. E. Ishmael, and M. Leid, "Isolation of a novel family of C(2)H(2) zinc finger proteins implicated in transcriptional repression mediated by chicken ovalbumin upstream promoter transcription factor (COUP-TF) orphan nuclear receptors," *The Journal of Biological Chemistry*, vol. 275, no. 14, pp. 10315–10322, 2000.

[222] D. Avram, A. Fields, T. Senawong, A. Topark-Ngarm, and M. Leid, "COUP-TF (chicken ovalbumin upstream promoter transcription factor)-interacting protein 1 (CTIP1) is a sequence-specific DNA binding protein," *Biochemical Journal*, vol. 368, no. Pt 2, pp. 555–563, 2002.

[223] T. Senawong, V. J. Peterson, D. Avram, D. M. Shepherd, R. A. Frye, S. Minucci, and M. Leid, "Involvement of the histone deacetylase SIRT1 in chicken ovalbumin upstream promoter transcription factor (COUP-TF)-interacting protein 2-mediated transcriptional repression," *The Journal of Biological Chemistry*, vol. 278, no. 44, pp. 43041–43050, 2003.

[224] V. B. Cismasiu, K. Adamo, J. Gecewicz, J. Duque, Q. Lin, and D. Avram, "BCL11B functionally associates with the NuRD complex in T lymphocytes to repress targeted promoter," *Oncogene*, vol. 24, no. 45, pp. 6753–6764, 2005.

[225] C. Marban, S. Suzanne, F. Dequiedt, S. de Walque, L. Redel, C. Van Lint, D. Aunis, and O. Rohr, "Recruitment of chromatin-modifying enzymes by CTIP2 promotes HIV-1 transcriptional silencing," *The EMBO Journal*, vol. 26, no. 2, pp. 412–423, 2007.

[226] V. B. Cismasiu, E. Paskaleva, S. Suman Daya, M. Canki, K. Duus, and D. Avram, "BCL11B is a general transcriptional repressor of the HIV-1 long terminal repeat in T lymphocytes through recruitment of the NuRD complex," *Virology*, vol. 380, no. 2, pp. 173–181, 2008.

[227] L. J. Zhang, W. K. Vogel, X. Liu, A. Topark-Ngarm, B. L. Arbogast, C. S. Maier, T. M. Filtz, and M. Leid, "Coordinated regulation of transcription factor Bcl11b activity in thymocytes by the mitogen-activated protein kinase (MAPK) pathways and protein sumoylation," *The Journal of Biological Chemistry*, vol. 287, no. 32, pp. 26971–26988, 2012.

[228] V. B. Cismasiu, S. Ghanta, J. Duque, D. I. Albu, H. M. Chen, R. Kasturi, and D. Avram, "BCL11B participates in the activation of IL2 gene expression in CD4+ T lymphocytes," *Blood*, vol. 108, no. 8, pp. 2695–2702, 2006.

[229] F. M. Abboud and J. H. Huston, "Measurement of arterial aging in hypertensive patients," *Journal of Clinical Investigation*, vol. 40, pp. 1915–1921, 1961.

[230] D. I. Albu, D. Feng, D. Bhattacharya, N. A. Jenkins, N. G. Copeland, P. Liu, and D. Avram, "BCL11B is required for positive selection and survival of double-positive thymocytes," *The Journal of Experimental Medicine*, vol. 204, no. 12, pp. 3003–3015, 2007.

[231] L. Li, M. Leid, and E. V. Rothenberg, "An early T cell lineage commitment checkpoint dependent on the transcription factor Bcl11b," *Science*, vol. 329, no. 5987, pp. 89–93, 2010.

[232] C. C. Tydell, E. S. David-Fung, J. E. Moore, L. Rowen, T. Taghon, and E. V. Rothenberg, "Molecular dissection of prethymic progenitor entry into the T lymphocyte developmental pathway," *The Journal of Immunology*, vol. 179, no. 1, pp. 421–438, 2007.

[233] W. A. Dik, K. Pike-Overzet, F. Weerkamp, D. de Ridder, E. F. de Haas, M. R. Baert, P. van der Spek, E. E. Koster, M. J. Reinders, J. J. van Dongen, A. W. Langerak, and F. J. Staal, "New insights on human T cell development by quantitative T cell receptor gene rearrangement studies and gene expression profiling," *The Journal of Experimental Medicine*, vol. 201, no. 11, pp. 1715–1723, 2005.

[234] H. Y. Kueh, M. A. Yui, K. K. Ng, S. S. Pease, J. A. Zhang, S. S. Damle, G. Freedman, S. Siu, I. D. Bernstein, M. B. Elowitz, and E. V. Rothenberg, "Asynchronous combinatorial action of four

regulatory factors activates Bcl11b for T cell commitment," *Nature Immunology*, vol. 17, no. 8, pp. 956–965, 2016.

[235] T. Ikawa, S. Hirose, K. Masuda, K. Kakugawa, R. Satoh, A. Shibano-Satoh, R. Kominami, Y. Katsura, and H. Kawamoto, "An essential developmental checkpoint for production of the T cell lineage," *Science*, vol. 329, no. 5987, pp. 93–96, 2010.

[236] V. L. Ha, A. Luong, F. Li, D. Casero, J. Malvar, Y. M. Kim, R. Bhatia, G. M. Crooks, and C. Parekh, "The T-ALL related gene BCL11B regulates the initial stages of human T-cell differentiation," *Leukemia*, 2017.

[237] J. Inoue, T. Kanefuji, K. Okazuka, H. Watanabe, Y. Mishima, and R. Kominami, "Expression of TCR alpha beta partly rescues developmental arrest and apoptosis of alpha beta T cells in Bcl11b-/- mice," *The Journal of Immunology*, vol. 176, no. 10, pp. 5871–5879, 2006.

[238] P. Li, S. Burke, J. Wang, X. Chen, M. Ortiz, S. C. Lee, D. Lu, L. Campos, D. Goulding, B. L. Ng, G. Dougan, B. Huntly, B. Gottgens, N. A. Jenkins, N. G. Copeland, F. Colucci, and P. Liu, "Reprogramming of T cells to natural killer-like cells upon Bcl11b deletion," *Science*, vol. 329, no. 5987, pp. 85–89, 2010.

[239] P. Kastner, S. Chan, W. K. Vogel, L. J. Zhang, A. Topark-Ngarm, O. Golonzhka, B. Jost, S. Le Gras, M. K. Gross, and M. Leid, "Bcl11b represses a mature T-cell gene expression program in immature CD4(+)CD8(+) thymocytes," *European Journal of Immunology*, vol. 40, no. 8, pp. 2143–2154, 2010.

[240] D. I. Albu, J. VanValkenburgh, N. Morin, D. Califano, N. A. Jenkins, N. G. Copeland, P. Liu, and D. Avram, "Transcription factor Bcl11b controls selection of invariant natural killer T-cells by regulating glycolipid presentation in double-positive thymocytes," *Proceedings of the National Academy of Sciences*, vol. 108, no. 15, pp. 6211–6216, 2011.

[241] J. Vanvalkenburgh, D. I. Albu, C. Bapanpally, S. Casanova, D. Califano, D. M. Jones, L. Ignatowicz, S. Kawamoto, S. Fagarasan, N. A. Jenkins, N. G. Copeland, P. Liu, and D. Avram, "Critical role of Bcl11b in suppressor function of T regulatory cells and prevention of inflammatory bowel disease," *The Journal of Experimental Medicine*, vol. 208, no. 10, pp. 2069–2081, 2011.

[242] D. Califano, K. J. Sweeney, H. Le, J. VanValkenburgh, E. Yager, W. O'Connor, J. S. Kennedy, D. M. Jones, and D. Avram, "Diverting T helper cell trafficking through increased plastic-

ity attenuates autoimmune encephalomyelitis," *Journal of Clinical Investigation*, vol. 124, no. 1, pp. 174–187, 2014.

[243] X. Huang, Q. Shen, S. Chen, L. Yang, J. Weng, X. Du, P. Grabarczyk, G. K. Przybylski, C. A. Schmidt, and Y. Li, "Gene expression profiles in BCL11B-siRNA treated malignant T cells," *Journal of Hematology and Oncology*, vol. 4, p. 23, 2011.

[244] N. K. Karanam, P. Grabarczyk, E. Hammer, C. Scharf, S. Venz, M. Gesell-Salazar, W. Barthlen, G. K. Przybylski, C. A. Schmidt, and U. Völker, "Proteome analysis reveals new mechanisms of Bcl11b-loss driven apoptosis," *Journal of Proteome Research*, vol. 9, no. 8, pp. 3799–3811, 2010.

[245] P. Grabarczyk, V. Nähse, M. Delin, G. Przybylski, M. Depke, P. Hildebrandt, U. Völker, and C. A. Schmidt, "Increased expression of bcl11b leads to chemoresistance accompanied by G1 accumulation," *PLoS ONE*, vol. 5, no. 9, 2010.

[246] P. Grabarczyk, G. K. Przybylski, M. Depke, U. Völker, J. Bahr, K. Assmus, B. M. Bröker, R. Walther, and C. A. Schmidt, "Inhibition of BCL11B expression leads to apoptosis of malignant but not normal mature T cells," *Oncogene*, vol. 26, no. 26, pp. 3797–3810, 2007.

[247] P. Arlotta, B. J. Molyneaux, J. Chen, J. Inoue, R. Kominami, and J. D. Macklis, "Neuronal subtype-specific genes that control corticospinal motor neuron development in vivo," *Neuron*, vol. 45, no. 2, pp. 207–221, 2005.

[248] T. Enomoto, M. Ohmoto, T. Iwata, A. Uno, M. Saitou, T. Yamaguchi, R. Kominami, I. Matsumoto, and J. Hirota, "Bcl11b/Ctip2 controls the differentiation of vomeronasal sensory neurons in mice," *Journal of Neuroscience*, vol. 31, no. 28, pp. 10159–10173, 2011.

[249] P. Arlotta, B. J. Molyneaux, D. Jabaudon, Y. Yoshida, and J. D. Macklis, "Ctip2 controls the differentiation of medium spiny neurons and the establishment of the cellular architecture of the striatum," *Journal of Neuroscience*, vol. 28, no. 3, pp. 622–632, 2008.

[250] R. Simon, H. Brylka, H. Schwegler, S. Venkataramanappa, J. Andratschke, C. Wiegreffe, P. Liu, E. Fuchs, N. A. Jenkins, N. G. Copeland, C. Birchmeier, and S. Britsch, "A dual function of Bcl11b/Ctip2 in hippocampal neurogenesis," *The EMBO Journal*, vol. 31, no. 13, pp. 2922–2936, 2012.

[251] B. Chen, S. S. Wang, A. M. Hattox, H. Rayburn, S. B. Nelson, and S. K. McConnell, "The Fezf2-Ctip2 genetic pathway regulates the fate choice of subcortical projection neurons in the

developing cerebral cortex," *Proceedings of the National Academy of Sciences*, vol. 105, no. 32, pp. 11382–11387, 2008.

[252] R. Simon, L. Baumann, J. Fischer, F. A. Seigfried, E. De Bruyckere, P. Liu, N. A. Jenkins, N. G. Copeland, H. Schwegler, and S. Britsch, "Structure-function integrity of the adult hippocampus depends on the transcription factor Bcl11b/Ctip2," *Genes, Brain and Behaviour*, vol. 15, no. 4, pp. 405–419, 2016.

[253] B. Tang, P. Di Lena, L. Schaffer, S. R. Head, P. Baldi, and E. A. Thomas, "Genome-wide identification of Bcl11b gene targets reveals role in brain-derived neurotrophic factor signaling," *PLoS ONE*, vol. 6, no. 9, p. e23691, 2011.

[254] O. Golonzhka, X. Liang, N. Messaddeq, J. M. Bornert, A. L. Campbell, D. Metzger, P. Chambon, G. Ganguli-Indra, M. Leid, and A. K. Indra, "Dual role of COUP-TF-interacting protein 2 in epidermal homeostasis and permeability barrier formation," *Journal of Investigative Dermatology*, vol. 129, no. 6, pp. 1459–1470, 2009.

[255] Z. Wang, L. J. Zhang, G. Guha, S. Li, K. Kyrylkova, C. Kioussi, M. Leid, G. Ganguli-Indra, and A. K. Indra, "Selective ablation of Ctip2/Bcl11b in epidermal keratinocytes triggers atopic dermatitis-like skin inflammatory responses in adult mice," *PLoS ONE*, vol. 7, no. 12, p. e51262, 2012.

[256] G. Ganguli-Indra, X. Liang, S. Hyter, M. Leid, J. Hanifin, and A. K. Indra, "Expression of COUP-TF-interacting protein 2 (CTIP2) in human atopic dermatitis and allergic contact dermatitis skin," *Experimental Dermatology*, vol. 18, no. 11, pp. 994–996, 2009.

[257] S. Bhattacharya, S. Li, H. Wheeler, R. Wang, C. V. Lohr, M. Leid, G. Ganguli-Indra, and A. K. Indra, "Ablation of Ctip2/Bcl11b in Adult Epidermis Enhances TPA/UV-Induced Proliferation and Increases Susceptibility to DMBA/TPA-Induced Epidermal Carcinogenesis," *Journal of Investigative Dermatology*, vol. 137, no. 7, pp. 1594–1598, 2017.

[258] Y. D. Zhang, Z. Chen, Y. Q. Song, C. Liu, and Y. P. Chen, "Making a tooth: growth factors, transcription factors, and stem cells," *Cell Research*, vol. 15, no. 5, pp. 301–316, 2005.

[259] K. Kyrylkova, S. Kyryachenko, B. Biehs, O. Klein, C. Kioussi, and M. Leid, "BCL11B regulates epithelial proliferation and asymmetric development of the mouse mandibular incisor," *PLoS ONE*, vol. 7, no. 5, p. e37670, 2012.

[260] Y. Katsuragi, J. Anraku, M. Nakatomi, H. Ida-Yonemochi, M. Obata, Y. Mishima, Y. Sakuraba, Y. Gondo, Y. Kodama, A. Nishikawa, R. Takagi, H. Ohshima, and R. Kominami, "Bcl11b transcription factor plays a role in the maintenance of the ameloblast-progenitors in mouse adult maxillary incisors," *Mechanisms of Development*, vol. 130, no. 9-10, pp. 482–492, 2013.

[261] Z. Li, G. Chen, Y. Yang, W. Guo, and W. Tian, "Bcl11b regulates enamel matrix protein expression and dental epithelial cell differentiation during rat tooth development," *Molecular Medicine Reports*, vol. 15, no. 1, pp. 297–304, 2017.

[262] J. Inoue, Y. Ihara, D. Tsukamoto, K. Yasumoto, T. Hashidume, K. Kamimura, S. Hirano, M. Shimizu, R. Kominami, and R. Sato, "BCL11B gene heterozygosity causes weight loss accompanied by increased energy consumption, but not defective adipogenesis, in mice," *Bioscience, Biotechnology, and Biochemistry*, vol. 81, no. 5, pp. 922–930, 2017.

[263] K. Kamimura, H. Ohi, T. Kubota, K. Okazuka, Y. Yoshikai, Y. Wakabayashi, Y. Aoyagi, Y. Mishima, and R. Kominami, "Haploinsufficiency of Bcl11b for suppression of lymphomagenesis and thymocyte development," *Biochemical and Biophysical Research Communications*, vol. 355, no. 2, pp. 538–542, 2007.

[264] K. De Keersmaecker, P. J. Real, G. D. Gatta, T. Palomero, M. L. Sulis, V. Tosello, P. Van Vlierberghe, K. Barnes, M. Castillo, X. Sole, M. Hadler, J. Lenz, P. D. Aplan, M. Kelliher, B. L. Kee, P. P. Pandolfi, D. Kappes, F. Gounari, H. Petrie, J. der Meulen, F. Speleman, E. Paietta, J. Racevskis, P. H. Wiernik, J. M. Rowe, J. Soulier, D. Avran, H. Cavé, N. Dastugue, S. Raimondi, J. P. Meijerink, C. Cordon-Cardo, A. Califano, and A. A. Ferrando, "The TLX1 oncogene drives aneuploidy in T cell transformation," *Nature Medicine*, vol. 16, no. 11, pp. 1321–1327, 2010.

[265] Y. Yoshikai, T. Sato, S. Morita, Y. Kohara, R. Takagi, Y. Mishima, and R. Kominami, "Effect of Bcl11b genotypes and gamma-radiation on the development of mouse thymic lymphomas," *Biochemical and Biophysical Research Communications*, vol. 373, no. 2, pp. 282–285, 2008.

[266] A. Sakamaki, Y. Katsuragi, K. Otsuka, M. Tomita, M. Obata, T. Iwasaki, M. Abe, T. Sato, M. Ochiai, Y. Sakuraba, Y. Aoyagi, Y. Gondo, K. Sakimura, H. Nakagama, Y. Mishima, and R. Kominami, "Bcl11b SWI/SNF-complex subunit modulates intestinal adenoma and regeneration after γ-irradiation through Wnt/β-catenin pathway," *Carcinogenesis*, vol. 36, no. 6, pp. 622–631, 2015.

[267] A. Gutierrez, A. Kentsis, T. Sanda, L. Holmfeldt, S. C. Chen, J. Zhang, A. Protopopov, L. Chin, S. E. Dahlberg, D. S. Neuberg, L. B. Silverman, S. S. Winter, S. P. Hunger, S. E. Sallan, S. Zha,

F. W. Alt, J. R. Downing, C. G. Mullighan, and A. T. Look, "The BCL11B tumor suppressor is mutated across the major molecular subtypes of T-cell acute lymphoblastic leukemia," *Blood*, vol. 118, no. 15, pp. 4169–4173, 2011.

[268] G. K. Przybylski, W. A. Dik, J. Wanzeck, P. Grabarczyk, S. Majunke, J. I. Martin-Subero, R. Siebert, G. Dölken, W. D. Ludwig, B. Verhaaf, J. J. van Dongen, C. A. Schmidt, and A. W. Langerak, "Disruption of the BCL11B gene through inv(14)(q11.2q32.31) results in the expression of BCL11B-TRDC fusion transcripts and is associated with the absence of wild-type BCL11B transcripts in T-ALL," *Leukemia*, vol. 19, no. 2, pp. 201–208, 2005.

[269] V. Bezrookove, S. L. van Zelderen-Bhola, A. Brink, K. Szuhai, A. K. Raap, R. Barge, G. C. Beverstock, and C. Rosenberg, "A novel t(6;14)(q25-q27;q32) in acute myelocytic leukemia involves the BCL11B gene," *Cancer Genetics and Cytogenetics*, vol. 149, no. 1, pp. 72–76, 2004.

[270] S. Torkildsen, L. Gorunova, K. Beiske, G. E. Tjønnfjord, S. Heim, and I. Panagopoulos, "Novel ZEB2-BCL11B fusion gene identified by RNA-sequencing in acute myeloid leukemia with t(2;14)(q22;q32)," *PLoS ONE*, vol. 10, no. 7, p. e0132736, 2015.

[271] J. R. Batanian, C. H. Dunphy, G. Gale, and N. Havlioglu, "Is t(6;14) a non-random translocation in childhood acute mixed lineage leukemia?," *Cancer Genetics and Cytogenetics*, vol. 90, no. 1, pp. 29–32, 1996.

[272] S. C. Raimondi, D. K. Kalwinsky, Y. Hayashi, F. G. Behm, J. Mirro, and D. L. Williams, "Cytogenetics of childhood acute nonlymphocytic leukemia," *Cancer Genetics and Cytogenetics*, vol. 40, no. 1, pp. 13–27, 1989.

[273] X. Huang, S. Chen, Q. Shen, L. Yang, P. Grabarczyk, G. K. Przybylski, C. A. Schmidt, and Y. Li, "Down regulation of BCL11B expression inhibits proliferation and induces apoptosis in malignant T cells by BCL11B-935-siRNA," *Hematology*, vol. 16, no. 4, pp. 236–242, 2011.

[274] B. W. Kunkle, J. Jaworski, S. Barral, B. Vardarajan, G. W. Beecham, E. R. Martin, L. S. Cantwell, A. Partch, T. D. Bird, W. H. Raskind, A. L. DeStefano, R. M. Carney, M. Cuccaro, J. M. Vance, L. A. Farrer, A. M. Goate, T. Foroud, R. P. Mayeux, G. D. Schellenberg, J. L. Haines, and M. A. Pericak-Vance, "Genome-wide linkage analyses of non-Hispanic white families identify novel loci for familial late-onset Alzheimer's disease," *Alzheimers and Dementia*, vol. 12, no. 1, pp. 2–10, 2016.

[275] B. Connor, D. Young, Q. Yan, R. L. Faull, B. Synek, and M. Dragunow, "Brain-derived neurotrophic factor is reduced in Alzheimer's disease," *Molecular Brain Research*, vol. 49, no. 1-2, pp. 71–81, 1997.

[276] P. A. Desplats, J. R. Lambert, and E. A. Thomas, "Functional roles for the striatal-enriched transcription factor, Bcl11b, in the control of striatal gene expression and transcriptional dysregulation in Huntington's disease," *Neurobiology of Diseases*, vol. 31, no. 3, pp. 298–308, 2008.

[277] I. Ahmed, J. I. Sbodio, M. M. Harraz, R. Tyagi, J. C. Grima, L. K. Albacarys, M. E. Hubbi, R. Xu, S. Kim, B. D. Paul, and S. H. Snyder, "Huntington's disease: Neural dysfunction linked to inositol polyphosphate multikinase," *Proceedings of the National Academy of Sciences*, vol. 112, no. 31, pp. 9751–9756, 2015.

[278] D. Punwani, Y. Zhang, J. Yu, M. J. Cowan, S. Rana, A. Kwan, A. N. Adhikari, C. O. Lizama, B. A. Mendelsohn, S. P. Fahl, A. Chellappan, R. Srinivasan, S. E. Brenner, D. L. Wiest, and J. M. Puck, "Multisystem Anomalies in Severe Combined Immunodeficiency with Mutant BCL11B," *New England Journal of Medicine*, vol. 375, no. 22, pp. 2165–2176, 2016.

[279] L. R. You, F. J. Lin, C. T. Lee, F. J. DeMayo, M. J. Tsai, and S. Y. Tsai, "Suppression of Notch signalling by the COUP-TFII transcription factor regulates vein identity," *Nature*, vol. 435, no. 7038, pp. 98–104, 2005.

[280] V. B. Cismasiu, J. Duque, E. Paskaleva, D. Califano, S. Ghanta, H. A. Young, and D. Avram, "BCL11B enhances TCR/CD28-triggered NF-kappaB activation through up-regulation of Cot kinase gene expression in T-lymphocytes," *Biochemical Journal*, vol. 417, no. 2, pp. 457–466, 2009.

[281] A. Topark-Ngarm, O. Golonzhka, V. J. Peterson, B. Barrett, B. Martinez, K. Crofoot, T. M. Filtz, and M. Leid, "CTIP2 associates with the NuRD complex on the promoter of p57KIP2, a newly identified CTIP2 target gene," *Journal of Biological Chemistry*, vol. 281, no. 43, pp. 32272–32283, 2006.

[282] S. Chen, X. Huang, L. Yang, Q. Shen, H. Zheng, B. Li, P. Grabarczyk, G. K. Przybylski, C. A. Schmidt, and Y. Li, "The role of BCL11B in regulating the proliferation of human naive T cells," *Human Immunology*, vol. 73, no. 5, pp. 456–464, 2012.

[283] S. Cai, T. Kalisky, D. Sahoo, P. Dalerba, W. Feng, Y. Lin, D. Qian, A. Kong, J. Yu, F. Wang, E. Y. Chen, F. A. Scheeren, A. H. Kuo, S. S. Sikandar, S. Hisamori, L. J. van Weele, D. Heiser, S. Sim,

J. Lam, S. Quake, and M. F. Clarke, "A Quiescent Bcl11b High Stem Cell Population Is Required for Maintenance of the Mammary Gland," *Cell Stem Cell*, vol. 20, no. 2, pp. 247–260.e5, 2017.

[284] N. J. McCarthy and M. R. Bennett, "The regulation of vascular smooth muscle cell apoptosis," *Cardiovascular Research*, vol. 45, no. 3, pp. 747–755, 2000.

[285] X. Chen, C. C. Yan, X. Zhang, and Z. H. You, "Long non-coding RNAs and complex diseases: from experimental results to computational models," *Briefings in Bioinformatics*, vol. 18, no. 4, pp. 558–576, 2016.

[286] A. Saxena and P. Carninci, "Long non-coding RNA modifies chromatin: epigenetic silencing by long non-coding RNAs," *Bioessays*, vol. 33, no. 11, pp. 830–839, 2011.

[287] P. Grote and B. G. Herrmann, "The long non-coding RNA Fendrr links epigenetic control mechanisms to gene regulatory networks in mammalian embryogenesis," *RNA Biology*, vol. 10, no. 10, pp. 1579–1585, 2013.

[288] Z. Chen, J. L. Li, S. Lin, C. Cao, N. T. Gimbrone, R. Yang, D. A. Fu, M. B. Carper, E. B. Haura, M. B. Schabath, J. Lu, A. L. Amelio, W. D. Cress, F. J. Kaye, and L. Wu, "cAMP/CREB-regulated LINC00473 marks LKB1-inactivated lung cancer and mediates tumor growth," *Journal of Clinical Investigation*, vol. 126, no. 6, pp. 2267–2279, 2016.

[289] S. Y. Li and K. Susztak, "The long noncoding RNA Tug1 connects metabolic changes with kidney disease in podocytes," *Journal of Clinical Investigation*, vol. 126, no. 11, pp. 4072–4075, 2016.

[290] L. Korostowski, N. Sedlak, and N. Engel, "The Kcnq1ot1 long non-coding RNA affects chromatin conformation and expression of Kcnq1, but does not regulate its imprinting in the developing heart," *PLoS Genetics*, vol. 8, no. 9, p. e1002956, 2012.

[291] P. Han, W. Li, C. H. Lin, J. Yang, C. Shang, S. T. Nuernberg, K. K. Jin, W. Xu, C. Y. Lin, C. J. Lin, Y. Xiong, H. Chien, B. Zhou, E. Ashley, D. Bernstein, P. S. Chen, H. V. Chen, T. Quertermous, and C. P. Chang, "A long noncoding RNA protects the heart from pathological hypertrophy," *Nature*, vol. 514, no. 7520, pp. 102–106, 2014.

[292] N. M. White, C. R. Cabanski, J. M. Silva-Fisher, H. X. Dang, R. Govindan, and C. A. Maher, "Transcriptome sequencing reveals altered long intergenic non-coding RNAs in lung cancer," *Genome Biology*, vol. 15, no. 8, p. 429, 2014.

[293] J. Long, S. S. Badal, Z. Ye, Y. Wang, B. A. Ayanga, D. L. Galvan, N. H. Green, B. H. Chang, P. A. Overbeek, and F. R. Danesh, "Long noncoding RNA Tug1 regulates mitochondrial bioenergetics in diabetic nephropathy," *Journal of Clinical Investigation*, vol. 126, no. 11, pp. 4205–4218, 2016.

[294] P. Grote, L. Wittler, D. Hendrix, F. Koch, S. Währisch, A. Beisaw, K. Macura, G. Bläss, M. Kellis, M. Werber, and B. G. Herrmann, "The tissue-specific lncRNA Fendrr is an essential regulator of heart and body wall development in the mouse," *Developmental Cell*, vol. 24, no. 2, pp. 206–214, 2013.

[295] M. A. Faghihi, F. Modarresi, A. M. Khalil, D. E. Wood, B. G. Sahagan, T. E. Morgan, C. E. Finch, G. St Laurent, P. J. Kenny, and C. Wahlestedt, "Expression of a noncoding RNA is elevated in Alzheimer's disease and drives rapid feed-forward regulation of beta-secretase," *Nature Medicine*, vol. 14, no. 7, pp. 723–730, 2008.

[296] E. Pasmant, A. Sabbagh, M. Vidaud, and I. Bièche, "ANRIL, a long, noncoding RNA, is an unexpected major hotspot in GWAS," *FASEB Journal*, vol. 25, no. 2, pp. 444–448, 2011.

[297] Q. Zhang, C. Y. Chen, V. S. Yedavalli, and K. T. Jeang, "NEAT1 long noncoding RNA and paraspeckle bodies modulate HIV-1 posttranscriptional expression," *MBio*, vol. 4, no. 1, pp. e00596–12, 2013.

[298] S. Chung, H. Nakagawa, M. Uemura, L. Piao, K. Ashikawa, N. Hosono, R. Takata, S. Akamatsu, T. Kawaguchi, T. Morizono, T. Tsunoda, Y. Daigo, K. Matsuda, N. Kamatani, Y. Nakamura, and M. Kubo, "Association of a novel long non-coding RNA in 8q24 with prostate cancer susceptibility," *Cancer Science*, vol. 102, no. 1, pp. 245–252, 2011.

[299] J. Jendrzejewski, H. He, H. S. Radomska, W. Li, J. Tomsic, S. Liyanarachchi, R. V. Davuluri, R. Nagy, and A. de la Chapelle, "The polymorphism rs944289 predisposes to papillary thyroid carcinoma through a large intergenic noncoding RNA gene of tumor suppressor type," *Proceedings of the National Academy of Sciences*, vol. 109, no. 22, pp. 8646–8651, 2012.

[300] X. Zhang, L. Zhou, G. Fu, F. Sun, J. Shi, J. Wei, C. Lu, C. Zhou, Q. Yuan, and M. Yang, "The identification of an ESCC susceptibility SNP rs920778 that regulates the expression of lncRNA HOTAIR via a novel intronic enhancer," *Carcinogenesis*, vol. 35, no. 9, pp. 2062–2067, 2014.

[301] A. Castellanos-Rubio, N. Fernandez-Jimenez, R. Kratchmarov, X. Luo, G. Bhagat, P. H. Green, R. Schneider, M. Kiledjian, J. R. Bilbao, and S. Ghosh, "A long noncoding RNA associated with susceptibility to celiac disease," *Science*, vol. 352, no. 6281, pp. 91–95, 2016.

[302] N. Jariwala and D. Sarkar, "Emerging role of lncRNA in cancer: a potential avenue in molecular medicine," *Annals of Translational Medicine*, vol. 4, no. 15, p. 286, 2016.

[303] W. T. Godbey, K. K. Wu, and A. G. Mikos, "Poly(ethylenimine) and its role in gene delivery," *Journal of Controlled Release*, vol. 60, no. 2-3, pp. 149–160, 1999.

[304] D. Latorra, K. Arar, and J. M. Hurley, "Design considerations and effects of LNA in PCR primers," *Molecular and Cellular Probes*, vol. 17, no. 5, pp. 253–259, 2003.

[305] R. V. f. A. S. Collaboration, "Determinants of pulse wave velocity in healthy people and in the presence of cardiovascular risk factors: 'establishing normal and reference values'," *European Heart Journal*, vol. 31, no. 19, pp. 2338–2350, 2010.

[306] A. P. Avolio, S. G. Chen, R. P. Wang, C. L. Zhang, M. F. Li, and M. F. O'Rourke, "Effects of aging on changing arterial compliance and left ventricular load in a northern Chinese urban community," *Circulation*, vol. 68, no. 1, pp. 50–58, 1983.

[307] R. Virmani, A. P. Avolio, W. J. Mergner, M. Robinowitz, E. E. Herderick, J. F. Cornhill, S. Y. Guo, T. H. Liu, D. Y. Ou, and M. O'Rourke, "Effect of aging on aortic morphology in populations with high and low prevalence of hypertension and atherosclerosis. Comparison between occidental and Chinese communities," *American Journal of Pathology*, vol. 139, no. 5, pp. 1119–1129, 1991.

[308] W. H. Pearce, M. S. Slaughter, S. LeMaire, A. N. Salyapongse, J. Feinglass, W. J. McCarthy, and J. S. Yao, "Aortic diameter as a function of age, gender, and body surface area," *Surgery*, vol. 114, no. 4, pp. 691–697, 1993.

[309] L. Jia, G. Landan, M. Pomerantz, R. Jaschek, P. Herman, D. Reich, C. Yan, O. Khalid, P. Kantoff, W. Oh, J. R. Manak, B. P. Berman, B. E. Henderson, B. Frenkel, C. A. Haiman, M. Freedman, A. Tanay, and G. A. Coetzee, "Functional enhancers at the gene-poor 8q24 cancer-linked locus," *PLoS Genetics*, vol. 5, no. 8, p. e1000597, 2009.

[310] O. Harismendy, D. Notani, X. Song, N. G. Rahim, B. Tanasa, N. Heintzman, B. Ren, X. D. Fu, E. J. Topol, M. G. Rosenfeld, and K. A. Frazer, "9p21 DNA variants associated with coronary artery disease impair interferon-γ signalling response," *Nature*, vol. 470, no. 7333, pp. 264–268, 2011.

[311] N. Ahmadiyeh, M. M. Pomerantz, C. Grisanzio, P. Herman, L. Jia, V. Almendro, H. H. He, M. Brown, X. S. Liu, M. Davis, J. L. Caswell, C. A. Beckwith, A. Hills, L. Macconaill, G. A.

Coetzee, M. M. Regan, and M. L. Freedman, "8q24 prostate, breast, and colon cancer risk loci show tissue-specific long-range interaction with MYC," *Proceedings of the National Academy of Sciences*, vol. 107, no. 21, pp. 9742–9746, 2010.

[312] F. Innocenti, G. M. Cooper, I. B. Stanaway, E. R. Gamazon, J. D. Smith, S. Mirkov, J. Ramirez, W. Liu, Y. S. Lin, C. Moloney, S. F. Aldred, N. D. Trinklein, E. Schuetz, D. A. Nickerson, K. E. Thummel, M. J. Rieder, A. E. Rettie, M. J. Ratain, N. J. Cox, and C. D. Brown, "Identification, replication, and functional fine-mapping of expression quantitative trait loci in primary human liver tissue," *PLoS Genetics*, vol. 7, no. 5, p. e1002078, 2011.

[313] W. G. McMaster, A. Kirabo, M. S. Madhur, and D. G. Harrison, "Inflammation, immunity, and hypertensive end-organ damage," *Circulation Research*, vol. 116, no. 6, pp. 1022–1033, 2015.

[314] P. Desplats, W. Dumaop, D. Smith, A. Adame, I. Everall, S. Letendre, R. Ellis, M. Cherner, I. Grant, and E. Masliah, "Molecular and pathologic insights from latent HIV-1 infection in the human brain," *Neurology*, vol. 80, no. 15, pp. 1415–1423, 2013.

[315] F. M. Vega, A. Sevilla, and P. A. Lazo, "p53 Stabilization and accumulation induced by human vaccinia-related kinase 1," *Molecular and Cellular Biology*, vol. 24, no. 23, pp. 10366–10380, 2004.

[316] I. López-Sánchez, A. Valbuena, M. Vázquez-Cedeira, J. Khadake, M. Sanz-García, A. Carrillo-Jiménez, and P. A. Lazo, "VRK1 interacts with p53 forming a basal complex that is activated by UV-induced DNA damage," *FEBS Letters*, vol. 588, no. 5, pp. 692–700, 2014.

[317] D. Gomez, K. Kessler, J. B. Michel, and R. Vranckx, "Modifications of chromatin dynamics control Smad2 pathway activation in aneurysmal smooth muscle cells," *Circulation Research*, vol. 113, no. 7, pp. 881–890, 2013.

[318] C. Ihling, T. Szombathy, K. Nampoothiri, J. Haendeler, F. Beyersdorf, M. Uhl, A. M. Zeiher, and H. E. Schaefer, "Cystic medial degeneration of the aorta is associated with p53 accumulation, Bax upregulation, apoptotic cell death, and cell proliferation," *Heart*, vol. 82, no. 3, pp. 286–293, 1999.

[319] Y. Wang, B. Zhang, L. Zhang, L. An, J. Xu, D. Li, M. N. K. Choudhary, Y. Li, M. Hu, R. Hardison, T. Wang, and F. Yue, "The 3D Genome Browser: a web-based browser for visualizing 3D genome organization and long-range chromatin interactions," *bioRxiv*, 2017.

[320] Y. Yang, L. Wen, and H. Zhu, "Unveiling the hidden function of long non-coding RNA by identifying its major partner-protein," *Cell Biosciences*, vol. 5, p. 59, 2015.

[321] E. J. Hennessy, "Cardiovascular Disease and Long Noncoding RNAs: Tools for Unraveling the Mystery Lnc-ing RNA and Phenotype," *Circulation: Cardiovascular Genetics*, vol. 10, no. 4, p. e001556, 2017.

[322] A. N. Lyle and U. Raaz, "Killing me unsoftly: Causes and mechanisms of arterial stiffness," *Arteriosclerosis, Thrombosis, and Vascular Biology*, vol. 37, no. 2, pp. e1–e11, 2017.

[323] K. Ding and I. J. Kullo, "Methods for the selection of tagging SNPs: a comparison of tagging efficiency and performance," *European Journal of Human Genetics*, vol. 15, no. 2, pp. 228–36, 2007.

[324] R. V. Iozzo and L. Schaefer, "Proteoglycan form and function: A comprehensive nomenclature of proteoglycans," *Matrix Biology*, vol. 42, pp. 11–55, 2015.

[325] H. Watanabe, L. Gao, S. Sugiyama, K. Doege, K. Kimata, and Y. Yamada, "Mouse aggrecan, a large cartilage proteoglycan: protein sequence, gene structure and promoter sequence," *The Biochemical Journal*, vol. 308 (Pt 2), pp. 433–440, 1995.

[326] Y. Huang, E. B. Askew, C. B. Knudson, and W. Knudson, "CRISPR/Cas9 knockout of HAS2 in rat chondrosarcoma chondrocytes demonstrates the requirement of hyaluronan for aggrecan retention," *Matrix Biology*, vol. 56, pp. 74–94, 2016.

[327] K. J. Doege, M. Sasaki, T. Kimura, and Y. Yamada, "Complete coding sequence and deduced primary structure of the human cartilage large aggregating proteoglycan, aggrecan. Human-specific repeats, and additional alternatively spliced forms," *Journal of Biological Chemistry*, vol. 266, no. 2, pp. 894–902, 1991.

[328] J. Dudhia, "Aggrecan, aging and assembly in articular cartilage," *Cellular and Molecular Life Sciences*, vol. 62, no. 19-20, pp. 2241–2256, 2005.

[329] E. Arciniegas, C. Y. Neves, D. Candelle, and D. Parada, "Differential versican isoforms and aggrecan expression in the chicken embryo aorta," *The Anatomical Record Part A Discoveries in Molecular Cellular and Evolutionary Biology*, vol. 279, no. 1, pp. 592–600, 2004.

[330] H. Watanabe, S. C. Cheung, N. Itano, K. Kimata, and Y. Yamada, "Identification of hyaluronan-binding domains of aggrecan," *Journal of Biological Chemistry*, vol. 272, no. 44, pp. 28057–28065, 1997.

[331] K. Matsumoto, M. Shionyu, M. Go, K. Shimizu, T. Shinomura, K. Kimata, and H. Watanabe, "Distinct Interaction of Versican/PG-M with Hyaluronan and Link Protein," *Journal of Biological Chemistry*, vol. 278, no. 42, pp. 41205–41212, 2003.

[332] C. Kiani, V. Lee, L. Cao, L. Chen, Y. Wu, Y. Zhang, M. E. Adams, and B. B. Yang, "Roles of aggrecan domains in biosynthesis, modification by glycosaminoglycans and product secretion.," *The Biochemical Journal*, vol. 354, pp. 199–207, 2001.

[333] A. Aspberg, "The versican C-type lectin domain recognizes the adhesion protein tenascin-R," *Proceedings of the National Academy of Sciences*, vol. 92, no. November, pp. 10590–10594, 1995.

[334] A. Aspberg, S. Adam, G. Kostka, R. Timpl, and D. Heinegard, "Fibulin-1 is a ligand for the C-type lectin domains of aggrecan and versican," *Journal of Biological Chemistry*, vol. 274, no. 29, pp. 20444–20449, 1999.

[335] A. I. Olin, M. Mörgelin, T. Sasaki, R. Timpl, D. Heinegård, and A. Aspberg, "The proteoglycans aggrecan and versican form networks with fibulin-2 through their lectin domain binding," *Journal of Biological Chemistry*, vol. 276, no. 2, pp. 1253–1261, 2001.

[336] Z. Isogai, A. Aspberg, D. R. Keene, R. N. Ono, D. P. Reinhardt, and L. Y. Sakai, "Versican interacts with fibrillin-1 and links extracellular microfibrils to other connective tissue networks," *Journal of Biological Chemistry*, vol. 277, no. 6, pp. 4565–4572, 2002.

[337] S. Saleque, N. Ruiz, and K. Drickamer, "Expression and characterization of a carbohydrate-binding fragment of rat aggrecan," *Glycobiology*, vol. 3, no. 2, pp. 185–190, 1993.

[338] R. Miura, A. Aspberg, I. M. Ethell, K. Hagihara, R. L. Schnaar, E. Ruoslahti, and Y. Yamaguchi, "The proteoglycan lectin domain binds sulfated cell surface glycolipids and promotes cell adhesion," *Journal of Biological Chemistry*, vol. 274, no. 16, pp. 11431–11438, 1999.

[339] C. Fülöp, E. Walcz, M. Valyon, and T. T. Glant, "Expression of alternatively spliced epidermal growth factor-like domains in aggrecans of different species: Evidence for a novel module," *Journal of Biological Chemistry*, vol. 268, no. 23, pp. 17377–17383, 1993.

[340] J. M. Day, A. I. Olin, A. D. Murdoch, A. Canfield, T. Sasaki, R. Timpl, T. E. Hardingham, and A. Aspberg, "Alternative Splicing in the Aggrecan G3 Domain Influences Binding Interactions with Tenascin-C and Other Extracellular Matrix Proteins," *Journal of Biological Chemistry*, vol. 279, no. 13, pp. 12511–12518, 2004.

[341] T. E. Hardingham and A. J. Fosang, "The structure of aggrecan and its turnover in cartilage," *Journal of Rheumatology*, vol. 22, no. 43, pp. 86–90, 1995.

[342] J. S. Mort, M. C. Magny, and E. R. Lee, "Cathepsin B: an alternative protease for the generation of an aggrecan 'metalloproteinase' cleavage neoepitope.," *The Biochemical Journal*, vol. 335 (Pt 3), pp. 491–494, 1998.

[343] C. B. Little, C. T. Meeker, S. B. Golub, K. E. Lawlor, P. J. Farmer, S. M. Smith, and A. J. Fosang, "Blocking aggrecanase cleavage in the aggrecan interglobular domain abrogates cartilage erosion and promotes cartilage repair," *Journal of Clinical Investigation*, vol. 117, no. 6, pp. 1627–1636, 2007.

[344] C. Kiani, L. Chen, Y. J. Wu, A. J. Yee, and B. B. Yang, "Structure and function of aggrecan," *Cell Research*, vol. 12, no. 1, pp. 19–32, 2002.

[345] P. J. Roughley and E. R. Lee, "Cartilage proteoglycans: Structure and potential functions," *Microscopy Research and Technique*, vol. 28, no. 5, pp. 385–397, 1994.

[346] S. Miyata and H. Kitagawa, "Chondroitin 6-Sulfation Regulates Perineuronal Net Formation by Controlling the Stability of Aggrecan," *Neural Plasticity*, vol. 2016, p. 1305801, 2016.

[347] R. D. Young, E. C. Gealy, M. Liles, B. Caterson, J. R. Ralphs, and A. J. Quantock, "Keratan sulfate glycosaminoglycan and the association with collagen fibrils in rudimentary lamellae in the developing avian cornea," *Investigative Ophthalmology and Visual Science*, vol. 48, no. 7, pp. 3083–3088, 2007.

[348] H. Hedlund, E. Hedbom, D. Heinegård, S. Mengarelli-Widholm, F. P. Reinholt, and O. Svensson, "Association of the aggrecan keratan sulfate-rich region with collagen in bovine articular cartilage," *Journal of Biological Chemistry*, vol. 274, no. 9, pp. 5777–5781, 1999.

[349] P. J. Roughley, R. J. White, and T. T. Glant, "The structure and abundance of cartilage proteoglycans during early development of the human fetus," *Pediatric Research*, vol. 22, no. 4, pp. 409–413, 1987.

[350] a. Maroudas, M. T. Bayliss, N. Uchitel-Kaushansky, R. Schneiderman, and E. Gilav, "Aggrecan turnover in human articular cartilage: use of aspartic acid racemization as a marker of molecular age," *Archives of Biochemistry and Biophysics*, vol. 350, no. 1, pp. 61–71, 1998.

[351] S. S. Sivan, E. Tsitron, E. Wachtel, P. J. Roughley, N. Sakkee, F. Van Der Ham, J. DeGroot, S. Roberts, and A. Maroudas, "Aggrecan turnover in human intervertebral disc as determined

by the racemization of aspartic acid," *Journal of Biological Chemistry*, vol. 281, no. 19, pp. 13009–13014, 2006.

[352] M. C. Bolton, J. Dudhia, and M. T. Bayliss, "Age-related changes in the synthesis of link protein and aggrecan in human articular cartilage: implications for aggregate stability," *Biochemical Journal*, vol. 337 (Pt 1), pp. 77–82, 1999.

[353] G. Verbruggen, M. Cornelissen, K. F. Almqvist, L. Wang, D. Elewaut, C. Broddelez, L. de Ridder, and E. M. Veys, "Influence of aging on the synthesis and morphology of the aggrecans synthesized by differentiated human articular chondrocytes," *Osteoarthritis and Cartilage*, vol. 8, no. 3, pp. 170–179, 2000.

[354] M. T. Bayliss, S. Howat, C. Davidson, and J. Dudhia, "The organization of aggrecan in human articular cartilage. Evidence for age-related changes in the rate of aggregation of newly synthesized molecules," *Journal of Biological Chemistry*, vol. 275, no. 9, pp. 6321–6327, 2000.

[355] K. Yokosuka, J. S. Park, K. Jimbo, K. Yamada, K. Sato, M. Tsuru, M. Takeuchi, S.-I. Yamagishi, and K. Nagata, "Advanced glycation end-products downregulating intervertebral disc cell production of proteoglycans in vitro," *Journal of Neurosurgery: Spine*, vol. 5, no. 4, pp. 324–329, 2006.

[356] P. A. C. Cloos and S. Christgau, "Non-enzymatic covalent modifications of proteins: Mechanisms, physiological consequences and clinical applications," *Matrix Biology*, vol. 21, no. 1, pp. 39–52, 2002.

[357] C. R. Flannery, M. W. Lark, and J. D. Sandy, "Identification of a stromelysin cleavage site within the interglobular domain of human aggrecan: Evidence for proteolysis at this site in vivo in human articular cartilage," *Journal of Biological Chemistry*, vol. 267, no. 2, pp. 1008–1014, 1992.

[358] A. J. Fosang, P. J. Neame, T. E. Hardingham, G. Murphy, and J. A. Hamilton, "Cleavage of cartilage proteoglycan between G1 and G2 domains by stromelysins," *Journal of Biological Chemistry*, vol. 266, no. 24, pp. 15579–15582, 1991.

[359] A. J. Fosang, P. J. Neame, K. Last, T. E. Hardingham, G. Murphy, and J. A. Hamilton, "The interglobular domain of cartilage aggrecan is cleaved by PUMP, gelatinases, and cathepsin B," *Journal of Biological Chemistry*, vol. 267, no. 27, pp. 19470–19474, 1992.

[360] A. J. Fosang, K. Last, P. J. Neame, G. Murphy, V. Knauper, H. Tschesche, C. E. Hughes, B. Caterson, and T. E. Hardingham, "Neutrophil collagenase (MMP-8) cleaves at the aggrecanase site

E373-A374 in the interglobular domain of cartilage aggrecan," *Biochemical Journal*, vol. 304 (Pt 2, pp. 347–351, 1994.

[361] A. J. Fosang, K. Last, V. Knäuper, G. Murphy, and P. J. Neame, "Degradation of cartilage aggrecan by collagenase 3 (MMP-13)," *FEBS Letters*, vol. 380, no. 1-2, pp. 17–20, 1996.

[362] K. Kuno, Y. Okada, H. Kawashima, H. Nakamura, M. Miyasaka, H. Ohno, and K. Matsushima, "ADAMTS-1 cleaves a cartilage proteoglycan, aggrecan," *FEBS Letters*, vol. 478, no. 3, pp. 241–245, 2000.

[363] L. A. Collins-Racie, C. R. Flannery, W. Zeng, C. Corcoran, B. Annis-Freeman, M. J. Agostino, M. Arai, E. Diblasio-Smith, A. J. Dorner, K. E. Georgiadis, M. Jin, X. Y. Tan, E. A. Morris, and E. R. Lavallie, "ADAMTS-8 exhibits aggrecanase activity and is expressed in human articular cartilage," *Matrix Biology*, vol. 23, no. 4, pp. 219–230, 2004.

[364] W. Zeng, C. Corcoran, L. A. Collins-Racie, E. R. LaVallie, E. A. Morris, and C. R. Flannery, "Glycosaminoglycan-binding properties and aggrecanase activities of truncated ADAMTSs: Comparative analyses with ADAMTS-5, -9, -16 and -18," *Biochimica et Biophysica Acta - General Subjects*, vol. 1760, no. 3, pp. 517–524, 2006.

[365] C. Gendron, M. Kashiwagi, H. L. Ngee, J. J. Enghild, I. B. Thøgersen, C. Hughes, B. Caterson, and H. Nagase, "Proteolytic activities of human ADAMTS-5: Comparative studies with ADAMTS-4," *Journal of Biological Chemistry*, vol. 282, no. 25, pp. 18294–18306, 2007.

[366] M. T. Mok, M. Z. Ilic, C. J. Handley, and H. C. Robinson, "Cleavage of proteoglycan aggregate by leucocyte elastase," *Archives of Biochemistry and Biophysics*, vol. 292, no. 2, pp. 442–447, 1992.

[367] A. Chamberland, E. Wang, A. R. Jones, L. A. Collins-Racie, E. R. LaVallie, Y. Huang, L. Liu, E. A. Morris, C. R. Flannery, and Z. Yang, "Identification of a novel HtrA1-susceptible cleavage site in human aggrecan. Evidence for the involvement of HtrA1 in aggrecan proteolysis in vivo," *Journal of Biological Chemistry*, vol. 284, no. 40, pp. 27352–27359, 2009.

[368] R. Sztrolovics, M. Alini, P. J. Roughley, and J. S. Mort, "Aggrecan degradation in human intervertebral disc and articular cartilage," *The Biochemical Journal*, vol. 326, pp. 235–41, 1997.

[369] T. Wells, C. Davidson, M. Mörgelin, J. L. E. Bird, M. T. Bayliss, and J. Dudhia, "Age-related changes in the composition, the molecular stoichiometry and the stability of proteoglycan aggregates extracted from human articular cartilage.," *The Biochemical Journal*, vol. 370, pp. 69–79, 2003.

[370] M. W. Lark, E. K. Bayne, J. Flanagan, C. F. Harper, L. A. Hoerrner, N. I. Hutchinson, I. I. Singer, S. A. Donatelli, J. R. Weidner, H. R. Williams, R. A. Mumford, and L. S. Lohmander, "Aggrecan degradation in human cartilage: Evidence for both matrix metalloproteinase and aggrecanase activity in normal, osteoarthritic, and rheumatoid joints," *Journal of Clinical Investigation*, vol. 100, no. 1, pp. 93–106, 1997.

[371] E. R. Bastow, K. Last, S. Golub, J. L. Stow, A. C. Stanley, and A. J. Fosang, "Evidence for lysosomal exocytosis and release of aggrecan-degrading hydrolases from hypertrophic chondrocytes, in vitro and in vivo.," *Biology Open*, vol. 1, no. 4, pp. 318–28, 2012.

[372] J. S. Mort, Y. Geng, W. D. Fisher, and P. J. Roughley, "Aggrecan heterogeneity in articular cartilage from patients with osteoarthritis," *BMC Musculoskeletal Disorders*, vol. 17, p. 89, 2016.

[373] M. Z. Ilic, C. J. East, F. M. Rogerson, A. J. Fosang, and C. J. Handley, "Distinguishing aggrecan loss from aggrecan proteolysis in ADAMTS-4 and ADAMTS-5 single and double deficient mice," *Journal of Biological Chemistry*, vol. 282, no. 52, pp. 37420–37428, 2007.

[374] G. M. Brown, T. N. Huckerby, M. T. Bayliss, and I. A. Nieduszynski, "Human aggrecan keratan sulfate undergoes structural changes during adolescent development," *Journal of Biological Chemistry*, vol. 273, no. 41, pp. 26408–26414, 1998.

[375] T. N. Huckerby, I. A. Nieduszynski, M. T. Bayliss, and G. M. Brown, "600 MHz NMR studies of human articular cartilage keratan sulfates," *European Journal of Biochemistry*, vol. 266, no. 3, pp. 1174–1183, 1999.

[376] A. McAlinden, J. Dudhia, M. C. Bolton, P. Lorenzo, D. Heinegård, and M. T. Bayliss, "Age-related changes in the synthesis and mRNA expression of decorin and aggrecan in human meniscus and articular cartilage," *Osteoarthritis Cartilage*, vol. 9, no. 1, pp. 33–41, 2001.

[377] R. E. Wilusz, J. Sanchez-Adams, and F. Guilak, "The structure and function of the pericellular matrix of articular cartilage," *Matrix Biology*, vol. 39, pp. 25–32, 2014.

[378] P. J. Roughley and J. S. Mort, "The role of aggrecan in normal and osteoarthritic cartilage," *Journal of Experimental Orthopaedics*, vol. 1, no. 1, p. 8, 2014.

[379] M. Yang, L. Zhang, J. Stevens, and G. Gibson, "CRISPR/Cas9 mediated generation of stable chondrocyte cell lines with targeted gene knockouts; analysis of an aggrecan knockout cell line," *Bone*, vol. 69, pp. 118–125, 2014.

[380] S. S. Sivan, E. Wachtel, and P. Roughley, "Structure, function, aging and turnover of aggrecan in the intervertebral disc," *Biochimica et Biophysica Acta*, vol. 1840, no. 10, pp. 3181–3189, 2014.

[381] W. E. B. Johnson, B. Caterson, S. M. Eisenstein, and S. Roberts, "Human intervertebral disc aggrecan inhibits endothelial cell adhesion and cell migration in vitro.," *Spine*, vol. 30, no. 10, pp. 1139–1147, 2005.

[382] W. E. B. Johnson, B. Caterson, S. M. Eisenstein, D. L. Hynds, D. M. Snow, and S. Roberts, "Human intervertebral disc aggrecan inhibits nerve growth in vitro.," *Arthritis and Rheumatology*, vol. 46, no. 10, pp. 2658–64, 2002.

[383] M. Valiyaveettil, J. S. Mort, and C. A. McDevitt, "The concentration, gene expression, and spatial distribution of aggrecan in canine articular cartilage, meniscus, and anterior and posterior cruciate ligaments: A new molecular distinction between hyaline cartilage and fibrocartilage in the knee joint," *Connective Tissue Research*, vol. 46, pp. 83–91, jan 2005.

[384] M. S. Domowicz, M. Cortes, J. G. Henry, and N. B. Schwartz, "Aggrecan modulation of growth plate morphogenesis," *Developmental Biology*, vol. 329, no. 2, pp. 242–257, 2009.

[385] S. Byers, J. C. van Rooden, and B. K. Foster, "Structural changes in the large proteoglycan, aggrecan, in different zones of the ovine growth plate," *Calcified Tissue International*, vol. 60, no. 1, pp. 71–78, 1997.

[386] S. Mundlos, R. Meyer, Y. Yamada, and B. Zabel, "Distribution of Cartilage Proteoglycan (Aggrecan) Core Protein and Link Protein Gene Expression during Human Skeletal Development," *Matrix*, vol. 11, no. 5, pp. 339–346, 1991.

[387] D. Virgintino, D. Perissinotto, F. Girolamo, M. T. Mucignat, L. Montanini, M. Errede, T. Kaneiwa, S. Yamada, K. Sugahara, L. Roncali, and R. Perris, "Differential distribution of aggrecan isoforms in perineuronal nets of the human cerebral cortex," *Journal of Cellular and Molecular Medicine*, vol. 13, no. 9 B, pp. 3151–3173, 2009.

[388] M. Morawski, G. Brückner, T. Arendt, and R. T. Matthews, "Aggrecan: Beyond cartilage and into the brain," *International Journal of Biochemistry & Cell Biology*, vol. 44, no. 5, pp. 690–693, 2012.

[389] S. Popp, P. Maurel, J. S. Andersen, and R. U. Margolis, "Developmental changes of aggrecan, versican and neurocan in the retina and optic nerve," *Experimental Eye Research*, vol. 79, no. 3, pp. 351–356, 2004.

[390] P. Milev, P. Maurel, A. Chiba, M. Mevissen, S. Popp, Y. Yamaguchi, R. U. K. Margolis, and R. U. K. Margolis, "Differential regulation of expression of hyaluronan-binding proteoglycans in developing brain: aggrecan, versican, neurocan, and brevican.," *Biochemical and Biophysical Research Communications*, vol. 247, no. 2, pp. 207–212, 1998.

[391] R. T. Matthews, G. M. Kelly, C. a. Zerillo, G. Gray, M. Tiemeyer, and S. Hockfield, "Aggrecan glycoforms contribute to the molecular heterogeneity of perineuronal nets.," *The Journal of Neuroscience*, vol. 22, no. 17, pp. 7536–7547, 2002.

[392] H. Li, M. Domowicz, A. Hennig, and N. B. Schwartz, "S103L reactive chondroitin sulfate proteoglycan (aggrecan) mRNA expressed in developing chick brain and cartilage is encoded by a single gene," *Molecular Brain Research*, vol. 36, no. 2, pp. 309–321, 1996.

[393] A. Suttkus, S. Rohn, S. Weigel, P. Glöckner, T. Arendt, and M. Morawski, "Aggrecan, link protein and tenascin-R are essential components of the perineuronal net to protect neurons against iron-induced oxidative stress," *Cell Death and Disease*, vol. 5, no. 3, p. e1119, 2014.

[394] M. Morawski, G. Brückner, C. Jäger, G. Seeger, and T. Arendt, "Neurons associated with aggrecan-based perineuronal nets are protected against tau pathology in subcortical regions in Alzheimer's disease," *Neuroscience*, vol. 169, no. 3, pp. 1347–1363, 2010.

[395] M. Morawski, M. K. Brückner, P. Riederer, G. Brückner, and T. Arendt, "Perineuronal nets potentially protect against oxidative stress," *Experimental Neurology*, vol. 188, no. 2, pp. 309–315, 2004.

[396] P. a. McRae, M. M. Rocco, G. Kelly, J. C. Brumberg, and R. T. Matthews, "Sensory deprivation alters aggrecan and perineuronal net expression in the mouse barrel cortex," *The Journal of Neuroscience*, vol. 27, no. 20, pp. 5405–5413, 2007.

[397] M. S. Domowicz, D. Mangoura, and N. B. Schwartz, "Aggrecan regulates telencephalic neuronal aggregation in culture," *Developmental Brain Research*, vol. 143, no. 2, pp. 207–216, 2003.

[398] W. Härtig, A. Derouiche, K. Welt, K. Brauer, J. Grosche, M. Mäder, A. Reichenbach, and G. Brückner, "Cortical neurons immunoreactive for the potassium channel Kv3.1b subunit are predominantly surrounded by perineuronal nets presumed as a buffering system for cations," *Brain Research*, vol. 842, no. 1, pp. 15–29, 1999.

[399] M. S. Domowicz, T. A. Sanders, C. W. Ragsdale, and N. B. Schwartz, "Aggrecan is expressed by embryonic brain glia and regulates astrocyte development," *Developmental Biology*, vol. 315, no. 1, pp. 114–124, 2008.

[400] M. W. Lark, E. K. Bayne, and L. S. Lohmander, "Aggrecan degradation in osteoarthritis and rheumatoid arthritis.," *Acta Orthopaedica Scandinavica. Supplementum*, vol. 266, pp. 92–97, 1995.

[401] L. Stefan Lohmander, P. J. Neame, and J. D. Sandy, "The structure of aggrecan fragments in human synovial fluid. evidence that aggrecanase mediates cartilage degradation in inflammatory joint disease, joint injury, and osteoarthritis," *Arthritis and Rheumatism*, vol. 36, no. 9, pp. 1214–1222, 1993.

[402] L. Troeberg and H. Nagase, "Proteases involved in cartilage matrix degradation in osteoarthritis," *Biochimica et Biophysica Acta - Proteins and Proteomics*, vol. 1824, no. 1, pp. 133–145, 2012.

[403] E. Mariani, L. Pulsatelli, and A. Facchini, "Signaling pathways in cartilage repair," *International Journal of Molecular Sciences*, vol. 15, no. 5, pp. 8667–8698, 2014.

[404] A. Hanyecz, T. Bárdos, S. E. Berlo, E. Buzás, A. B. Nesterovitch, K. Mikecz, and T. T. Glant, "Induction of arthritis in SCID mice by T cells specific for the "Shared Epitope" sequence in the G3 domain of human cartilage proteoglycan," *Arthritis and Rheumatism*, vol. 48, no. 10, pp. 2959–2973, 2003.

[405] E. I. Buzás, A. Végvári, Y. M. Murad, A. Finnegan, K. Mikecz, and T. T. Glant, "T-cell recognition of differentially tolerated epitopes of cartilage proteoglycan aggrecan in arthritis," *Cellular Immunology*, vol. 235, no. 2, pp. 98–108, 2005.

[406] T. T. Glant, E. I. Buzás, A. Finnegan, G. Negroiu, G. Cs-Szabó, and K. Mikecz, "Critical roles of glycosaminoglycan side chains of cartilage proteoglycan (aggrecan) in antigen recognition and presentation," *Journal of Immunology*, vol. 160, no. 8, pp. 3812–9, 1998.

[407] A. Hanyecz, K. Olasz, O. Tarjanyi, P. Nemeth, K. Mikecz, T. T. Glant, and F. Boldizsar, "Proteoglycan aggrecan conducting T cell activation and apoptosis in a murine model of rheumatoid arthritis," *BioMed Research International*, vol. 2014, p. 13, 2014.

[408] C. Melin Fürst, M. Mörgelin, K. Vadstrup, D. Heinegård, A. Aspberg, and A. M. Blom, "The C-type lectin of the agrecan G3 domain activates complement," *PLoS ONE*, vol. 8, no. 4, 2013.

[409] A. O. Snorradottir, H. J. Isaksson, S. A. Kaeser, A. A. Skodras, E. Olafsson, A. Palsdottir, and B. T. Bragason, "Deposition of collagen IV and aggrecan in leptomeningeal arteries of hereditary brain haemorrhage with amyloidosis," *Brain Research*, vol. 1535, pp. 106–114, 2013.

[410] Z. Z. Wang, O. Jensson, L. Thorsteinsson, and H. V. Vinters, "Microvascular degeneration in hereditary cystatin C amyloid angiopathy of the brain.," *APMIS*, vol. 105, no. 1, pp. 41–47, 1997.

[411] J. E. Wagenseil and R. P. Mecham, "Vascular Extracellular Matrix and Arterial Mechanics," *Physiological Reviews*, vol. 89, no. 3, pp. 957–989, 2009.

[412] E. U. Azeloglu, M. B. Albro, V. A. Thimmappa, G. A. Ateshian, and K. D. Costa, "Heterogeneous transmural proteoglycan distribution provides a mechanism for regulating residual stresses in the aorta," *The American Journal of Physiology-Heart and Circulatory Physiology*, vol. 294, no. 3, pp. H1197–205, 2008.

[413] V. K. Krishnamurthy, A. N. Evans, J. P. Wansapura, H. Osinska, K. E. Maddy, S. V. Biechler, D. A. Narmoneva, R. L. Goodwin, and R. B. Hinton, "Asymmetric cell-matrix and biomechanical abnormalities in elastin insufficiency induced aortopathy," *Annals of Biomedical Engineering*, vol. 42, no. 10, pp. 2014–2028, 2014.

[414] J. J. Maleszewski, D. V. Miller, J. Lu, H. C. Dietz, and M. K. Halushka, "Histopathologic Findings in Ascending Aortas From Individuals With Loeys-Dietz Syndrome (LDS)," *The American Journal of Surgical Pathology*, vol. 33, pp. 194–201, 2009.

[415] S. Roccabianca, G. A. Ateshian, and J. D. Humphrey, "Biomechanical roles of medial pooling of glycosaminoglycans in thoracic aortic dissection," *Biomechanics and Modeling in Mechanobiology*, vol. 13, no. 1, pp. 13–25, 2014.

[416] P. Talusan, S. Bedri, S. Yang, T. Kattapuram, N. Silva, P. J. Roughley, and J. R. Stone, "Analysis of intimal proteoglycans in atherosclerosis-prone and atherosclerosis-resistant human arteries by mass spectrometry.," *Molecular and Cellular Proteomics*, vol. 4, no. 9, pp. 1350–7, 2005.

[417] M. Fakhry, M. Roszkowska, A. Briolay, C. Bougault, A. Guignandon, J. I. Diaz-Hernandez, M. Diaz-Hernandez, S. Pikula, R. Buchet, E. Hamade, B. Badran, L. Bessueille, and D. Magne, "TNAP stimulates vascular smooth muscle cell trans-differentiation into chondrocytes through calcium deposition and BMP-2 activation: Possible implication in atherosclerotic plaque stability," *Biochimica et Biophysica Acta - Molecular Basis of Disease*, vol. 1863, no. 3, pp. 643–653, 2017.

[418] E. Neven, V. Persy, S. Dauwe, T. De Schutter, M. E. De Broe, and P. C. Dhaese, "Chondrocyte rather than osteoblast conversion of vascular cells underlies medial calcification in uremic rats," *Arteriosclerosis, Thrombosis, and Vascular Biology*, vol. 30, no. 9, pp. 1741–1750, 2010.

[419] S. W. Tompson, B. Merriman, V. A. Funari, M. Fresquet, R. S. Lachman, D. L. Rimoin, S. F. Nelson, M. D. Briggs, D. H. Cohn, and D. Krakow, "A Recessive Skeletal Dysplasia, SEMD Aggrecan Type, Results from a Missense Mutation Affecting the C-Type Lectin Domain of Aggrecan," *American Journal of Human Genetics*, vol. 84, no. 1, pp. 72–79, 2009.

[420] E. L. Stattin, F. Wiklund, K. Lindblom, P. Önnerfjord, B. A. Jonsson, Y. Tegner, T. Sasaki, A. Struglics, S. Lohmander, N. Dahl, D. Heinegård, and A. Aspberg, "A Missense Mutation in the Aggrecan C-type Lectin Domain Disrupts Extracellular Matrix Interactions and Causes Dominant Familial Osteochondritis Dissecans," *American Journal of Human Genetics*, vol. 86, no. 2, pp. 126–137, 2010.

[421] O. Nilsson, M. H. Guo, N. Dunbar, J. Popovic, D. Flynn, C. Jacobsen, J. C. Lui, J. N. Hirschhorn, J. Baron, and A. Dauber, "Short stature, accelerated bone maturation, and early growth cessation due to heterozygous aggrecan mutations," *The Journal of Clinical Endocrinology & Metabolism*, vol. 99, no. 8, pp. E1510–E1518, 2014.

[422] J. B. Quintos, M. H. Guo, and A. Dauber, "Idiopathic short stature due to novel heterozygous mutation of the aggrecan gene," *Journal of Pediatric Endocrinology & Metabolism*, vol. 28, no. 7-8, pp. 927–932, 2015.

[423] M. van der Steen, R. Pfundt, S. J. W. H. Maas, W. M. Bakker-vanWaarde, R. J. Odink, and A. C. S. Hokken-Koelega, "ACAN gene mutations in short children born SGA and response to Growth Hormone treatment.," *The Journal of Clinical Endocrinology & Metabolism*, vol. 102, no. 5, pp. 1458–1467, 2016.

[424] A. Gkourogianni, M. Andrew, L. Tyzinski, M. Crocker, J. Douglas, N. Dunbar, J. Fairchild, M. F. A. Funari, K. E. Heath, A. A. Jorge, T. Kurtzman, S. LaFranchi, S. Lalani, J. Lebl, Y. Lin, E. Los, D. Newbern, C. Nowak, M. Olson, J. Popovic, Š. PrÅŕhová, L. Elblova, J. B. Quintos, E. Segerlund, L. Sentchordi, M. Shinawi, E.-L. Stattin, J. Swartz, G.-d. A. Ariadna, D.-C. Sinhué, H. Hosono, P. A. Sanchez-Lara, V. Hwa, J. Baron, O. Nilsson, and A. Dauber, "Clinical characterization of patients with autosomal dominant short stature due to aggrecan mutations," *The Journal of Clinical Endocrinology & Metabolism*, vol. 102, no. 2, pp. jc.2016–3313, 2016.

[425] L. Gleghorn, R. Ramesar, P. Beighton, and G. Wallis, "A mutation in the variable repeat region of the aggrecan gene (AGC1) causes a form of spondyloepiphyseal dysplasia associated with severe, premature osteoarthritis.," *American Journal of Human Genetics*, vol. 77, no. 3, pp. 484–90, 2005.

[426] S. Dateki, A. Nakatomi, S. Watanabe, H. Shimizu, Y. Inoue, H. Baba, K.-i. Yoshiura, and H. Moriuchi, "Identification of a novel heterozygous mutation of the Aggrecan gene in a family with idiopathic short stature and multiple intervertebral disc herniation," *Journal of Human Genetics*, vol. 62, pp. 717–721, jul 2017.

[427] S. Solovieva, N. Noponen, M. Männikkö, P. Leino-Arjas, K. Luoma, R. Raininko, L. Ala-Kokko, and H. Riihimäki, "Association between the aggrecan gene variable number of tandem repeats polymorphism and intervertebral disc degeneration," *Spine*, vol. 32, no. 16, pp. 1700–5, 2007.

[428] N. K. Kim, D. A. Shin, I. B. Han, E. H. Yoo, S. H. Kim, and S. S. Chung, "The association of aggrecan gene polymorphism with the risk of intervertebral disc degeneration," *Acta Neurochirurgica*, vol. 153, no. 1, pp. 129–133, 2011.

[429] K. J. Doege, S. N. Coulter, L. M. Meek, K. Maslen, and J. G. Wood, "A human-specific polymorphism in the coding region of the aggrecan gene: Variable number of tandem repeats produce a range of core protein sizes in the general population," *Journal of Biological Chemistry*, vol. 272, no. 21, pp. 13974–13979, 1997.

[430] J. Gu, F. Guan, G. Guan, G. Xu, X. Wang, W. Zhao, Y. Ji, and J. Yan, "Aggrecan variable number of tandem repeat polymorphism and lumbar disc degeneration: A meta-analysis," *Spine*, vol. 38, no. 25, pp. E1600–7, 2013.

[431] Y. Kawaguchi, R. Osada, M. Kanamori, H. Ishihara, K. Ohmori, H. Matsui, and T. Kimura, "Association between an aggrecan gene polymorphism and lumbar disc degeneration," *Spine*, vol. 24, no. 23, pp. 2456–2460, 1999.

[432] R. S. Perera, P. H. Dissanayake, U. Senarath, L. S. Wijayaratne, A. L. Karunanayake, and V. H. W. Dissanayake, "Single nucleotide variants of candidate genes in aggrecan metabolic pathway are associated with lumbar disc degeneration and modic changes," *PLoS ONE*, vol. 12, no. 1, p. e0169835, 2017.

[433] R. Perera, P. Dissanayake, U. Senarath, L. Wijayaratne, A. Karunanayake, and V. Dissanayake, "Variants of ACAN are associated with severity of lumbar disc herniation in patients with chronic low back pain," *PLoS ONE*, vol. 12, no. 7, p. e0181580, 2017.

[434] H. Watanabe, K. Kimata, S. Line, D. Strong, L. Y. Gao, C. A. Kozak, and Y. Yamada, "Mouse cartilage matrix deficiency (cmd) caused by a 7 bp deletion in the aggrecan gene," *Nature Genetics*, vol. 7, pp. 154–7, jun 1994.

[435] H. Watanabe, K. Nakata, K. Kimata, I. Nakanishi, and Y. Yamada, "Dwarfism and age-associated spinal degeneration of heterozygote cmd mice defective in aggrecan.," *Proceedings of the National Academy of Sciences*, vol. 94, no. 13, pp. 6943–7, 1997.

[436] J. R. Korenberg, X. N. Chen, H. Tran, and W. S. Argraves, "Localisation of the human gene for fibulin-1 (FBLN1) to chromosome band 22q13.3," *Cytogenics and Cell Genetics*, vol. 68, no. 3-4, pp. 192–193, 1995.

[437] J. M. Muriel, C. Dong, H. Hutter, and B. E. Vogel, "Fibulin-1C and Fibulin-1D splice variants have distinct functions and assemble in a hemicentin-dependent manner.," *Development*, vol. 132, no. 19, pp. 4223–34, 2005.

[438] N. Miosge, W. Götz, T. Sasaki, M. L. Chu, R. Timpl, and R. Herken, "The extracellular matrix proteins fibulin-1 and fibulin-2 in the early human embryo," *The Histochemical Journal*, vol. 28, no. 2, pp. 109–116, 1996.

[439] H. Y. Zhang, R. Timpl, T. Sasaki, M. L. Chu, and P. Ekblom, "Fibulin-1 and fibulin-2 expression during organogenesis in the developing mouse embryo," *Developmental Dynamics*, vol. 205, no. 3, pp. 348–364, 1996.

[440] E. F. Roark, D. R. Keene, C. C. Haudenschild, S. Godyna, C. D. Little, and W. S. Argraves, "The association of human fibulin-1 with elastic fibers: an immunohistological, ultrastructural, and RNA study," *Journal of Histochemistry and Cytochemistry*, vol. 43, no. 4, pp. 401–411, 1995.

[441] N. Kobayashi, G. Kostka, J. H. O. Garbe, D. R. Keene, H. P. Bächinger, F.-G. Hanisch, D. Markova, T. Tsuda, R. Timpl, M.-L. Chu, and T. Sasaki, "A comparative analysis of the fibulin protein family. Biochemical characterization, binding interactions, and tissue localization.," *The Journal of Biological Chemistry*, vol. 282, no. 16, pp. 11805–11816, 2007.

[442] V. M. Fresco, X. C. B. Kern, M. Mohammadi, and X. W. O. Twal, "Fibulin-1 binds to fibroblast growth factor 8 with high affinity: Effects on embryo survival," *Journal of Biological Chemistry*, vol. 291, no. 36, pp. 18730–18739, 2016.

[443] R. Timpl, T. Sasaki, G. Kostka, and M.-L. Chu, "Fibulins: a versatile family of extracellular matrix proteins," *Nature Reviews Molecular Cell Biology*, vol. 4, no. 6, pp. 479–489, 2003.

[444] T. Sasaki, G. Kostka, W. Göhring, H. Wiedemann, K. Mann, M. L. Chu, and R. Timpl, "Structural characterization of two variants of fibulin-1 that differ in nidogen affinity," *Journal of Molecular Biology*, vol. 245, no. 3, pp. 241–250, 1995.

[445] P. Maurer and E. Hohenester, "Structural and functional aspects of calcium binding in extracellular matrix proteins," *Matrix Biology*, vol. 15, no. 8-9, pp. 569–580, 1997.

[446] T. Sasaki, K. Mann, G. Murphy, M. L. Chu, and R. Timpl, "Different susceptibilities of fibulin-1 and fibulin-2 to cleavage by matrix metalloproteinases and other tissue proteases," *European Journal of Biochemistry*, vol. 240, no. 2, pp. 427–434, 1996.

[447] S. Adam, W. Göhring, H. Wiedemann, M. L. Chu, R. Timpl, and G. Kostka, "Binding of fibulin-1 to nidogen depends on its C-terminal globular domain and a specific array of calcium-binding epidermal growth factor- like (EG) modules," *Journal of Molecular Biology*, vol. 272, no. 2, pp. 226–236, 1997.

[448] T. Pan, M. Kluge, R. Zhang, U. Mayer, R. Timpl, and M. Chu, "Sequence of extracellular mouse protein BMâĂŘ90/fibulin and its calciumâĂŘdependent binding to other basementâĂŘmembrane ligands," *European Journal of Biochemistry*, vol. 215, no. 3, pp. 733–740, 1993.

[449] H. Tran, W. J. VanDusen, and W. S. Argraves, "The self-association and fibronectin-binding sites of fibulin-1 map to calcium-binding epidermal growth factor-like domains," *Journal of Biological Chemistry*, vol. 272, no. 36, pp. 22600–22606, 1997.

[450] J. M. Muriel, E. Xu, J. M. Kramer, and B. E. Vogel, "Selective assembly of fibulin-1 splice variants reveals distinct extracellular matrix networks and novel functions for perlecan/UNC-52 splice variants," *Developmental Dynamics*, vol. 235, no. 10, pp. 2632–2640, 2006.

[451] M. Overgaard, C. Cangemi, M. L. Jensen, W. S. Argraves, and L. M. Rasmussen, "Total and isoform-specific quantitative assessment of circulating fibulin-1 using selected reaction monitoring MS and time-resolved immunofluorometry," *Proteomics Clinical Applications*, vol. 9, pp. 767–775, aug 2015.

[452] G. Liu, M. A. Cooley, A. G. Jarnicki, A. C.-Y. Hsu, P. M. Nair, T. J. Haw, M. Fricker, S. L. Gellatly, R. Y. Kim, M. D. Inman, G. Tjin, P. A. Wark, M. M. Walker, J. C. Horvat, B. G. Oliver, W. S. Argraves, D. A. Knight, J. K. Burgess, and P. M. Hansbro, "Fibulin-1 regulates the pathogenesis of tissue remodeling in respiratory diseases," *JCI Insight*, vol. 1, no. 9, p. e86380, 2016.

[453] N. V. Lee, J. C. Rodriguez-Manzaneque, S. N. M. Thai, W. O. Twal, A. Luque, K. M. Lyons, W. S. Argraves, and M. L. Iruela-Arispe, "Fibulin-1 acts as a cofactor for the matrix metalloprotease ADAMTS-1," *Journal of Biological Chemistry*, vol. 280, no. 41, pp. 34796–34804, 2005.

[454] D. R. McCulloch, C. M. Nelson, L. J. Dixon, D. L. Silver, J. D. Wylie, V. Lindner, T. Sasaki, M. A. Cooley, W. S. Argraves, and S. S. Apte, "ADAMTS Metalloproteases Generate Active Versican Fragments that Regulate Interdigital Web Regression," *Developmental Cell*, vol. 17, no. 5, pp. 687–698, 2009.

[455] H. Zhang, X. Gao, C. Weng, and Z. Xu, "Interaction between angiogenin and fibulin 1: Evidence and implication," *Acta Biochimica et Biophysica Sinica*, vol. 40, no. 5, pp. 375–380, 2008.

[456] I. Ohsawa, C. Takamura, and S. Kohsaka, "Fibulin-1 binds the amino-terminal head of beta-amyloid precursor protein and modulates its physiological function," *Journal of Neurochemistry*, vol. 76, no. 5, pp. 1411–20, 2001.

[457] N. Fujimoto, J. Terlizzi, R. Brittingham, A. Fertala, J. A. McGrath, and J. Uitto, "Extracellular matrix protein 1 interacts with the domain III of fibulin-1C and 1D variants through its central tandem repeat 2," *Biochemical and Biophysical Research Communications*, vol. 333, no. 4, pp. 1327–1333, 2005.

[458] H. Tran, A. Tanaka, S. V. Litvinovich, L. V. Medved, C. C. Haudenschild, and W. S. Argraves, "The interaction of fibulin-1 with fibrinogen: A potential role in hemostasis and thrombosis," *Journal of Biological Chemistry*, vol. 270, no. 33, pp. 19458–19464, 1995.

[459] W. O. Twal, A. Czirok, B. Hegedus, C. Knaak, M. R. Chintalapudi, H. Okagawa, Y. Sugi, and W. S. Argraves, "Fibulin-1 suppression of fibronectin-regulated cell adhesion and motility," *Journal of cell science*, vol. 114, no. Pt 24, pp. 4587–4598, 2001.

[460] S. De Vega, T. Iwamoto, T. Nakamura, K. Hozumi, D. A. McKnight, L. W. Fisher, S. Fukumoto, and Y. Yamada, "TM14 is a new member of the fibulin family (fibulin-7) that interacts with extracellular matrix molecules and is active for cell binding," *Journal of Biological Chemistry*, vol. 282, no. 42, pp. 30878–30888, 2007.

[461] J. S. Brooke, J.-H. Cha, and L. Eidels, "Latent transforming growth factor β-binding protein-3 and fibulin-1C interact with the extracellular domain of the heparin-binding EGF-like growth factor precursor," *BMC Cell Biology*, vol. 3, no. 1, p. 2, 2002.

[462] J. H. Miner and P. D. Yurchenco, "Laminin functions in tissue morphogenesis," *Annual Review of Cell and Developmental Biology*, vol. 20, no. 1, pp. 255–284, 2004.

[463] K. M. Ng, M. G. Catalano, T. Pinós, D. M. Selva, G. V. Avvakumov, F. Munell, and G. L. Hammond, "Evidence that fibulin family members contribute to the steroid-dependent extravascular sequestration of sex hormone-binding globulin," *Journal of Biological Chemistry*, vol. 281, no. 23, pp. 15853–15861, 2006.

[464] M. A. Cooley, V. M. Fresco, M. E. Dorlon, W. O. Twal, N. V. Lee, J. L. Barth, C. B. Kern, M. L. Iruela-Arispe, and W. S. Argraves, "Fibulin-1 is required during cardiac ventricular morphogenesis for versican cleavage, suppression of ErbB2 and Erk1/2 activation, and to attenuate trabecular cardiomyocyte proliferation," *Developmental Dynamics*, vol. 241, no. 2, pp. 303–314, 2012.

[465] G. Kostka, R. Giltay, W. Bloch, K. Addicks, R. Timpl, R. Fassler, and M. L. Chu, "Perinatal lethality and endothelial cell abnormalities in several vessel compartments of fibulin-1-deficient mice," *Molecular and Cellular Biology*, vol. 21, no. 20, pp. 7025–7034, 2001.

[466] C. Cangemi, V. Skov, M. K. Poulsen, J. Funder, W. O. Twal, M. A. Gall, V. Hjortdal, M. L. Jespersen, T. A. Kruse, J. Aagard, H. H. Parving, S. Knudsen, P. F. Høilund-Carlsen, P. Rossing, J. E. Henriksen, W. S. Argraves, and L. M. Rasmussen, "Fibulin-1 is a marker for arterial extracellular matrix alterations in type 2 diabetes," *Clinical Chemistry*, vol. 57, no. 11, pp. 1556–1565, 2011.

[467] M. A. Cooley, C. B. Kern, V. M. Fresco, A. Wessels, R. P. Thompson, T. C. McQuinn, W. O. Twal, C. H. Mjaatvedt, C. J. Drake, and W. S. Argraves, "Fibulin-1 is required for morphogenesis of neural crest-derived structures," *Developmental Biology*, vol. 319, no. 2, pp. 336–345, 2008.

[468] S. Godyna, M. Diaz-Ricart, and W. S. Argraves, "Fibulin-1 mediates platelet adhesion via a bridge of fibrinogen," *Blood*, vol. 88, no. 7, pp. 2569–2577, 1996.

[469] W. S. Argraves, A. Tanaka, E. P. Smith, W. O. Twal, K. M. Argraves, D. Fan, and C. C. Haudenschild, "Fibulin-1 and fibrinogen in human atherosclerotic lesions," *Histochemistry and Cell Biology*, vol. 132, no. 5, pp. 559–565, 2009.

[470] J. S. Dahl, J. E. Møller, L. Videbæk, M. K. Poulsen, T. R. Rudbæk, P. A. Pellikka, W. Scott Argraves, and L. M. Rasmussen, "Plasma fibulin-1 is linked to restrictive filling of the left ventricle and to mortality in patients with aortic valve stenosis," *Journal of the American Heart Association*, vol. 1, no. 6, p. e003889, 2012.

[471] A. Scholze, E.-M. Bladbjerg, J. J. Sidelmann, A. C. P. Diederichsen, H. Mickley, M. Nybo, W. S. Argraves, P. Marckmann, and L. M. Rasmussen, "Plasma concentrations of extracellular matrix protein fibulin-1 are related to cardiovascular risk markers in chronic kidney disease and diabetes," *Cardiovascular Diabetology*, vol. 12, p. 6, 2013.

[472] M. Neiman, J. J. Hedberg, P. R. D??nnes, I. Schuppe-Koistinen, S. Hanschke, R. Schindler, M. Uhl??n, J. M. Schwenk, and P. Nilsson, "Plasma profiling reveals human fibulin-1 as candidate marker for renal impairment," *Journal of Proteome Research*, vol. 10, no. 11, pp. 4925–4934, 2011.

[473] M. L. Hansen, J. S. Dahl, W. S. Argraves, A. Irmukhamedov, and L. M. Rasmussen, "Aortic valve stenosis and atrial fibrillation influence plasma fibulin-1 levels in patients treated with coronary bypass surgery," *Cardiology*, vol. 126, no. 3, pp. 202–206, 2013.

[474] E. Laugesen, P. Hoyem, J. S. Christiansen, S. T. Knudsen, K. W. Hansen, W. S. Argraves, T. K. Hansen, P. L. Poulsen, and L. M. Rasmussen, "Plasma levels of the arterial wall protein fibulin-1 are associated with carotid-femoral pulse wave velocity: a cross-sectional study," *Cardiovascular Diabetology*, vol. 12, no. 1, p. 107, 2013.

[475] L. Mikhaylova, J. Malmquist, and M. Nurminskaya, "Regulation of in vitro vascular calcification by BMP4, VEGF and Wnt3a," *Calcified Tissue International*, vol. 81, no. 5, pp. 372–381, 2007.

[476] B. L. Cheuk and S. W. Cheng, "Differential expression of elastin assembly genes in patients with Stanford Type A aortic dissection using microarray analysis," *Journal of Vascucal Surgery*, vol. 53, no. 4, pp. 1071–1078.e2, 2011.

[477] S. A. Mohamed, H. H. Sievers, T. Hanke, D. Richardt, C. Schmidtke, E. I. Charitos, G. Belge, and J. Bullerdiek, "Pathway analysis of differentially expressed genes in patients with acute aortic dissection," *Biomarker Insights*, vol. 4, pp. 81–90, 2009.

[478] J. Zheng, Y. Chen, B. Pat, L. A. Dell'italia, M. Tillson, A. R. Dillon, P. C. Powell, K. Shi, N. Shah, T. Denney, A. Husain, and L. J. Dell'Italia, "Microarray identifies extensive downregulation of noncollagen extracellular matrix and profibrotic growth factor genes in chronic isolated mitral regurgitation in the dog," *Circulation*, vol. 119, no. 15, pp. 2086–2095, 2009.

[479] A. Garcia, S. Eiras, A. F. Parguina, J. Alonso, I. Rosa, A. Salgado-Somoza, T. Y. Rico, E. Teijeira-Fernandez, and J. R. Gonzalez-Juanatey, "High-resolution two-dimensional gel electrophoresis

analysis of atrial tissue proteome reveals down-regulation of fibulin-1 in atrial fibrillation," *International Journal of Cardiology*, vol. 150, no. 3, pp. 283–290, 2011.

[480] V. Beisvag, P. K. Lehre, H. Midelfart, H. Aass, O. Geiran, A. K. Sandvik, A. Lægreid, J. Komorowski, and Ø. Ellingsen, "Aetiology-specific patterns in end-stage heart failure patients identified by functional annotation and classification of microarray data," *European Journal of Heart Failure*, vol. 8, no. 4, pp. 381–389, 2006.

[481] J. Y. Lau, B. G. Oliver, M. Baraket, E. L. Beckett, N. G. Hansbro, L. M. Moir, S. D. Wilton, C. Williams, P. S. Foster, P. M. Hansbro, J. L. Black, and J. K. Burgess, "Fibulin-1 is increased in asthma - a novel mediator of airway remodeling?," *PLoS ONE*, vol. 5, no. 10, 2010.

[482] J. Jaffar, S. Unger, T. J. Corte, M. Keller, P. J. Wolters, L. Richeldi, S. Cerri, C. M. Prele, P. M. Hansbro, W. S. Argraves, R. A. Oliver, B. G. Oliver, J. L. Black, and J. K. Burgess, "Fibulin-1 predicts disease progression in patients with idiopathic pulmonary fibrosis," *Chest*, vol. 146, no. 4, pp. 1055–1063, 2014.

[483] Q. Ge, L. Chen, J. Jaffar, W. S. Argraves, W. O. Twal, P. Hansbro, J. L. Black, J. K. Burgess, and B. Oliver, "Fibulin1C peptide induces cell attachment and extracellular matrix deposition in lung fibroblasts," *Science Reports*, vol. 5, p. 9496, 2015.

[484] P. Debeer, E. F. P. M. Schoenmakers, W. O. Twal, W. S. Argraves, L. De Smet, J. P. Fryns, and W. J. M. Van De Ven, "The fibulin-1 gene (FBLN1) is disrupted in a t(12;22) associated with a complex type of synpolydactyly," *Journal of Medical Genetics*, vol. 39, no. 2, pp. 98–104, 2002.

[485] S. Bohlega, H. Al-Ajlan, and A. Al-Saif, "Mutation of fibulin-1 causes a novel syndrome involving the central nervous system and connective tissues," *European Journal of Human Genetics*, vol. 22, no. 5, pp. 640–643, 2014.

[486] Yasmin and K. M. O'Shaughnessy, "Genetics of arterial structure and function: towards new biomarkers for aortic stiffness?," *Clinical Science*, vol. 114, no. 11, pp. 661–677, 2008.

[487] C. M. McEniery, Yasmin, S. Wallace, K. Maki-Petaja, B. McDonnell, J. E. Sharman, C. Retallick, S. S. Franklin, M. J. Brown, R. C. Lloyd, J. R. Cockcroft, I. B. Wilkinson, and E. S. Investigators, "Increased stroke volume and aortic stiffness contribute to isolated systolic hypertension in young adults," *Hypertension*, vol. 46, no. 1, pp. 221–226, 2005.

[488] N. Risch and H. Zhang, "Extreme discordant sib pairs for mapping quantitative trait loci in humans.," *Science (New York, N.Y.)*, vol. 268, no. 5217, pp. 1584–9, 1995.

[489] G. Consortium, "The Genotype-Tissue Expression (GTEx) project," *Nature Genetics*, vol. 45, no. 6, pp. 580–585, 2013.

[490] J. K. Wittke-Thompson, A. Pluzhnikov, and N. J. Cox, "Rational inferences about departures from Hardy-Weinberg equilibrium.," *American Journal of Human Genetics*, vol. 76, no. 6, pp. 967–986, 2005.

[491] A. Grupe, R. Abraham, Y. Li, C. Rowland, P. Hollingworth, A. Morgan, L. Jehu, R. Segurado, D. Stone, E. Schadt, M. Karnoub, P. Nowotny, K. Tacey, J. Catanese, J. Sninsky, C. Brayne, D. Rubinsztein, M. Gill, B. Lawlor, S. Lovestone, P. Holmans, M. O'Donovan, J. C. Morris, L. Thal, A. Goate, M. J. Owen, and J. Williams, "Evidence for novel susceptibility genes for late-onset Alzheimer's disease from a genome-wide association study of putative functional variants," *Human Molecular Genetics*, vol. 16, no. 8, pp. 865–873, 2007.

[492] Y. Zhang, L. Cao, B. L. Yang, and B. B. Yang, "The G3 domain of versican enhances cell proliferation via epidermial growth factor-like motifs," *Journal of Biological Chemistry*, vol. 273, no. 33, pp. 21342–21351, 1998.

[493] Y. Zhang, L. Cao, C. G. Kiani, B. L. Yang, and B. B. Yang, "The G3 domain of versican inhibits mesenchymal chondrogenesis via the epidermal growth factor-like motifs," *Journal of Biological Chemistry*, vol. 273, no. 49, pp. 33054–33063, 1998.

[494] Y. Zhang, Y. Wu, L. Cao, V. Lee, L. Chen, Z. Lin, C. Kiani, M. E. Adams, and B. B. Yang, "Versican modulates embryonic chondrocyte morphology via the epidermal growth factor-like motifs in G3," *Experimental Cell Research*, vol. 263, no. 1, pp. 33–42, 2001.

[495] P. A. Arakaki, M. R. Marques, and M. C. Santos, "MMP-1 polymorphism and its relationship to pathological processes," *Journal of Biosciences*, vol. 34, no. 2, pp. 313–320, 2009.

[496] A. M. Langers, H. W. Verspaget, D. W. Hommes, and C. F. Sier, "Single-nucleotide polymorphisms of matrix metalloproteinases and their inhibitors in gastrointestinal cancer.," *World Journal of Gastrointestinal Oncology*, vol. 3, no. 6, pp. 79–98, 2011.

[497] J. Dudhia, C. M. Davidson, T. M. Wells, D. H. Vynios, T. E. Hardingham, and M. T. Bayliss, "Age-related changes in the content of the C-terminal region of aggrecan in human articular cartilage," *Biochemical Journal*, vol. 313 (Pt 3, pp. 933–940, 1996.

[498] P. J. Roughley, L. I. Melching, and A. D. Recklies, "Changes in the expression of decorin and biglycan in human articular cartilage with age and regulation by TGF-beta," *Matrix Biology*, vol. 14, no. 1, pp. 51–59, 1994.

[499] T. E. Hardingham, A. J. Fosang, and J. Dudhia, "The structure, function and turnover of aggrecan, the large aggregating proteoglycan from cartilage," *European Journal of Clinical Chemistry and Clinical Biochemistry*, vol. 32, no. 4, pp. 249–257, 1994.

[500] S. Sahebjam, R. Khokha, and J. S. Mort, "Increased collagen and aggrecan degradation with age in the joints of Timp3(-/-) mice," *Arthritis and Rheumatology*, vol. 56, no. 3, pp. 905–909, 2007.

[501] J. R. Dunlevy and J. A. Rada, "Interaction of lumican with aggrecan in the aging human sclera," *Investigative Ophthalmology and Visual Science*, vol. 45, no. 11, pp. 3849–3856, 2004.

[502] N. Adhikari, M. Carlson, B. Lerman, and J. L. Hall, "Changes in expression of proteoglycan core proteins and heparan sulfate enzymes in the developing and adult murine aorta," *Journal of Cardiovascular Translational Research*, vol. 4, no. 3, pp. 313–320, 2011.

[503] A. M. Tovar, D. C. Cesar, G. C. Leta, and P. A. Mourão, "Age-related changes in populations of aortic glycosaminoglycans: species with low affinity for plasma low-density lipoproteins, and not species with high affinity, are preferentially affected," *Arteriosclerosis, Thrombosis, and Vascular Biology*, vol. 18, no. 4, pp. 604–614, 1998.

[504] G. Manley, R. N. Mullinger, and P. H. Lloyd, "Properties of heparan sulphate and chondroitin sulphate from young and old human aortae," *Biochemical Journal*, vol. 114, no. 1, pp. 89–96, 1969.

[505] A. Struglics and M. Hansson, "Calpain is involved in C-terminal truncation of human aggrecan," *Biochemical Journal*, vol. 430, no. 3, pp. 531–538, 2010.

[506] Z. Li, J. Froehlich, Z. S. Galis, and E. G. Lakatta, "Increased expression of matrix metalloproteinase-2 in the thickened intima of aged rats," *Hypertension*, vol. 33, no. 1, pp. 116–123, 1999.

[507] M. McNulty, P. Spiers, E. McGovern, and J. Feely, "Aging is associated with increased matrix metalloproteinase-2 activity in the human aorta," *American Journal of Hypertension*, vol. 18, no. 4 (Pt 1), pp. 504–509, 2005.

[508] M. Wang, G. Takagi, K. Asai, R. G. Resuello, F. F. Natividad, D. E. Vatner, S. F. Vatner, and E. G. Lakatta, "Aging increases aortic MMP-2 activity and angiotensin II in nonhuman primates," *Hypertension*, vol. 41, no. 6, pp. 1308–1316, 2003.

[509] L. Jiang, M. Wang, J. Zhang, R. E. Monticone, R. Telljohann, G. Spinetti, G. Pintus, and E. G. Lakatta, "Increased aortic Calpain-1 activity mediates age-associated angiotensin II signaling of vascular smooth muscle cells," *PLoS ONE*, vol. 3, no. 5, p. e2231, 2008.

[510] A. Aspberg, "The different roles of aggrecan interaction domains," *Journal of Histochemistry and Cytochemistry*, vol. 60, no. 12, pp. 987–996, 2012.

[511] B. M. Vertel, "The ins and outs of aggrecan," *Trends in Cell Biology*, vol. 5, no. 12, pp. 458–464, 1995.

[512] E. D. Eanes and A. W. Hailer, "Effect of ultrafilterable fragments from chondroitinase and protease-treated aggrecan on calcium phosphate precipitation in liposomal suspensions," *Calcified Tissue International*, vol. 55, no. 3, pp. 176–179, 1994.

[513] L. Schaefer and R. V. Iozzo, "Biological functions of the small leucine-rich proteoglycans: From genetics to signal transduction," *Journal of Biological Chemistry*, vol. 283, no. 31, pp. 21305–21309, 2008.

[514] W. C. O'Neill, "Pyrophosphate, alkaline phosphatase, and vascular calcification," *Circulation Research*, vol. 99, no. 2, 2006.

[515] M. M. Adeva-Andany, C. Fernandez-Fernandez, R. Sanchez-Bello, C. Donapetry-Garcia, and J. Martinez-Rodriguez, "The role of carbonic anhydrase in the pathogenesis of vascular calcification in humans," *Atherosclerosis*, vol. 241, no. 1, pp. 183–191, 2015.

[516] G. Mucchiano, G. G. Cornwell, and P. Westermark, "Senile aortic amyloid. Evidence for two distinct forms of localized deposits," *The American Journal of Pathology*, vol. 140, no. 4, pp. 871–7, 1992.

[517] T. M. Hughes, L. H. Kuller, E. J. M. Barinas-Mitchell, E. M. McDade, W. E. Klunk, A. D. Cohen, C. A. Mathis, S. T. Dekosky, J. C. Price, and O. L. Lopez, "Arterial stiffness and β-amyloid progression in nondemented elderly adults," *JAMA Neurology*, vol. 71, no. 5, pp. 562–8, 2014.

[518] S. Sharma, A. Lee, K. Choi, K. Kim, I. Youn, S. B. Trippel, and A. Panitch, "Biomimetic aggrecan reduces cartilage extracellular matrix from degradation and lowers catabolic activity in ex vivo and in vivo models," *Macromolecular Bioscience*, vol. 13, no. 9, pp. 1228–1237, 2013.

[519] S. Sharma, A. Panitch, and C. P. Neu, "Incorporation of an aggrecan mimic prevents proteolytic degradation of anisotropic cartilage analogs," *Acta Biomaterialia*, vol. 9, no. 1, pp. 4618–4625, 2013.

[520] A. M. Gilbert, J. a. Bikker, and S. V. O'Neil, "Advances in the development of novel aggrecanase inhibitors.," *Expert Opinion on Therapeutic Patents*, vol. 21, no. 1, pp. 1–12, 2011.

[521] J. Larkin, T. A. Lohr, L. Elefante, J. Shearin, R. Matico, J. L. Su, Y. Xue, F. Liu, C. Genell, R. E. Miller, P. B. Tran, A. M. Malfait, C. C. Maier, and C. J. Matheny, "Translational development of an ADAMTS-5 antibody for osteoarthritis disease modification," *Osteoarthritis and Cartilage*, vol. 23, no. 8, pp. 1254–1266, 2015.

[522] K. R. Hutchinson, J. A. Stewart, and P. A. Lucchesi, "Extracellular matrix remodeling during the progression of volume overload-induced heart failure," *Journal of Molecular and Cellular Cardiology*, vol. 48, no. 3, pp. 564–569, 2010.

[523] M. L. Hansen and L. M. Rasmussen, "Associations between plasma fibulin-1, pulse wave velocity and diabetes in patients with coronary heart disease," *Journal of Diabetes and its Complications*, vol. 29, no. 3, pp. 362–366, 2015.

[524] C. Oxlund, C. Cangemi, J. Henriksen, I. Jacobsen, J. Gram, K. Schousboe, L. Tarnow, W. Argraves, and L. Rasmussen, "Low-dose spironolactone reduces plasma fibulin-1 levels in patients with type 2 diabetes and resistant hypertension," *Journal of Human Hypertension*, vol. 29, no. 1, pp. 28–32, 2015.

[525] K. Harikrishnan, M. A. Cooley, Y. Sugi, J. L. Barth, L. M. Rasmussen, C. B. Kern, K. M. Argraves, and W. S. Argraves, "Fibulin-1 suppresses endothelial to mesenchymal transition in the proximal outflow tract," *Mechanisms of Development*, vol. 136, pp. 123–132, 2015.

[526] A. Struglics and M. Hansson, "MMP proteolysis of the human extracellular matrix protein aggrecan is mainly a process of normal turnover," *Biochemical Journal*, vol. 446, no. 2, pp. 213–223, 2012.

[527] J. H. Moore, "The ubiquitous nature of epistasis in determining susceptibility to common human diseases," *Human Heredity*, vol. 56, no. 1-3, pp. 73–82, 2003.

[528] S. L. Edwards, J. Beesley, J. D. French, and M. Dunning, "Beyond GWASs: Illuminating the dark road from association to function," *American Journal of Human Genetics*, vol. 93, no. 5, pp. 779–797, 2013.